Holographic Quantum Liquids

Nikolaos Kaplis
Magdalen College
University of Oxford

A thesis submitted for the degree of
Doctor of Philosophy
Trinity 2013

Abstract

In this thesis, applications of Holography in the context of Condensed Matter Physics and in particular hydrodynamics, will be studied. Holography or gauge/gravity duality has been an enormously useful tool in studying strongly-coupled Field Theories with particular success in their low-frequency and large-wavelength fluctuation regime, i.e the hydrodynamical regime. Here, following a phenomenological approach, gravitational systems, simple enough to be properly examined, will be studied in order to derive as much information as possible about their dual theories, given that their exact form is not accessible in this way. After a review of the most important elements of standard Condensed Matter Theory, the gauge/gravity duality itself will be presented, along with some of its most important achievements. Having established the framework of this work, the main results of this thesis will be presented. Initially the sound channel of the theory dual to the anti-de Sitter Reissner–Nordström black hole space-time will be studied, at finite temperature and finite chemical potential. Hydrodynamical properties of the boundary theory will be of major interest. Following that, focus will be shifted towards another gravitational system, namely the Electron Star. There, the shear channel of the dual theory will be mainly examined. The goal will be, as before, to extract information about the hydrodynamical properties of the boundary theory.

To my parents.

Γράφω γιὰ κείνους ποὺ δὲν ξέρουν νὰ διαβάσουν
γιὰ τοὺς ἐργάτες ποὺ γυρίζουνε τὸ βράδι μὲ τὰ μάτια κόκκινα ἀπ᾽ τὸν ἄμμο
γιὰ σᾶς, χωριάτες, ποὺ ἤπιαμε μαζὶ στὰ χάνια τὶς χειμωνιάτικες νύχτες τοῦ ἀγώνα
ἐνῶ μακριὰ ἀκουγότανε τὸ ντουφεκίδι τῶν συντρόφων μας.
Γράφω νὰ μὲ διαβάζουν αὐτοὶ ποὺ μαζεύουν τὰ χαρτιὰ ἀπ᾽ τοὺς δρόμους
καὶ σκορπίζουνε τοὺς σπόρους ὅλων τῶν αὐριανῶν μας τραγουδιῶν
γράφω γιὰ τοὺς καρβουνιάρηδες, γιὰ τοὺς γυρολόγους καὶ τὶς πλύστρες.
Γράφω γιὰ σᾶς
ἀδέρφια μου στὸ θάνατο
συντρόφοι μου στὴν ἐλπίδα
ποὺ σᾶς ἀγάπησα βαθειὰ κι ἀπέραντα
ὅπως ἑνώνεται κανεὶς μὲ μιὰ γυναίκα.

Κι ὅταν πεθάνω καὶ δὲ θἄμαι οὔτε λίγη σκόνη πιὰ μέσα στοὺς δρόμους σας
τὰ βιβλία μου, στέρεα κι ἁπλά
θὰ βρίσκουν πάντοτε μιὰ θέση πάνω στὰ ξύλινα τραπέζια
ἀνάμεσα στὸ ψωμὶ
καὶ τὰ ἐργαλεῖα τοῦ λαοῦ.

Ποιητικὴ, Τάσος Λειβαδίτης

Acknowledgements

I would like to thank my supervisor, Andrei Starinets, for his guidance and support over the course of my studies. I would also like to thank my colleagues, Richard Davison and Sašo Grozdanov, for a very fruitful and enjoyable cooperation. Furthermore I would like to acknowledge the Greek State Scholarship Foundation (IKY), without the financial support of which I would not have been able to pursuit my degree. Similarly I would like to thank my college, Magdalen, for their assistance - financial and otherwise - that made my studies a pleasant and untroubled experience. Finally I would like to thank my family and friends for their forbearance throughout this rather demanding part of my life. Their support allowed me to overcome the more arduous parts of the last few years.

Contents

List of Figures

List of Tables

Chapter 1

Introduction

Over the past fifteen years an amazing development coming from String Theory, has created a novel and fast growing sector in the field of Theoretical Physics. This development is Holography or what was originally named AdS/CFT correspondence or later gauge/gravity duality [5–8]. Holography has had a twofold effect - on the one hand it has significantly revitalized String Theory releasing it from the singular pursuit of a Theory of Everything, posing new problems for investigation and pointing at new directions to be explored. On the other hand it has proven to be a stupendously useful computational tool (which also provides unique insights) that can be applied to a vast variety of problems seemingly unrelated to String Theory. One may call it a tool instead of an actual physical theory, because it maps physically interesting systems to artificial (though not necessarily) configurations that fall under the purview of String Theory, where they can be solved or at the very least be addressed in an unprecedented and almost always useful way. Though the specifics of Holography will be developed in a following chapter, it should be noted from this point that this aspect of Holography, i.e. the practical one, that is going to be explored in this thesis.

Temporarily postponing any technical description, Holography in its very essence provides a map (and the tools to implement it) between strongly interacting theories of some kind and weakly coupled ones of a completely different kind. In particular Quantum Field Theories (QFTs) at strong coupling are mapped to weakly coupled gravitational theories in higher dimensions. It is hard to over-emphasize the importance of this statement, given that strongly coupled problems have forever plagued Theoretical Physics, limiting one to perturbative descriptions of most phenomena. Holography offers a path around this restriction, since for each intractable problem it substitutes a solvable one or at least one that can be systematically studied. This feature was immediately appreciated and from the very early stages Holographic applications were sought in almost every strongly coupled system of interest. The most

noticeable examples of application fields include Heavy Ion Physics (and in particular the study of Quark Gluon Plasma) [9] and Condensed Matter Physics [10]. The latter will be the most pertinent to this thesis.

In Condensed Matter Physics one studies systems consisting of large number of components, or said in a better way, degrees of freedom. Systems like that include gases, liquids, metals, plasmas as well as more exotic configurations. Despite the long and successful history of this field there are still a lot of outstanding problems, e.g. high-temperature superconductivity, strange metals, non-Fermi liquids and others. The difficulties are primarily focused on developing a deeper understanding of the mechanisms that lead to the emergence of these phenomena. These difficulties are attributed, to a great extent, to the strongly-coupled nature of those systems, because of which standard perturbation theory breaks down and one is left without reliable, systematic tools to use. The break-through brought about by Holography is what one could colloquially call "transmutation" of degrees of freedom. That is the realization that the fundamental degrees of freedom (dof), appropriate to describe a system, and consequently the appropriate perturbative scheme, in its weak regime are not necessarily suitable to describe the same system in its strongly-coupled phase. In fact in going from the former to the latter the dof can change so dramatically that the resulting system may be difficult to identify with or even relate to the original.

Even after more than a decade of intensive study the single most examined and better understood system is that of the $\mathcal{N} = 4$ Super Yang-Mills (SYM) non-Abelian Quantum Field Theory, with $SU(N_c)$ $N_c \to \infty$ gauge group at four dimensions ($d = 4$). This system is dual to a String Theory (Type-IIB) in a particular background, namely $AdS_5 \times S^5$. It should be noted at this point that Holography takes its name from the fact that the dimensionality of the dual theories differ by one, and in fact one is defined on the boundary of the other, hence the holographic interpretation. The innovative part is that difficult, i.e. strongly-coupled, problems in the Field Theory side can be translated into weakly-coupled ones on the String Theory (actually gravity) side where the perturbative arsenal is still available, solved and then the solution can be translated back, or at the very least some useful intuition can be gained.

However, what can a highly super-symmetric, non-Abelian theory at $N_c \to \infty$ tell one about regular Condensed Matter? The first and easy answer is that even though $\mathcal{N} = 4$ SYM is not a realistic theory, it provides a very well-controlled toy model, in the strongly-coupled regime, that can be used to extract new insights into how to address such systems. The most interesting answer though came as people started

understanding better the nature and mechanics of the duality, realizing that one can engineer Holographic duals, i.e. stringy/gravitational, systems (backgrounds), suitable for the Condensed Matter problem in question, overcoming the limitation posed by excessive and often exotic symmetries. Thus began what is commonly known as "bottom-up" approaches to Holography. That is one first decides the essential ingredients of the boundary theory and then "tailors" the (minimal) appropriate gravitational dual, respecting of course the Holographic principles, which is then used to compute interesting and previously inaccessible properties of the boundary theory. Examples of this method will be examined in this thesis. This approach has become so wide-spread that it nowadays goes by its own name, that is AdS-CMT [10–18].

Besides being a computational tool, Holography has provided some amazing insights too. One of the most interesting ones is the emergence of universalities in strongly-coupled systems. By allowing the treatment of system in that regime, inaccessible by conventional perturbative methods, it has shown that quite distinct weakly-coupled theories flow, in the RG[1] sense, to similar duals on the other end of the coupling scale. As an illustration it is worth mentioning that most Holographic models have a common gravitational sector, the Einstein-Hilbert action, that seems to provide a basic set of characteristics for all these strongly (in fact infinitely) coupled theories. The emergence of common behaviour is more apparent in a regime where Holography is particularly powerful - that is hydrodynamics or in other words the regime of low-frequency and large-wavelength fluctuations. Hydrodynamics emerge for almost every theory as a low-energy effective theory. Through Holography they are mapped, to the low-frequency regime of gravity. Exactly because the Holographic dual is essentially horizon dynamics within classical gravity, for which quite a lot is known, Holography has had such a remarkable success in hydrodynamics [19].

In particular, the thermodynamic and near-equilibrium properties of such strongly-coupled field theories can be obtained relatively easily from their dual gravitational descriptions. Initial studies of these properties concentrated on field theories at non-zero temperature T (most notably $\mathcal{N} = 4$ $SU(N_c)$ super-symmetric Yang-Mills theory with $N_c \to \infty$) and were motivated by experimentally-observed properties of thermal field theories [9]. For perturbations whose frequency ω and momentum q are much less than T, these field theories were found to obey the laws of hydrodynamics and their transport coefficients, such as shear viscosity, charge diffusion constant etc. were calculated (see [20–22] and subsequent work). More recently, there has been a lot of interest in studying field theories at *zero* temperature but with a non-zero

[1]Renormalization Group.

density of a conserved global $U(1)$ charge - these are analogues of strongly-coupled condensed matter systems with a non-zero density of particles (see [10, 18, 23, 24] for some introductions to the field).

This thesis will be structured as follows. In the chapter following this introduction, aspects of Condensed Matter Physics will be reviewed. This will familiarize one with the field into which Holographic applications will be later attempted. This review will also provide the framework into which any Holographic results concerning Condensed Matter systems should belong, as well as a baseline against which the novelty and sensibility of any Holographic result will be measured.

In the next chapter more detailed aspects of Holography itself will be presented. The technical details that have been avoided in this introduction, to the detriment of specificity, will be provided. The String Theory/gravity framework in which Holography "lives" will also be addressed. Towards the end of this section some celebrated Holographic results, particularly of hydrodynamic/CM nature, will be reviewed, in order to demonstrate the power of the Duality.

In the fourth chapter the $AdS_4 - RN$ system will be studied. This system consists, on the gravity side, of a Reissner–Nordström black hole in a four-dimensional anti-de Sitter space-time. The properties of the dual theory, i.e. a $2+1$-dimensional theory, will be examined. Even though the exact nature of the theory on the boundary is not known, as this system does not come directly from some UV-complete configuration, very interesting information can still be extracted. In particular the long-lived modes of the charge density and energy density correlators will be studied, in the strongly-coupled, finite density and temperature phase of the theory dual to this gravitational system.

In the fifth chapter the properties of a different gravitational system, namely the Electron Star, will be investigated. This system consists of a four-dimensional RN-AdS background, as before, in which fermions are introduced. More specifically the fermions are assumed to populate the available states to form a star-like object, i.e. a system of charged fermions at gravitational equilibrium, that has not however gone through collapse. In other words the fermionic matter does not introduce a horizon. For simplicity the fermions[2] are assumed to behave like an ideal fermionic liquid. The total system has therefore two kinds of charge available - that which comes from behind the horizon and that coming directly from the bulk. The relation between these two will be of particular interest. The shear channel of this system will be

[2]In this context the terms fermions and electrons will be used interchangeably.

primarily examined while only some preliminary results on the longitudinal one will be presented.

Finally this thesis will be concluded by a summary of the most important findings and some discussion regarding the prospects of this work.

Chapter 2

Elements of Condensed Matter Physics

In this chapter, which is of auxiliary nature, a set of fundamental ideas and results from Condensed Matter Theory, will be reviewed. The purpose of this presentation is twofold. Firstly it will provide context for some of the most important results of Holography, which are related to strongly coupled hydrodynamics. Secondly it will guide one's physical intuition through the unfamiliar regime of strongly coupled dynamics and provide the contrast, given that it typically refers to weakly interacting systems, necessary to appreciate the novelty of Holographic calculations.

The structure of this chapter is the following. In the first section the standard approach to both ideal and viscous hydrodynamics, will be presented. Following that the relativistic approach to hydrodynamics will be reviewed, which is the most relevant in the Holographic context. Next quantum aspects of Hydrodynamics will be addressed, which formally fall into the purview of finite-temperature and finite-density Field Theory. Finally the most characteristic example of a quantum liquid in the context of Condensed Matter Physics (Fermi liquid), will be examined in some detail. This example will prove to be particularly useful as it will act as the yardstick against which the Holographic results, can be compared.

2.1 Hydrodynamics

One might wonder why Hydrodynamics are relevant to our discussion. On the face of it, they seem to describe rather trivial and exhausted systems. However if viewed as the dynamics of long-wavelength fluctuations of any given system they acquire a highly universal and modern character [25, 26]. Essentially any theory describing a physical system (i.e. a Quantum Field Theory) at the limit of long wavelengths and

small frequencies admits a hydrodynamic description. This universality is particularly useful in the case of Holography as in many cases the exact microscopic theory describing the relevant system is not known. Nonetheless the hydrodynamic limit of such a theory can still be studied and important properties can be revealed. A spectacular example of this phenomenon is the case of Heavy Ion Collisions and studies of Quark Gluon Plasma [27]. In that system the specific microscopic dynamics are extremely difficult to track, given that QCD is still in its strongly-coupled phase. However one can still study the hydrodynamical properties of the system, which turn out to be the primary route of access to that regime.

Perfect fluids

Let us start this presentation with the simplest system - that of an ideal fluid. The current presentation follows very closely the standard textbook [28]. An ideal fluid is a classical multi-particle system treated as a continuum with the following scale restriction - the unit volume of this fluid, even if considered infinitesimal around a point, has to be much larger than the characteristic inter-particle distances or in other words even infinitesimal fluid volumes must contain a very large number of constituent particles. Additionally an ideal fluid is characterized by the absence of heat exchange and dissipation, or equivalently there is no thermal conductivity or viscosity. Consequently the motion of such fluid is adiabatic, i.e. $\frac{ds}{dt} = 0$, where s is the entropy density. In order to describe the dynamics of ideal fluids one uses the velocity $\boldsymbol{v}(t, \boldsymbol{r})$, energy density ($\rho(t, \boldsymbol{r})$) and pressure $\boldsymbol{p}(t, \boldsymbol{r})$ fields, which are functions of space-time, with the aforementioned caveat regarding scales. The dynamics are governed by the continuity and Euler equations. The continuity equation

$$\partial_t \rho + \boldsymbol{\nabla}(\rho \boldsymbol{v}) = 0 \tag{2.1}$$

is just a representation of the conservation of matter (i.e the rate of change of the amount of fluid within some volume is equal to the amount crossing the boundary of said volume). Defining the flux vector $\boldsymbol{j} := \rho \boldsymbol{v}$ this equation can be written as

$$\partial_t \rho + \rho \nabla \boldsymbol{v} + \boldsymbol{v} \cdot \boldsymbol{\nabla} \rho = 0 \tag{2.2}$$

Similarly by considering the force that is exerted on a unit volume due to pressure, $-\oint p d\boldsymbol{S} = -\int dV \boldsymbol{\nabla} p$ (where $\boldsymbol{dS}$ is the infinitesimal surface bounding the infinitesimal volume dV), and essentially writing Newton's law one gets Euler's equation

$$\rho \frac{d\boldsymbol{v}}{dt} = -\boldsymbol{\nabla} p \tag{2.3}$$

Taking into account that the time derivative is a total one, i.e. it contains the implicit dependence through the fluid's flow, one arrives at the familiar form

$$\partial_t \boldsymbol{v} + (\boldsymbol{v} \cdot \boldsymbol{\nabla})\boldsymbol{v} = -\frac{1}{\rho}\boldsymbol{\nabla} p \tag{2.4}$$

Specifying $\boldsymbol{v}, \rho, \boldsymbol{p}$ along with the appropriate boundary conditions, fully determines the system.

Given that such fluids are adiabatic one can make use of the constancy of entropy in order to re-write Euler's equation (2.4) with respect to macroscopic quantities. Starting from the definition of enthalpy $dw = Tds + Vdp$ (where T is the temperature and $V = 1/\rho$ is the specific volume) which for adiabatic systems becomes $dw = Vdp$, one gets $\frac{1}{\rho}\boldsymbol{\nabla} p = \boldsymbol{\nabla} w$. Equation (2.4) therefore becomes

$$\partial_t \boldsymbol{v} + (\boldsymbol{v} \cdot \boldsymbol{\nabla})\boldsymbol{v} = -\boldsymbol{\nabla} w \tag{2.5}$$

By applying some trivial vector calculus one can recast this in the following form

$$\partial_t \boldsymbol{v} - \boldsymbol{v} \times \boldsymbol{\nabla} \times \boldsymbol{v} = -\boldsymbol{\nabla}(w + \frac{1}{2}v^2) \Rightarrow \partial_t(\boldsymbol{\nabla} \times \boldsymbol{v}) = \boldsymbol{\nabla} \times (\boldsymbol{v} \times \boldsymbol{\nabla} \times \boldsymbol{v}) \tag{2.6}$$

This particular form is special because it only involves the velocity field.

In anticipation of the viscous fluids results, as well as the Holographic results, let us define the quantities of energy and momentum flux. Starting from the energy contained in a unit volume $\frac{1}{2}\rho v^2 + \rho\epsilon$ one has

$$\partial_t(\frac{1}{2}\rho v^2) = -\frac{1}{2}v^2\nabla(\rho\boldsymbol{v}) - \boldsymbol{v} \cdot \boldsymbol{\nabla} p - \rho\boldsymbol{v} \cdot (\boldsymbol{v} \cdot \boldsymbol{\nabla})\boldsymbol{v} \tag{2.7}$$

for the first term. Using, as before, thermodynamic quantities, this equations becomes

$$\partial_t(\frac{1}{2}\rho v^2) = -\frac{1}{2}v^2\nabla(\rho\boldsymbol{v}) - \rho\boldsymbol{v} \cdot \boldsymbol{\nabla}(\frac{1}{2}v^2 + w) + \rho T\boldsymbol{v} \cdot \boldsymbol{\nabla} s \tag{2.8}$$

Moving now to the second term of the energy

$$\partial_t(\rho\epsilon) = w\partial_t\rho + \rho T\partial_t s = -w\nabla(\rho\boldsymbol{v}) - \rho T\boldsymbol{v} \cdot \boldsymbol{\nabla} s \tag{2.9}$$

where the first law of thermodynamics $d\epsilon = Tds - pdV = Tds + (\frac{p}{\rho^2})d\rho$ has been used. By adding the two terms up and integrating over the relevant volume one immediately sees that

$$\begin{aligned} \partial_t \int dV(\frac{1}{2}\rho v^2 + \rho\epsilon) &= -\int dV\nabla(\rho\boldsymbol{v}(\frac{1}{2}v^2 + w)) \\ \Rightarrow \partial_t \int dV(\frac{1}{2}\rho v^2 + \rho\epsilon) &= -\oint \rho\boldsymbol{v}(\frac{1}{2}v^2 + w) \cdot d\boldsymbol{S} \end{aligned} \tag{2.10}$$

It therefore becomes obvious that the quantity $\rho \boldsymbol{v}(\frac{1}{2}v^2 + w)$ is the energy flux density vector, i.e. the energy that flows through a surface that bounds a volume in which the energy changes in time.

One can repeat the same process with respect to the momentum contained in a unit volume $\rho \boldsymbol{v}$

$$\partial_t(\rho v_i) = -\frac{\partial \boldsymbol{p}}{\partial x_i} - \frac{\partial(\rho v_i v_j)}{\partial x_j} = -\frac{\partial \Pi_{ij}}{\partial x_j} \tag{2.11}$$

with the definition of the symmetric tensor $\Pi_{ij} = p\delta_{ij} + \rho v_i v_j$, where both the continuity (2.1)and Euler's (2.4) equations have been used. In order to make the physical content of this tensor clear, one can integrate over a certain volume

$$\partial_t \int dV \rho v_i = -\oint \Pi_{ij} dS_j \tag{2.12}$$

where $d\boldsymbol{S}$ is the vector perpendicular to the surface surrounding the integration volume. It is now obvious that Π_{ij} represents the ith component of momentum flowing through an infinitesimal surface element oriented along the jth direction (encoded in the normal vector). In the next section it will be seen how this is related to the stress-energy tensor, which is central in interpreting the Holographic results.

Viscous fluids

Departing from the perfect fluid, towards a more realistic system, viscous fluids will now be examined, by allowing energy dissipation. Dissipation is tightly related to thermodynamic irreversibility. Formally this can be treated through the study of Liouville equation for an $N-$particle system [29]

$$\partial_t f_N = \{H, f_N\} \tag{2.13}$$

where f_N is the $N-$particle probability function. For statistical systems $N \to \infty$, hence in order to make the system manageable one would like to reduce the previous equation down to one for the single-particle probability function, by integrating out higher-particle contributions

$$f_1 = N \int \prod_{i=2}^{N} f_i \tag{2.14}$$

In this way the BBGKY [1] hierarchy of equations emerges

$$\partial_t f_i = \{H_i, f_i\} + \sum_{j=1}^{i} \int \frac{\partial U}{\partial x_j} \cdot \frac{\partial f_{i+1}}{\partial p_j} \tag{2.15}$$

[1]The acronym stands for Bogoliubov, Born, Green, Kirkwood and Yuan

where H_i is the effective Hamiltonian

$$H_n = \sum_{j=1}^{n} \left(\frac{\boldsymbol{p}_i^2}{2m} + V(\boldsymbol{r}_i) \right) + \sum_{i<j<n} U(\boldsymbol{r}_i - \boldsymbol{r}_j) \tag{2.16}$$

for an overall potential V and inter-particle interaction potential U. BBGKY is particularly convenient as an approximation scheme, provided that reliable assumptions can be made about the magnitude of the $i-$th-particle function.

In a more intuitive way one can attribute irreversibility and therefore dissipation, to internal friction (encoded in the viscosity of the fluid) and thermal conduction. How does one incorporate this into the fluid dynamics description, without changing the degrees of freedom (d.o.f.), i.e. the velocity, density, pressure etc. fields? Another element that one cannot change is the continuity equation, since it is just a manifestation of the conservation of mass which should not be altered by the existence of dissipation. Hence Euler's equation (2.4) must be modified in such a way that it does not represent the reversible mechanical interaction of constituent particles. Equipped with the momentum flux tensor that was previously defined, one can write (2.4) as

$$\partial_t(\rho v_i) = -\frac{\partial \Pi_{ij}}{\partial x_j} \tag{2.17}$$

and modify Π_{ij} so that transfer of energy from high to low velocity regions of the fluid, is achieved. This can be accomplished by writing

$$\Pi_{ij} = p\delta_{ij} + \rho v_i v_j - \tilde{\sigma}_{ij} \tag{2.18}$$

where $\tilde{\sigma}_{ij}$ is the viscous stress tensor which along with $p\delta_{ij}$ form the stress-energy tensor $\sigma_{ij} = -p\delta_{ij} + \tilde{\sigma}_{ij}$. The particular form of the viscous stress tensor is

$$\tilde{\sigma}_{ij} = \eta \left(\frac{\partial u_i}{\partial x_j} + \frac{\partial u_j}{\partial x_i} - \frac{2}{3}\delta_{ij} \frac{\partial u_k}{\partial x_k} \right) + \zeta \delta_{ij} \frac{\partial v_k}{\partial x_k} \tag{2.19}$$

where η, ζ are constants (know as first order transport coefficients, which however still depend on temperature and pressure), namely the shear and bulk viscosity. The form of the viscous stress tensor requires some explanation. As mentioned before one would like $\tilde{\sigma}_{ij}$ to encode transfer of energy from high velocity areas to low velocity ones. It should therefore depend on spatial derivatives of velocities. Generically $\tilde{\sigma}_{ij}$ can be written as a gradient expansion of velocities and to first order (which is sufficient for small gradients) it only depends linearly on velocity derivatives. However rigid rotation of a fluid cannot result in dissipation. It therefore follows that this linear dependence must not contain the antisymmetric combinations (which correspond to

Fluid	$\eta(10^{-3}kgm^{-1}s^{-1})$
Water	0.891
Ethanol	1.06
Mercury	1.55
Sulphuric acid	27

Table 2.1: Shear viscosity values for various fluids at $T = 298K$ [4]

rotations), so that it vanishes when in uniform rotation. Under these conditions (2.19) is the most general rank-2 tensor that one can write. Having determined the viscous stress tensor one has fully determined, to first order in the gradient expansion, the equations of motion for a viscous fluid.

If one assumes, furthermore, that shear and bulk viscosities remain constant throughout the fluid, Euler's equation (2.17) becomes

$$\rho\left(\partial_t \boldsymbol{v} + (\boldsymbol{v}\cdot\boldsymbol{\nabla})\boldsymbol{v}\right) = -\boldsymbol{\nabla}p + \eta\triangle\boldsymbol{v} + (\zeta + \frac{1}{3}\eta)\boldsymbol{\nabla}\boldsymbol{\nabla}\cdot\boldsymbol{v} \tag{2.20}$$

which is the Navier-Stokes equation. Expecting the results from Holography, it is worth writing down this equation for the case of incompressible fluids, i.e. $\boldsymbol{\nabla}\cdot\boldsymbol{v} = 0$

$$\partial_t \boldsymbol{v} + (\boldsymbol{v}\cdot\boldsymbol{\nabla})\boldsymbol{v} = -\frac{1}{\rho}\boldsymbol{\nabla}p + \frac{\eta}{\rho}\triangle\boldsymbol{v} \tag{2.21}$$

In terms of the stress-energy tensor this means that

$$\sigma_{ij} = -p\delta_{ij} + \eta\left(\frac{\partial v_i}{\partial x_j} + \frac{\partial v_j}{\partial x_i}\right) \tag{2.22}$$

Let this section end by presenting a table of typical values for the shear viscosity for a selection of fluids, as seen in table 2.1. This is particularly interesting since Holography makes a prediction for a related quantity (namely $\frac{\eta}{s}$), and it would be helpful to develop some intuition.

Sound

A highly interesting property of these systems (i.e. compressible fluids) is that they can support sound-wave propagation. Such waves correspond to fluctuations of pressure / density. In order to study these fluctuations the pressure and density fields are written as

$$\begin{aligned} p &= p_0 + \delta p \\ \rho &= \rho_0 + \delta\rho \end{aligned} \tag{2.23}$$

where p_0, ρ_0 are the unperturbed / equilibrium values of pressure and density. The continuity and Euler's equations, therefore become

$$\begin{aligned} \partial_t \delta\rho + \rho_0 \nabla \boldsymbol{v} &= 0 \\ \partial_t \boldsymbol{v} + \left(\frac{1}{\rho_0}\right) \boldsymbol{\nabla} \delta p &= 0 \end{aligned} \tag{2.24}$$

In the previous set of equations the term $(\boldsymbol{v} \cdot \boldsymbol{\nabla})\boldsymbol{v}$ from (2.4) has been dismissed because of the small-velocity approximation and only fist-order terms have been consistently kept. An extra condition that needs to be satisfied in order for this approximation to be valid is that the velocity of the constituents particles must be much smaller that the speed of sound (which will henceforth be denoted by c),i.e. $v \ll c$, which is equivalent to demanding that the density perturbations are much smaller than the unperturbed value, i.e. $\delta\rho \ll \rho_0$.

Equations (2.24) can be simplified if one can reliably assume that the process (of the travelling wave inside the fluid) is adiabatic, as is the case for ideal fluids, because

$$\delta p = \left(\frac{\partial p}{\partial \rho_0}\right) \delta\rho$$

which makes the first of (2.24)

$$\partial_t \delta p + \rho_0 \left(\frac{p}{\rho_0}\right)_s \nabla \boldsymbol{v} = 0 \tag{2.25}$$

Although the second of equations (2.24) along with (2.25) fully describe the (adiabatic) propagation of waves, they do not look like the regular wave equation. This can be rectified by introducing the velocity potential $\phi : \boldsymbol{v} = \boldsymbol{\nabla}\phi$ so that $\delta p = -\rho_0 \partial_t \phi$. Hence

$$\partial_t^2 \phi - c^2 \triangle \phi = 0 \tag{2.26}$$

with $c^2 = \left(\frac{\partial p}{\partial \rho}\right)_s$ the speed of sound. This is the familiar form of the wave equation (admitting the expected solutions). The individual equations for $\boldsymbol{v}, p, \rho$ can be then derived from (2.26).

What happens though if one takes into account phenomena of dissipation, due to viscosity or thermal conductivity? For this purpose it is necessary to compute the rate of loss of energy $\dot{E} = -\left(\frac{\partial E}{\partial S}\right) \dot{S}$, where S is the entropy. At this point one can lift the results from thermal conduction in fluids, from which one knows that

$$\dot{S} = \int dV \frac{\kappa}{T^2} (\boldsymbol{\nabla} T)^2 + \int dV \frac{\eta}{2T} \left(\frac{\partial v_i}{\partial x_j} + \frac{\partial v_j}{\partial x_i} - \frac{2}{3}\delta_{ij} \frac{\partial v_i}{\partial x_i}\right)^2 + \int dV \frac{\zeta}{T} (\nabla \boldsymbol{v})^2 \tag{2.27}$$

from which one gets

$$\dot{E} = -\frac{\kappa}{T}\int dV(\boldsymbol{\nabla} T)^2 - \frac{1}{2}\eta\int dV\left(\frac{\partial v_i}{\partial x_j} + \frac{\partial v_j}{\partial x_i} - \frac{2}{3}\delta_{ij}\frac{\partial v_i}{\partial x_i}\right) - \zeta\int dV(\nabla \boldsymbol{v})^2 \quad (2.28)$$

where κ is the thermal conductivity. For simplicity and without loss of generality one can choose a particular configuration, namely a wave travelling along the x axis of the form $v_x = v_0\cos(kx-\omega t), v_y = v_z = 0$. Taking the time average one has

$$\langle\dot{E}\rangle = -\frac{1}{2}k^2 v_0^2 V_0\left((\frac{4}{3}\eta+\zeta) + \kappa(\frac{1}{c_V} - \frac{1}{c_p})\right) \quad (2.29)$$

where V_0 is the volume of the fluid and c_V, c_p are the heat capacities under constant volume and pressure respectively. Furthermore the total energy of the sound wave is $\langle E_t\rangle = \frac{1}{2}\rho v_0^2 V_0$. There are enough ingredients now to compute the damping coefficient $v_0 \propto \exp[-\gamma x]$

$$\gamma = \frac{\langle\dot{E}\rangle}{2c\langle E_t\rangle} = \frac{\omega^2}{2\rho c^3}\left\{(\frac{4}{3}\eta+\zeta) + \kappa\left(\frac{1}{c_V} - \frac{1}{c_p}\right)\right\} := \alpha\omega^2 \quad (2.30)$$

Finally in the presence of damping the wave-vector will become complex and in particular

$$k = \frac{\omega}{c} + \imath\alpha\omega^2 \quad (2.31)$$

Relativistic Hydrodynamics

So far the fluid dynamics treatment presented has been non-relativistic. However most results coming from Holography are of relativistic nature, since they refer to the hydrodynamic limit of Quantum Field Theories (QFTs). It is worth noting though that this is not exclusively the case, as a lot of studies have been focused on various departures from relativistic dynamics. In this section the most noteworthy elements of relativistic hydrodynamics will be reviewed [30, 31].

The first thing that needs to be reconsidered is the degrees of freedom, with which the fluid dynamics will be described. This is quite obvious since the 3-velocity, scalar density and 3-vector pressure, are not well-defined objects in a four-dimensional space-time. The fields appropriate for relativistic hydrodynamics are the 4-velocity u^μ and the energy-momentum tensor $T_{\mu\nu}$. Another detail to be taken under consideration is that the mass density ρ, used so far, is not a good degree of freedom since it cannot account for the kinetic energy, of the system, that can now become comparable to the mass. In its place one should use the total energy, which will be denote by $\epsilon(x^\mu)$. As expected $\lim_{\frac{v}{c}\to 0}\epsilon = \rho$. It should be noted that although the 4-velocity has apparently

four degrees of freedom corresponding to the four components, this is not the case since there is also a constraint, namely $u^2 = -1$ [2]

In order to determine the dynamics, one needs first to determine the energy-momentum tensor form. Starting from the case of ideal fluids[3], one notices that the energy-momentum tensor has to be built out of ϵ, p, u^μ and the metric tensor $g^{\mu\nu}$. $T_{\mu\nu}$ must also be a symmetric rank - 2 tensor (i.e. have a well-defined Lorentz transformation). The most general such tensor can be written as

$$T^{\mu\nu}_{(0)} = \epsilon\left(\alpha g^{\mu\nu} + \beta u^\mu u^\nu\right) + p\left(\gamma g^{\mu\nu} + \delta u^\mu u^\nu\right) \tag{2.32}$$

In the fluid's rest frame $T^{00}_{(0)}$ should reduce to the total energy ϵ. Additionally in the rest frame $T^{0i}_{(0)} = 0, \forall i \in \{1,2,3\}$ and $T^{ij}_{(0)} = p\delta^{ij}, i,j \in \{1,2,3\}$. Applying these constraints on the general form of the energy-momentum tensor one gets the following system of equations

$$\begin{aligned}(\alpha+\beta)\epsilon + (\gamma+\delta)p &= \epsilon \\ -\alpha\epsilon - \gamma p &= p\end{aligned}$$

which result in $\alpha = 0$, $\beta = 1$, $\gamma = -1$, $\delta = 1$, or

$$T^{\mu\nu}_{(0)} = \epsilon u^\mu u^\nu - p(g^{\mu\nu} - u^\mu u^\nu) \tag{2.33}$$

The form of the energy-momentum tensor suggests the definition of the projection tensor $\Delta^{\mu\nu} = g^{\mu\nu} - u^\mu u^\nu$ which projects on the space orthogonal to the fluid velocity u^μ. It is obvious that $\Delta^{\mu\nu}u_\mu = \Delta^{\mu\nu}u_\nu = 0$ and $\Delta^\rho_\nu = \Delta^{\mu\rho}$. Using the projection tensor the energy-momentum tensors can be written as

$$T^{\mu\nu}_{(0)} = \epsilon u^\mu u^\nu - p\Delta^{\mu\nu} \tag{2.34}$$

In the absence of external sources, conservation of the energy-momentum tensor reads

$$\partial_\mu T^{\mu\nu}_{(0)} = 0 \tag{2.35}$$

which encodes the equations of motion for the fluid dynamics. One can use the projection tensor to split these equations into directions parallel (i.e. $u_\nu\partial_\mu T^{\mu\nu}_{(0)}$) and perpendicular (i.e. $\Delta^\sigma_\nu\partial_\mu T^{\mu\nu}_{(0)}$) to the fluid velocity. One therefore has

$$u_\nu\partial_\mu T^{\mu\nu}_{(0)} = u^\mu\partial_\mu\epsilon + \epsilon(\partial_\mu u^\mu) + \epsilon u_\nu u^\mu\partial_\mu u^\nu - p u_\nu\partial_\mu\Delta^{\mu\nu} = (\epsilon+p)\partial_\mu u^\mu + u^\mu\partial_\mu\epsilon = 0 \tag{2.36}$$

[2]There is a sign ambiguity in this expression, which depends on the metric signature used.

[3]When ideal fluids are considered, this will be denoted by a 0 index

and

$$\Delta^\sigma_\nu \partial_\mu T^{\mu\nu}_{(0)} = \epsilon u^\mu \Delta^\sigma_\nu \partial_\mu u^\nu - \Delta^{\mu\sigma}(\partial_\mu p) + p u^\mu \Delta^\sigma_\nu \partial_\mu u^\nu = (\epsilon + p) u^\mu \partial_\mu u^\sigma - \Delta^{\mu\sigma}\partial_\mu p = 0 \tag{2.37}$$

Introducing, for conciseness, the operators $D := u^\mu \partial_\mu$ and $\nabla^\sigma := \Delta^{\mu\sigma}\partial_\mu$, one can rewrite the equations of motion in a compact form

$$D\epsilon + (\epsilon + p)\partial_\mu u^\mu = 0 \tag{2.38}$$

$$(\epsilon + p) D u^\sigma - \nabla^\sigma p = 0 \tag{2.39}$$

One can now make a connection to the non-relativistic case by taking the small velocity limit $\frac{|\boldsymbol{v}|}{c} \to 0$

$$D = u^\mu \partial_\mu \to \partial_t + \boldsymbol{v} \cdot \boldsymbol{\nabla} + \mathcal{O}(v^2) \tag{2.40}$$

$$\nabla^i = \Delta^{i\mu}\partial_\mu \to \partial^i + \mathcal{O}(v) \tag{2.41}$$

In other words D and ∇^i reduce to the time and space derivatives, respectively. If one further demands that the energy is primarily that corresponding to the mass density, i.e. $\epsilon \simeq \rho$ and that $p \ll \epsilon$ (in the appropriate units), one retrieves the non-relativistic continuity and Euler's equations.

So far only ideal relativistic fluids have been considered. Introducing dissipation effects, as is the case when one does not neglect viscosity, the energy-momentum tensor has to be modified, in the same spirit as in the non-relativistic case

$$T^{\mu\nu} = T^{\mu\nu}_{(0)} + \Pi^{\mu\nu} \tag{2.42}$$

where $T^{\mu\nu}_{(0)}$ is the previously defined energy-momentum tensor for ideal fluids, while $\Pi^{\mu\nu}$ is the viscous stress tensor. The equations of motion get modified to

$$u_\nu \partial_\mu T^{\mu\nu} = D\epsilon + (\epsilon + p)\partial_\nu u^\mu + u_\nu \partial_\mu \Pi^{\mu\nu} = 0 \tag{2.43}$$

$$\Delta^\sigma_\nu \partial_\mu T^{\mu\nu} = (\epsilon + p) D u^\sigma - \nabla^\sigma p + \Delta^\sigma_\nu \partial_\mu \Pi^{\mu\nu} = 0 \tag{2.44}$$

Note now that $u_\nu \partial_\mu \Pi^{\mu\nu} = \partial_\mu (u_\nu \Pi^{\mu\nu}) - \Pi^{\mu\nu}\partial_{(\mu} u_{\nu)}$ (where parentheses around indices imply symmetrization) and $\partial_\mu = u_\mu D + \nabla_\mu$. Putting all this together one gets the final version of the equations of motion

$$D\epsilon + (\epsilon + p)\partial_\mu u^\mu - \Pi^{\mu\nu}\nabla_{(\mu} u_{\nu)} = 0 \tag{2.45}$$

$$(\epsilon + p) D u^\sigma - \nabla^\sigma p + \Delta^\sigma_\nu \partial_\mu \Pi^{\mu\nu} = 0 \tag{2.46}$$

It is necessary at this point to emphasize that the viscous stress tensor still needs to be determined. One way of achieving that is to assume local thermodynamic equilibrium in which case the local version of the Second Law of Thermodynamics is $\partial_\mu s^\mu \geq 0$, where s^μ is the entropy 4-current, which in local equilibrium is $s^\mu = su^\mu$. Using the basic thermodynamic relations (in the absence of conserved charges)

$$\epsilon + p = Ts$$
$$Tds = d\epsilon$$

the divergence of the entropy current becomes

$$\partial_\mu s^\mu = Ds + s\partial_\mu u^\mu = \frac{1}{T} D\epsilon + \frac{\epsilon + p}{T} \partial_\mu u^\mu = \frac{1}{T} \Pi^{\mu\nu} \nabla_{(\mu} u_{\nu)} \geq 0 \tag{2.47}$$

Conventionally one writes $\Pi^{\mu\nu} = \pi^{\mu\nu} + \Delta^{\mu\nu}\Pi$, which is a splitting into a traceless part and the remainder. It is also convenient to define the traceless part of $\nabla_{(\mu} u_{\nu)}$

$$\nabla_{\langle\mu} u_{\nu\rangle} := 2\nabla_{(\mu} u_{\nu)} - \frac{2}{3} \Delta_{\mu\nu} \nabla_\sigma u^\sigma \tag{2.48}$$

The entropy current divergence is hence rewritten as

$$\partial_\mu s^\mu = \frac{1}{2T} \pi^{\mu\nu} \nabla_{\langle\mu} u_{\nu\rangle} + \frac{1}{T} \Pi \nabla_\sigma u^\sigma \geq 0 \tag{2.49}$$

This is satisfied if $\pi^{\mu\nu} = \eta \nabla^{\langle\mu} u^{\nu\rangle}$ and $\Pi = \zeta \nabla_\sigma u^\sigma$, with $\eta \geq 0$ and $\zeta \geq 0$. In the non-relativistic limit η and ζ reduce to the shear and bulk viscosity, respectively.

There is an interesting caveat in the presentation so far. That is, the fluids considered have been uncharged, or more precisely there have been no conserved charges. This is important because the existence of conserved charges implies the existence of a charge current J^μ, which can be used to define the fluid velocity. This allows one to consider two different frames choices. In one of them (Landau) one defines the local rest frame as the frame where energy density is at rest, while in the other (Eckart) the local rest frame is identified with the frame in which the charge density is at rest. This choice is a redundancy of the description and physical content should not depend on it. The result of this freedom of choice is that what is interpreted as charge diffusion in one frame is thermal conduction in the other.

Having cleared this intricacy, the relativistic hydrodynamics of charged fluids will now be presented [32]. In addition to the conservation of energy-momentum tensor $\partial_\mu T^{\mu\nu} = 0$, one now has the conservation of current density $\partial_\mu J^\mu = 0$. Moreover the constitutive equations are

$$T^{\mu\nu} = (\epsilon + p) u^\mu u^\nu + p g^{\mu\nu} + \Pi^{\mu\nu} \tag{2.50}$$
$$J^\mu = \rho u^\mu + \nu^\mu \tag{2.51}$$

where ϵ is the local energy density, p the local pressure density, $\Pi^{\mu\nu}$ the dissipative part of the energy-momentum tensor and ν^μ the dissipative part of the charge current. The choice one can make at this point is $u_\mu \Pi^{\mu\nu} = u_\mu \nu^\mu = 0$. As before one can derive the form of the dissipative parts, from the Second Law. The thermodynamic relations for a charged fluid are

$$\epsilon + p = Ts + \mu\rho \tag{2.52}$$

$$d\epsilon = Tds + \mu d\rho \tag{2.53}$$

where μ is the chemical potential. One can now compute the divergence of the entropy current, using in addition the fact that $u_\nu \partial_\mu T^{\mu\nu} = 0$

$$\begin{aligned} \partial_\mu (s^\mu) = \frac{\mu}{T}\partial_\mu \nu^\mu - \frac{\Pi^{\mu\nu}}{T}\partial_\mu u_\nu \Rightarrow \\ \partial_\mu \left(s u^\mu - \frac{\mu}{T}\nu^\mu \right) = -\nu^\mu \partial_\mu \frac{\mu}{T} - \frac{\Pi^{\mu\nu}}{T}\partial_\mu \nu^\mu \end{aligned} \tag{2.54}$$

Defining the left-hand side of (2.54) as the entropy current, one has to demand that the right-hand side is positive. Hence it follows that

$$\nu^\mu = -\kappa \left(\partial^\mu \frac{\mu}{T} + u^\mu u^\nu \partial_\nu \frac{\mu}{T} \right) \tag{2.55}$$

$$\Pi^{\mu\nu} = -\eta \left(\partial^\mu u^\nu + \partial^\nu u^\mu + u^\mu u^\sigma \partial_\sigma u^\nu + u^\nu u^\sigma \partial_\sigma u^\mu \right) - \left(\zeta - \frac{2}{3}\eta \right) (g^{\mu\nu} + u^\mu u^\nu)\partial_\sigma u^\sigma \tag{2.56}$$

where η, ζ are the shear and bulk viscosity respectively and κ is the thermal conductivity.

2.2 Quantum Hydrodynamics

One of the most celebrated achievements of Holography is the ability to describe strongly interacting systems, away but very close to equilibrium. For weakly interacting systems this is the purview of Linear Response. In this section Linear Response of a generic quantum system will be presented, so as to lay the foundation and set the context for the Holographic results. This will also serve as an introduction to the presentation of purely quantum systems (with no classical analogue) such as Fermi liquids, which are of high interest from a Holographic point of view.

Linear Response treats a system under an external stimulus, like an electromagnetic field, a temperature or pressure fluctuation. In the framework of Quantum Mechanics the dynamics of a system are encoded in its Hamiltonian, $\hat{H}$. Similarly an

observable is mapped into an operator, say $\hat{O}$. The goal is to study the system under some perturbation. Such a perturbation is described by the addition of a term in the Hamiltonian

$$\hat{H} \to \hat{H} + \hat{H}_{pert}$$

where

$$\hat{H}_{pert} := \phi\hat{O}$$

The coefficient field corresponding to an observable $\hat{O}$ is referred to as the source of said observable and plays the role of the external stimulus. The introduction of $\hat{H}_{pert}$ deforms the original theory, modifying the equations of motion, in which one now finds the field ϕ in addition to the original degrees of freedom.

Generically this problem is difficult to address, hence the first step is to assume that the response of the system under the external perturbation, remains linear. In other words the change in the expectation value of an operator (corresponding to an observable) is a linear function of the external source[4]

$$\delta\langle O(t)\rangle = \int dt'\chi(t,t')\phi(t') \tag{2.57}$$

This is the case for sources that are small in comparison with the relative scales. The function $\chi(t,t')$ is called the response function. It is obvious from the above definitions that the response function is nothing more than the Green's function, of the system and the terms will be henceforth used interchangeably. If the system is endowed with space-time symmetries, like time reversal (and similarly translational invariance) one can simplify things significantly by writing the linear response relation (2.57) in Fourier space

$$\delta\langle O(\omega)\rangle = \int dt'dte^{\imath\omega t}\chi(t-t')\phi(t') = \tilde{\chi}(\omega)\tilde{\phi}(\omega) \tag{2.58}$$

where $\tilde{\chi}(\omega)$ and $\tilde{\phi}(\omega)$ are the Fourier transformations of the response function and the source respectively. Moreover the product is to be understood as the convolution of the two functions. The simplification in working in Fourier space, lies in the fact that what is a bi-local function ($\chi(t-t')$) in coordinate space is a local function in frequency space ($\tilde{\chi}(\omega)$).

Writing it in frequency space, allows one to easily uncover further properties of the response function. Note first that since $\hat{O}$ correspond to an observable, it has to be Hermitian as an operator and hence its expectation value has to be real. Assuming

[4]Here the Heisenberg picture is adopted, in which time dependence is included in the operators.

that the external source is also real one concludes that the response function is real in coordinate space ($\chi(t,t') \in \mathbb{R}$). In Fourier space though $\chi(\omega) \in \mathbb{C}$, with its real ($\Re\chi(\omega)$) and imaginary ($\Im\chi(\omega)$) parts having distinct interpretations. The imaginary part can be written

$$\Im\chi(\omega) \equiv -\frac{\imath}{2}\left(\chi(\omega) - \bar{\chi}(\omega)\right) = -\frac{\imath}{2}\int dt\chi(t)\left(e^{\imath\omega t} - e^{-\imath\omega t}\right) \tag{2.59}$$

$$= -\frac{\imath}{2}\int dt e^{\imath\omega t}\left(\chi(t) - \chi(-t)\right) \tag{2.60}$$

Similarly for the real part

$$\Re\chi(\omega) \equiv \frac{1}{2}\left(\chi(\omega) + \bar{\chi}(\omega)\right) = \frac{1}{2}\int dt e^{\imath\omega t}\left(\chi(t) + \chi(-t)\right) \tag{2.61}$$

It becomes clear from the above expressions that the imaginary part of the response function is not symmetric under time reversal, while the real part is. Given that on a microscopic level, dynamics are assumed to be time reversible, the imaginary part must originate from dissipative effects. $\Im\chi$ is therefore called the dissipative part of the response function and is also referred to as the spectral function.

Another interesting aspect of the response function is its detailed relation to the Green's function. In real-time Quantum dynamics (as opposed to Euclidean time) there are more than one Green's functions (i.e. retarded (G_R), advanced (G_A), Feynman (G_F)). By demanding causality, i.e. no response prior to the appearance of the external source, assuming that at $t = 0$ the source is turned on, one has $\chi(t < 0) = 0$. This relates the response function to the retarded Green's function. Borrowing from the analytic properties of Green's functions one can translate this requirement into a requirement about the analytic structure of $\chi(\omega)$ for complex frequencies ($\omega \in \mathbb{C}$). For $t < 0$ the Fourier integral

$$\chi(t) = \int \frac{d\omega}{2\pi} e^{-\imath\omega t}\chi(\omega)$$

has to follow a contour that closes in the upper complex plane (Fig.2.1). In order for χ to vanish, it is therefore required that it has no poles for $\Im\omega > 0$. The requirement that $\chi(\omega)$ is analytic in the upper ω-plane induces a relation between its real and imaginary part, known as the Krammers-Kronig relation. In particular by making use of the Principal Value one can write the Krammers-Kronig relations

$$\Re\chi(\omega) = \mathcal{P}\int \frac{d\omega'}{\pi}\frac{\Im\chi(\omega')}{\omega' - \omega} \tag{2.62}$$

$$\Im\chi(\omega) = -\mathcal{P}\int \frac{d\omega'}{\pi}\frac{\Re\chi(\omega')}{\omega' - \omega} \tag{2.63}$$

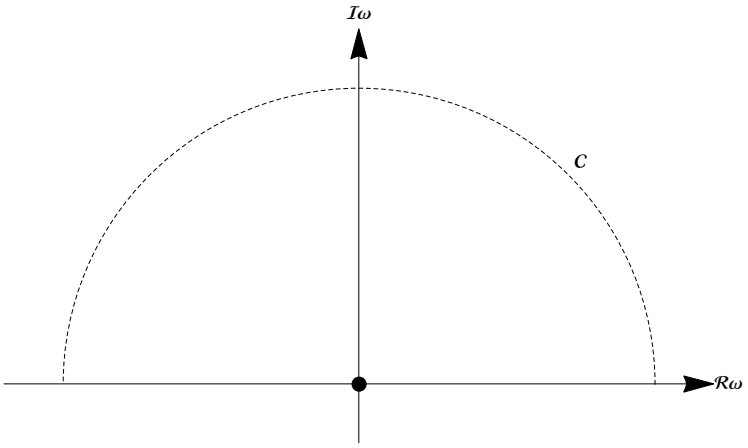

Figure 2.1: Integration contour in the complex ω plane.

At this point two comments are in order. Firstly these relations are derived purely from causality, without any extra assumption and details about the dynamics. However the cost for such a broad result is that one needs the full analytic structure of the imaginary part of the response function in order to reconstruct the real part and vice versa. A rephrasing of this result is that one can write the full response function, knowing only its imaginary or dissipative part. To see this one needs to write the principal value as a deformation of the integration contour. In particular if one defines $g(\omega) := (1/\imath\pi)\int d\omega' \chi(\omega)/(\omega' - \omega)$, then

$$\mathcal{P}\int d\omega' \frac{\chi(\omega)}{\omega' - \omega} := \frac{\imath\pi}{2}\left(g(\omega + \imath\epsilon) + g(\omega - \imath\epsilon)\right) \tag{2.64}$$

By Cauchy's theorem one also has that $\chi(\omega) = (1/2)\left(g(\omega + \imath\epsilon) - g(\omega - \imath\epsilon)\right)$ and hence one writes

$$\int \frac{d\omega'}{\imath\pi}\frac{\Im\chi(\omega')}{\omega' - \omega - \imath\epsilon} = \Im\chi(\omega) + \mathcal{P}\int \frac{d\omega'}{\imath\pi}\frac{\Im\chi(\omega')}{\omega' - \omega - \imath\epsilon} = \Im\chi(\omega) - \imath\Re\chi(\omega) \tag{2.65}$$

which then leads to

$$\chi(\omega) = \int \frac{d\omega'}{\pi}\frac{\Im\chi(\omega')}{\omega' - \omega - \imath\epsilon} \tag{2.66}$$

It is then apparent that the imaginary (or dissipative) part of the response function (i.e. the spectral function) contains the full information about the system studied and this is why it will play a very important role in what follows. This fact also highlights the importance of being able to compute the spectral function of strongly interacting systems by Holographic means.

A quantity that can immediately be computed from the response function is susceptibility ($\tilde{\chi}$). For an external source ϕ corresponding to the observable $\hat{O}$, causing a change of the expectation value $\delta\langle O\rangle$ susceptibility is

$$\tilde{\chi} := \left.\frac{\partial\delta\langle O\rangle}{\partial\phi}\right|_{\omega=0} \tag{2.67}$$

which by the definition of the response function means that

$$\tilde{\chi} = \lim_{\omega\to 0}\chi(\omega) \tag{2.68}$$

or in integral form

$$\tilde{\chi} = \int \frac{d\omega'}{\pi}\frac{\Im\chi(\omega')}{\omega' - \imath\epsilon} \tag{2.69}$$

It is appropriate at this point to make an aside to established a connection with what was presented before, with respect to classical hydrodynamics. To achieve this a simple dissipative hydrodynamics model will be examined, in which one adds a diffusive current on top of an ideal fluid, along with and external driving force

$$\boldsymbol{J} = -D\boldsymbol{\nabla}\rho + \boldsymbol{f} \tag{2.70}$$

where D is the diffusion constant and $\boldsymbol{f}$ is the driving force. From the continuity equation (2.1) one has

$$\partial_t\rho - D\nabla^2\rho = -\boldsymbol{\nabla}\cdot\boldsymbol{f} \tag{2.71}$$

Treating $\boldsymbol{f}$ as the external source here, the observables would be the density ρ and the current $\boldsymbol{J}$ and it is the response to these that one wants to study. Using (2.57) one writes

$$\rho(t,x) = \int dt'dx'\chi_{\rho J}(t',x';t'x)f(t',x') \tag{2.72}$$

$$J(t,x) = \int dt'dx'\chi_{JJ}(t',x';t'x)f(t',x') \tag{2.73}$$

where the indices in the response function appear now because there are two correlated responses to the external source. Hence there is a current-density response, i.e. the external source drives the current which in turn perturbs the density, and a current-current response, i.e. the immediate response of the current to the external force. Assuming full space-time translational symmetry and Fourier transforming, as before, the responses become

$$\rho(\omega,k) = \chi_{\rho J}(\omega,k)f(\omega,k) \tag{2.74}$$

$$J(\omega,k) = \chi_{JJ}(\omega,k)f(\omega,k) \tag{2.75}$$

Plugging into (2.71) the Fourier transformations for ρ, J and the linear response relations (2.74,2.75) the density-current response function is

$$\chi_{\rho J} = \frac{-\imath k}{\imath\omega - Dk^2} \tag{2.76}$$

Then from the definition of the current $\boldsymbol{J}$ one also gets the current-current response function

$$\chi_{JJ} = \frac{\imath\omega}{\imath\omega - Dk^2} \tag{2.77}$$

From (2.76,2.77) it is obvious that both response functions have a pole at $\omega = -\imath Dk^2$. This is the well-known diffusion pole that governs the diffusive behaviour of the system. This pole will re-appear in the Holographic context demonstrating the persistence of hydrodynamics even in strongly interacting systems.

One of the last pieces necessary to have a relatively complete picture of hydrodynamics and linear response on the quantum level, is the celebrated Kubo formulae. These are relations, derived in the context of quantum statistical mechanics, which relate the response of a system under perturbation, to the two-point function of the relevant observable. In order to arrive at the Kubo formula, one needs to do first-order perturbation of a quantum system, described by a density matrix ρ.[5] As before the perturbation is encoded in the Hamiltonian, through $H_{pert} := \phi_i O_j$, where the index indicates that there can be more than one sources, for more than one observables. [6] Following standard perturbation theory one defines the time evolution operator

$$U(t, t') = \mathcal{T} \exp\left(-\imath \int_{t'}^{t} dt' H_{pert}\right) \tag{2.78}$$

which satisfies Schrödinger's equation

$$\imath\partial_t U = H_{pert} U \tag{2.79}$$

and governs the time evolution of the wave-functions

$$|\psi(t)\rangle = U(t, t_0)|\psi(t_0)\rangle \tag{2.80}$$

Similarly the density matrix evolves as

$$\rho(t) = U(t, t_0)\rho_0 U^{-1}(t, t_0) \tag{2.81}$$

[5]Not to be confused with the energy density for which this symbol has been used previously.
[6]Here Einstein's index summation convention is adopted.

where ρ_0 is the density matrix at a distant enough time ($t_0 \to -\infty$) that the perturbation has died off. One is in position now to compute the expectation value of an operator, for a non-vanishing external source ϕ

$$\langle O(t)\rangle|_\phi \equiv Tr\rho(t)O(t) = Tr\rho_0 U^{-1}OU \tag{2.82}$$

$$= Tr\rho_0\left(O + \imath\int_{-\infty}^{t} dt'\,[H_{pert}, O] + \ldots\right) = \langle O\rangle|_{\phi=0} + \imath\int_{-\infty}^{t} dt'\langle[H_{pert}, O]\rangle + \ldots \tag{2.83}$$

The change in the expectation value $\delta\langle O\rangle := \langle O\rangle_\phi - \langle O\rangle_{\phi=0}$ can be written, taking into account the explicit form of the perturbation, as

$$\delta\langle O\rangle = \imath\int_{-\infty}^{t} dt'\langle[O(t'), O(t)]\rangle\phi(t') \tag{2.84}$$

or in order to make the integration interval symmetric, one can introduce a step function, resulting in

$$\delta\langle O\rangle = \imath\int_{-\infty}^{+\infty} dt'\theta(t-t')\langle[O(t'), O(t)]\rangle\phi(t') \tag{2.85}$$

A simple comparison of the last equation with (2.57) reveals that the response function is

$$\chi(t-t') = -\imath\theta(t-t')\langle[O(t), O(t')]\rangle \tag{2.86}$$

which is the well-known Kubo formula. From this point it is straightforward to generalize to Quantum Field Theory, which is more relevant to Holography, by allowing the operators as well as the response function to depend in space in addition to time. The Kubo formula becomes then

$$\chi_{ij}(t', \boldsymbol{x}'; t, \boldsymbol{x}) = -\imath\theta(t-t')\langle[O_i(t, \boldsymbol{x}), O_j(t', \boldsymbol{x}')]\rangle \tag{2.87}$$

where the indices account for multiple operators.

The usefulness of Kubo's formula is most easily demonstrated by straightforwardly calculating two quantities that come up almost constantly in Holographic calculations, and which sparked interest in using Holography as a computational tool. The first quantity is conductivity. Assume a system that possesses a global $U(1)$ symmetry. For this symmetry there is a corresponding conserved current J^μ. This current plays the role of the operator in the previous discussion. The external source is the electromagnetic field A_μ and the perturbation Hamiltonian reads

$$H_{pert} = \int d^d x A_\mu J^\mu \tag{2.88}$$

where d is the number of spatial dimensions. By restricting the electromagnetic field to a purely electric one, the (electrical) conductivity is defined as the response function relative to the electric field

$$\langle J_i(\omega, \boldsymbol{k})\rangle = \sigma_{ij}(\omega, \boldsymbol{k}) E_j(\omega, \boldsymbol{k}) \tag{2.89}$$

Applying Kubo's formula for this perturbation gives

$$\delta\langle J_\mu\rangle \equiv \langle J_\mu\rangle - \langle J_\mu\rangle_0 = -\imath \int d^4x' \langle [J_\mu(x'), J_\nu(x)]\rangle_0 A_\mu(x') \tag{2.90}$$

Now by working in a gauge where $A_0 = 0$, the $U(1)$ field in Fourier space is just $E_i(\omega) = \imath\omega A_i(\omega)$ and hence the change in the current's expectation value can be put into the Ohm's law form (2.89) by setting the conductivity tensor to be

$$\sigma_{ij} = \frac{\alpha}{\imath\omega}\delta_{ij} + \frac{\chi_{ij}(\omega, \boldsymbol{k})}{\imath\omega} \tag{2.91}$$

The second term in the above sum, which is the relevant one for this discussion, comes directly from the current-current Green's function

$$\chi_{ij}(\omega, \boldsymbol{k}) = -\imath \int d^4x \theta(t) e^{\imath kx} \langle [J_i(x), J_j(0)]\rangle \tag{2.92}$$

It should be noted here that the first term in (2.91) derives from the background, $\langle J_i\rangle_0 = e^2 A_i \rho$, where ρ, allowing for some abuse of the notation, is the charge density. Hence $\alpha = -e\rho$ in (2.91).

The second, even more celebrated in the Holographic context, quantity that can be computed using Kubo's formula, is the shear viscosity. In this case the operator involved is the energy-momentum tensor $T_{\mu\nu}$ and the response function has a tensor structure because of the different configurations possible. For this example a situation where momentum injected in x_1 direction gets diffused into x_2, is picked. This scenario involves the T_{12} components of the energy-momentum tensor. The relevant components of the response function are therefore

$$\chi_{12,12}(\omega, \boldsymbol{k}) = -\imath \int d^4x \theta(t) e^{\imath kx} \langle [T_{12}(x), T_{12}(0)]\rangle \tag{2.93}$$

Compared to the case of conductivity there is no background contribution, since in the unperturbed state there is no net momentum diffusion. Finally to get the actual viscosity one needs to apply the zero frequency limit

$$\eta = \lim_{\omega\to 0} \frac{1}{\imath\omega} \chi_{12,12}(\omega, 0) \tag{2.94}$$

given that viscosity is related to constant external force (source).

Fermi Liquids

In this final section of the present chapter the theory of Fermi liquids will be reviewed [33–37]. Fermi liquids are quintessentially quantum mechanical in nature, and as it will soon become apparent, possess characteristics that survive into the strongly interacting regime, making them a very interesting test-bed for Holographic calculations. In particular the systematic Holographic reconstruction of one of their most important feature, i.e. the existence of a Fermi surface, is a constant goal of Holographic models. The starting point will be the standard phenomenological approach, followed by a quick microscopical justification. Towards the end of this section, the Renormalization Group analysis of Fermi surfaces, will be presented as the background necessary to justify the discussion of Fermi surfaces in the context of strongly interacting theories and Holography.

The term Fermi Liquid is used to generically describe a multi-particle state of fermions at non-vanishing density. One of the most striking characteristics of Fermi liquids is that, even in the non-zero interaction regime, they retain properties of the free Fermion gas system. Free multi-particle fermion states are organized based on Pauli's exclusion principle, into shells, resulting in the Fermi surface, defined as the last occupied shell. It should be noted that this surface lives in momentum space. Low-energy excitations around this ground states involve quasi-particles, which resemble particles, above and holes below the Fermi surface. Examples of Fermi liquids include ^{4}He and the electron gas of metals.

The free action of a spin-1/2 fermion $\psi_s(k)$, of spin s and momentum k (in d spatial dimensions) is

$$S_{free} = \int d\tau \int \frac{d^d k}{(2\pi)^d} \psi_s^\dagger(k) \left(\partial_\tau + \epsilon(k)\right) \psi_s(k) \tag{2.95}$$

The corresponding Green's function is therefore

$$G_0(\omega_n, k) = \frac{1}{-\imath\omega_n + \epsilon(k)} \tag{2.96}$$

Analytically continuing to real frequencies, reveals that (2.96) has a simple pole at energy $E = \epsilon(k)$ with residue 1. This pole corresponds to quasi-particle excitations, which can have either positive (particle-like) or negative (hole-like) energies. The locus of points in the phase space where the energy flips sign, is exactly the Fermi surface, i.e. it is the surface that divides particle-like from hole-like excitations. [7]

[7] It should be noted here that the appearance of negative energies should not be interpreted as the emergence of an instability. This is just a result of artificially combining particles and holes in the same propagator, through identifying hole-like excitations with the negative-energy counterpart of the particle-like ones.

In studying further the quasi-particle excitations it is important to take into account the complications imposed by the fact that these do not occur in some empty, uniform space, but rather around the Fermi surface. This means that there could be excitations travelling tangentially to the Fermi surface, with $\epsilon(k) = 0$. In order to accommodate for this particularity, it is convenient assign $\boldsymbol{k}_F(\boldsymbol{n})$ to the actual Fermi surface and then define momenta with respect to that as

$$\boldsymbol{k} = \boldsymbol{k}_F(\boldsymbol{n}) + k_\perp \boldsymbol{n} \tag{2.97}$$

where $\boldsymbol{n}$ is the unit vector perpendicular to the Fermi surface, pointing outwards

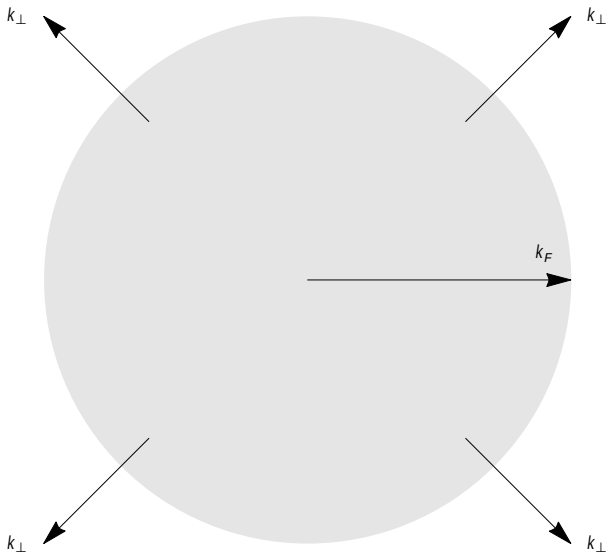

Figure 2.2: Momenta defined relative to the Fermi surfaces.

($\boldsymbol{n} := \frac{\boldsymbol{k}_F}{|\boldsymbol{k}_F|}$) (Fig.2.2). Now any momenta expansion is considered around the Fermi surface, i.e. with respect to $k_\perp$. One can now rescale the original fermion fields as

$$\psi_s(\boldsymbol{k}) \to \frac{1}{V_F}\psi_{s,\boldsymbol{n}}(k_\perp) \tag{2.98}$$

where V_F is the area of the Fermi surface. Another, more intuitive, way of understanding this reformulation is that because motion tangentially to the Fermi surface corresponds to $\epsilon(k) = 0$, one needs to expand around every point of the surface. Taking this into account the effective action becomes

$$S_{FL} = \int d\Omega_n \int dk_\perp \psi^\dagger_{s,\boldsymbol{n}}(k_\perp)\left(\partial_\tau - \imath v_F(\boldsymbol{n}\partial_{k_\perp})\right)\psi_{s,\boldsymbol{n}}(k_\perp) \tag{2.99}$$

where v_F is the Fermi velocity which corresponds to the energy gradient on the Fermi surface, i.e. $v_F(\boldsymbol{n}) = |\nabla_k \epsilon_{k_F}|$. Intuitively this effective action describes the Fermi

surface as an infinite collection of (one for each point of the surface) fermions, moving in a transverse to the surface direction. The effective action (2.99), does not take into account excitations moving along the surface. To address this issue one can work with fermions living in the full d-dimensional space, instead of just on the surface. Then one splits the coordinates into $k_\perp$ which is perpendicular to the Fermi surface and $\boldsymbol{k}_{//}$ normal to the $k_\perp$ direction. With that in mind the effective action can be recast in the form

$$S = \int d\tau \int dk_\perp \int d\boldsymbol{k}_{//} \psi_s^\dagger \left(\partial_\tau - v_F \partial_{k_\perp} - \frac{\kappa}{2} \nabla_{//}^2 \right) \psi_s \tag{2.100}$$

where κ encodes the curvature of the Fermi surface. The benefit of using this action now becomes apparent, as one can immediately extract the dispersion relation

$$v_F k_\perp + \kappa \frac{k_{//}^2}{2} = 0 \tag{2.101}$$

Having given a very brief, definitional overview of Fermi liquids, one can now approach them from a more phenomenological (statistical) point of view. Temporarily ignoring interactions, the energy of a system consisting of N free fermions (i.e. a free Fermi gas) is

$$E = \sum_{\boldsymbol{k}} \frac{k^2}{2m} n(\boldsymbol{k}) \tag{2.102}$$

where $n(\boldsymbol{k} = 2\theta(k_F - |\boldsymbol{k}|)$ is the occupation number for a state of momentum $\boldsymbol{k}$. If one applies an external stimulus on the system the energy will get shifted implicitly, through the change in the occupation number

$$\delta E = \sum_{\boldsymbol{k}} = \frac{k^2}{2m} \delta n(\boldsymbol{k}) \tag{2.103}$$

To the extent that the external field applied remains small, the occupation number will be a distribution concentrated around the Fermi surface.

The next step is to allow for inter-particle interactions. A critical point in doing so, is that interactions need to be turned on adiabatically, so that one retains a one-to-one correspondence between the free and interacting states. In other words one does not want bound states created as one introduces interactions, which would drastically change the true degrees of freedom. As a results the picture of Fermi surface and particle or hole-like excitations around it, coming from the free system, remains valid. Since interactions are now present, apart from the quasi-particle's energy $\epsilon(k)$ (while $\epsilon_0(k)$ will be the unperturbed energy) there is also the interaction energy, denoted by $f(k, k')$, where k, k' are the momenta of the quasi-particles involved. Applying a

weak external field on the interacting system, the induced change of energy for the system is

$$\delta E = \sum_{\boldsymbol{k}} \epsilon_0(\boldsymbol{k})\delta n(\boldsymbol{k}) + \frac{1}{2V}\sum_{\boldsymbol{k},\boldsymbol{k'}} f(\boldsymbol{k},\boldsymbol{k'})\delta n(\boldsymbol{k})\delta n(\boldsymbol{k'}) \tag{2.104}$$

where V is the volume occupied by the system. From (2.104) one can now compute the "dressed" (i.e. the perturbed) energy of each quasi-particle

$$\epsilon(\boldsymbol{k}) = \frac{\delta E}{\delta n(\boldsymbol{k})} = \epsilon_0(\boldsymbol{k}) + \frac{1}{V}\sum_{\boldsymbol{k'}} f(\boldsymbol{k},\boldsymbol{k'})\delta n(\boldsymbol{k'}) \tag{2.105}$$

while the interaction energy is given by

$$f(\boldsymbol{k},\boldsymbol{k'}) = V\frac{\delta^2 E}{\delta n(\boldsymbol{k})\delta n(\boldsymbol{k'})} \tag{2.106}$$

Here one can make use, again, of the adiabaticity to note that interacting quasi-particles, stemming from fermions, will obey Fermi-Dirac statistics and hence the occupation number is

$$n(\boldsymbol{k}) = \frac{1}{e^{\frac{\epsilon(\boldsymbol{k})}{T}-\mu}+1} \tag{2.107}$$

where μ is the system's chemical potential.

With this description at hand one can calculate various observable / phenomenological properties of Fermi liquids, which will be very useful to compare with Holographic results, testing whether the latter constitute or not true Fermi liquids. One such quantity of particular interest is specific heat. By definition

$$c_V = \frac{1}{V}\left.\frac{\partial E}{\partial T}\right|_V \tag{2.108}$$

The change of temperature affects the energy indirectly through the change of the occupation number, hence

$$c_V = \frac{1}{V}\sum_{\boldsymbol{k}} \frac{\partial E}{\partial n(\boldsymbol{k})}\frac{\partial n(\boldsymbol{k})}{\partial T} \tag{2.109}$$

which by using (2.104) becomes

$$c_V = \frac{1}{V}\sum_{\boldsymbol{k}} \epsilon(\boldsymbol{k})\frac{\partial n(\boldsymbol{k})}{\partial \epsilon(\boldsymbol{k})}\left(\frac{\mu-\epsilon(\boldsymbol{k})}{T} + \frac{\partial(\epsilon(k)-\mu)}{\partial T}\right) \tag{2.110}$$

At this point one needs to notice that at low temperatures ($\beta \to \infty$) the interaction part of (2.104) goes like β^{-2} or T^2 which means that it can be ignored compared to

$\epsilon_0(\boldsymbol{k})$ and therefore one can just use the latter. An immediate result of this approximation is that the sum over momenta can be substituted by a sum over energies. At low temperatures, the sum can then be computed giving

$$c_V = \frac{1}{3} m^* k_F k_B T \tag{2.111}$$

where k_B is the Boltzmann constant and m^* the effective mass. The effective mass comes as the modification of the dispersion relation, by the self energy and can be extracted from

$$\epsilon_0(k) = \mu + (k - k_F)\frac{k_F}{m^*} \tag{2.112}$$

$$m^* = \frac{k_F}{v_F} \tag{2.113}$$

where $v_F = \frac{\partial \epsilon_0(\boldsymbol{k})}{\partial \boldsymbol{k}}$. The linear temperature dependence of the specific heat is one of the most commonly used tests, in Holography, to verify whether the system studied is dominated by fermions.

Another interesting quantity is the speed of sound, also referred to as first sound to contrast it with zero-sound which will be presented momentarily. The thermodynamic speed of sound is defined as

$$c_1^2 = \frac{1}{m}\frac{\partial P}{\partial \rho} = \frac{1}{m\rho\chi} \tag{2.114}$$

where m is the bare fermion mass, $\rho = \frac{N}{V}$ the density and χ the compressibility which is defined as

$$\chi^{-1} = -V\frac{\partial P}{\partial V} = \rho\frac{\partial P}{\partial \rho} \tag{2.115}$$

In order to relate the speed of sound to the, by now familiar, interaction function $f(\boldsymbol{k}, \boldsymbol{k}')$, one needs to first employ the Free Energy to write the compressibility in term of the chemical potential, which is then related to the energy on the Fermi surface. Then using (2.104) one write c_1 in terms of $f(\boldsymbol{k}, \boldsymbol{k}')$ and more specifically in terms of spatial averages of the first two multi-pole components of the interaction function, known as Landau parameters. In particular, one starts from the pressure

$$P = -\frac{\partial F}{\partial V} = \mathrm{f} - \rho\frac{\partial \mathrm{f}}{\partial \rho} \tag{2.116}$$

where F is the Free Energy and $\mathrm{f} = F/V$ the Free Energy per unity volume. Hence

$$\chi^{-1} = \rho^2\frac{\partial^2 \mathrm{f}}{\partial \rho^2} \tag{2.117}$$

By definition of the chemical potential

$$\mu = \frac{\partial F}{\partial N} = \frac{\partial \mathrm{f}}{\partial \rho} \tag{2.118}$$

and therefore $\chi^{-1} = \rho^2 \frac{\partial \mu}{\partial \rho}$. Then noting that $\mu = \epsilon(k_F, n)$ one can use (2.104) to write

$$\frac{\partial \mu}{\partial \rho} = \frac{\partial \epsilon_0(k_F)}{\partial k_F}\frac{\partial k_F}{\partial \rho} + \sum \int \frac{d^3k'}{(2\pi)^3} f(k_F, \boldsymbol{k}')\frac{\partial n(\boldsymbol{k}')}{\partial k_F}\frac{\partial k_F}{\partial \rho} \tag{2.119}$$

The remaining sum in the previous expression is over the spin degrees of freedom. Employing the following properties of Fermi liquids

$$\rho = \frac{k_F^3}{3\pi^2} \tag{2.120}$$

$$\frac{\partial \epsilon_0}{\partial k_F} = \frac{k_F}{m^*} \tag{2.121}$$

$$\frac{\partial n(k')}{\partial k_F} = \delta(k' - k_F) \tag{2.122}$$

(2.119) can be rewritten as

$$\rho\frac{\partial \mu}{\partial \rho} = \rho\frac{k_F}{\partial \rho}\left(\frac{k_F}{m^*} + \frac{k_F^2}{(2\pi)^3}\sum \int d\Omega f\right) = \frac{k_F^2}{3m^*}(1 + F_0) \tag{2.123}$$

Here F_0 is just the spherically symmetric average of the interaction function, or in other words the first term in its multi-pole expansion. By borrowing the expression for the effective mass from [34] in terms of Landau parameters one writes

$$\chi^{-1} = \frac{\rho k_F^2}{m}\frac{1 + F_0}{3 + F_1} \tag{2.124}$$

where F_1 is the next term in the multi-pole expansion of f. Consequently

$$c_1^2 = \frac{k_F^2}{m^2}\frac{1 + F_0}{3 + F_1} \tag{2.125}$$

First, or regular thermodynamic, sound dies off as $T \to 0$. In particular for a sound wave of frequency ν its life-time goes like $\tau \sim (\epsilon - \epsilon_F)^{-2}$ and its energy like $(\epsilon(k) - \epsilon_F) \sim k_B T$ and therefore in order to have sound, temperature has to be $T^2 \gg \nu$. Intuitively in the $T^2 \ll \nu$ limit, inter-particle collisions cease to exists and liquid perturbations cannot propagate. However in this collision-less regime another collective mode emerges out of the Boltzmann equation. In particular, Boltzmann's equation is

$$\partial_t n + \partial_{\boldsymbol{r}} n \partial_{\boldsymbol{k}} \epsilon - \partial_{\boldsymbol{k}} n \partial_{\boldsymbol{r}} \epsilon = I(n) \tag{2.126}$$

where $I(n)$ encodes quasi-particle collisions. Hence one can look for propagating solution to (2.126) in its collision-less regime, where $I(n) = 0$. Since one looks for wave-like solutions, one writes

$$\delta n(\boldsymbol{k}, \boldsymbol{r}, t) = \exp[\imath(\boldsymbol{q} \cdot \boldsymbol{r} - \omega t)]\phi_{\boldsymbol{k}} \tag{2.127}$$

and then the linearised version of Boltzmann's equations becomes

$$(\boldsymbol{q} \cdot \boldsymbol{v}_k - \omega)\phi_{\boldsymbol{k}} + \boldsymbol{q} \cdot \boldsymbol{v}_{\boldsymbol{k}} \delta(\mu - \epsilon(k)) \frac{1}{V} \sum_{\boldsymbol{k}'} f(\boldsymbol{k}, \boldsymbol{k}')\phi_{\boldsymbol{k}'} = 0 \tag{2.128}$$

where $\boldsymbol{v}_k = \boldsymbol{k}/m^*$. Rescaling the solution like

$$\phi_{\boldsymbol{k}} := \delta(\epsilon(k) - \mu) v_F u(\boldsymbol{k}) \tag{2.129}$$

so that $u(\boldsymbol{k})$ measure the displacement of the Fermi surface, one gets

$$(\boldsymbol{q} \cdot \boldsymbol{v}_k - \omega)u(\boldsymbol{k}) + \boldsymbol{q} \cdot \boldsymbol{v}_k \frac{1}{V} \sum_{\boldsymbol{k}'} f(\boldsymbol{k}, \boldsymbol{k}')\delta(\epsilon_{k'} - \mu)u(k') = 0 \tag{2.130}$$

Since the momentum is restricted on the Fermi surface, the remaining dependence is on the angles ($\{\theta, \phi\} =: \Omega$) defining the direction of $\boldsymbol{k}$ and of course spin. Writing all the parameters of (2.128) in terms of the Fermi momentum k_F, one eventually gets

$$(s - \cos\theta)u(\Omega, s) = \cos\theta \sum_{s'} \int \frac{d^3k'}{(2\pi)^3} \delta(\frac{k_F}{m^*}(k - k_F)) f(k, k'; s, s')u(\Omega, s') \tag{2.131}$$

where $s = \frac{\omega}{qv_F}$.

From the discussion so far it has become abundantly clear that the key object in the Fermi liquid description is the interaction function $f(\boldsymbol{k}, \boldsymbol{k}')$. It is therefore important to see how it is related to the microscopic degrees of freedom of the theory. In this part of the section, it will be presented how this can be achieved. In fact it will be shown that $f(\boldsymbol{k}, \boldsymbol{k}')$ is related to a particular limit of the four-point Green's function (or to be more precise the vertex function, i.e. the sum of the one-particle irreducible amputated Feynman diagrams). In order to keep the discussion concise and given that the details of these calculations are not the purpose of this section, elements of finite-temperature perturbation theory will be borrowed from standard textbooks treatments [34–36]. For purposes of simplicity of the notation the convention of [34] will be adopted, so that all the degrees of freedom associated with a particle will be encoded in a number representing said particle (e.g. $\{\boldsymbol{x}_1, s_1, \ldots\} \to 1$).

The first object needed is the two-point Green's function (or propagator)

$$G(1, 2) = -\imath\langle\psi_0|T\left\{\psi(1), \psi^\dagger(2)\right\}|\psi_0\rangle \tag{2.132}$$

where $|\psi_0\rangle$ is the ground state and $T\{\ldots\}$ represents the time-ordered product. In momentum space the propagator can be written

$$G_2(\boldsymbol{p}) = \frac{1}{\omega - \frac{p^2}{2m} - \Sigma(\omega, \boldsymbol{p})} \tag{2.133}$$

where $\Sigma(\omega, \boldsymbol{p})$ is the standard self-energy. Rewriting this around the Fermi surface one gets

$$G_2(\boldsymbol{p}) = \frac{a}{\omega - \epsilon_F - v_F(p - k_F) + \imath\zeta sgn(\omega - \epsilon_F)} \tag{2.134}$$

where $a = (1 - \partial_\epsilon \Sigma)^{-1}$ is the residue of the quasi-particle pole, ϵ_F the Fermi energy, $v_F = k_F/m^*$ and ζ just a positive infinitesimal constant.

The next object one needs, is the four-point Green's function

$$G_4(1,2;3,4) = \langle\psi_0|T\left\{\psi(1)\psi(2)\psi^\dagger(3)\psi^\dagger(4)\right\}|\psi_0\rangle \tag{2.135}$$

which following standard perturbation procedures is split into disconnected and 1PI parts

$$\begin{aligned} G_4(1,2;3,4) &= G_2(1,3)G_2(2,4) - G_2(1,4)G_2(2,3) \\ &+ \imath \int d1'd2'd3'd4' G_2(1,1')G_2(2,2')G_2(3,3')G_2(4,4')\Gamma_4(1',2';3',4') \end{aligned} \tag{2.136}$$

or in momentum space

$$\begin{aligned} G_4(\boldsymbol{p}_1,\boldsymbol{p}_2;\boldsymbol{p}_3,\boldsymbol{p}_4) &= (2\pi)^8 G_2(\boldsymbol{p_1})G_2(\boldsymbol{p_2})\left(\delta(\boldsymbol{p}_1 - \boldsymbol{p}_3)\delta(\boldsymbol{p}_2 - \boldsymbol{p}_4) - \delta(\boldsymbol{p}_1 - \boldsymbol{p}_4)\delta(\boldsymbol{p}_2 - \boldsymbol{p}_3)\right) \\ &+ \imath(2\pi)^4 G_2(\boldsymbol{p_1})G_2(\boldsymbol{p_2})G_2(\boldsymbol{p_3})G_2(\boldsymbol{p_4})\delta(\boldsymbol{p}_1 + \boldsymbol{p}_2 - \boldsymbol{p}_3 - \boldsymbol{p}_4)\Gamma_4(\boldsymbol{p}_1,\boldsymbol{p}_2;\boldsymbol{p}_3,\boldsymbol{p}_4) \end{aligned} \tag{2.137}$$

The analytic structure of Γ_4 is then of prime interest, since its poles correspond to different states of the system. In particular the specific time ordering determines this state. Since here the Fermi liquids dynamics are of interest, the relevant ordering is $\psi(1)\psi(3)^\dagger\psi(2)\psi(4)^\dagger$, which in turn means that poles should be found in the $\omega(3)-\omega(1)$ channel, i.e. the particle-hole channel. In order to remain within the regime of validity of Fermi liquid description both energy and momentum should remain small and close to the Fermi surface. It is then convenient to write $p_3 = p_1 + k$ and $p_4 = p_2 - k$, where $k = (\omega, \boldsymbol{k})$ is a small four-vector. Putting all these together one can now write down the Feynman diagrams involved in computing Γ_4. In Fig.2.3 the first two orders of perturbation series are presented. Given that the momentum with respect to which the poles should be studied is k, it is convenient to write $\Gamma(p_1, p_2; k) = \Gamma_4(p_1, p_2; p_3, p_4)$.

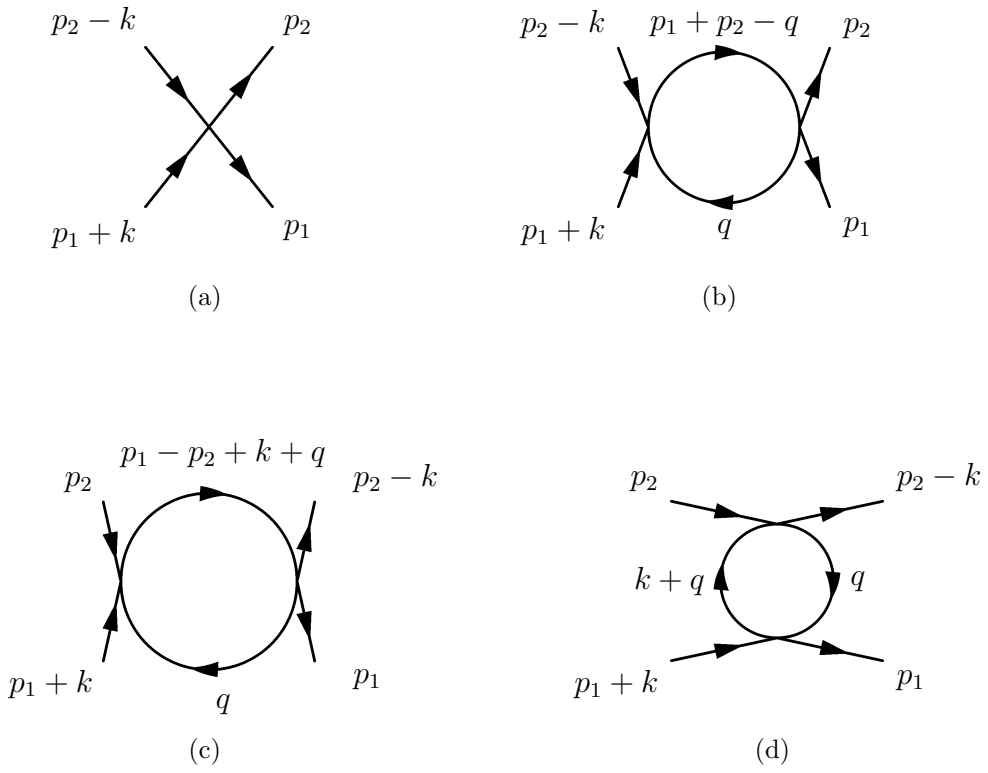

Figure 2.3: Feynman diagrams corresponding to Γ_4 up to one loop.

Out of the one-loop graphs in Fig.2.3 the first two behave nicely in the limit $k \to 0$, so one can just set $k = 0$ for them. On the other hand in the last graph as $k \to 0$ the two propagators $G_2(q)$ and $G_2(k+q)$ come together, making the graph apparently divergent. Defining $\tilde{\Gamma}(p_1, p_2) := \Gamma(p_1, p_2; k = 0)$ as the finite part of the vertex function one can write the integral equation that governs Γ_4

$$\Gamma_4(p_1, p_2; k) = \tilde{\Gamma}(p_1, p_2) - \imath \int \frac{d^4q}{(2\pi)^4} \tilde{\Gamma}(p_1, q) G_2(q) G_2(q+k) \Gamma_4(q, p_2; k) \tag{2.138}$$

Now one uses expression (2.134) to explicitly write the product of the two propagators as

$$\begin{aligned} G_2(q)G_2(q+k) =& \frac{a}{\epsilon - \epsilon_F - v_F(q - k_F) + \imath\zeta sgn(\epsilon - \epsilon_F)} \\ & \cdot \frac{a}{\omega + \epsilon - \epsilon_F - v_F((k+q) - k_F) + \imath\zeta sgn(\omega + \epsilon - \epsilon_F)} \end{aligned} \tag{2.139}$$

The regime of interest is the Hydrodynamic one, meaning long wavelengths and small frequencies, i.e. $k \to 0$ and $\omega \to 0$. In this limit one can split the product of the propagators into divergent and regular part

$$G_2(q)G_2(q+k) \underset{k \to 0}{=} Res(\theta)\delta(\epsilon - \epsilon_F)\delta(q - k_F) + Reg(q) \tag{2.140}$$

where $Reg(q)$ is the regular part and $Res(\theta)$ is the residue ($\theta = \cos^{-1}(\frac{q\cdot k}{|k||q|})$). Following standard procedures the residue can be computed by carefully taking the integration over the complex plane, resulting in

$$Res(\theta) \underset{k\to 0}{=} \frac{2\imath a^2 k\cos\theta}{\omega - v_F k\cos\theta} \tag{2.141}$$

making the product of propagators

$$G_2(q)G_2(q+k) \underset{k\to 0}{=} \frac{2\imath a^2 \hat{q}\cdot k}{\omega - v_F\cos\theta}\delta(\epsilon-\epsilon_F)\delta(q-k_F) + Reg(q) \tag{2.142}$$

where the following identity has been used: $k\cos\theta = \hat{q}\cdot k$. Putting all the pieces together the four-point function (to first order) becomes

$$\begin{aligned}\Gamma_4(p_1,p_2;k) = \tilde{\Gamma}(p_1,p_2) - \imath\int\frac{d^4q}{(2\pi)^4}\tilde{\Gamma}(p_1,\theta)Reg(q)\Gamma_4(q,p_2;k)\\ + \frac{a^2k_F}{(2\pi)^3}\int d\Omega\tilde{\Gamma}(p_1,q)\frac{\hat{q}\cdot k}{\omega - v_F\hat{q}\cdot k}\Gamma_4(q,p_2;k)\end{aligned} \tag{2.143}$$

where $d^4q = q^2dqd\epsilon d\Omega$ and $d\Omega$ is the solid angle. At this point one encounters a crucial detail - the way the Hydrodynamic limit is taken. In other words the two limits involved, i.e. $k\to 0$ and $\omega\to 0$ are not commuting. For the present purposes the one that will be used is $\lim_{\omega\to 0}\lim_{k\to 0}$. [8] Consequently

$$\lim_{\omega\to 0}\lim_{k\to 0}\left(\frac{\hat{q}\cdot k}{\omega - v_F\hat{q}\cdot k}\right) = 0 \tag{2.144}$$

and the vertex function, which in this limit will be denoted as Γ^ω becomes

$$\Gamma^\omega(p_1,p_2) = \tilde{\Gamma}(p_1,p_2) - \imath\int\frac{d^4q}{(2\pi)^4}\tilde{\Gamma}(p_1,q)Reg(q)\Gamma^\omega(q,p_2) \tag{2.145}$$

and eliminating $Reg(q)$

$$\Gamma_4(p_1,p_2;k) = \Gamma^\omega(p_1,p_2) + \frac{a^2k_F^2}{(2\pi)^3}\int d\Omega\Gamma^\omega(p,q)\frac{\hat{q}\cdot k}{\omega - v_F\hat{q}\cdot k}\Gamma_4(q,p_2;k) \tag{2.146}$$

Now all the components are in place to take the Hydrodynamic limit

$$\Gamma_4(p_1,p_2;k) \underset{k\to 0}{=} \frac{a^2k_F^2}{(2\pi)^3}\int d\Omega\Gamma^\omega(p_1,q)\frac{\hat{q}\cdot k}{\omega - v_F\hat{q}\cdot k}\Gamma_4(q,p_2;k) \tag{2.147}$$

where the fact that energy and momentum is very close to the Fermi values, i.e. $p_1 = (\epsilon_F, k_F\hat{p}_1)$ and $p_2 = (\epsilon_F, k_F\hat{p}_2)$, where $\hat{p}_1$ and $\hat{p}_2$ are unit vectors and $\lim_{k\to 0}\Gamma^\omega = 0$,

[8] The other limit, i.e. $\lim_{k\to 0}\lim_{\omega\to 0}$, results in a Γ_4 that corresponds to physical forward scattering of quasi-particles off the the Fermi surface, while the limit used in the text, corresponds to virtual excitations.

has been used. In the last equation the only real variable is $\hat{p}_1$ and hence is can be manipulated into a familiar form so that the connection with the interaction function $f(k, k')$ can be made. Namely one writes it as

$$\left(\frac{\omega}{kv_F} - \cos\theta\right) u(\hat{p}) = \cos\theta \frac{m^* k_F}{2\pi^2} \int \frac{d\Omega}{4\pi} a^2 \Gamma^\omega(\hat{p}, \hat{q}) u(\hat{q}) \tag{2.148}$$

where

$$u(\hat{q}) = \frac{\hat{q} \cdot k}{\omega - v_F \hat{q} \cdot k} \Gamma_4(\hat{q}) \tag{2.149}$$

Comparing the last equation with (2.131) one immediately sees that the sought after relation between $f(k, k')$ and the vertex function is

$$f(\hat{p}, \hat{q}) = a^2 \Gamma^\omega(\hat{p}, \hat{q}) \tag{2.150}$$

The significance of this result needs to be stressed, since it relates a phenomenologically introduced function that encodes the interaction energy between quasi-particles, with a microscopic quantity, the vertex function, that is well grounded on Quantum Field Theory and can be perturbatively calculated in a systematic way. It is also important to explicitly state the physical content of this statement. It describes the scattering of a particle-hole pair from one point of the Fermi surface to another.

To conclude this presentation of Fermi liquids, the resilience of their description by Landau's theory and of the presence of a Fermi surface, will be reviewed. Landau's theory is in essence an effective theory and as such it can be examined using the standard toolbox of effective field theories. Here [33, 37] will be followed. What will be shown is that interaction terms of this theory, can be effectively integrated out resulting in a theory with almost no relevant or marginal operators.

The starting point will be the non-interacting action encountered before

$$\int dt d^3p \left\{ \imath \psi_s(p)^\dagger \partial_t \psi_s(p) - (\epsilon(p) - \epsilon_F) \psi_s(p)^\dagger \psi_s(p) \right\} \tag{2.151}$$

with the ground state corresponding to the Fermi sea, with filled states for $\epsilon < \epsilon_F$ and empty ones for $\epsilon > \epsilon_F$. In order to make the presence of the Fermi surface explicit one writes, as done previously, the momentum as $\boldsymbol{p} = \boldsymbol{k} + \boldsymbol{l}$, where $\boldsymbol{k}$ is vector on the Fermi surface and $\boldsymbol{l}$ is orthogonal to it. The single-particle energy therefore becomes $\epsilon(p) - \epsilon_F = l v_F + \mathcal{O}(l^2)$.

In order to study the effects of adding interactions to this theory, one does what is usually done with effective theories, that is write down all the terms allowed by the symmetries of the system and study their scaling behaviour. Assuming that an

effective theory is studied at a scale Λ the interaction terms at this scale can be written as a series of operators

$$S_\Lambda = \int d^d x \sum_i g_i O_i \tag{2.152}$$

with the i-th term scaling as $\int d^d x O_i \sim E^{\delta_i - d}$ or written in terms of a dimensionless parameter $\lambda_i \left(E/\Lambda\right)^{\delta_i - d}$. If $\delta_i > d$, O_i is irrelevant, i.e. it becomes less important as energy becomes lower ($E \to 0$). If $\delta_i < d$, O_i is relevant, i.e. it becomes more important as energy becomes lower. If $\delta_i = d$, O_i is marginal and it is equally important at all energy scales. Marginal operators can turn relevant or irrelevant depending or higher interaction terms. This is determined by the beta-function

$$E\partial_E g = bg^2 + \mathcal{O}(g^3) \tag{2.153}$$

If $b > 0$ then the corresponding operator is marginally irrelevant, while if $b < 0$ it is marginally relevant. In the case where $b = 0$ for all higher orders then the operator is truly marginal.

The symmetries of this theory include number of particle and space-time symmetries, which for the case of realistic scenarios break down to lattice symmetries. Additionally in the non-relativistic limit ($c \to \infty$), where spin and rotational symmetries get decoupled, one gets an additional $SU(2)$ internal spin symmetry.

If energies get rescaled as $E \to \lambda E$, where $\lambda < 1$, then $k \to k$, $l \to \lambda l$, $dt \to \lambda^{-1} dt$, $dk \to dk$, $dl \to \lambda dl$ and $\partial_t \to \lambda \partial_t$. The action then scales as $\lambda\times$ (scaling of $\psi^\dagger \psi$), which means the $\psi \sim \lambda^{-1/2}$. The scaling of possible interaction terms will now be examined. A quadratic term

$$\int dt d^2 k dl \mu(k) \psi_s(p)^\dagger \psi_s(p) \sim \lambda^{-1} \tag{2.154}$$

This looks like a mass term and it is relevant but it can be absorbed into the definition of $\epsilon(p)$. Next a quartic term will be examined

$$\begin{aligned} &\int dt d^2 k_1 dl_1 d^2 k_2 dl_2 d^2 k_3 dl_3 d^2 k_4 dl_4 V(k_1, k_2, k_3, k_4) \\ &\quad \psi_s(p_1)^\dagger \psi_s(p_3) \psi_{s'}(p_2)^\dagger \psi_{s'}(p_4) \delta^{(3)}(p_1 + p + 2 - p_3 - p_4) \sim \lambda^1 \times \lambda_\delta \end{aligned} \tag{2.155}$$

where λ_δ is the scaling of the delta-function. If one naively assumes that the scaling of the delta-function goes like λ^0 because

$$\delta^{(3)}(p_1 + p_2 - p_3 - p_4) = \delta^{(3)}(k_1 + k_2 - k_3 - k_4 + l_1 + l_2 - l_3 - l_4) \simeq \delta^{(3)}(k_1 + k_2 - k_3 - k_4) \tag{2.156}$$

since l scales to 0, then the overall scaling of the quartic operator is λ^1, which makes it irrelevant. It therefore seems that quadratic and quartic terms are irrelevant indicating that at low energies the theory becomes "freer" - almost like a free electron gas.

However there are two caveats that require further examination. The first one involves phonon interactions, while the second one stems from the delta-function scaling. Starting from the phonon interactions, one notices that the presence of a crystal lattice breaks space-time symmetries giving rise to Goldstone bosons. This bosons must be included in the low-energy theory and therefore one introduces a phonon field $\boldsymbol{D}(\boldsymbol{r})$ which is proportional the displacement of the ions from their equilibrium position times their mass ($M^{1/2}$). The kinetic plus restoring force part of the action describing the phonon field is

$$\frac{1}{2}\int dtd^3q\left(\partial_t D_i(\boldsymbol{q})\partial_t D_i(-\boldsymbol{q}) - M^{-1}\Delta_{ij}(\boldsymbol{q})D_i(\boldsymbol{q})D_j(-\boldsymbol{q})\right) \tag{2.157}$$

The scaling of the phonon field can be determined by the free action and then used to derive the scaling of the phonon-fermion interaction term. In particular close to the Fermi surface the particles' momenta scale as $q \sim \lambda^0$ while the integration variables and the derivatives of the kinetic term contribute another λ^1. Overall then the phonon field's scaling is $\lambda^{-1/2}$. If one now examines the first of possible phonon-particle interaction terms

$$\int dtd^3qd^2l_1dl_1d^2l_2dl_2M^{-1/2}g_i(\boldsymbol{q},\boldsymbol{k}_1,\boldsymbol{k}_2)D_i(\boldsymbol{q})\psi_s(\boldsymbol{p}_1)^\dagger\psi_s(\boldsymbol{p}_2)\delta^{(3)}(\boldsymbol{p}_1-\boldsymbol{p}_2-\boldsymbol{q}) \tag{2.158}$$

scales as $\lambda^{-1/2}$ assuming that one treats the delta-function as before, i.e. scaling as λ^0. That makes the term relevant. However the term gets suppressed by a factor of $(m/M)^{1/4}$. Note here that below the Debye energy $(m/M)^{1/2}E_0$, where E_0 is the characteristic energy scale, the restoring force is larger than the kinetic term and it is therefore what should be used to determine the scaling of D. In that case $D \sim \lambda^{1/2}$ and similarly (2.158)$\sim \lambda^{1/2}$, making the interaction term irrelevant below E_1.

Finally one needs to address the issue of the scaling of the delta-function. So far it has been assumed that it scales as λ^0. This is a valid assumption when particles scattered with generic initial momenta. Assume that two particles of momenta p_1 and p_2 scatter into p_3 and p_4. One can then write

$$p_3 = p_1 + \delta k_3 + \delta l_3 \tag{2.159}$$

$$p_4 = p_2 + \delta k_4 + \delta l_4 \tag{2.160}$$

and the corresponding delta-function becomes $\delta^{(d)}(\delta k_3 + \delta k_4 + \delta l_3 + \delta l_4)$. Recall that, as before, $l-$ momenta are perpendicular to the Fermi surface and $k-$momenta tangential. Now for generic momenta, δk_i are linearly independent, hence the argument of the delta-function is dominated by those and neglecting the δl_i parts is reasonable, leading to the scaling λ^0. However in the special case where the initial momenta add up to zero, i.e. $p_1 = -p_2$, then $\delta^{(d)}(\delta k_3 + \delta k_4)$ becomes degenerate and one needs to take into account the perpendicular momenta l_i. This leads to a λ^{-1} scaling for the delta-function which in turn makes the quartic interaction term scale as λ^0, i.e. marginal. The rest of the interaction terms remain irrelevant. As for the phonon-particle interactions one can integrate out the phonons leading back to the quartic interaction term. The effect of the presence of a marginal operator is that the one-loop (and higher) correction to a diagram involving external momenta, restricted to sum up to zero, is not suppressed and need to be explicitly calculated and taken into account. These corrections can be summed up into a geometric series and their effect is a modification of the expectation values of currents, compared to the free case.

Chapter 3

Aspects of Holography

Following the review of some fundamental aspects of Condensed Matter, a detour will be attempted in order to provide an overview of Holography itself. In this chapter some of its most important elements will be presented, starting from its origins in String Theory and ending at its application to strongly coupled Condensed Matter systems. The structure of this chapter is the following. Firstly a brief history of Holography and strong-weak dualities will be presented. Then the practical tools of Holography (which is usually refereed to as the Holographic dictionary) will be reviewed. Finally those tools, will be used in practical applications and contact with Condensed Matter Theory will be attempted.

3.1 History

Holography can be considered as the most successful and most influential example of a strong-weak duality. It is highly interesting to note though that it is neither the only nor the first one. As early as the forties it was noticed that in the context of Lattice Field Theory one encounters such dualities. In particular Krammers and Wannier [38, 39] noticed that for $d = 2$ Ising model on a square lattice, with nearest-neighbour interactions, where the partition function is

$$Z[J] = \sum_{s=\pm 1} \exp\left[J \sum_{\langle ij \rangle} s_i s_j \right] \tag{3.1}$$

one can do the following transformation $J \to J^* = -\frac{1}{2} \ln \tanh J$ resulting in the transformed partition function $Z[J] \to Z[J] = C(J) Z^*[J^*]$ or explicitly

$$Z[J] = \frac{1}{2} \left(\cosh J \sinh J \right)^N \sum_{s^*=\pm 1} \exp\left[J^* \sum_{\langle ij \rangle} s_i^* s_j^* \right] \tag{3.2}$$

where N is number of sites of the lattice. It is then obvious that in the starred coordinates one gets an identical (self-dual) system with a new coupling constant J^*. What gives rise to the strong-weak duality, is the relation between the two coupling constants J and J^*. As shown in fig. 3.1 when the system in its strongly-coupled regime in the starred coordinates, it is in its weak regime in the un-starred coordinates and vice-versa. It should be noted here, that the emergence of a self-dual

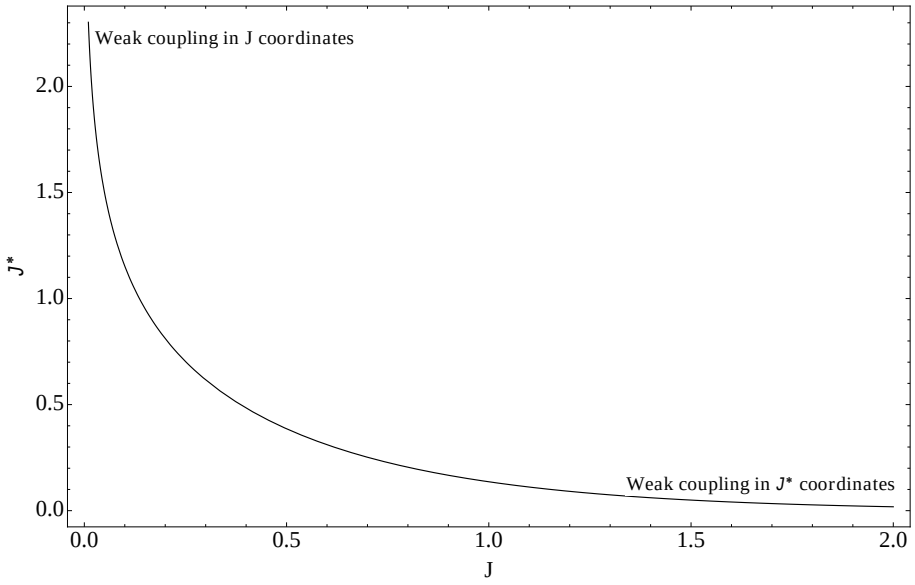

Figure 3.1: The relation between the coupling coefficients between the two dual theories in Krammers-Wannier system.

system under this transformation is specific to the $d = 2$ case. In higher dimensions the system is not necessarily self-dual. This system contains a phase transition at J_C such that $\sinh^2 2J_C = 1$ [40]. It is important to note that the simplicity of this model is predicated on the symmetry group (which for the $d = 2$ Ising model is $\mathbb{Z}_2$) being Abelian. If this is not the case the treatment is much more involved and leads to what is referred to as Tannaka-Krein duality [41]. Further information on this subject can be found in the excellent review of R.Savit [42].

Another such system, that develops strong-weak duality is the Sin-Gordon model [43]. The standard action is

$$S_{SG} = \int d^2x \left\{ \frac{1}{2}\partial_\mu\phi\partial^\mu\phi + \frac{\alpha}{\beta^2}\left(\cos\beta\phi - 1\right) \right\} \tag{3.3}$$

In this theory there are two types of excitations: meson ($M_{mes} = \sqrt{\alpha}$) and solitons ($M_{sol} = \frac{8\sqrt{\alpha}}{\beta^2}$). The perturbative regime of this theory is $\beta^2 \ll 1$ where $M_{sol} \gg M_{mes}$,

where β^2 is the relevant coupling constant. It turns out that this model is dual (through bosonization) to the Thirring model, described by the action

$$S_T = \int d^2x \left\{ \bar{\psi} \imath \gamma_\mu \partial^\mu \psi + m \bar{\psi} \psi - \frac{g}{2} \bar{\psi} \gamma^\mu \psi \bar{\psi} \gamma_\mu \psi \right\} \tag{3.4}$$

The excitations of this theory consist of fundamental fermions (dual to solitons in the Sin-Gordon model) and fermion-anti-fermion bound states (dual to meson in the Sin-Gordon model). The duality relates the coupling constants of the two models as

$$\frac{\beta^2}{4\pi} = \frac{1}{1 + \frac{g}{\pi}} \tag{3.5}$$

which makes it clear that when on side of the duality pair is at its weakly-coupled regime, then the other is at its strongly-coupled regime and vice-versa. It should be noted here that in this case the dual degrees of freedom are fundamental quanta on the on side and solitons on the other, while Noether charges are interchanged with topological charges.

Strong-weak dualities are not restricted to low-dimensional models. There are numerous higher-dimensional cases, which however are usually super-symmetric. Such examples include the Montonen-Olive duality [44] as well as the Seiberg-Witten duality [45].

Having established that weak-strong dualities are not a rare and exotic phenomenon but rather abundant one can now turn two Holography. As it will be argued momentarily Holography is based on a similar duality but involving gravitational degrees of freedom. What is even more striking is that the dual degrees of freedom are not gravitational. There are many reviews on this subject, of which a few are used and cited here [8, 46–52].

The historic context within which Holography emerged was that of attempting to describe in a microscopic way (within String Theory most commonly), Black Holes and their thermodynamic properties in particular (e.g. see [53]). This properties are nicely reviewed in [54] and more recent progress presented in [55]. These attempts brought into the foreground the extended objects which naturally occur in String Theory, i.e. branes and emphasized their importance in extending one's understanding of String Theory. The origins of Holography itself can be traced back to the seminal work of Maldacena [5], Witten [7] and Gubser, Klebanov, Polyakov [6]. These constitute the foundational works of Holography, that sparked an enormous interest on the subject and motivated a huge body of work, that extends from fundamental, mathematical aspects of Holography, all the way to applications to "real-life" systems (e.g. Heavy Ion physics [27] and high-T_C superconductivity [12]).

3.2 Background

The framework of Holography is String Theory [56–59], which started as the quantum theory describing interacting strings but it became quickly apparent that it quite naturally includes other extended objects, i.e. branes [60–62].

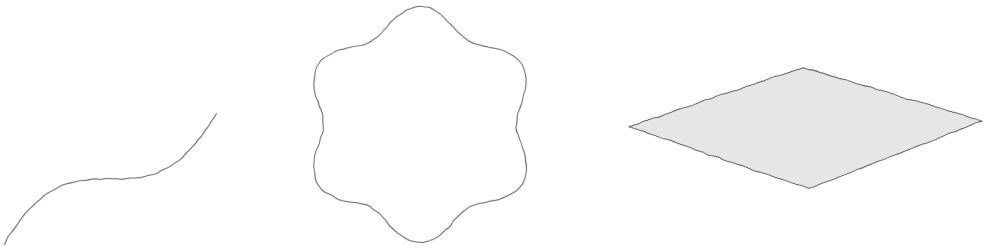

(a) Open string (b) Closed string (c) Brane

Figure 3.2: The objects of String Theory.

In the full quantum theory apart from the open-closed string interaction, there are interactions between open-closed strings and branes, as schematically depicted in fig. 3.7. The dynamics of the string is governed by the action

$$S = -T \int d^2\sigma \sqrt{-g} \tag{3.6}$$

where

$$g_{\alpha\beta} = G_{\mu\nu} \frac{\partial X^\mu}{\partial \sigma^\alpha} \frac{\partial X^\nu}{\partial \sigma^\beta} \ , \ X^\mu = X^\mu(\sigma) \tag{3.7}$$

and T is the string tension. This is the fundamental parameter of String Theory and

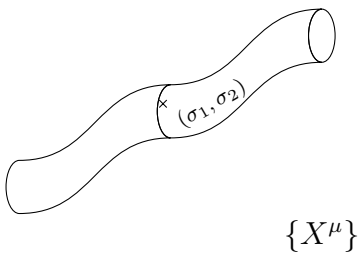

Figure 3.3: The world-sheet of a closed string.

is often written as $T = \frac{1}{4\pi\alpha'}$, with $\alpha' = l_s^2$ where l_s is the fundamental string length. Strings are quantized in the first quantization formalism and once super-symmetric

extensions are included one gets a finite number of massless states along with an infinite number of massive modes, the mass of which is $M \sim m_s l_s^{-1}$. Depending on the boundary conditions imposed, one finds five self-consistent string theories. Namely Type-IIA, Type-IIB, Type-I, Heterotic $SO(32)$ and Heterotic $E_8 \times E_8$, all of which are considered as limits of an eleven-dimensional theory, i.e. M-theory [63]. The requirement of no negative-norm states fixes the dimensionality to $D = 10$. When weak string interactions are included one gets a scheme similar to the perturbation theory in QFTs (i.e. Feynman diagrams) where the summation is over distinct world-sheet topologies (fig. 3.4). The string length or equivalently α' controls the departure

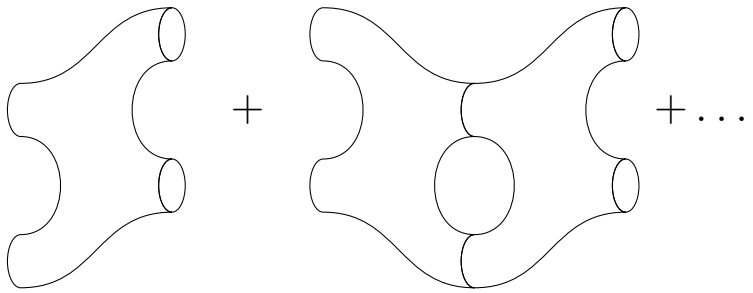

Figure 3.4: Perturbation series of String Theory - sum over topologies.

of string amplitudes from the corresponding point-like particle amplitudes, so that at $l_s \to 0$ one recovers the standard perturbative series (fig. 3.5). Similarly the string

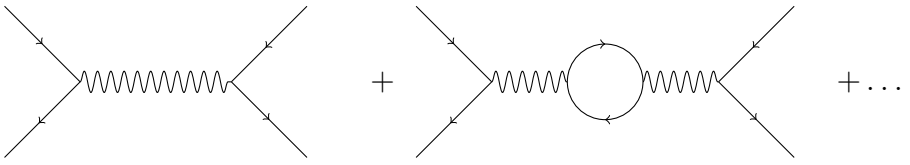

Figure 3.5: As $l_s \to 0$ the String Theory perturbation series reduces to the standard Feynman perturbation series.

coupling g_s which is related to the string length and the ten-dimensional Newton's constant through $16\pi G = (2\pi)^7 g_s^2 l_s^8$ and is attached to each vertex (as depicted in fig. 3.6), controls the convergence of the topological series (fig. 3.4). For each diagram in this series one gets a factor of g_s^{2h+1}, where h is the number of holes of the world-sheet surface. It should be noted here that g_s is not a free parameter (as is the case in QFTs) but rather is related to the dilaton (ϕ) through $g_s = \exp[\langle\phi\rangle]$. In the context of Holography the gauge-string duality is often approximated by the gauge-gravity duality, which involves the following limits: $L \gg l_s$ and $g_s \ll 1$, where L is the

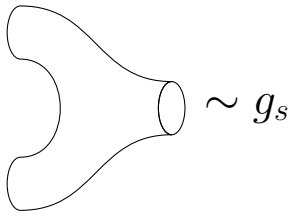

Figure 3.6: Closed string vertex.

characteristic length scale. The former guarantees that the string-length effects can be safely neglected, while the latter, which is equivalent to the requirement that the dilaton remains small, allows the use of only the first term in the perturbative series (fig. 3.4), i.e allows one to neglect quantum corrections.

Before proceeding further towards the presentation of the Holographic duality, one needs to introduce branes and in particular D-branes. Within String Theory branes enter as non-perturbative (with respect to g_s) higher-dimensional objects with tension (i.e. energy per unit volume) $T_s \sim \frac{1}{g_s}$. D_p- branes are topological defects in the $D-$dimensional space-time, with $(p+1)-$dimensional world-volume, on which open strings can end (hence the name D from the Dirichlet boundary conditions imposed) [61]. It should be noted here that D_p-branes are by no means the only type of extended objects "living" within String Theory, but they are the most relevant to Holography, at least as it was originally formulated. Apart from having open strings ending on them, D_p-branes can emit and absorb closed strings, as they carry tension, i.e. energy and therefore they gravitate (with gravity belonging to the closed string spectrum) (fig. 3.7). At low energies, i.e. for $E \ll m_s \sim \frac{1}{l_s}$, only the lowest states are relevant. Taking Type-IIB String Theory as a working example (which is also the most relevant for Holography), the low-energy spectrum includes the fields listed in table 3.1, which constitutes a $\mathcal{N} = 2$ ten-dimensional Super-gravity (SUGRA) [64].

$g_{\mu\nu}$	Graviton
ϕ, C	Dilaton and Axion
$B_{\mu\nu}$, $A_{\mu\nu}$	Rank-2 anti-symmetric tensors
$A^{\dagger}_{\mu\nu\rho\sigma}$	Rank-4, anti-symmetric, self-dual tensor
$\psi^{I=1,2}_{\mu,\alpha}$	Majorana-Weyl gravitini
$\lambda^{I=1,2}_{\alpha}$	Dilatini

Table 3.1: Low-energy spectrum of Type-IIB String Theory.

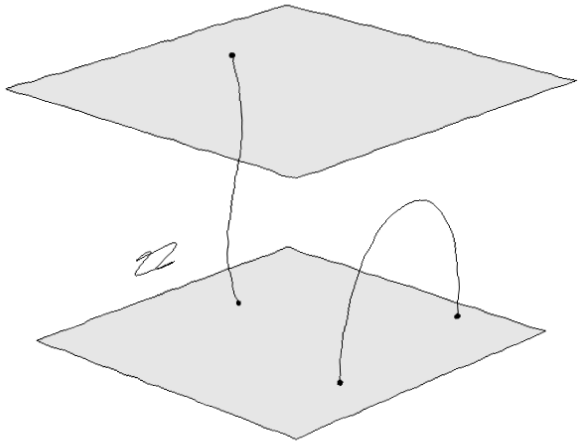

Figure 3.7: Schematic of interactions between strings and branes.

Next one writes down the Polyakov action

$$S_P = -\frac{1}{4\pi\alpha'}\int d^x\sqrt{-h}h^{\alpha\beta}\partial_\alpha X^\mu\partial_\beta X^\nu g_{\mu\nu} \tag{3.8}$$

where $g_{\mu\nu}$ is the ten-dimensional metric, X^μ the embedding functions, $h^{\alpha\beta}$ the world-sheet metric and h its determinant. Demanding the preservation of the symmetries (like conformal symmetry) of the Polyakov action on the quantum level one gets a set of restrictions which appear as the beta functionals of the theory [65]

$$\beta_{\mu\nu}(X) = R_{\mu\nu} + \frac{1}{4}H^{\lambda\sigma}{}_\mu H_{\nu\lambda\sigma} - 2D_\mu D_\nu\phi + \mathcal{O}(\alpha') \stackrel{!}{=} 0 \tag{3.9}$$

where $H_{\mu\nu\rho} := \partial_\mu B_{\nu\rho} + \partial_\nu B_{\mu\rho} + \partial_\rho B_{\mu\nu}$ is a generalization of the Faraday tensor $F_{\mu\nu} = \partial_\mu A_\nu - \partial_\nu A_\mu$. Similarly there are more beta functionals

$$\begin{aligned} R_{\mu\nu} = {} & \frac{1}{2}\partial_\mu\phi\partial_\nu\phi + \frac{1}{4}\exp[-\phi]\left\{H_{\mu\alpha\beta}H_\nu{}^{\alpha\beta} - \frac{1}{2}g_{\mu\nu}H^2\right\} + \exp[2\phi]\frac{1}{2}\partial_\mu C\partial_\nu C \\ & + \exp[\phi]\frac{1}{4}\left\{\tilde{F}_{\mu\lambda\sigma}F_\nu{}^{\lambda\sigma} - \frac{1}{2}g_{\mu\nu}\tilde{F}^2_{(3)}\right\} + \frac{1}{96}F_{\mu\lambda\rho\sigma\kappa}F_\nu{}^{\lambda\rho\sigma\kappa} \end{aligned} \tag{3.10}$$

$$\nabla^2\phi = \exp[2\phi]\partial_\mu C\partial^\mu C - \frac{1}{12}\exp[-\phi]H_3^2 + \frac{1}{12}\exp[\phi]\tilde{F}^2_{(3)} \tag{3.11}$$

$$\partial_\mu\left\{\sqrt{-g}g^{\mu\nu}\exp[2\phi]\partial_\nu C\right\} = -\frac{1}{6}\exp[\phi]H_{\mu\nu\sigma}\tilde{F}^{\mu\nu\sigma} \tag{3.12}$$

$$d\star\tilde{F}_5 = H_3\wedge F_3 \tag{3.13}$$

$$d\star\left(\exp[\phi]\tilde{F}_3\right) = \tilde{F}_5 \wedge H_3 \tag{3.14}$$

$$d\star\left(C\tilde{F}_3\exp[\phi] - H_3\exp[-\phi]\right) = \tilde{F}_3 \wedge F_3 \tag{3.15}$$

$$\tilde{F}_5 = \star\tilde{F}_5 \tag{3.16}$$

where $\tilde{F}_3 = F_3 - CH_3$, $F_3 = dA_2$ (noting that $A_2 \leftrightarrow A_{\mu\nu}$), $H_3 = dB_2$ (noting that $B_2 \leftrightarrow B_{\mu\nu}$). On top of the beta functionals there are a couple of Bianchi identities

$$d\tilde{F}_3 = -dC \wedge H_3 \ , \ d\tilde{F}_5 = H_3 \wedge F_3 \tag{3.17}$$

This set of equations constitute the equations of motion of the low energy theory, and can be derived from and action

$$S_{IIB}^{low\ energy} = S_{NS} + S_R + S_{CS} + fermions \tag{3.18}$$

with

$$S_{NS} = \frac{1}{2\kappa_{10}^2}\int d^{10}\sqrt{-g}\left\{R - \frac{1}{2}\partial_\mu\phi\partial^\mu\phi - \frac{1}{2}\exp[-\phi]|H_3|^2\right\} \tag{3.19}$$

$$S_R = \frac{1}{4\kappa_{10}^2}\int d^{10}\sqrt{-g}\left\{\exp[2\phi]|F_1|^2 + \exp[\phi]|\tilde{F}_3|^2 + \frac{1}{2}|\tilde{F}_5|^2\right\} \tag{3.20}$$

$$S_{CS} = \frac{1}{4\kappa_{10}^2}\int A_4 \wedge H_3 \wedge F_3 \tag{3.21}$$

where $F_1 = dC$. A word of caution is appropriate here - these equations of motion receive string-length corrections (i.e. $\alpha' \neq 0$), which signify a departure from Super-gravity towards String Theory. For example the action contains corrections like $\gamma\exp[-\frac{3}{2}\phi]W$ with

$$W = C^{hmnk}C_{pmnq}c_h{}^{rsp}C^q{}_{rsk} + \ldots \tag{3.22}$$

where C^{hmnk} is the Weyl tensor[1] and $\gamma = \frac{1}{8}\zeta(3)\alpha'^3$.

Most solutions to the Type-IIB equations of motion receive α' corrections with some exceptions the most striking of which is Minkowski and $AdS_5 \times S^5$ space-times, which are highly relevant to Holography. Generically if one has a classical solution to the Super-gravity equations of motion, characterized by some length scale L (as is the case for the Schwarzschild black hole solution where $L = r_S$) then this solution will receive string corrections ($\alpha' \neq 0$) and quantum corrections ($g_s \neq 0$) unless $L \gg l_s$ and $L \gg l_p$ (where l_p is the Planck length) respectively. The equations of motion (eqs. (3.9) to (3.16)) have an extremely rich structure resulting in numerous solutions.

[1] $C_{abcd} = R_{abcd} - \frac{2}{d-2}\left(g_{a[c}R_{b]d} - g_{b[c}R_{d]a}\right) + \frac{2}{(d-1)(d-2)}Rg_{a[c}g_{a]b}$

However, there is also a sub-sector of the fields that can be isolated and excited separately so that one can consistently eliminate the rest. One such example studied in [32] among other places, involves keeping only gravitational degrees of freedom $g_{\mu\nu}$ and the five-form field F_5 (also keeping the dilaton (ϕ) constant). Setting all other fields to zero, one gets a much simpler set of equations of motion

$$R_{\mu\nu} = \frac{1}{96} F_{\mu abcd} F_{\nu}{}^{abcd} \tag{3.23}$$

$$F_5 = \star F_5 \tag{3.24}$$

which can be solved by

$$ds_{10}^2 = H^{-\frac{1}{2}}(r)\left(-f(r)dt + dx^2 + dy^2 + dz^2\right) + H^{\frac{1}{2}}\left(\frac{1}{f(r)}dr^2 + r^2 d\Omega_5^2\right) \tag{3.25}$$

$$F_5 = -\frac{4L^2}{H^2 r^5}\sqrt{r_0^4 + L^4}\,(1+\star)\,dt \wedge dx \wedge dy \wedge dz \wedge dr \tag{3.26}$$

where $f(r) = 1 - \frac{r_0^4}{r^4}$, $H(r) = 1 + \frac{L^4}{r^4}$. This solution corresponds to a black 3−brane with r_0 being the horizon's radial position. An interesting limit emerges when this solution is examined near its horizon. In particular in the limit where $r \ll L$ one can bring the metric solution (3.25) in the following form (changing coordinates to $u := \frac{r_0^2}{r^2}$)

$$ds_{10}^2 = \frac{(\pi T L)^2}{u}\left(-f(u)dt^2 + dx^2 + dy^2 + dz^2\right) + \frac{L^2}{4u^2 f(u)}du^2 + L^2 d\Omega_5^2 \tag{3.27}$$

where $T = \frac{r_0}{\pi L^2}$ is the temperature corresponding to the solution's horizon. If furthermore, one takes the zero-temperature limit $T \to 0$ and going to the original coordinates, the metric becomes

$$ds_{10}^2 = \frac{r^2}{L^2}\left(-dt^2 + dx^2 + dy^2 + dz^2\right) + \frac{L^2}{r^2}\left(dr^2 + r^2 d\Omega_5^2\right) \tag{3.28}$$

It is then clear that the space-time described by this metric is $AdS_5 \times S^5$ [2], which will be crucial in what follows.

Reviewing the ingredients of this restricted theory, one sees that on a perturbative level, i.e. where the relevant degrees of freedom are (potentially interacting) open and closed strings, there are gravitons g_μ and a gauge field $A^\dagger_{\mu\nu\lambda\rho}$. On the non-perturbative level there is a variety of higher-dimensional objects appearing like the D_p−branes. As mentioned before these are dynamical hyper-surfaces, with $(p+1)$−dimensional world-volumes, on which open strings can end. They are charged objects (under the

[2] In particular this is the Poincaré patch of AdS_5

gauge field $A_4^\dagger$), of solitonic nature (with respect to SUGRA), that carry finite tension T_D. Given their definition as the locus of open-string endpoints, it is not surprising that their fluctuations are determined by the quantum spectrum of the attached open strings. This spectrum consists of a massless sector, including a $U(1)$ gauge field $A_\mu(x^i)$, $i = 0, \ldots, p$ and $(9-p)$ scalars $\phi^i(x)$, $i = 1 \ldots (9-p)$ corresponding to transverse fluctuations, along with their super-partners, and a massive sector with energies $E \sim m_s \sim \frac{1}{l_s}$. Considering the D_p- branes as solitons the massless modes correspond to the collective modes of said soliton [43].

Now assume that instead of just one brane, two of them are present. The configuration looks like fig. 3.8. The two gauge fields extending between the two branes are

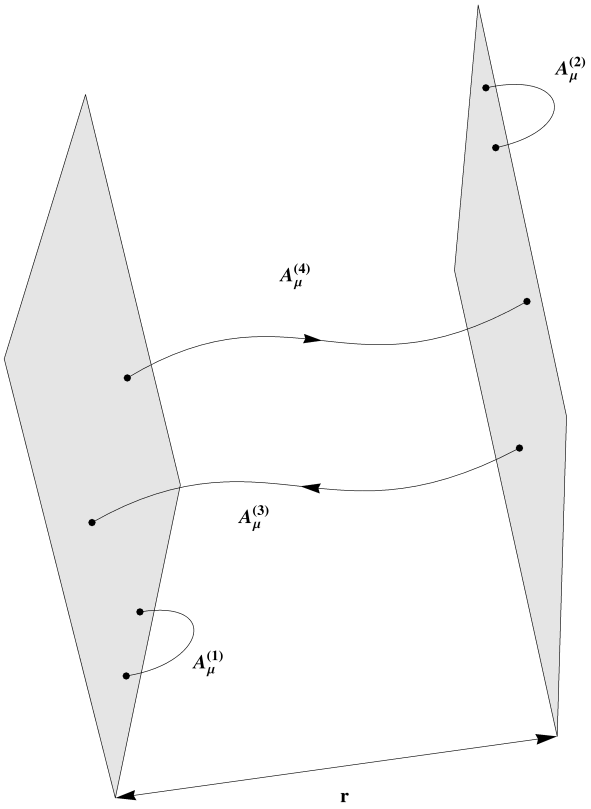

Figure 3.8: Possible configurations of open string between two branes.

now massive, in fact $m \sim \frac{r}{2\pi\alpha'}$, both of them carrying $U(1)$ charges at their end-points. If one takes them limit $r \to 0$ then the two branes get superimposed, the gauge fields become massless and the gauge symmetry gets enhanced into a $U(2)$ consisting of the fields $(A_\mu)^\alpha_\beta$, $\alpha, \beta = 1, 2$. Along with the gauge fields there are also scalars $(\phi^i)^\alpha_\beta$ [66]. The dynamics of the massless modes now constitute a non-Abelian gauge theory. One can take this process further, superimposing N_c D_3-branes (fig. 3.9).

The massless spectrum of this system consists of A_μ , ϕ^i , $i = 1, \ldots, 6$ along with the

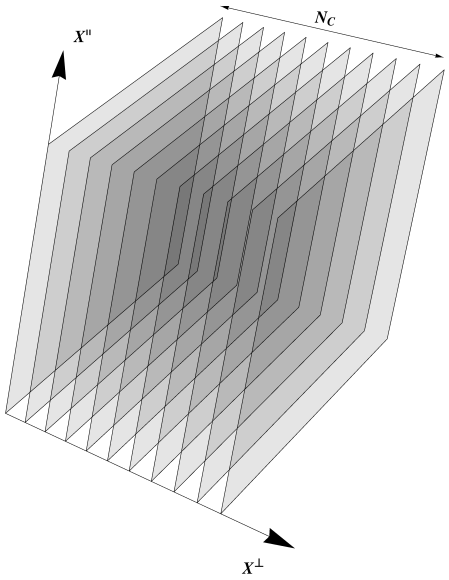

Figure 3.9: A stack of N_c D_3-branes.

super-partners - four Weyl fermions in the adjoint of $U(N_c)$. The low-energy effective action describing this system would then be

$$\mathcal{L} = -\frac{1}{g_{YM}^2} Tr \left\{ \frac{1}{4} F_{\mu\nu} F^{\mu\nu} + \frac{1}{2} D_\mu \phi^i D^\mu \phi^i + \left[\phi^i, \phi^j\right]^2 + fermions \right\} \tag{3.29}$$

where $g_{YM}^2 = 4\pi {g_s}^3$. In other words the low-energy effective action of a stack of D_3-branes correspond to an $\mathcal{N} = 4$, $U(N_c)^4$ Super-Yang-Mills theory in four dimensions ($d = 4$). This is a rather special and particularly interesting theory. For example it has an identically vanishing beta-function, i.e. it is scale invariant and its coupling constant does not run (can be set to an arbitrary value and it will remain there). This is a striking difference with ordinary, less symmetric Quantum Field Theories where the beta-functions are either positive or negative, but certainly non-zero.

The effective super-symmetric theory is governed by two parameters - N_c and g_{YM}. It is however convenient to combine them into the 'tHooft coupling $\lambda = g_{YM}^2 N_c$, as in the large-N_c limit the perturbative expansion of any amplitude $\mathcal{A}(g_{YM}, N_c)$ can be

[3]This can be derived from DBI action, describing a single D_p-brane with constant (or slowly varying) world-volume fields, re-summing the α' corrections [61].

[4]The $U(N_c)$ group is decomposed into $SU(N_c) \otimes U(1)$ with the $U(1)$ component describing the motion of the centre of mass of the brane system, essentially resulting in the more familiar $SU(N_c)$, $\mathcal{N} = 4$ SYM.

written as

$$\mathcal{A}(g_{YM}, N_c) = \sum_{g=0}^{\infty} N^{2-2g} f_g(\lambda) \tag{3.30}$$

where g is the genus of the diagram [67].

The content and the symmetries of this theory are highly relevant to the AdS/CFT conjecture as the constitute the first tests one can perform on it. As mentioned earlier the field content consists of A_μ, ϕ^i and λ^a_α, i.e. gauge field, scalars and fermions. The theory's symmetries are

- Conformal symmetry $SO(2,4)$, with generators P_μ, $L_{\mu\nu}$, D, K_μ
- R-Symmetry $SO(6) \sim SU(4)_R$
- Poincaré SUSY, with generators Q^a_α, $\bar{Q}_{a,\dot{\alpha}}$, $a = 1, \ldots, 4$
- Conformal SUSY, with generators $s_{\alpha,a}$, $\bar{S}^a_{\dot{\alpha}}$, $a = 1, \ldots, 4$

It should not be overlooked that the action (3.29) is an effective one and therefore receives corrections, which take the form of higher derivative terms. This corrections however are suppressed by factors of $E^2\alpha'$, where E is the energy scale. The brane-system also includes closed strings which interact with a strength $G_{10} \sim g_s^2 l_s^8$ meaning that interaction terms will come with factors of $E^8 G_{10}$ and can be neglected for small enough energies, i.e. for $E \ll \frac{1}{l_s}$. At this energy regime closed string do not interact (i.e. one is in the classical gravity regime) and they decouple from the open string sector which in this limit reduces to the $\mathcal{N} = 4$ SYM in $d = 4$. More formally the system's action is

$$S = S_{brane} + S_{bulk} + S_{interaction} \tag{3.31}$$

At the low energy regime $S_{interaction}$ can be neglected ($\sim \mathcal{O}(E^8 G_{10})$), S_{brane} is the $\mathcal{N} = 4$, $SU(N_c)$ SYM in $d = 3 + 1$ dimensions (plus corrections $\mathcal{O}(E^2 l_s^2)$) and S_{bulk} corresponds to $d = 10$ Minkowski gravity (plus corrections $\mathcal{O}(E^8 G_{10})$). More specifically as the number of branes grows the gravitational field they induce increases, since each one carries a finite tension. The resulting gravitational system, at low energies, is one that has been encountered before (3.25), i.e the $p = 3$ black $p-$brane solution of Type-IIB super-gravity. Noticing that $\int_{S^{8-p}} \star F_5 = Q \Rightarrow L^4 = 4\pi g_s N_c l_s^4$ which is the relevant scale. Therefore the gravitational system at $r \ll L$ (near-horizon limit) simplifies to $AdS_5 \times S^5$.

Given that it has been established that the brane-system gravitates, it is interesting to estimate at which point of the parameter space, the gravitational effects are

significant. In general an extended $p-$dimensional object will produce a gravitation field $\sim \frac{G_{10}M_{tot}}{r^{d-p-3}}$. Specifically for a D_3-brane this field is $\sim \frac{G_{10}N_cT_{(3)}}{r^4}$ or written in terms of the theory's parameters

$$gravity\ field\ for\ D_3-brane \sim \frac{g_sN_cl_s^4}{r^4} \tag{3.32}$$

This now allows one to estimate the regime of validity for each picture, i.e. that of the stack of branes embedded in flat space-time (fig. 3.9) or that of the black brane space-time (fig. 3.10). In particular one has

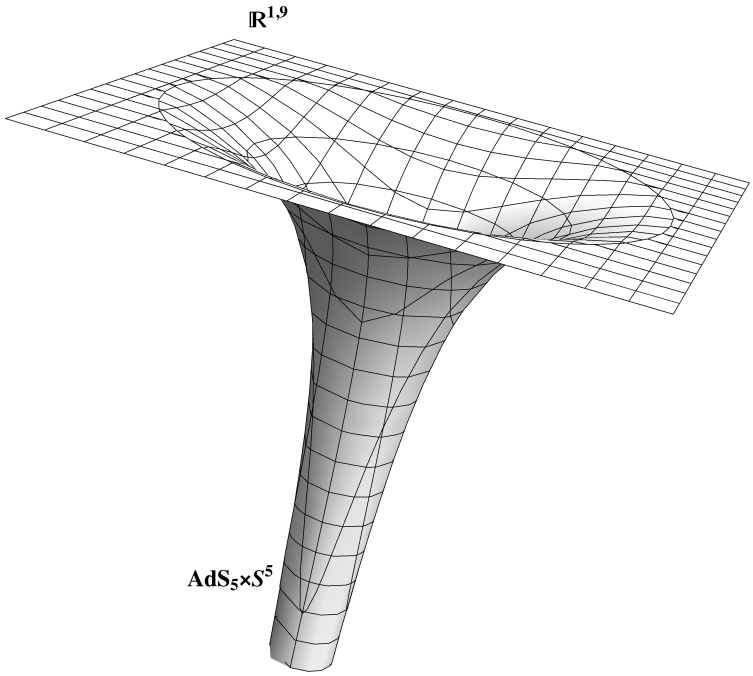

Figure 3.10: Ten-dimensional space-time from the closed-string or gravitational perspective for $g_sN_c \gg 1$ and $N_c \gg 1$. There are two distinct regimes - the near-horizon "throat" and the asymptotic boundary.

- for $g_sN_c \ll 1$ gravity corrections are of order $\mathcal{O}(1)$ for $r \ll l_s$
- for $g_sN_c \gg 1$ gravity corrections are of order $\mathcal{O}(1)$ for $r \gg l_s$

Beyond these limits there is another, more subtle one that needs to be examined, particularly if one intends to ignore quantum gravity corrections. Suppression of quantum effects occurs when $L \gg l_p \Leftrightarrow \frac{L^4}{l_p^4} \gg 1$. Recalling that $(l_p^{(10)})^8 = \frac{\hbar G_{10}}{c^3}$ and $G_{10} \sim g_s^2 l_s^8$ one sees that

$$\frac{L^4}{l_p^4} \sim \frac{g_sN_cl_s^4}{G_{10}^{1/2}} \sim N_c \tag{3.33}$$

It is then apparent that in order for quantum gravity effects to be negligible $N_c \gg 1$, independently of any other limits.

To summarize, the system consisting of a stack of N_c D_3-branes admits the following two descriptions

- at $g_s N_c \ll 1$ or equivalently $\lambda \ll 1$, the open-string picture prevails, giving rise to the effective action corresponding to a $\mathcal{N} = 4$ $SU(N_c)$ SYM
- at $g_s N_c \gg 1$ or equivalently $\lambda \gg 1$ and $N_c \gg 1$, the closed-string picture prevails, giving rise to the geometric black brane description

In principle both these descriptions should be valid for any value of the parameters λ, N_c and it is only a matter of one's ability to track the theory at each limit that these convenient effective theories emerge. In other words each of them is limited to a particular area of the parameter space (fig. 3.11), only because of the difficulty (and potentially inability) to compute the higher corrections necessary to extend the regime of validity.

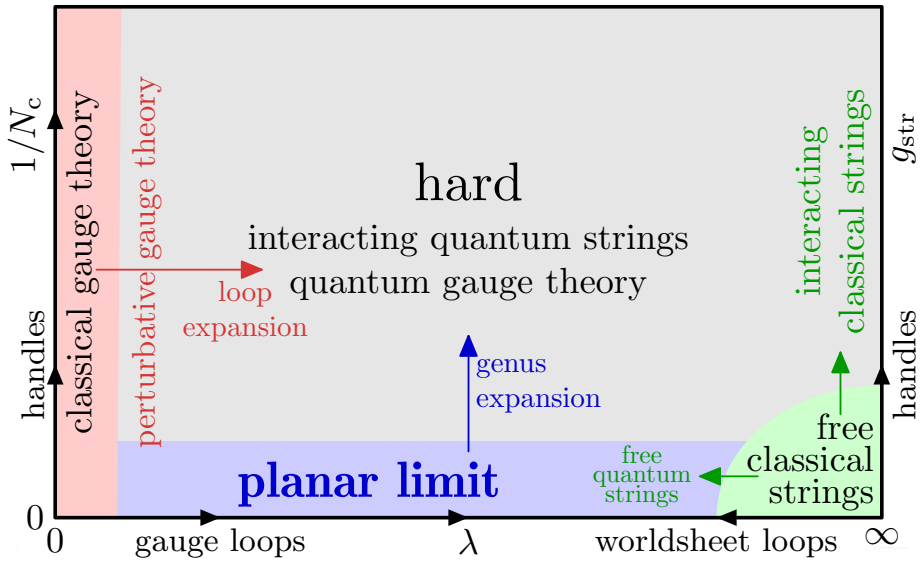

Figure 3.11: The Holographic parameter space. Figure taken from [1].

Having established the relation of this two regimes and the corresponding theories, as limits of a common starting point, one is now in a position to explicitly state the AdS/CFT conjecture:

The AdS/CFT Conjecture.

$$\mathcal{N} = 4 \ , \ SU(N_c) \ SYM \ @d = 3 + 1 = TypeIIB \ superstring \ theory \ on \ AdS_5 \times S^5 \tag{3.34}$$

This is a weak-strong duality, in which the relevant degrees of freedom are very different - on the one side they are gauge ones and on the other side they are gravitational. The characterization of this duality as Holographic, stems from the fact that the gravity side lives on a five (in fact $5+5$) dimensional space-time while the gauge side lives on the boundary of this space-time, in one dimension less, i.e. $d = 3+1$. In a more formal way one can write down the duality using the partition functions on each side

$$\mathcal{Z}_{d=3+1,\mathcal{N}=4SYM}\left[J\right] = \mathcal{Z}_{TypeIIB@AdS_5\times S^5}\left[J\right] \tag{3.35}$$

The very first test one performs on this duality, as mentioned earlier, is to check if the symmetries on the two sides match. As seen in table 3.2 that appears to be the case.

$\mathcal{N}=4$ SYM $d=3+1$	$AdS_5 \times S^5$
$SO(4,2)$ (conformal) $\times$ $SO(6)_R$ (R-symmetry)	$SO(4,2) \times SO(6)$ (isometries)
$SL(2,\mathbb{Z})$	$SL(2,\mathbb{Z})$

Table 3.2: The symmetries of the theories on the two sides of the Holographic duality.

Another revealing comparison that can be made, is that of the entropy density (s) on the two sides. As seen in [68] using Holographic techniques one gets

$$s_H = \frac{\pi^2}{2} N_c^2 T^3 \tag{3.36}$$

This should match the entropy density for $\mathcal{N}=4$ SYM at the $\lambda \to \infty$, $N_c \to \infty$ limit. From standard perturbative approaches [35, 36] (i.e. $\lambda \ll 1$) it is known that

$$s_{YM}|_{\lambda\to 0} = \frac{4\pi^2}{90} T^3 \left(N_B + \frac{7}{8} N_F\right) \tag{3.37}$$

where N_B and N_F are the number of bosons and fermions respectively. For the particular field content of $\mathcal{N}=4$ SYM this reduces to

$$s(\lambda \to 0) = \frac{2\pi^2}{3} N_c^2 T^3 \tag{3.38}$$

This expression though receives λ correction, which one necessarily needs to include in order to depart from the strict $\lambda \to 0$ limit. In fact as seen in [69, 70] for $\lambda > 0$

$$s(\lambda) = \frac{2\pi^2}{3} N_c^2 T^3 f(\lambda) \tag{3.39}$$

where

$$f(\lambda) = 1 - \frac{3}{2\pi^2}\lambda + \frac{3+\sqrt{2}}{\pi^3}\lambda^{\frac{3}{2}} + \dots \tag{3.40}$$

Similarly in order to depart from the strict $\lambda \to \infty$ limit, on the other side, one needs to include $\frac{1}{\lambda}$ corrections. This is done in [68], resulting in

$$f(\lambda) = \frac{3}{4} + \frac{45}{32}\zeta(3)\lambda^{-\frac{3}{2}} + \dots \tag{3.41}$$

It is therefore presumed that $f(\lambda)$ interpolates between the two limiting values $f(0) = 1$ and $f(\infty) = \frac{3}{4}$.

3.3 Holographic toolbox

Having stated the AdS/CFT conjecture, established its connections to String Theory and glossed over its derivation, the next step is to examine how one can make practical use out of it. To do that one notices that on the right-hand-side of eq. (3.35) saddle point approximation can be used to give

$$\mathcal{Z}_{IIB\ ST@AdS_5\times S^5} \overset{saddle}{\underset{point}{\simeq}} \exp\left[-S_{IIB\ SUGRA}\right] + \mathcal{O}(\frac{1}{N_c^2}, \lambda^{-\frac{3}{2}}) \tag{3.42}$$

where $\mathcal{O}(\frac{1}{N_c^2})$ corresponds to quantum corrections and $\mathcal{O}(\lambda^{-\frac{3}{2}})$ to higher-derivative terms. This is a much more tractable theory and can even be consistently truncated down to regular gravity. Given this approximation one can then compute expectation values of operators $\langle O(x_1)\dots O(x_n)\rangle_{YM}$ in the dual theory since

$$\langle \exp\left[\int d^4x JO\right]\rangle_{YM} = \exp\left[-S_{grav}[J]\right] \tag{3.43}$$

The question then becomes what plays the role of J on the gravity side. For this purpose it is instructive to recall that the string coupling constant $g_s = 4\pi g_{YM}^2$ is related to the expectation value of the dilaton at the AdS boundary, i.e. $g_s = \exp\left[\langle\phi_\infty\rangle\right]$. Deforming the gauge theory (on the boundary), meaning that one changes the coupling constant is equivalent to changing the boundary value of a bulk field, namely the dilaton. This can be extended so that generically a deformation of the YM theory is of the form

$$S_{YM} \to S_{YM} + \int d^4x \phi(x) O(x) \tag{3.44}$$

where $O(x)$ is a local, gauge-invariant operator (e.g. $O = TrF^2$) and $\phi(x)$ is a source. Then

$$\phi(x) = \Phi_{bulk}|_{\partial AdS}(x) = \lim_{r\to\infty} \Phi_{bulk}(r, x) \tag{3.45}$$

This process leads quite naturally to the field-operator correspondence. That is for every boundary operator $O(x)$ there is a bulk field, the boundary value of which acts as a source for that operator. In some cases where both gravity and boundary theories are well-controlled and fully understood this field-operator matching comes directly (e.g. DBI action can help in these identifications). This however is not always possible in which case a more phenomenological approach is needed. For example one looks for fields such that the quantum numbers of the global symmetries in both sides match. For conserved currents such as $O^{\mu}(x) = J^{\mu}(x)$ or $O^{\mu\nu}(x) = T^{\mu\nu}(x)$ the appropriate terms are easy to identify, namely

$$\int d^4x A_{\mu}(x) J^{\mu} \rightarrow A_{\mu}(x,r) \ @d = 5 \tag{3.46}$$

$$\int d^4x g_{\mu\nu}(x) T^{\mu\nu}(x) \rightarrow g_{\mu\nu}(x,r) \ @d = 5 \tag{3.47}$$

$$\int d^4x \phi(x) O(x) \rightarrow \phi(x,r) \ @d = 5 \tag{3.48}$$

Out of these considerations a Holographic "dictionary" emerges

$\hat{O}$ (boundary operator)	$\delta\phi$ (bulk field)
$T_{\mu\nu}$	$\delta g_{\mu\nu}$
J_{μ}	A_{μ}
TrF^2	ϕ

Table 3.3: Operator-field mapping within the Holographic dictionary.

One therefore is equipped with a tool to compute strongly-coupled (in fact infinitely-coupled) correlators of the boundary theory, the most important of which is the two-point (Green's) function (or propagator). This is achieved by taking functional derivatives of the (on-shell) gravitational action with respect to the boundary values of the field corresponding to the operator, the correlator of which one wants to compute. Since in most Holographic calculations the goal (at least initially) is the computation of some theory's propagators, the discussion about a subtlety is in order. When working in Euclidean signature the propagator G_E is uniquely defined, without any ambiguity.

$$G_E(k_E) = \int d^4x_E \exp\left[\imath k_E x_E\right] \langle T_E \hat{O}(x_E) \hat{O}(0) \rangle_T \tag{3.49}$$

For finite temperature this becomes the Matsubara propagator defined at $\omega_E = 2\pi T n$ for boson and $\omega_E = 2\pi T(n + 1/2)$ for fermions [35]. In fact the first Holographic calculations were done in Euclidean signature [7].

It was soon realized though that this poses some difficulties particularly if one tries to compute non-zero temperature and chemical potential correlators as well as real-time dynamics (small deviations from equilibrium). In principal one would expect that this could be achieved through an analytic continuation, however this poses problems since there is not a unique way to do this continuation. Additionally in many cases of practical interest propagators can only be calculated numerically, in which case it is not clear how one could analytically continue a numerical function. These limitations were realized and addressed in [71, 72] which laid the foundations for real-time Holography. Moreover this opened the way for a more phenomenological approach to Holography.

From ordinary Quantum Field Theory (at finite temperature) it is already known that [35, 36] there are four distinct propagators in Minkowski signature, namely

$$G^R(k) = \imath \int d^4x \exp[-\imath kx]\Theta(t)\langle\Big[\hat{O}(x), \hat{O}(0)\Big]\rangle_T \tag{3.50}$$

$$G^A(k) = \imath \int d^4x \exp[-\imath kx]\Theta(-t)\langle\Big[\hat{O}(x), \hat{O}(0)\Big]\rangle_T \tag{3.51}$$

$$G(k) = \frac{1}{2}\int d^4x \exp[-\imath kx]\langle\hat{O}(x)\hat{O}(0) + \hat{O}(0)\hat{O}(x)\rangle_T \tag{3.52}$$

$$G^F(k) = -\imath \int d^4x \exp[-\imath kx]\langle T\hat{O}(x)\hat{O}(0)\rangle_T \tag{3.53}$$

where the expectation values are $\langle\hat{A}\rangle := Tr\hat{\rho}\hat{A}$, with $\hat{\rho} = \exp[-\beta\hat{H} + \mu_A\hat{Q}_A]$ and $T(\ldots)$ is the time-ordering. In the order that they appear these are the Retarded, Advanced, Wightman and Feynman propagators, respectively. It is important to note that these are not all independent. In fact using the spectral representation of the propagators one can write

$$G^F = \frac{1}{2}\left(G^R + G^A\right) - \imath G \tag{3.54}$$

$$G(k) = -\coth\frac{\omega}{2T}\Im G^R \tag{3.55}$$

$$G^F(k) = \Re G^R + \imath\coth\frac{\omega}{2T}\Im G^R \tag{3.56}$$

$$G^A(k) = G^R(-k) = (G^R)^* \tag{3.57}$$

and moreover at the zero-temperature limit $T \to 0$, $G^F(k) = ReG^R + \imath sgn\omega ImG^R$. Out of this set of Green's functions causality picks out the retarded one, because, as seen in the Linear Response section, one does not want a response prior to the appearance of the external stimulus.

All the elements are in place now to write down the "recipe" for Holographic calculation of correlation functions

- identify the bulk field $\delta\phi$ corresponding to the operator $\hat{O}$ of interest
- solve the equations of motion (to linear order if one is interested in Linear Response) for $\delta\phi$ with the boundary condition that $\phi(boundary) = J$
- compute the on-shell action $S_{grav}[J]$
- compute correlators by taking functional derivatives $\frac{\delta}{\delta J}\exp\left[-S_{grav}[J]\right]$

This concludes the recipe for the cases of Euclidean signature. In order to compute real-time Green's functions this recipe needs to be amended to

- Fourier decompose the bulk field $\delta\phi(r,x)\int d^dk\exp[\imath k\cdot x]f_k(r)\phi_0(k)$
- solve equations of motion with boundary conditions $f_k(r\to\partial)=1$ and impose incoming wave conditions at the horizon
- write the on-shell action in the form $S=\int^d k\phi_0(-k)\ \mathcal{F}(k,r)\phi_0(k)|_{r\to\partial}^{r=r_H}$
- extract the retarded Green's function $G_R(k)=-2\mathcal{F}(k,r)|_{r\to\partial}$

This section will end by presenting a simple example of such a Holographic calculation, which will smoothly transition to one of the most celebrated results of Holography, namely the calculation of the ratio of shear viscosity over the entropy density $\frac{\eta}{s}$.

The background will be an AdS space-time,

$$ds^2=\frac{r^2}{L^2}\left(-dt^2+dx_1^2+dx_2^2dx_3^2\right)+\frac{L^2}{r^4}dr^2+L^2d\Omega_5^2 \tag{3.58}$$

or making the radial coordinate transformation $r\to z=\frac{L^2}{r}$[5]

$$ds^2=\frac{L^2}{z^2}\left(dz^2+dx_1^2+dx_3^2+dx_4^2\right) \tag{3.59}$$

where the sphere part is left out. Now consider in this background a massive scalar field describe by the action

$$S_E=\frac{\pi^2L^8}{4\kappa_{10}^2}\int\frac{d^4xdz}{z^3}\left[(\partial_z\phi)^2+(\partial_i\phi)^2+\frac{m^2L^2}{z^2}\phi^2\right] \tag{3.60}$$

Following the procedure described previously, one first Fourier decomposes the field in

$$\phi(z,k)=\int\frac{d^4k}{(2\pi)^4}\exp[\imath kx]f_k(z)\phi_0(k) \tag{3.61}$$

[5]Note that in these coordinates the AdS boundary $r\to\infty$ is now at $z=0$.

The equations of motion are then

$$f_k''(z) - \frac{3}{z} f_k'(z) - (k_E^2 + \frac{m^2 L^2}{z^2}) f_k(z) = 0 \tag{3.62}$$

with the boundary condition $f_k(z \to 0) = 1$ as well as the demand for regularity. The on-shell action then becomes

$$S_E = \frac{\pi^3 L^8}{4\kappa_{10}^2} \int_\epsilon^\infty \int \frac{d^4k}{(2\pi)^4} d^4k' \frac{1}{z} \delta(k+k') \left[\partial_z f_k \partial_z f_{k'} + kk' f_k f_{k'} + \frac{m^2 L^2}{z^2} f_k f_{k'} \right] \phi_0(k) \phi_0(k') \tag{3.63}$$

where ϵ is a small number setting the lower end of the integral close to but not on the AdS boundary. This is because divergences emerge as one approaches the boundary that need to be carefully renormalized, giving rise to additional terms in the action (i.e. Holographic counter-terms). This is the subject of Holographic Renormalization discussed in [73, 74], but will not be pursued here as it doesn't affect the results. The solutions of eq. (3.62) are of the form

$$f_k(z) = A z^\nu I_\nu(kz) + B z^\nu K_\nu(kz) \tag{3.64}$$

where $k = |k_E|$, $\nu = (4 + m^2 L^2)^{1/2}$ and I, K are the modified Bessel functions of the first and second kind (following the standard Frobenious theory for Ordinary Differential Equations (ODE) [75]). The asymptotic behaviour of the Bessel functions, i.e. $K_\nu(x \to \infty) \sim \exp[-x]$ while $I_\nu(x \to \infty) \sim \exp[x]$, allows one, by demanding finiteness to exclude the latter. Hence the solution is (for the massless case, which means $\nu = 2$)

$$f_k(z) = \frac{z^2 K_2(kz)}{\epsilon^2 K_2(k\epsilon)} \tag{3.65}$$

such that $f_k(\epsilon) = 1$. Plugging this back into the on-shell action, it can be written as

$$S_E = \frac{\pi^3 L^8}{4\kappa_{10}^2} \int \frac{d^4k d^4k'}{(2\pi)^4} \delta(k+k') \phi_0(k) \phi_0(k') \left. \frac{f_{k'} \partial_z f_k(z)}{z^3} \right|_\epsilon^\infty = \int \frac{d^4k d^4k'}{(2\pi)^8} \phi_0(k) \phi_0(k') \left. \mathcal{F} \right|_\epsilon^\infty \tag{3.66}$$

which allows one to compute the two-point function

$$\begin{aligned} \langle \hat{O}(k) \hat{O}(k') \rangle &= \frac{1}{\mathcal{Z}} \left. \frac{\delta^2 \mathcal{Z}[\phi_0]}{\delta\phi_0(k) \delta\phi_0(k')} \right|_{\phi_0 = 0} = -2\mathcal{F}(z, k, k')|_\epsilon^\infty \\ &= -(2\pi)^4 \delta(k + k') \frac{\pi^3 L^8}{2\kappa_{10}^2} \left. \frac{f_{k'} \partial_z f_k}{z^3} \right|_\epsilon^\infty \end{aligned} \tag{3.67}$$

or recalling that $\kappa_{10} = 2\pi^{5/2} \frac{L^4}{N_c}$, the Euclidean propagator becomes

$$\langle \hat{O}(k) \hat{O}(k') \rangle_E = \frac{N_c^2}{8\pi^2} \delta(k + k') \frac{f'(\epsilon)}{\epsilon^3} \tag{3.68}$$

in the limit $\epsilon \to 0$. In this limit, properly treating the Holographic counter-terms, and neglecting contact ones (non singular terms), one finds that

$$\lim_{\epsilon\to 0} \frac{f'}{\epsilon^3} = -\frac{k^4}{8} \ln k^2 \tag{3.69}$$

Hence

$$\langle \hat{O}(k)\hat{O}(k')\rangle_E = -\frac{N_c^2}{64\pi^2}(2\pi)^4 \delta(k+k') k_E^2 \ln k_E^2 \tag{3.70}$$

There is an interesting observation to be made at this point. From perturbative calculations one knows that

$$\langle \hat{O}(x)\hat{O}(y)\rangle_{pert} \sim \frac{1}{|x-y|^8} =: \frac{1}{|x-y|^{2\Delta_0}} \tag{3.71}$$

resulting in $\Delta_0 = 4$. By Fourier transforming the Holographic result back into coordinate space one

$$\langle \hat{O}(k)\hat{O}(k')\rangle \sim \frac{N_c^2}{|x-y|^8} \tag{3.72}$$

yielding $\Delta(\lambda = 0) = \Delta(\lambda = \infty) = 4$. This is consistent with what is known for $\mathcal{N} = 4$ SYM (non-renormalization theorems), which is scale invariant. However not all $\mathcal{N} = 4$ operators are protected against running so generically one expects $\Delta = \Delta(\lambda)$ to be a non-trivial function.

The calculation presented so far has been in Euclidean signature. The Minkowski version will now be presented. The background metric is now

$$ds^2 = \frac{L^2}{z^2}\left[dz^2 + \eta_{\mu\nu} dx^\mu dx^\nu\right] \tag{3.73}$$

where $\eta_{\mu\nu} = diag[- + \ldots +]$. The Fourier decomposition is

$$\phi(z,x) = \int \frac{d^4k}{(2\pi)^4} \exp[-\imath\omega t + \imath kx] f_k(z)\phi_0(k) \tag{3.74}$$

the action

$$S = -\frac{\pi^3 L^8}{4\kappa_{10}^2} \int d^4x \int_\epsilon^\infty \frac{dz}{z^3} \left\{ (\partial_z \phi)^2 + \eta^{\mu\nu}\partial_\mu\phi\partial_\nu\phi + \frac{m^2L^2}{z^2}\phi^2 \right\} \tag{3.75}$$

the equations of motion

$$f_k''(z) - \frac{3}{z} f_k'(z) - \left(k^2 + \frac{m^2L^2}{z^2}\right) f_k = 0 \tag{3.76}$$

but note that here k^2 can be either positive or negative. The on-shell action becomes

$$S = \int \frac{d^4k}{(2\pi)^4} \left(\mathcal{F}(k,\infty) - \mathcal{F}(k,\epsilon)\right) \phi_0(-k)\phi_0(k) \tag{3.77}$$

where $\mathcal{F}(k,z) = -\frac{\pi^3 L^8}{4\kappa_{10}^2}\frac{f_{-\imath}\partial_z f_k}{z^3}$. It should be mentioned here that for space-like momenta $k^2 > 0$, the situation is similar to the Euclidean case. For time-like momenta $k^2 < 0$ requiring non-diverging solutions, results in usual instead of modified Bessel functions. In particular setting $q = \sqrt{-k^2}$

$$f_k(z) = \frac{z^2 H_\nu^{(1)}(qz)}{\epsilon^2 H_\nu^{(1)}(q\epsilon)}\ ,\ \omega > 0 \tag{3.78}$$

$$f_k(z) = \frac{z^2 H_\nu^{(2)}(qz)}{\epsilon^2 H_\nu^{(2)}(q\epsilon)}\ ,\ \omega < 0 \tag{3.79}$$

with H_ν being the Hankel function $H_\nu^{(1,2)} = J_\nu \pm \imath Y_\nu$. Incoming wave conditions need to be imposed now. To do this notice first that the asymptotic behaviour of Hankel functions is

$$\lim_{z\to\infty} H_\nu^{(1,2)}(z) = \sqrt{\frac{2}{\pi z}}\exp\left[\pm\imath\left(z - \frac{\nu\pi}{2} - \frac{\pi}{4}\right)\right] \tag{3.80}$$

and therefore imposing incoming conditions at $z \to \infty$ means that for $\omega > 0$ picks out $H_\nu^{(1)}$ and for $\omega < 0$, $H_\nu^{(1)}$. The incoming conditions also pick out the retarded Green's function G^R. Putting all these together one gets

$$G^R(k) = \frac{N_c k^4}{64\pi^2}\left(\ln|k^2| - \imath\pi\Theta(-k^2)sgn\omega\right) \tag{3.81}$$

which a posteriori can be easily checked to be the proper analytic continuation of the Euclidean propagator G_E.

The above calculation can be easily extended to higher dimensions, where the metric is

$$ds_{d+1}^2 = \frac{L^2}{z^2}\left(dz^2 + \eta_{\mu\nu}dx^\mu dx^\nu\right) \tag{3.82}$$

and the equations of motion

$$z^{d+1}\partial_z\left(z^{1-d}\partial_z\phi\right) - k^2 z^2\phi - m^2 L^2\phi = 0 \tag{3.83}$$

The solution near the boundary ∂AdS ($z \to 0$) can be written as [6]

$$\phi(z,k) = \mathcal{A}(k)z^{d-\Delta} + \ldots + \mathcal{B}(k)z^\Delta + \ldots \tag{3.84}$$

where $\Delta = \frac{d}{2} + \nu$, with $\nu = \left(\frac{d^2}{4} + m^2L^2\right)^{1/2}$. This "anomalous" dimension, that controls whether a mode is normalizable or non-normalizable [7], raises an interesting

[6] This comes again from Frobenious theory [30].

[7] Normalizability is determined with respect to the AdS inner product that is defined, according to [76], as $(\phi_1,\phi_2) = -\imath\int_{\Sigma_t} dtd^dx\sqrt{-g}g^{tt}(\phi_1^*\partial_t\phi_2 - \phi_2\partial_t\phi_1^*)$.

issue. It has to be real and that can be achieved when $m^2L^2 \geq -\frac{d^2}{4}$, i.e there is a small negative window of mass that is allowed. This is the well-known Breitenlohner-Freedman bound [77]. The modes with masses above the BF bound are split into two categories

- $-\frac{d^2}{4} \leq m^2L^2 \leq -\frac{d^2}{4}+1$
- $-\frac{d^2}{4}+1 \leq m^2L^2$

In the first case both $z^{d-\Delta}$ and z^{Δ} are normalizable. In the case where the mass is unbounded from above, i.e . $m^2L^2 \geq -\frac{d^2}{4}+1$, the term $\phi \sim z^{d-\Delta}$ is non-normalizable while the term $\phi_2 \sim z^{\Delta}$ is normalizable. The non-normalizable term (at the boundary) plays the role of the source for the boundary operator operator $\hat{O}$ whereas the normalizable mode correspond to the its expectation value $\langle\hat{O}\rangle$. In particular on the boundary

$$S_{\partial AdS} \to S_{\partial AdS} + \int d^dx J(x)O(x) \tag{3.85}$$

with

$$J(x) = \phi|_{\partial AdS} = \lim_{z\to 0} z^{\Delta-d}\phi(z,x) \tag{3.86}$$

In other words if the bulk field ϕ correspond to the boundary operator $\hat{O}$, using eq. (3.84), $J \leftrightarrow \mathcal{A}$ and $\langle\hat{O}\rangle \leftrightarrow \mathcal{B}$.

This section will end with the presentation of the Holographic hydrodynamical limit, that will allow a smooth transition to the Condensed Matter applications of Holography (as it actually happened historically). For this purpose the prototypical example of $\mathcal{N}=4$ SYM at finite temperature, will be used. The dual background to this theory, as seen above, is the black brane configuration

$$d_5^2 = \frac{(\pi TL)^2}{u}\left(-f(u)dt^2 + d\boldsymbol{x}^2\right) + \frac{L^2}{4f(u)u^2}du^2 \tag{3.87}$$

with $u = \frac{r_0^2}{r^2}$ and $T = \frac{r_0}{\pi L^2}$. In order to study the hydrodynamical limit, one needs to perturb the system (remaining close to equilibrium. For this purpose one expands the gravity field as $g_{\mu\nu} = g^{(0)}_{\mu\nu} + \delta g_{\mu\nu}(t,\boldsymbol{x},u)$. It is then straightforward to write the linearised version of Einstein's equation

$$R_{\mu\nu} = R^{(0)}_{\mu\nu} + R^{(1)}_{\mu\nu} + \ldots = \frac{2\Lambda}{3}\left(g^{(0)}_{\mu\nu} + \delta g_{\mu\nu} + \ldots\right) \tag{3.88}$$

Using the symmetries of the system one can pick, without loss of generality, the direction into which the metric perturbation propagates, the presence of which breaks rotational symmetry. Fortunately the resulting system still possesses enough symmetry to split the metric perturbations into three families

- δg_{xy}, called tensor channel
- $\{\delta g_{xt},\ \delta g_{xt},\ \delta g_{ty},\ \delta g_{yz}\}$, called vector (or shear) channel
- $\{\delta g_{tz}, \delta g_{ii}\}$, called scalar (or sound) channel

assuming that the perturbation travels along the z direction. Since the elements of each channel cannot mix with any other, Einstein's equations also split along these channels, significantly simplifying treatment of the system. Focusing, for now, on the shear channel, the relevant Einstein's equations are

$$H_t' + \frac{\bar{q}}{\bar{\omega}} f H_z' = 0 \tag{3.89}$$

$$H_t'' - \frac{1}{u} H_t' - \frac{\bar{\omega}\bar{q}}{uf^2} H_z - \frac{\bar{q}^2}{uf} H_t = 0 \tag{3.90}$$

$$H_z'' - \frac{1+u^2}{uf} H_z' + \frac{\bar{\omega}^2}{uf^2} H_z + \frac{\bar{\omega}\bar{q}}{uf^2} H_t = 0 \tag{3.91}$$

where $H_t := \frac{u\delta g_{tx}}{(\pi TL)^2}$, $H_z := \frac{u\delta g_{zx}}{(\pi TL)^2}$, $\bar{\omega} = \frac{\omega}{2\pi T}$ and $\bar{q} = \frac{q}{2\pi T}$. Considering that one wants to compute correlation functions of gauge invariant operators and given that individual metric components are not invariant under diffeomorphism transformations (which are the gauge transformations of gravity) it is necessary to combine the fundamental degrees of freedom into gauge invariant ones. For this case one defines

$$Z_1 := \bar{q} H_t + \bar{\omega} H_z \tag{3.92}$$

Taking the Lie derivative of Z_1 one sees that $\mathcal{L}_\xi Z_1 = 0$ [8]. The shear Einstein's equations can be combined into a single equation for this gauge invariant degree of freedom, namely

$$Z_1'' + \left\{ \frac{(\bar{\omega}^2 - \bar{q}^2 f) f - u\bar{\omega}^2 f'}{uf(\bar{q}^2 f - \bar{\omega}^2)} \right\} Z_1' + \left\{ \frac{\bar{\omega}^2 - \bar{q}^2 f}{uf^2} \right\} Z_1 = 0 \tag{3.93}$$

Near the boundary ($u = 0$) the solution of this equation can be expanded as $Z_1 = \mathcal{A}_1(1 + \ldots) + \mathcal{B}_1(u^2 + \ldots)$. As seen before, once one has this expansion extracting the Green's functions is straightforward, i.e.

$$G_1(\bar{\omega}, \bar{q}) = -\pi^2 N_c^2 T^4 \frac{\mathcal{B}_1(\bar{\omega}, \bar{q})}{\mathcal{A}_1(\bar{\omega}, \bar{q})} \tag{3.94}$$

At this stage one can impose the hydrodynamical limit, by looking for solutions G perturbatively in $\bar{\omega}$, $\bar{q}$. In other words the hydrodynamic limit is valid for small $\bar{\omega}$

[8] Recall that $\mathcal{L}_\xi g_{\mu\nu} = \nabla_\mu \xi_\nu + \nabla_\nu \xi_\mu$.

and $\bar{q}$. To see why this is the case, first notice that for finite-temperature $\mathcal{N}=4$ SYM there is only one scale, that of the temperature T. Therefore the free mean path scales like $l_{mfp} \sim \frac{1}{T}$. In terms of the free mean path the hydrodynamic limit is $l_{mfp} \ll l \ll L$. It is then apparent that this limit is equivalent to $q l_{mfp} \ll 1$ or $\frac{q}{2\pi T} \ll 1$ and similarly $\frac{\omega}{T} \ll 1$. One then writes Z_1 as a series over $\bar{\omega}$ and $\bar{q}$

$$Z_1(u) = C_1 f(u)^{-\imath\bar{\omega}/2}\left(1 + \frac{\imath\bar{q}^2 f}{2\bar{\omega}} + \mathcal{O}(\bar{\omega}^2, \bar{q}^2, \bar{\omega}\bar{q})\right) \tag{3.95}$$

Imposing Dirichlet boundary conditions on the boundary, i.e. $Z_1(0) = 0$, yields the dispersion relation

$$\omega = -\frac{\imath}{4\pi T} q^2 + \mathcal{O}(q^4) \tag{3.96}$$

This is the Holographic result for $\mathcal{N}=4$ SYM at $\lambda \to \infty$ and $N_c \to \infty$. From general dissipative hydrodynamics it is known that from the dispersion relation one can extract the diffusion coefficient D, since $\omega = \imath D q^2 + \ldots$. Hence the Holographic prediction is that $D = \frac{1}{4\pi T}$. It is also the case that $D = \frac{\eta}{\epsilon + p}$, where η is the shear viscosity, ϵ the energy density and p the pressure. For a system where the chemical potential vanishes, i.e.$\mu = 0$, thermodynamic relations dictate that $\epsilon + p = sT$, where s is the entropy density. Therefore $D = \frac{\eta}{sT}$. Combining this with the Holographic result one gets the famous result [71, 78].

$$\frac{\eta}{s} = \frac{1}{4\pi} \tag{3.97}$$

This has been a very impactful result and it has been conjectured that it constitutes a lower bound for a certain class of Holographic theories. Its corrections have also been studied quite extensively and it is known that to first λ correction it is

$$\frac{\eta}{s} = \frac{\hbar}{4\pi k_B}\left(1 + \frac{15\zeta(3)}{\lambda^{3/2}}\right) \tag{3.98}$$

where all the units have been put back in explicitly. In general it is expected that at $N_c \to \infty$ viscosity itself (that is extracting $s = \frac{\pi^2}{2} N_c^2 T^3$) is $\eta(\lambda) = f(\lambda) N_c^2 T^3$, where $f(\lambda)$ is a function interpolating between $\pi/8$ at $\lambda \gg 1$ and $\lambda^{-2} \ln^{-1} \frac{1}{\lambda}$ at $\lambda \ll 1$, i.e. between the strongly-coupled and the perturbative results.

3.4 AdS-CMT

In the final section of this chapter further Holographic calculations pertaining to Condensed Matter systems will be presented.

Sound

The starting point will be sound propagation. This is a natural point to begin, since it is closely related to the calculation of shear viscosity. In particular the underlying system is the same and one only changes the channel studied [21]. The background metric is again

$$ds^2 = \frac{(\pi TL)^2}{u}\left(-f(u)dt^2 + dx^2 + dy^2 + dz^2\right) + \frac{L^2}{4u^2 f(u)}du^2 \tag{3.99}$$

As expected by the listing of the fundamental components $\delta g_{\mu\nu}$ in the sound channel above, the linearised Einstein's equation are more numerous and less simple. In particular (using radial gauge where $\delta g_{u\mu} = 0$) and reducing to the independent set one has

$$H''_{tt} - \frac{3u}{f}H'_t - H''_{ii} + \frac{u}{f}H'_{ii} = 0 \tag{3.100}$$

$$\bar{\omega}\left(H'_{ii} + \frac{u}{f}H_{ii}\right) + \bar{q}\left(H'_{tz} + \frac{2u}{f}H_{tz}\right) = 0 \tag{3.101}$$

$$\bar{q}\left(fH'_{tt} - uH_{tt}\right) + \bar{\omega}H'_{tz} - \bar{q}H'_{aa} = 0 \tag{3.102}$$

$$H'_{ii} - \frac{3fH'_{tt}}{3-u^2} - \frac{2}{f(3-u^2)}\left(\bar{\omega}^2 H_{ii} + 2\bar{\omega}\bar{q}H_{tz} + \bar{q}^2 f(H_{tt} - H_{aa})\right) = 0 \tag{3.103}$$

where $H_{tt} := \frac{u}{f(\pi TL)^2}\delta g_{tt}$, $H_{tz} := \frac{u}{(\pi TL)^2}\delta g_{tz}$, $H_{ij} := \frac{u}{(\pi TL)^2}\delta g_{ij}$, $H_{aa} : H_{xx} + H_{yy}$ and $H_{ii} := H_{aa} + H_{zz}$. The equations of motion still have some residual gauge symmetry, thus one can construct solution to them by acting on the trivial solution $H_{\mu\nu} = 0$ with the generating transformations of said symmetry. This are by construction pure gauge solutions and are linear combinations of the terms

$$H^I_{tz} = \bar{\omega} \tag{3.104}$$

$$H^I_{zz} = -2\bar{q} \tag{3.105}$$

$$H^{II}_{tt} = -2\bar{\omega} \tag{3.106}$$

$$H^{II}_{tz} = \bar{q}f \tag{3.107}$$

$$H^{III}_{tt} = \frac{1 + u^2 + 2\bar{\omega}^2 u}{\sqrt{f}} \tag{3.108}$$

$$H^{III}_{tz} = -\bar{q}\bar{\omega}\arcsin u - \bar{q}\bar{\omega}u\sqrt{f} \tag{3.109}$$

$$H^{III}_{aa} = -2\sqrt{f} \tag{3.110}$$

$$H^{III}_{zz} = 2\bar{q}^2 \arcsin i - \sqrt{f} \tag{3.111}$$

as found in [21]. Proceeding further one employs the standard Frobenius procedure, on top of which the small frequency and long wavelength ($\bar{\omega} \ll 1$ and $\bar{q} \ll 1$) limit is

taken, along with the incoming boundary conditions, one gets (to second order in $\bar{\omega}$ and $\bar{q}$)

$$H_{tt} = \frac{\bar{q}^2}{3}(1-u) \tag{3.112}$$

$$H_{ii} = \bar{q}^2(1-u) \tag{3.113}$$

$$H_{tz} = -\imath\frac{\bar{q}}{2}(1-u^2) + \frac{\bar{\omega}\bar{q}}{2}u(1-u) - \frac{\bar{\omega}\bar{q}}{4}(1-u^2)\ln\frac{2(1-u)}{1+u} \tag{3.114}$$

$$\begin{aligned} H_{aa} = 1 &- \imath\frac{\bar{\omega}}{2}\ln\frac{1-u^2}{2} - \frac{\bar{\omega}^2}{8}\ln^2(1-u) - \frac{\bar{\omega}^2}{4}\ln(1-u)\ln\frac{1+u}{2} \\ &+ \frac{2}{3}\bar{q}^2(1-u) + \frac{3\bar{\omega}^2+\bar{q}^2}{3}\ln\frac{1+u}{2} + \frac{\bar{\omega}^2}{8}\ln^2\frac{1+u}{2} - \frac{\bar{\omega}^2}{2}Li_2\frac{1-u}{2} \end{aligned} \tag{3.115}$$

To these solutions the pure gauge one can be added, yielding another solution. The general solution can then be deduced and given that the on-shell action can be computed. The action of the system, including the appropriate counter-terms [73], is

$$S = \frac{\pi^3 L^5}{2\kappa_{10}^2}\int_0^1 du d^4x\sqrt{-g}\,(R-2\Lambda) + 2\int d^4x\sqrt{-h}K - \frac{6}{L}\int d^4x\sqrt{-h} \tag{3.116}$$

where $h_{\mu\nu}$ is the induced metric (and h its determinant) and K the extrinsic curvature. On shell this reduces to

$$\begin{aligned} S_{OS}(\epsilon) = \frac{\pi^2 N_c^2 T^4}{8}\int d^4x \Bigg(&-1 + \frac{1}{2}(3H_{tt}+H_{ii}) \\ &+\frac{1}{8}(3H_{tt}^2 - 12H_{tz}^2 + 2H_{tt}H_{ii} + 2H_{zz}H_{aa} - H_{zz}^2) \\ &- \frac{1}{2\epsilon}(H_{tz}^2 + \frac{1}{4}H_{aa}^2 - H_{tt}H_{ii} + H_{zz}H_{aa})'\Bigg) \end{aligned} \tag{3.117}$$

for some infinitesimal $\epsilon > 0$. Plugging in the solutions, to linear order in $\bar{\omega}$ and $\bar{q}$ the action becomes

$$\begin{aligned} S_{OS} = \frac{\pi^2 N_c^2 T^4}{8}\Bigg(&V_4 + \frac{1}{3}(3H_{tt}^0 + H_{ii}^0) + \frac{1}{2(\bar{q}^2-3\bar{\omega}^2)}\left[(2\bar{q}H_{tz}^0 + \bar{\omega}H_{ii}^0)^2\right. \\ &+ \left. H_{tt}^0(3\bar{q}^2H_{tt}^0 + 12\bar{q}\bar{\omega}H_{tz}^0 + (3\bar{\omega}^2+\bar{q}^2)H_{ii}^0)\right] \\ &+ \frac{1}{8}\left[3(H_{tt}^0)^2 - 12(H_{tz}^0)^2 + 2H_{tt}^0H_{ii}^0 + 2H_{zz}^0H_{aa}^0 - (H_{zz}^0)^2\right]\Bigg) \end{aligned} \tag{3.118}$$

where V_4 is the four-dimensional volume, making the first term in the action the free energy $\mathcal{F} = -\frac{\pi^2}{8}N_c^2T^4V_4$. The zero index indicates non-dependence on $\bar{\omega}$ and $\bar{q}$. It is now possible to extract some useful information about the dual theory. Namely the

expectation values of the stress-energy tensor can be computed

$$\epsilon = \langle T^{tt} \rangle = 2\frac{\delta S_{OS}}{\delta H^0_{tt}} = \frac{3\pi^2}{8} N_c^2 T^4 \tag{3.119}$$

$$2p = \langle T^{aa} \rangle = 4\frac{\delta S_{OS}}{\delta H^0_{aa}} = \frac{\pi^2}{4} N_c^2 T^4 \tag{3.120}$$

$$p = \langle T^{zz} \rangle = 2\frac{\delta S_{OS}}{\delta H^0_{zz}} = \frac{\pi^2}{8} N_c^2 T^4 \tag{3.121}$$

Combining the above one sees that $\epsilon = 3P$. This is exactly what one would expect from a conformal theory, like the boundary one ($\mathcal{N} = 4$ SYM), which constitutes another test for the AdS/CFT correspondence. Beyond one-point function one can get the two-point function as well

$$G^{tttt}(\omega, q) = -4\frac{\delta^2 S_{OS}}{\delta (H^0_{tt})^2} = \frac{3N_c^2 \pi^2 T^4 q^2}{2(3\omega^2 - q^2)} - \frac{3\pi^2}{8} N_c^2 T^4 = 3p\frac{5q^2 - 3\omega^2}{3\omega^2 - q^2} \tag{3.122}$$

More information can be derived from this Green's function. In particular it has a pole at $\omega = \frac{1}{\sqrt{3}}k$. This pole corresponds to sound propagation (density fluctuations) and its velocity is exactly $v_s = \frac{1}{\sqrt{3}}$ (see relative section of previous chapter), which once again is exactly what is expected of a conformal boundary theory (in which the stress-energy tensor has to be trace-less). It should be noted that it is not just the position of the pole that matches but the full two-point function is identical to the one computed by field-theoretical tools (for $\mathcal{N} = 4$ SYM).

Zero sound

It has been seen that there is sound propagation in Holographic models and it is of the exact form expected for the relative field theory. One can then ask if it is possible to reconstruct Holographically zero-sound, which as seen in the previous chapter is a feature of quantum liquids (Fermi liquids in particular). This has actually been studied in [2, 79]. On the gravity side (IIB string theory) the system consists of intersecting N_c D_3-branes and N_f D_7-branes with the following configuration in the ten-dimensional space

	x_0	x_1	x_2	x_3	x_4	x_5	x_6	x_7	x_8	x_9
D3	×	×	×	×						
D7	×	×	×	×	×	×	×	×		

(3.123)

In the usual Holographic limits $N_c \to \infty$ and $\lambda \to \infty$ the D_3-branes reduce, as usual, to gravity in $AdS_5 \times S^2$, whereas the D_7-branes can be made into probes (that do not disturb the gravitational background) provided that $N_f \ll N_c$. The Holographic dual

of this system is $\mathcal{N}=4$ $SU(N_c)$ SYM with N_f massless $\mathcal{N}=2$ hyper-multiplet fields (flavours) at zero temperature. The gravitational background, in the near-horizon limit, is as seen previously

$$ds^2 = \frac{r^2}{L^2}\eta_{\nu\mu}dx^\mu dx^\nu + \frac{L^2}{r^2}\left(dr^2 + r^2 d\Omega\right) \tag{3.124}$$

In this background the action describing the dynamics of the D_7-branes is the DBI[9] action

$$S_{DBI} = -N_f T_{D_7}\int d^8\xi\sqrt{-det\left(g_{ab}+2\pi\alpha' F_{ab}\right)} \tag{3.125}$$

where ξ_a are the brane's world-volume coordinates, g_{ab} is the induced metric and F_{ab} the world-volume $U(1)$ gauge field. In order to induce a non-vanishing baryon density on the boundary one needs to turn on the zeroth component of the bulk gauge field A_0. This results in $\langle J^0\rangle \neq 0$, where J^μ is the flavour current, that belongs to the baryon number subgroup $(U(1)_B)$ of the $U(N_f)$ global symmetry, characterizing the $\mathcal{N}=2$ hyper-multiplet. This significantly simplifies the DBI action (3.125)

$$S_{DBI} = -\frac{\lambda N_f N_c}{(2\pi)^4}V_3\int dr r^3\sqrt{1-A_0'^2} \tag{3.126}$$

where a factor of $2\pi\alpha'$ has been absorbed by rescaling A_0 and V_3 is the volume of the boundary theory. In order to study the existence of zero-sound one needs to compute the current-density two-point (retarded) correlation function and check whether this has a pole at zero temperature. Following the standard Holographic recipe the system needs to be slightly perturbed, i.e.

$$A_\mu \to A_\mu + \delta A_\mu \tag{3.127}$$

Substituting this into the DBI action and expanding to first order with respect to the gauge field, leads to

$$S_2 = \frac{N}{2}\int d^4x dr r^3\left\{\frac{\delta A_t'^2}{(1-A_t'^2)^{3/2}} + \frac{(\partial_t A_z - \partial_z A_t)^2}{r^4\sqrt{1-A_t'^2}} - \frac{A_z'^2}{\sqrt{1-A_t'^2}}\right\} \tag{3.128}$$

where $N = \lambda N_f N_c/(2\pi)^4$. Continuing with the Holographic dictionary, the fluctuations are Fourier decomposed as

$$\delta A_\mu = \int\frac{d\omega dq}{(2\pi)^2}\exp[-\imath\omega t + \imath q x]\delta A_\mu \tag{3.129}$$

[9]Dirac-Born-Infeld.

and the equations of motion are

$$\left[\frac{r^3\delta A_t'}{(1-A_t'^2)^{3/2}}\right]' - \frac{1}{r\sqrt{1-A_t'^2}}\left(\omega q\delta A_z + q^2\delta A_t\right) = 0 \tag{3.130}$$

$$\left[\frac{r^3\delta A_z'}{\sqrt{1-A_t'^2}}\right]' + \frac{1}{r\sqrt{1-A_t'^2}}\left(\omega q\delta A_t + \omega^2\delta A_z\right) = 0 \tag{3.131}$$

$$\omega\delta A_t' + (1-A_t'^2)q\delta A_z' = 0 \tag{3.132}$$

where eq. (3.132) is just a constraint equation, resulting from the residual gauge symmetry. As seen before given that the goal is to calculate correlators of gauge-invariant operators on the boundary, it is very useful to construct a gauge invariant bulk field, out of the variables δA_t and δA_z. The gauge invariant variable is $Z = \omega\delta A_z + q\delta A_t$ and the equations of motion are combined into

$$Z'' + \left(\frac{f'(3q^2-\omega^2 f^2)}{f(q^2-\omega^2 f^2)} - \frac{1}{u}\right)Z' + \frac{\omega^2 f^2 - q^2}{f^2}Z = 0 \tag{3.133}$$

where variables have been switched $r \to u = 1/r$ and $f(u) = \sqrt{1+d^2u^6}$ where $d = (2\pi\alpha' N)^{-1}\rho$, with ρ being the baryon density. Imposing incoming boundary conditions close to the horizon at $u \to \infty$ the solution asymptotes to $E(u) \sim \frac{\exp[\imath\omega u]}{u}$. Assuming that $\omega u \ll 1$, $qu \ll 1$ with ω/q fixed, the equation of motion reduces to

$$Z'' + \left[\frac{f'(3q^2-\omega^2 f^2)}{f(q^2-\omega^2 f^2)} - \frac{1}{u}\right]E' = 0 \tag{3.134}$$

the solution of which is

$$Z = C_1 + C_2 u^2\left(\frac{q^2}{3f} + \frac{q^2-3\omega^2}{6}{}_2F_1\left(\frac{1}{2},\frac{1}{3};\frac{4}{3};-d^2u^6\right)\right) \tag{3.135}$$

where ${}_2F_1$ is the Hyper-geometric function. Using the asymptotic behaviour of ${}_2F_1$ one then finds

$$Z = C_1 + C_2\left(\frac{a}{u} + b\right) + \mathcal{O}(1/u^2) \tag{3.136}$$

where $a = \omega^2/d$ and $b = (q^2-3\omega^2)d^{2/3}\Gamma(1/3)\Gamma(1/6)(18\Gamma(1/2))^{-1}$. In order to determine the integration constants C_1 and C_2 this solution needs to be matched with the asymptotic behavior when $\omega z \ll 1$. In that case

$$Z = \frac{C}{u} + \imath\omega C \tag{3.137}$$

The matching of the two asymptotic expansions leads to $C_1 = (\imath\omega - b/a)C$ and $C_2 = C/a$. There is enough information in place to examine the existence of zero-sound. This is because zero-sound would appear as a pole of the two-point retarded

function, which from the gravity point of view would emerge as a quasi-normal mode of the field Z [80]. More precisely given that the hydrodynamic limit is of interest here, one needs to extract the lowest quasi-normal pole (i.e. the one with the smallest $|\omega|$). Seeing as an analytic solution is available for this case, it is easy to extract the lowest quasi-normal mode by just imposting the Dirichlet boundary conditions on the field Z, on the AdS boundary, i.e. $Z(0) = 0 \Leftrightarrow C_1 = 0$. This in turn yields

$$\imath\omega = \left(\frac{q^2}{\omega^2} - 3\right) \frac{d^{1/3}\Gamma(1/3)\Gamma(1/6)}{18\Gamma(1/6)} \tag{3.138}$$

In the hydrodynamic regime, i.e. for small ω and q this simplifies to

$$\omega = \pm\frac{q}{\sqrt{3}} - \frac{\imath\Gamma(1/2)q^2}{d^{1/3}\Gamma(1/3)\Gamma(1/6)} + \mathcal{O}(q^3) \tag{3.139}$$

or in a more convenient form

$$\omega = \pm\frac{q}{\sqrt{3}} - \frac{\imath q^2}{6\mu_0} + \mathcal{O}(q^3) \tag{3.140}$$

where the zero-temperature chemical potential has been used

$$\mu_0 = \Gamma(1/3)\Gamma(1/6)(6\Gamma(1/2))^{-1}d^{1/3} \tag{3.141}$$

In summary what has been shown in [79] is that the system of D_3/D_7 branes, in the probe limit, has a propagating mode at zero temperature. The identification of this mode as zero-sound, comes firstly from the dependence of its imaginary part on q, i.e. q^2. This is compatible with zero-sound. Moreover this dependence excludes the possibility of this mode corresponding to a super-fluid phonon. In fact this could not have been the case since the background preserves the particle number symmetry, meaning that the ground state cannot be a super-fluid. However, this particular zero-sound is not exactly the zero-sound of Fermi liquids. This is because its speed is the same at finite temperatures (first sound), whereas in the case of Fermi liquids zero and first sound differ by a factor of $\sqrt{3}$.

Fermi Liquids

It has just been reviewed how one can construct gravitational systems, that can reproduce Condensed Matter phenomena (like normal and zero-sound). Is it possible in a Holographic context to actually reconstruct Fermi liquids? The answer seems to be affirmative. Following [15, 16] a quick review of this answer, will be demonstrated

here. Once again the starting point is the Holographic ingredients. The system consists of a four-dimensional[10] gravitational background (AdS_4), a bulk gauge field (A_M) and a bulk, charged fermionic field (Ψ). It should be stressed here, that this is the phenomenological or bottom-up way of approaching the problem, i.e. including the minimum set of necessary ingredients without looking for a String Theory embedding. This may cause some worries and in general it needs to be addressed, however none of the relevant results are affected by this subtlety. Thus one can begin this analysis from the action

$$S = \frac{1}{\kappa_{10}} \int d^4x \sqrt{-g} \left\{ R + \frac{6}{L^2} + L^2 \left[-\frac{1}{4} F^2 - \bar{\Psi} e_A^M \Gamma^A D_M \Psi - m \bar{\Psi} \Psi \right] \right\} \tag{3.142}$$

containing all the aforementioned fields. In eq. (3.142) Γ^A are just the Dirac matrices ($\Gamma^A = \{\gamma^a, \gamma^4\}$) and e_A^M is the inverse vielbein. Moreover the covariant derivative, acting on the spinors is

$$D_M \Psi = \left(\partial_M + \frac{1}{8} \omega_M^{AB} \left[\Gamma_A, \Gamma_B \right] + \imath g A_M \right) \Psi \tag{3.143}$$

A solution to the equations of motion coming from this action contains and AdS_4 black-hole background

$$ds^2 = \frac{L^2 \alpha^2}{z^2} \left(-f dt^2 + dx^2 + dy^2 \right) + \frac{L^2}{z^2 f} dz^2 \tag{3.144}$$

a gauge field

$$A_0 = 2q\alpha(z-1) \tag{3.145}$$

where $f(z) = (1-z)(z^2 + z + 1 - q^2 z^2)$. For book-keeping reasons it should be noted that, in these coordinates, the horizon is located at $z = 1$ and the AdS boundary at $z = 0$. Temperature and chemical potential for this system are $T = \frac{\alpha}{4\pi}(3 - q^2)$ and $\mu = -2q\alpha$ respectively. Treatment of the fermions becomes more involved because of their action is first-order and hence on the boundary it vanishes identically, making it more tricky to set up the variational problem and use the boundary action as the generating functional for the boundary theory. This phenomenon is a side-effect of the fact that not all the components of the Dirac spinor are independent. However one can project out half of the spinor and use that to define the boundary action [81]. Following the careful analysis in [15] one can eventually derive the retarded fermionic Green's function and then from that the spectral function. Studying the behaviour

[10] This choice is made so that the dual theory is $2+1$ dimensional, which is the case for many relevant experimental configurations.

of the spectral function, the authors of [15] have established that in fact there is a parameter regime, within this model, that describes a Fermi liquid.

The examples presented here are in no way an exhaustive list. In fact over the last several years a lot of effort has been invested in understanding strongly coupled systems from Condensed Matter, using the tools of Holography. The systems studied include high-T_C superconductivity [12, 17], strange metals [82, 83], non-Fermi liquids [14], Josephson junctions [84], Mott insulators [85] and almost every other system of Condensed Matter interest. Here, just for completeness, the major references for each system are provided.

Chapter 4

Anti-de Sitter Reissner-Nordström

4.1 Introduction

In this chapter a Holographic study of the Anti-de Sitter Reissner-Nordström (RN-AdS) system will be presented [86]. As it may already be known the RN-AdS system is an extremely useful one, particularly from the phenomenological or bottom-up, approach to Holography, since it contains the necessary ingredients, that is gravity and a $U(1)$ gauge field, necessary to address a lot of interesting Condensed Matter problems. It is also very popular because it constitutes a realistic truncation of top-down models, presenting a quite universal character. It therefore provides an excellent toy model / laboratory to explore Holography. This system has been rather well-examined so this study comes as an addition to the existing body of work which most notably includes [3, 87, 88].

Over the years, the excitations present when $T = 0$ and $\omega, q \ll \mu$ in specific strongly-coupled field theories have attracted a lot of interest and a significant amount of scrutiny, and one common feature amongst many examples is a propagating longitudinal mode with the dispersion relation

$$\bar{\omega} = \pm v_s \bar{q} - i\Gamma_0 \bar{q}^2 + O\left(\bar{q}^3\right), \tag{4.1}$$

where

$$\bar{\omega} = \frac{\omega}{\mu}, \qquad \text{and} \qquad \bar{q} = \frac{q}{\mu}. \tag{4.2}$$

One can detect this feature in probe brane theories in different dimensions and with different UV symmetries (where the conserved charge is a density of fundamental matter - at least in the case where the background is derived from string theory) [79,89–96] as well as in 4D bulk Einstein-Maxwell theory with a cosmological constant (where the conserved charge is an R-charge density) [3].

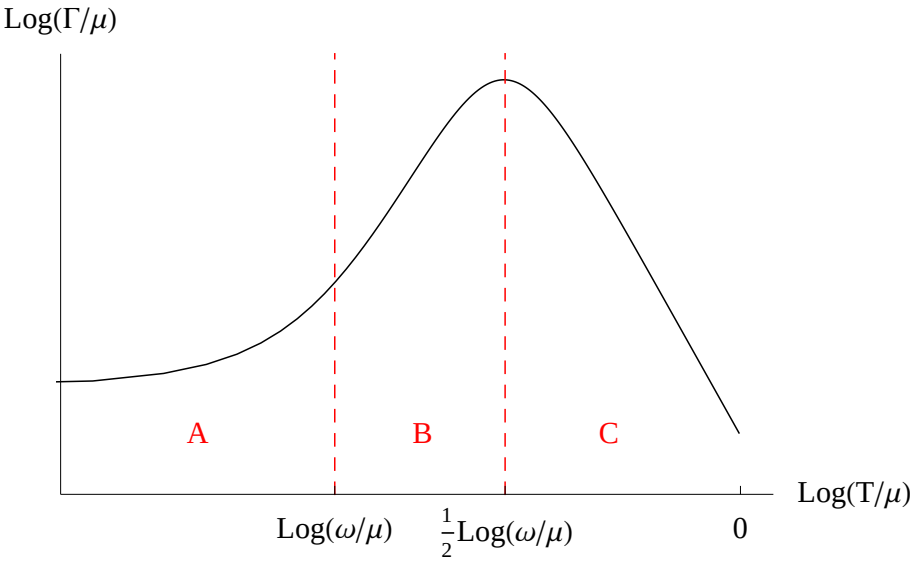

Figure 4.1: The sound attenuation Γ in an LFL as a function of temperature, at fixed ω and μ. A is the collisionless quantum regime, B is the collisionless thermal regime and C is the hydrodynamic regime.

In one of these probe brane theories (the D3/D7 theory in (3+1) dimensions), the behaviour of this zero temperature sound mode was analysed as the temperature was increased from $T = 0$ and it was found to behave similarly to the 'zero sound' mode due to the oscillation of the Fermi surface of a Landau Fermi liquid (LFL), despite the fact that some of its other properties are quite different from an LFL (e.g. its heat capacity is proportional to T^6 rather than T) [2]. The theory of an LFL is valid when $T \ll \mu$ and $\omega, q \ll \mu$ and it predicts three different regimes for the behaviour of the sound attenuation, as shown in figure 4.1 [97–101]. At $T = 0$, the sound mode has a non-zero attenuation Γ proportional to ω^2/μ. As the temperature is increased from zero (with ω and μ fixed), the attenuation of the sound mode remains approximately constant until $T/\mu \sim \omega/\mu$ (the 'collisionless quantum regime' denoted by A in figure 4.1). Above this, thermal excitations around the Fermi surface must be taken into account and collisions between these thermally-excited quasiparticles cause the sound attenuation to increase at a rate proportional to T^2/μ (the 'collisionless thermal regime' B). When T is sufficiently high such that $T/\mu \sim \sqrt{\omega/\mu}$, these thermal collisions become so frequent that the zero sound mode is no longer a long-lived mode. However, the thermal collisions support the hydrodynamic modes of sound and diffusion. This results in the 'collisionless/hydrodynamic crossover' and the sound attenuation begins to decrease at a rate proportional to $\mu\,(\omega/T)^2$ as the hydrodynamic sound mode stabilises.

These features were reproduced precisely in the strongly-coupled D3/D7 field theory except that there was no sound propagation in the hydrodynamic regime - this can be explained by the fact that the fluctuations of the bulk metric, which generate the hydrodynamic sound mode of the dual field theory, were explicitly suppressed for consistency with the probe limit. The collisionless/hydrodynamic crossover is most clearly exhibited in the D3/D7 theory via the poles of the charge density Green's function in the complex frequency plane [2]. As the temperature is raised, the low temperature poles corresponding to sound propagation approach the imaginary axis and collide to form two purely imaginary poles, one of which becomes the hydrodynamic diffusion mode as the temperature is raised further. The crossover can also be seen by examining the charge density spectral function - the tall, narrow peak corresponding to the sound mode becomes smaller and moves towards the origin as the temperature is raised, eventually forming a diffusive peak around $\bar{\omega} = 0$. A natural question to ask is whether similar behaviour is observed in the low temperature sound modes of other holographic theories at large chemical potential and hence whether they can all be characterised in this way as LFL-like 'zero sound' modes or not.

Here, the strongly-coupled field theory dual to the RN-AdS_4 black hole solution of 4D Einstein-Maxwell theory with a cosmological constant, will be studied. Many properties of this theory have been investigated in recent years as it is relatively simple and yet has very interesting behaviour. In particular when $T = 0$, the low energy behaviour of the field theory is governed by a CFT_1 dual to the AdS_2 factor of the black hole's $AdS_2 \times \mathbb{R}^2$ near-horizon geometry [16]. If one considers a probe Dirac action for fermions in this background, the field theory operators dual to these fermions exhibit Fermi surfaces of a non-Fermi liquid type [14–16]. If instead one considers a fermionic action which is the super-symmetric completion of the Einstein-Maxwell action, no such Fermi surfaces are observed [102–104].

The quasi-normal modes of the bulk bosonic fields, which correspond to the poles of the retarded Green's functions of the field theory energy-momentum tensor $T^{\mu\nu}$ and U(1) current J^μ, have also been studied at zero temperature. At $T = 0$ the transverse sector (i.e. transport perpendicular to the direction of the momentum flow) contains a branch cut along the negative imaginary frequency axis, and no long-lived modes (by which we mean no modes satisfying $\bar{\omega} \to 0$ as $\bar{q} \to 0$). At very small temperatures $T \ll \mu$, this branch cut becomes a series of poles, one of which has a dispersion relation of the form $\bar{\omega} = -i\mathcal{D}\bar{q}^2 + O(\bar{q}^3)$ [88, 105, 106]. This is an analogue of the

well-known hydrodynamic shear diffusive mode of the energy-momentum tensor [20]. At $T = 0$, the longitudinal sector (i.e. transport parallel to the direction of the momentum flow) also contains a branch cut along the negative imaginary frequency axis. Additionally, it has two propagating modes with dispersion relations of the form (4.1) with $v_s = \sqrt{(\partial P/\partial\epsilon)|_{T=0}}$ and $\Gamma_0 \approx \mu\eta_0/2(\epsilon + P)$, where η_0 is the 'zero temperature viscosity' derived via the 'Kubo formula'

$$\eta_0 = -\lim_{\omega\to 0}\frac{1}{\omega}\mathrm{Im}\left[G^R_{T^{xy}T^{xy}}(\omega, 0)\right]\Big|_{T=0}, \tag{4.3}$$

ϵ and P are the field theory's energy density and pressure respectively, and the '$\approx$' signifies that these are equal to within about 10% [3, 87].[1] A priori, this result is not obvious. It suggests that when $T = 0$, μ acts as an 'effective hydrodynamic scale', at least as far as sound propagation is concerned.

In this work, a numerical study of the behaviour of the longitudinal poles for a fixed momentum $\bar{q} < 1$ as the temperature is increased from $T = 0$ to $T \gg \mu$, will be presented. Of particular interest is the behaviour of the sound mode and whether there is a collisionless/hydrodynamic crossover as in the D3/D7 theory and Landau's theory of Fermi liquids. What is discovered is that the attenuation of the sound mode shows no significant temperature dependence over the range $T \lesssim \mu$ where we may have expected to find LFL-like behaviour and above this it approaches the $\mu = 0$ hydrodynamic result [107, 108] where the attenuation decreases like T^{-1}. Its speed is approximately $1/\sqrt{2}$ at all temperatures. This is in complete contrast to the results for an LFL (as shown in figure 4.1). Such an outcome is not particularly surprising since all available evidence suggests that this field theory is *not* an LFL. However, this is also true of the D3/D7 theory and yet it possesses an LFL-like zero sound mode. The present results show that this kind of mode is *not* generic to all strongly-coupled field theories at large chemical potential which have a gravitational dual.

The other long-lived, longitudinal mode of the theory corresponds to a purely imaginary pole that forms when the branch cut along the negative imaginary frequency axis dissolves at non-zero temperatures. This mode becomes more stable as the temperature increases and when $T \gg \mu$ its dispersion relation is that of the $\mu = 0$ hydrodynamic charge diffusion mode [108, 109].

[1] The sound attenuation Γ_0 is only known numerically and thus an exact comparison cannot be made.

In addition to the poles of the Green's functions, the spectral functions of energy density and charge density, is also computed, as the temperature is increased at fixed $\bar{q} < 1$. The energy density spectral function is dominated by the peak corresponding to sound propagation at all temperatures. In contrast to this, the charge density spectral function undergoes a crossover from being dominated by the sound peak at low temperatures to being dominated by the diffusion peak at high temperatures $T \gg \mu^2/q$. Note that this mechanism is quite different than in the D3/D7 theory where the sound poles collide to form the diffusion pole. Here, the sound and diffusion poles coexist at all non-zero temperatures (that we can access numerically) but their residues change and this results in the crossover. In the D3/D7 theory this crossover was reminiscent of that in an LFL, but here we know of no such comparison - in particular, the RN-AdS_4 crossover occurs outside of the 'quantum liquid' range $T \ll \mu$ where we may expect an LFL-like theory to apply.

As well as the previous results regarding the temperature dependence of the poles and spectral functions at fixed momentum, their momentum dependence at various fixed temperatures has also been calculated. The results show that the sound and purely imaginary modes exist at all non-zero temperatures that can be accessed numerically ($T \geq 0.0219\mu$) with the dispersion relations

$$\bar{\omega} = \frac{\bar{q}}{\sqrt{2}} - i\Gamma(T/\mu)\bar{q}^2 + O(\bar{q}^3), \tag{4.4}$$

and

$$\bar{\omega} = -iD(T/\mu)\bar{q}^2 + O(\bar{q}^3), \tag{4.5}$$

where the functions $D(T/\mu)$ and $\Gamma(T/\mu)$ are computed numerically. For this reason, and the fact that it becomes the $\mu = 0$ hydrodynamic charge diffusion mode in the $T \gg \mu$ limit, this purely imaginary mode will be labelled the diffusion mode. When $\bar{q} \gg 1$, these modes no longer dominate the low-energy properties of the theory and one must consider additional poles of the Green's functions also.

Finally, the properties of sound propagation in the theory, at some fixed momentum q, over the (T, μ) plane, are investigated. As discussed above, it is known that when $\mu = 0$, T is the hydrodynamic scale and sound will propagate provided its momentum satisfies $q \ll T$. It is also known that when $T = 0$, there is an effective hydrodynamic scale μ in that there is a long-lived sound mode provided that $q \ll \mu$. It is found that when both of these scales are non-zero, there will be a long-lived sound mode provided that any *one* of them is much larger than the momentum. In other words,

sound will propagate for *any* value of μ/T, provided that one considers small enough momenta.

The structure of the rest of this chapter is as follows. In section 4.2 the RN-AdS_4 solution of the four dimensional Einstein-Maxwell theory with a cosmological constant is presented, as well as the gauge-invariant fluctuations of the bulk fields that are used to compute the poles of the retarded Green's functions and the spectral functions. Section 4.3 contains the numerical results showing how the properties of the sound mode change as we increase the temperature at fixed $\bar{q} < 1$. In particular, it is demonstrated that these properties are significantly different from those of an LFL and of the D3/D7 theory. In section 4.4, the behaviour of the other long-lived mode of the system - the diffusion mode - as T is increased for $\bar{q} < 1$, is explored. The dependence of the energy and charge density spectral functions on T for $\bar{q} < 1$, is also examined. Section 4.5 contains results for the poles and spectral functions as a function of $\bar{q}$ at fixed temperature $T < \mu$. The existence of an effective hydrodynamic scale in section 4.6, is then studied, by examining the properties of the sound mode as a function of both q/μ and q/T.

4.2 The RN-AdS_4 background and fluctuations

The action and background solution

The gravitational theory under investigation is the four dimensional Einstein-Maxwell theory with a cosmological constant, described by the action

$$S = \frac{1}{2\kappa_4^2}\left[\int_{\mathcal{M}} d^4x\sqrt{-g}\left(R - 2\Lambda - L^2 F_{\mu\nu}F^{\mu\nu}\right) + 2\int_{\partial\mathcal{M}} d^3x\sqrt{|h|}\left(\mathcal{K} + \text{counterterms}\right)\right], \tag{4.6}$$

where $\Lambda = -3/L^2$, h is the induced metric on the boundary of the space-time, $\mathcal{K}$ is the extrinsic curvature on this boundary and $F_{\mu\nu}$ is the field strength of a $U(1)$ gauge field A_μ. This is a consistent truncation of $D = 11$ super-gravity [110, 111].

This theory has a charged, asymptotically-AdS black hole solution with a planar horizon: the planar AdS_4 Reissner-Nordström black hole (RN-AdS_4)

$$\begin{aligned} ds_4^2 &= -\frac{r^2 f(r)}{L^2}dt^2 + \frac{r^2}{L^2}dx^2 + \frac{r^2}{L^2}dy^2 + \frac{L^2}{r^2 f(r)}dr^2, \\ f(r) &= 1 - (1+Q^2)\left(\frac{r_0}{r}\right)^3 + Q^2\left(\frac{r_0}{r}\right)^4, \\ A_t &= \frac{Qr_0}{L^2}\left(1 - \frac{r_0}{r}\right), \end{aligned} \tag{4.7}$$

where r is the bulk radial co-ordinate, r_0 is the position of the horizon and Q determines the $U(1)$ charge of the black hole. In the full $D = 11$ supergravity theory, it is the decoupling limit of the geometry created by a stack of M2-branes which are rotating (in a specific way) in the directions transverse to their world-volume [111]. The bulk $U(1)$ gauge field is dual to a $U(1)$ R-current in the field theory on this world-volume.

This solution has one tunable dimensionless parameter Q which determines the ratio of the chemical potential in the field theory to the temperature

$$\frac{\mu}{T} = \frac{4\pi Q}{3 - Q^2}. \tag{4.8}$$

It takes values between 0 (the zero chemical potential limit) and $\sqrt{3}$ (the zero temperature limit). The thermodynamics of the dual field theory are well-known [110]. It is important to note that the entropy density has the unusual property of being non-zero when $T = 0$, which will naturally lead to the next system that will be studied, that of the Electron Star.

Fluctuations around equilibrium

Of interest is the response of the field theory to small perturbations around the equilibrium state - this is encoded holographically in the linear response of the black hole to perturbations around the background solution (4.7):

$$\begin{aligned} g_{\mu\nu} &\to g_{\mu\nu} + h_{\mu\nu}, \\ A_\mu &\to A_\mu + a_\mu. \end{aligned} \tag{4.9}$$

The residual rotational invariance in the (x, y)-plane is used to choose the momentum to flow only in the x-direction of the field theory, without loss of generality. One may then classify fluctuations according to their parity under $y \to -y$. The fluctuations which are even under this operation (h_{xx}, h_{yy}, h_{rr}, h_{tt}, h_{rt}, h_{rx}, h_{xt}, a_r, a_t and a_x)

decouple from those which are odd ($h_{yr},\ h_{yx},\ h_{yt}$ and a_y) at linear order [109]. The indices are raised and lowered with the background metric. In the following of interest are only the even fluctuations which will be referred to as 'longitudinal' henceforth, as they encode the response of the fields parallel to the direction of momentum flow. The metric and gauge field fluctuations are coupled within this longitudinal sector which means that the retarded Green's functions of the longitudinal components of the field theory energy-momentum tensor $T^{\mu\nu}$ and U(1) conserved current J^{μ} are not independent.

Two properties of the retarded Green's functions $G^R_{\mathcal{O}_A\mathcal{O}_B}$ will be particularly interesting. The first is the poles of the Green's functions in the complex frequency plane. These poles correspond to the field theory excitations - the real part of each pole is its propagating frequency and the imaginary part is its decay rate. One is primarily interested in the long-lived excitations - those with the smallest imaginary part. Note that if any excited bulk fields are coupled, their dual field theory operators share a common set of Green's function poles.

The second object of interest is the matrix of spectral functions

$$\chi_{AB}(\omega, q) \equiv i\left(G^R_{\mathcal{O}_A\mathcal{O}_B}(\omega, q) - G^R_{\mathcal{O}_B\mathcal{O}_A}(\omega, q)^*\right), \tag{4.10}$$

which contains information about the rate of work done on the system by small external sources for $\mathcal{O}_A$ and $\mathcal{O}_B$ with frequency ω (see, for example, [10]). Modes which couple strongly to external sources in this way are visible in the spectral functions as tall, narrow peaks centred on the propagating frequency and with a width proportional to their decay rate. Such a peak will be produced by a pole of the Green's function with small imaginary part provided that the residue of the Green's function is large enough at this pole and that there are no other poles near it in the complex frequency plane. Unlike the existence of a pole, the residue at a pole differs between the Green's functions of a set of coupled operators and hence despite the fact that they have a shared set of Green's function poles, the spectral functions of coupled operators can be very different. The focus of interest will be the energy density spectral function $\chi_{T^{tt}T^{tt}} \equiv \chi_{\epsilon\epsilon}$ and the charge density spectral function $\chi_{J^tJ^t} \equiv \chi_{QQ}$, which are real quantities, and dictate which modes couple strongly to external sources of energy density and charge density respectively.

Gauge-invariant variables and Ward identities

The retarded Green's functions can be computed from the on-shell action of the gravitational theory which generically has the form

$$S_{\text{on-shell}} = \int_{r\to\infty,\omega>0} \frac{d\omega d^2q}{(2\pi)^3}\Big[\phi_I(r,-\omega,-q)\mathcal{G}_{IJ}\partial_r\phi_J(r,\omega,q)+\phi_I(r,-\omega,-q)\mathcal{C}_{IJ}\phi_J(r,\omega,q)\Big], \tag{4.11}$$

where ϕ_I label the perturbations of bulk fields which are dual to field theory operators $\mathcal{O}_I$. To obtain the retarded Green's function of two operators $G^R_{\mathcal{O}_A\mathcal{O}_B}(\omega,q)$, one must find solutions to the bulk field equations which satisfy ingoing conditions at the black hole horizon and asymptote to

$$\phi_I\left(r\to\infty,-\omega,-q\right)\to\begin{cases}1, & I=A\\ 0, & I\neq A\end{cases}\qquad\text{and}\qquad \phi_J\left(r\to\infty,\omega,q\right)\to\begin{cases}1, & J=B\\ 0, & J\neq B\end{cases}, \tag{4.12}$$

near the boundary. $G^R_{\mathcal{O}_A\mathcal{O}_B}(\omega,q)$ is then given by the integrand of the on-shell action evaluated on these solutions [71, 112].

The longitudinal sector of the theory contains ten fields whose excitations are coupled. The equations of motion and on-shell action for the excited longitudinal fields can be simplified considerably by noting that the theory has a U(1) gauge symmetry which acts on the gauge field fluctuations as

$$a_\mu \to a_\mu - \partial_\mu\Lambda, \tag{4.13}$$

and a diffeomorphism symmetry which acts as

$$\begin{aligned} h_{\mu\nu} &\to h_{\mu\nu} - \nabla_\mu\xi_\nu - \nabla_\nu\xi_\mu,\\ a_\mu &\to a_\mu - \xi^\alpha\nabla_\alpha A_\mu - A_\alpha\nabla_\mu\xi^\alpha, \end{aligned} \tag{4.14}$$

to linear order, where ∇ is the covariant derivative with respect to the background metric [113]. One can form two linearly-independent variables which are invariant under these transformations

$$\begin{aligned} Z_1(r,\omega,q) &= \omega a_x(r,\omega,q) + q a_t(r,\omega,q) - \frac{qL^2A_t'(r)}{2r}h_{yy},\\ Z_2(r,\omega,q) &= \frac{2\omega q}{r^2}h_{xt} + \frac{\omega^2}{r^2}h_{xx} + \frac{q^2}{r^2}h_{tt} + \frac{q^2f(r)}{r^2}h_{yy}\left(1+\frac{rf'(r)}{2f(r)} - \frac{\omega^2}{q^2f(r)}\right), \end{aligned} \tag{4.15}$$

and to linear order in the fluctuations, one can write the theory in terms of these variables. In particular, this reduces the set of ten coupled equations to a set of two.

It also allows one to write the on-shell action in the form

$$S_{\text{on-shell}} = \int_{r\to\infty,\omega>0} \frac{d\omega d^2q}{(2\pi)^3}\Big[Z_i\left(r,-\omega,-q\right)\mathcal{G}_{ij}\partial_r Z_j\left(r,\omega,q\right)+\phi_I\left(r,-\omega,-q\right)\mathcal{C}_{IJ}\phi_J\left(r,\omega,q\right)\Big], \tag{4.16}$$

where $i = 1, 2$ and ϕ_I denote the fundamental fluctuations $\{h_{tt}, h_{xx}, h_{yy}, h_{tx}, a_t, a_x\}$. The $\mathcal{C}_{IJ}$ terms are analytic in ω, q and hence contribute only contact terms to the retarded Green's functions (i.e. terms analytic in ω, q). These Z_i variables are a generalisation of those of [114] to non-zero chemical potential (and in 3+1, rather than 4+1, dimensions).

Written in this way it is seen explicitly that, neglecting contact terms, the on-shell action for a solution that has the form $a_t\left(r\to\infty,\pm\omega,\pm q\right)\to 1$ (with all others fields zero in this limit) differs from that for a solution with $a_x\left(r\to\infty,\pm\omega,\pm q\right)\to 1$ (with all other fields zero in this limit) only by the factor q^2/ω^2 in the definition of the variables Z_i, and similarly for the other fields.

This property of bulk gauge-invariance thus generates a number of relationships between the retarded Green's functions of the corresponding field theory operators:

$$G^R_{J^xJ^t} = \frac{\omega}{q}G^R_{J^tJ^t}, \qquad G^R_{J^xJ^x} = \frac{\omega^2}{q^2}G^R_{J^tJ^t}, \tag{4.17}$$

$$G^R_{T^{xx}J^t} = \frac{\omega^2}{q^2}G^R_{T^{tt}J^t}, \quad G^R_{T^{tx}J^t} = \frac{\omega}{q}G^R_{T^{tt}J^t}, \quad G^R_{T^{yy}J^t} = \left(1-\frac{\omega^2}{q^2}\right)G^R_{T^{tt}J^t}, \ \ldots, \tag{4.18}$$

$$G^R_{T^{xx}T^{tt}} = \frac{\omega^2}{q^2}G^R_{T^{tt}T^{tt}}, \quad G^R_{T^{tx}T^{tt}} = \frac{\omega}{q}G^R_{T^{tt}T^{tt}}, \ \ldots, \tag{4.19}$$

where the '...' represents other similar relations, and these equations should be understood to hold up to contact terms. These are precisely the Ward identities of the field theory.

Thus not only do these gauge-invariant variables simplify the equations of motion for the bulk fluctuations, they also explicitly encode the Ward identities of the field theory. The contribution of the contact terms to the diagonal retarded Green's functions is purely real, and thus they don't affect our results for the spectral functions $\chi_{\epsilon\epsilon}$ and χ_{QQ}. Note that the contact terms cannot be written in terms of these gauge-invariant variables - it is believed that this is because the linear diffeomorphism transformations (4.14) are not the correct ones to apply to the action which is quadratic in fluctuations.

It should be noted that these are not the only possible gauge-invariant choice of variables. Another choice is the Kodama-Ishibashi variables which involve radial derivatives of the bulk fields, and have the advantage that the two equations of motion in these variables decouple [115].

Equations of motion and on-shell action in dimensionless variables

It is convenient to work with the dimensionless radial co-ordinate $u \equiv r/r_0$. For $T > 0$, the following gauge-invariant variables are used

$$\begin{aligned}
\bar{Z}_1(u,\omega,q) &= \bar{\omega}a_x + \bar{q}a_t - \frac{\bar{q}\mu}{2u}h^y_y, \\
\bar{Z}_2(u,\omega,q) &= i\mu\left[2\bar{\omega}\bar{q}h^x_t + \bar{\omega}^2 h^x_x - \bar{q}^2 f(u)h^t_t + \bar{q}^2 f(u)\left(1 + \frac{uf'(u)}{2f(u)} - \frac{\bar{\omega}^2}{\bar{q}^2 f(u)}\right)h^y_y\right],
\end{aligned} \tag{4.20}$$

where $f(u) = 1 - (1+Q^2)/u^3 + Q^2/u^4$. The two linearly-independent, coupled equations of motion in these variables, for $\bar{Z}_1(u,\bar{\omega},\bar{q})$ and $\bar{Z}_2(u,\bar{\omega},\bar{q})$ can be written in the form

$$\begin{aligned}
\bar{Z}_1''(u) + A_1\bar{Z}_1'(u) + A_2\bar{Z}_2'(u) + A_3\bar{Z}_1(u) + A_4\bar{Z}_2(u) = 0, \\
\bar{Z}_2''(u) + B_1\bar{Z}_1'(u) + B_2\bar{Z}_2'(u) + B_3\bar{Z}_1(u) + B_4\bar{Z}_2(u) = 0,
\end{aligned} \tag{4.21}$$

where the dependence of $\bar{Z}_{1,2}$ on $\bar{\omega}$ and $\bar{q}$ has been suppressed, and the coefficients are

$$
\begin{aligned}
A_1 &= \frac{u^5 f'(u)\bar{\omega}^2 + 2f(u)\left[Q^2\bar{q}^2 + u^4\left(\bar{\omega}^2 - f(u)\bar{q}^2\right)\right]}{u^5 f(u)\left(\bar{\omega}^2 - f(u)\bar{q}^2\right)},\\
A_2 &= -i\bar{q}\frac{u^5 f'(u)\bar{q}^2 + 2\left[Q^2\bar{q}^2 - u^4\left(\bar{\omega}^2 - f(u)\bar{q}^2\right)\right]}{u^6\left(\bar{\omega}^2 - f(u)\bar{q}^2\right)\left[uf'(u)\bar{q}^2 - 4\left(\bar{\omega}^2 - f(u)\bar{q}^2\right)\right]},\\
A_3 &= \frac{Q^2\left[u^2\left(\bar{\omega}^2 - f(u)\bar{q}^2\right) - 4f(u)\right]}{u^6 f(u)^2} + \frac{4Q^2\bar{q}^2}{u^6\left(\bar{\omega}^2 - f(u)\bar{q}^2\right)}\\
&\quad + \frac{8Q^2\bar{q}^2\left[u^4\left(\bar{\omega}^2 - f(u)\bar{q}^2\right) + Q^2\bar{q}^2\right]}{u^{10}\left(\bar{\omega}^2 - f(u)\bar{q}^2\right)\left[uf'(u)\bar{q}^2 - 4\left(\bar{\omega}^2 - f(u)\bar{q}^2\right)\right]},\\
A_4 &= i\bar{q}\frac{4Q^2 + u^5 f'(u)}{u^7 f(u)\left[uf'(u)\bar{q}^2 - 4\left(\bar{\omega}^2 - f(u)\bar{q}^2\right)\right]},\\
B_1 &= -i\bar{q}\frac{2Q^2\left[uf'(u)\bar{q}^2 - 4\left(\bar{\omega}^2 - f(u)\bar{q}^2\right)\right]}{u^4\left(\bar{\omega}^2 - f(u)\bar{q}^2\right)},\\
B_2 &= \frac{1}{u^5 f(u)\left(\bar{\omega}^2 - f(u)\bar{q}^2\right)\left[uf'(u)\bar{q}^2 - 4\left(\bar{\omega}^2 - f(u)\bar{q}^2\right)\right]}\Bigg\{-16u^4 f(u)^3\bar{q}^4\\
&\quad + 2f(u)^2\bar{q}^2\left[-4Q^2\bar{q}^2 + 16u^4\bar{\omega}^2 + u^5\left(f'(u) + uf''(u)\right)\bar{q}^2\right]\\
&\quad - f(u)\Big[-8Q^2\bar{q}^2\bar{\omega}^2 + 16u^4\bar{\omega}^4 + u\bar{q}^2\Big\{f'(u)\Big(2Q^2\bar{q}^2 - 2u^4\bar{\omega}^2 + u^5 f'(u)\bar{q}^2\Big)\\
&\quad + 2u^5 f''(u)\bar{\omega}^2\Big\}\Big] + u^5 f'(u)\bar{\omega}^2\left[uf'(u)\bar{q}^2 - 4\bar{\omega}^2\right]\Bigg\},
\end{aligned}
$$

$$
\begin{aligned}
B_3 &= \frac{8iQ^2\bar{q}}{u^9 f(u)\left(\bar{\omega}^2 - f(u)\bar{q}^2\right)\left[uf'(u)\bar{q}^2 - 4\left(\bar{\omega}^2 - f(u)\bar{q}^2\right)\right]}\Bigg\{u^5 f'(u)\bar{\omega}^2[uf'(u)\bar{q}^2 - 4\bar{\omega}^2]\\
&\quad - f(u)\bar{q}^2\left[-4Q^2\bar{\omega}^2 + uf'(u)\left(Q^2\bar{q}^2 - 3u^4\bar{\omega}^2 + u^5 f'(u)\bar{q}^2\right) + u^6 f''(u)\bar{\omega}^2\right]\\
&\quad + f(u)^2\bar{q}^4\left[-4Q^2 + u^5\left(f'(u) + uf''(u)\right)\right]\Bigg\},\\
B_4 &= \frac{1}{u^4 f(u)^2\left[uf'(u)\bar{q}^2 - 4\left(\bar{\omega}^2 - f(u)\bar{q}^2\right)\right]}\Bigg\{-4Q^2 f(u)^2\bar{q}^4 + Q^2\bar{\omega}^2\left[uf'(u)\bar{q}^2 - 4\bar{\omega}^2\right]\\
&\quad + f(u)\bar{q}^2\left[8Q^2\bar{\omega}^2 + uf'(u)\left(u^4 f''(u) + 5u^3 f'(u) - Q^2\bar{q}^2\right)\right]\Bigg\}.
\end{aligned}
\tag{4.22}
$$

In these variables, the off-shell action to quadratic order in the fluctuations is of

the form

$$S = \frac{r_0}{2\kappa_4^2}\int_1^\infty du \frac{d\omega d^2q}{(2\pi)^3}\Big[\mathcal{G}_{11}\partial_u\bar{Z}_1(u,-\bar{\omega},-\bar{q})\partial_u\bar{Z}_1(u,\bar{\omega},\bar{q}) + \mathcal{G}_{12}\partial_u\bar{Z}_1(u,-\bar{\omega},-\bar{q})\partial_u\bar{Z}_2(u,\bar{\omega},\bar{q}) + \mathcal{G}_{21}\partial_u\bar{Z}_2(u,-\bar{\omega},-\bar{q})\partial_u\bar{Z}_1(u,\bar{\omega},\bar{q}) + \mathcal{G}_{22}\partial_u\bar{Z}_2(u,-\bar{\omega},-\bar{q})\partial_u\bar{Z}_2(u,\bar{\omega},\bar{q}) + \ldots\Big], \tag{4.23}$$

where the coefficients are

$$\begin{aligned}
\mathcal{G}_{11} &= \frac{2u^2 f(u)}{\bar{\omega}^2 - f(u)\bar{q}^2}, \\
\mathcal{G}_{12} &= -\frac{2i\bar{q}uf(u)}{(\bar{\omega}^2 - f(u)\bar{q}^2)\left[-4\left(\bar{\omega}^2 - f(u)\bar{q}^2\right) + uf'(u)\bar{q}^2\right]}, \\
\mathcal{G}_{21} &= -\mathcal{G}_{12}, \\
\mathcal{G}_{22} &= \frac{2u^4 f(u)\left[(\bar{\omega}^2 - f(u)\bar{q}^2) + \frac{\bar{q}^2Q^2}{u^4}\right]}{Q^2\left(\bar{\omega}^2 - f(u)\bar{q}^2\right)\left[-4\left(\bar{\omega}^2 - f(u)\bar{q}^2\right) + \bar{q}^2uf'(u)\right]^2},
\end{aligned} \tag{4.24}$$

and the '...' represents terms with less than two u derivatives (which cannot generically be written in terms of these gauge-invariant variables). These coefficients, combined with the equations of motion listed previously, allow one to compute the Green's function's poles and spectral functions $\chi_{\epsilon\epsilon}$, χ_{QQ} by following the method of [112]. Note that the counter-terms in (4.6) (listed, for example, in [3]) do not affect these quantities.

To compute the poles and spectral functions, the numerical procedure described in [112] is used. This procedure involves a numerical check which relies on the coefficients of the one-derivative terms in the action in addition to the two-derivative terms. Hence to obtain a numerical check in the present gauge-invariant formalism, a boundary 'counter-term' has been added (distinct from those mentioned previously) to the off-shell action of the form

$$S^{\text{c.t.}} = \frac{r_0}{2\kappa_4^2}\int du \frac{d\omega d^2q}{(2\pi)^3}\frac{d}{du}\left[\phi_I\left(u,-\bar{\omega},-\bar{q}\right)\mathcal{D}^{\text{c.t.}}_{IJ}\left(u,\bar{\omega},\bar{q}\right)\phi_J\left(u,\bar{\omega},\bar{q}\right)\right], \tag{4.25}$$

where $\mathcal{D}^{\text{c.t.}}_{IJ}\left(u,\bar{\omega},\bar{q}\right)$ was chosen such that the full off-shell action could then be written in terms of the gauge-invariant variables $\bar{Z}_{1,2}$. This boundary term does not alter the equations of motion and as the coefficients $\mathcal{D}^{\text{c.t.}}_{IJ}$ are purely real, it does not have any effect upon the poles of the Green's functions or the diagonal spectral functions $\chi_{\epsilon\epsilon}$ and χ_{QQ}.

At $T = 0$, on the other hand, the Kodama-Ishibashi variables are used following the methods described in [3]. The equations of motion in these variables are given in

appendix A of [3]. Accurate numerics at $T = 0$ are only expected above $\bar{q} \gtrsim 0.1$, and hence only $T = 0$ results in this range are presented.

4.3 Temperature dependence of the sound mode

The primary motivation for studying this theory is that it supports stable, propagating excitations of energy and charge density at zero temperature and large chemical potential $\bar{q} \ll 1$. These sound modes at zero temperature have a dispersion relation of the form (4.1) where the speed is $v_s = 1/\sqrt{2}$ [3]. One would want to know what effect the increase of temperature has upon this mode - in particular one is interested to see if it shares the characteristics of the 'zero sound' mode of a Landau Fermi liquid. This comparison can be made by studying the sound attenuation as a function of temperature for $T \ll \mu$ and looking for the three different regimes shown in figure 4.1.

Note that when $\mu = 0$ and $\omega, q \ll T$, there are sound modes with the dispersion relation

$$\omega = \pm\frac{1}{\sqrt{2}}q - i\frac{1}{8\pi T}q^2 + O(q^3). \tag{4.26}$$

At non-zero μ, we would expect to recover these results when $\mu \ll \omega, q \ll T$, which is outside of the 'quantum liquid' regime $T \ll \mu$ where any LFL-like behaviour would be present.

The temperature dependence of the real and imaginary parts of the sound mode are shown in figures 4.2 and 4.3 for various $\bar{q} < 1$. The finite temperature numerical results are shown along with $T = 0$ numerical results (for $\bar{q} \geq 0.1$ where accurate results can be obtained) and the $\mu = 0$ analytic result (4.26).

The plots show that both the real and imaginary parts of the mode have a non-trivial temperature dependence. As the temperature is increased from zero, finite temperature corrections cause small changes to the real part of the sound mode whose sign depends upon the value of $\bar{q}$. At sufficiently high temperature, $T/\mu \gtrsim 1$, the real part quickly asymptotes to the $\mu = 0$ hydrodynamic result (4.26). The imaginary part of the sound mode shows similar behaviour. This is slightly surprising - it indicates that the $\mu = 0$ result (4.26) is valid when $q \ll \mu \ll T$. This will be reviewed in section 4.6.

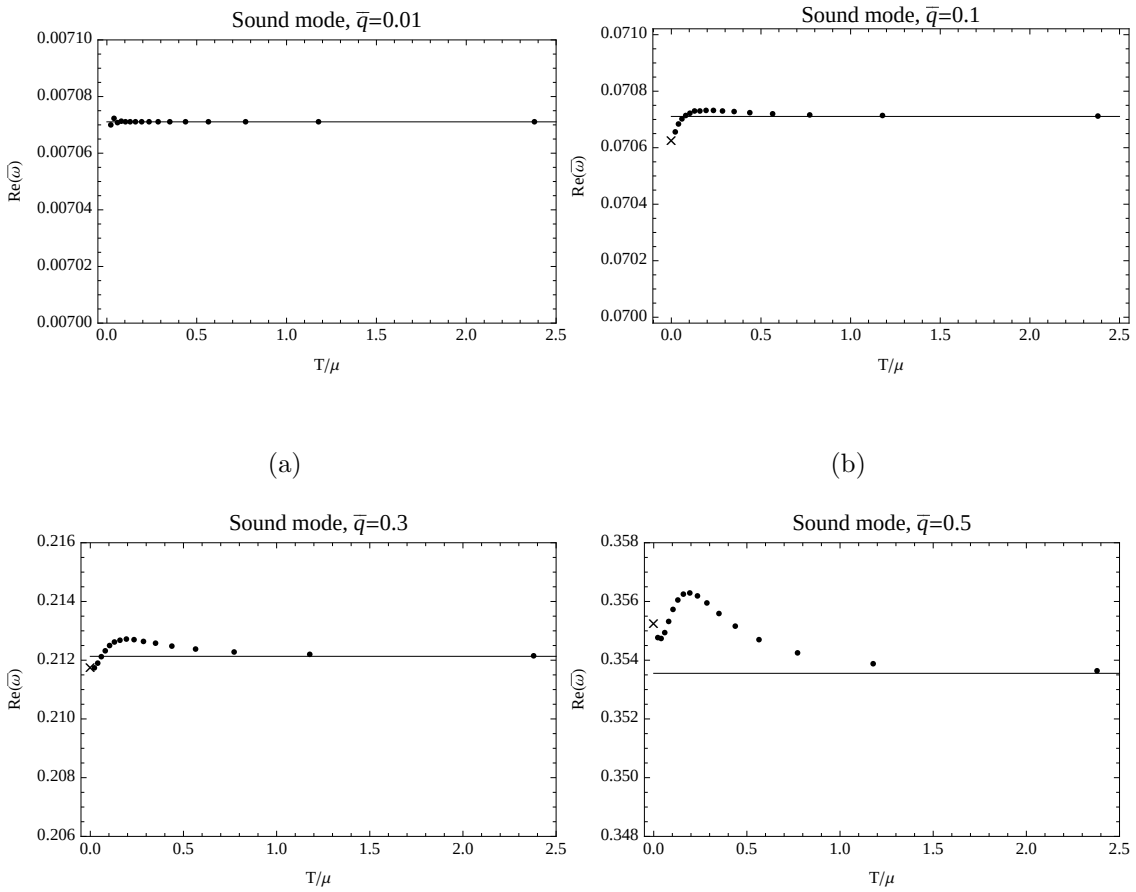

Figure 4.2: Variation of the real part of the sound mode as the temperature is increased. The crosses mark the $T = 0$ numerical results, the dots are the numerical results for $T > 0$, and the solid lines are the $\mu = 0$ analytic result (4.26).

To make an easier comparison with Landau Fermi liquid theory, the temperature dependence of the imaginary part of the sound mode is plotted on a logarithmic scale in figure 4.4. These plots show only the region $T < \mu$ where one may expect such a theory to apply, and the imaginary part of the sound mode is normalised by $\bar{\omega}_0$, its value at the lowest non-zero temperature that can be accessed.

There is a stark contrast between these plots and the results expected for an LFL zero sound mode, shown in figure 4.1.[2] Landau's theory predicts that as the tem-

[2]The magnitude of the frequency of the sound mode in the RN-AdS_4 theory is of the same order as its momentum for the results shown, and thus comparisons are made to the LFL results with $\omega \to q$.

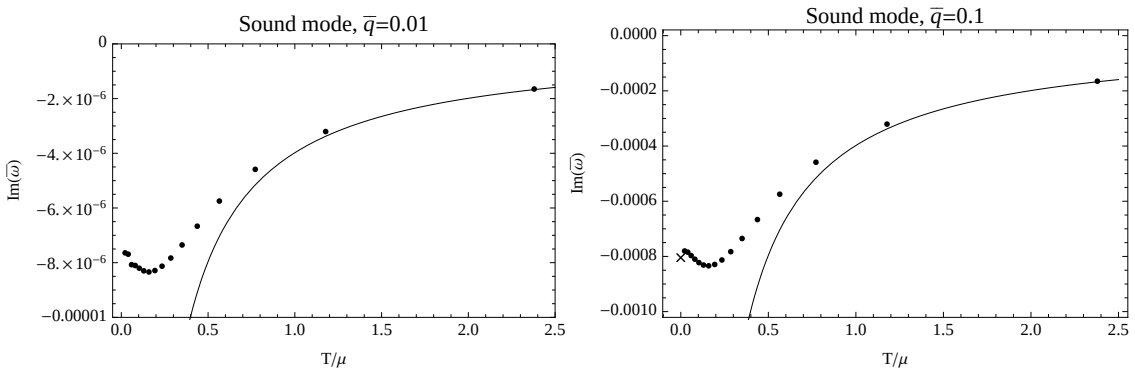

(a)

(b)

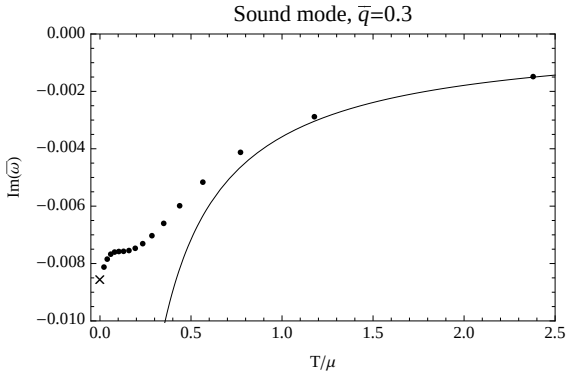

(c)

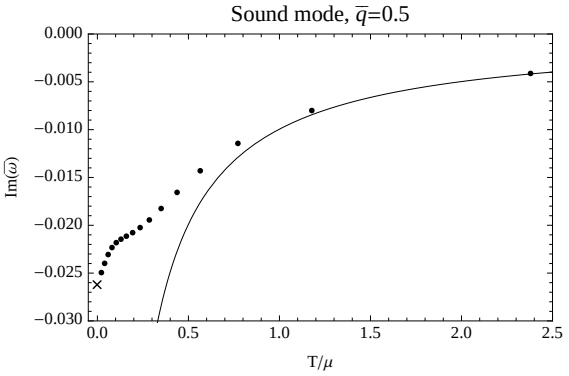

(d)

Figure 4.3: Variation of the imaginary part of the sound mode as the temperature is increased. The crosses marks the $T = 0$ numerical results, the dots are the numerical results for $T > 0$, and the solid lines are the $\mu = 0$ analytic result (4.26).

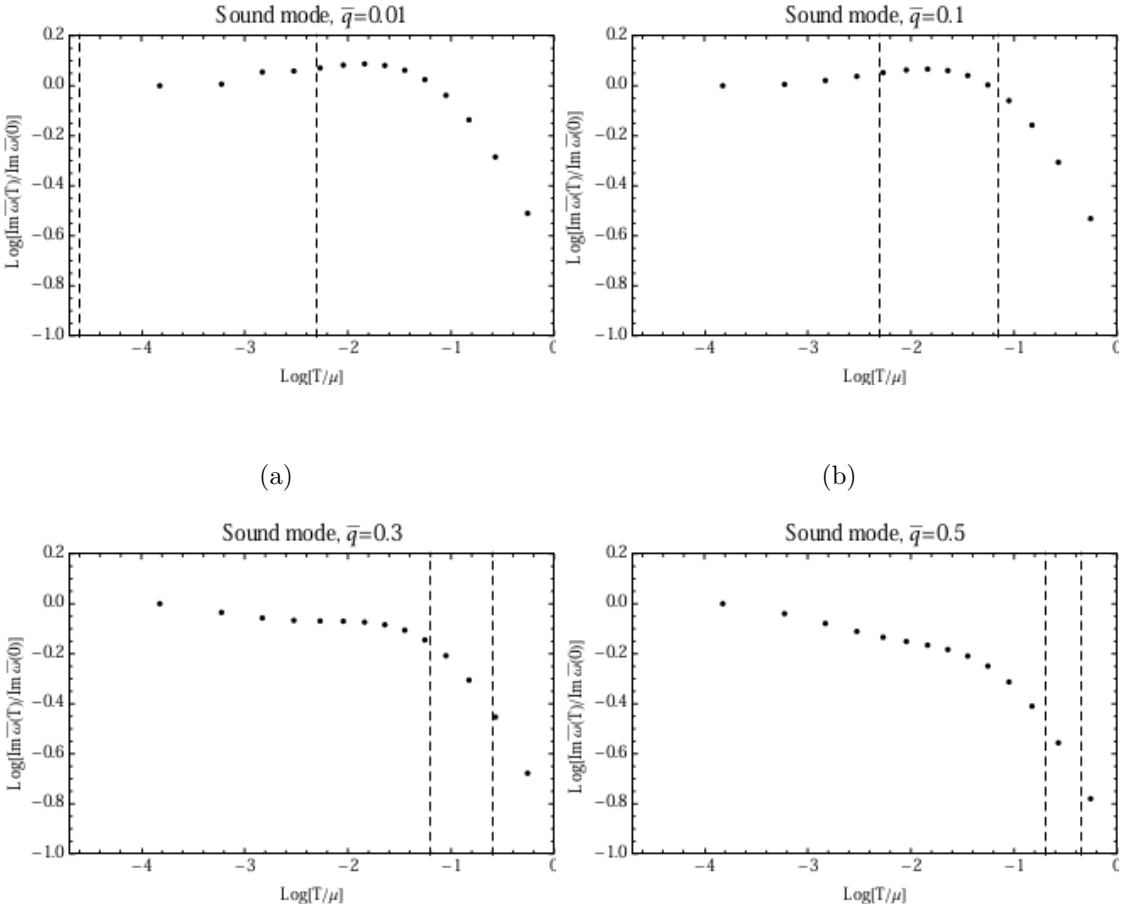

(a) (b)

(c) (d)

Figure 4.4: Variation of the imaginary part of the sound mode as the temperature is increased, in the regime $T < \mu$. The dots are the numerical results for $T > 0$, and the two dashed lines on each plot denote $T/\mu = q/\mu$ and $T/\mu = \sqrt{q/\mu}$ as one moves to the right along the plot.

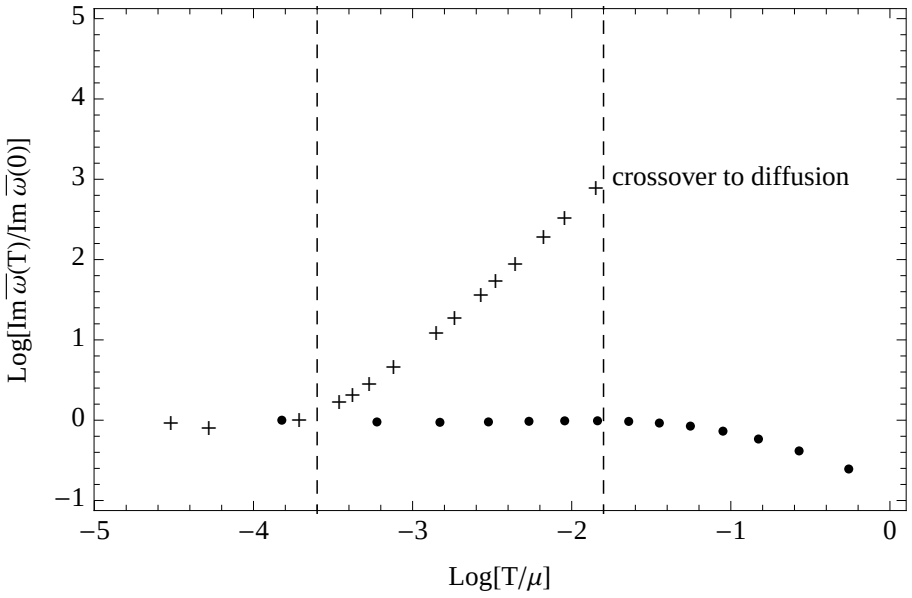

Figure 4.5: A superposition of the plots of the temperature dependence of the normalised imaginary part of the sound mode when $q/\mu = 0.2$ for both the D3/D7 theory and the RN-AdS_4 theory. Crosses denote the D3/D7 numerical results [2] and circles denote the RN-AdS_4 results. Moving from left to right, the dotted lines mark the transition points between the quantum and thermal collisionless regimes, and the thermal collisionless regime and the hydrodynamic regime, in the D3/D7 theory. These occur when $\omega \sim T$ and $\omega \sim T^2/\mu$ respectively. There are no results for the D3/D7 sound mode in the hydrodynamic regime since the hydrodynamic sound mode is suppressed in the probe brane limit. We refer the reader to [2] for a more detailed discussion of these features.

perature is increased at fixed q and μ, the imaginary part of the zero sound mode should be approximately constant up until $T/\mu \sim q/\mu$. Between $T/\mu \sim q/\mu$ and $T/\mu \sim \sqrt{q/\mu}$, it should increase like T^2. Above $T/\mu \sim \sqrt{q/\mu}$ and below $T/\mu \sim 1$, it should decrease like T^2. None of these features are present in our results. The magnitude of the imaginary part of the sound mode in our theory shows no significant temperature dependence until $T \sim \mu$. Above this, it begins to approach the $\mu = 0$, $\omega, q \ll T$ result (4.26) where it decreases as $1/T$.

An explicit comparison between these RN-AdS_4 results and the corresponding D3/D7 results is shown in figure 4.5. This highlights the fact that the D3/D7 sound mode behaves like the LFL zero sound mode, whereas the RN-AdS_4 sound mode does not.

4.4 Further temperature-dependent properties of the theory when $\bar{q} < 1$

In addition to the sound modes at $T = 0$, there are other propagating modes lying deeper in the complex frequency plane as well as a branch cut along the negative imaginary frequency axis [3]. In this section, changes in this configuration are studied as T/μ is increased at a fixed momentum $\bar{q} < 1$. In particular, attention is focused on the longest-lived purely imaginary mode - this exists at non-zero temperatures as the branch cut mentioned above dissolves into a series of poles when $T \neq 0$. We note here that when $\mu = 0$ and $\omega, q \ll T$, the longest-lived purely imaginary mode has the dispersion relation

$$\omega = -i\frac{3}{4\pi T}q^2 + O(q^3), \tag{4.27}$$

corresponding to hydrodynamic charge diffusion [109]. One expects to recover this behaviour at non-zero μ in the limit $\mu \ll \omega, q \ll T$.

It is also shown in this section how the energy density and charge density spectral functions of the theory change with the temperature, and in particular how the residues of the long-lived modes play an important role in the transition from sound domination of the charge density spectral function to diffusion domination.

Temperature dependence of the diffusion mode

The study begins with the longitudinal diffusion mode of the theory. At $T = 0$, the negative imaginary frequency axis is a branch cut [3]. At non-zero temperatures, this branch cut dissolves into a series of poles along the axis and generically these become less stable (they recede into the complex plane) as the temperature is increased. However, one of the modes is special in that it becomes more stable as the temperature is increased, and at very high temperatures it becomes the $\mu = 0$ hydrodynamic charge diffusion mode (4.27). Figure 4.6 shows how the imaginary part of this mode changes with the temperature. Its real part is always zero. Unlike for the sound mode, this plot has the same shape for all values of $0.01 \leq \bar{q} \leq 0.5$ and so we show only one for brevity. The decay rate of this mode decreases monotonically as the temperature is increased, and is described well by the $\mu = 0$ result (4.27) when $T \gtrsim \mu$. Again, it is non-trivial that the $\mu = 0$ result holds in the regime $q \ll \mu \ll T$. Note that there is no $T = 0$ point on this plot because it does not make sense to ask where the pole is in that case - the whole negative imaginary frequency axis forms a branch cut.

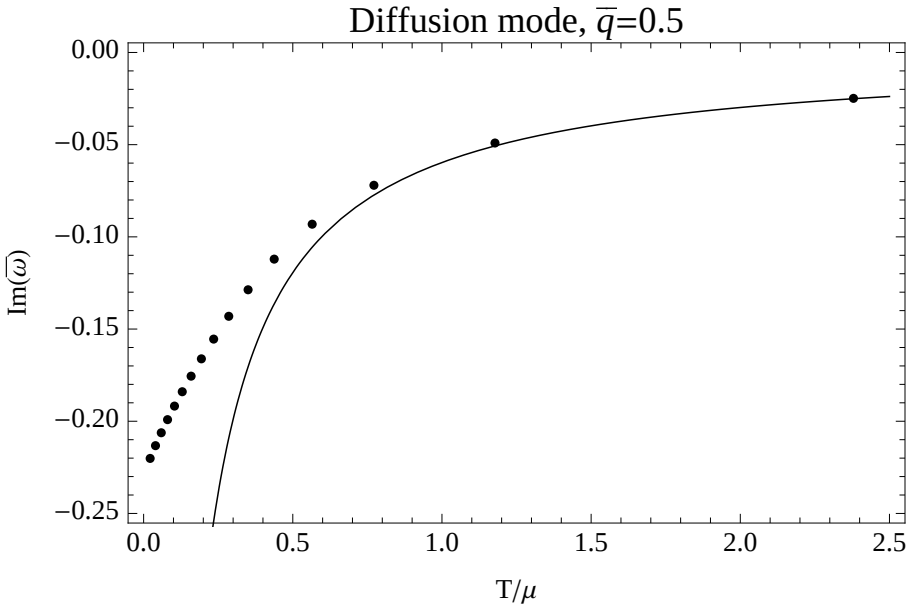

Figure 4.6: Variation of the imaginary part of the longitudinal diffusion mode as the temperature is increased. The dots are the numerical results for $T > 0$, and the solid line is the $\mu = 0$ analytic result (4.27).

Movement of the poles in the complex frequency plane with temperature

It is instructive to view the simultaneous movement of the Green's function poles described previously in the complex frequency plane as the temperature is increased - this is shown in figure 4.7. As described previously, the sound and diffusion modes both become more stable, approaching the real axis as the temperature is increased. Note that the sound mode is closer to the real axis than the diffusion mode for all values of the temperature and thus it is always the longest-lived mode of the theory. However this does not mean that it always dominates the low-energy properties of the theory, as it will be shown in the following subsection. Finally, it must be noted that both the sound and diffusion poles coexist for all non-zero values of the temperature that we can access numerically ($T \gtrsim 0.02\mu$). This is in contrast to the strongly-coupled D3/D7 field theory in which the low temperature sound poles collide to form the high temperature diffusion pole [2].

In addition to the sound and diffusion poles, there are 'secondary' modes corresponding to poles lying deeper in the complex frequency plane. These are much shorter-lived than the sound and diffusion poles when $\bar{q} < 1$ and become less stable

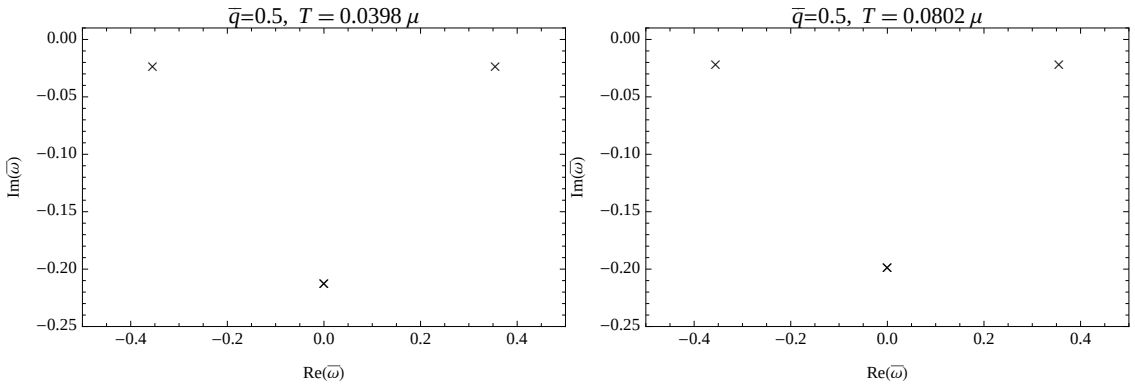

(a) (b)

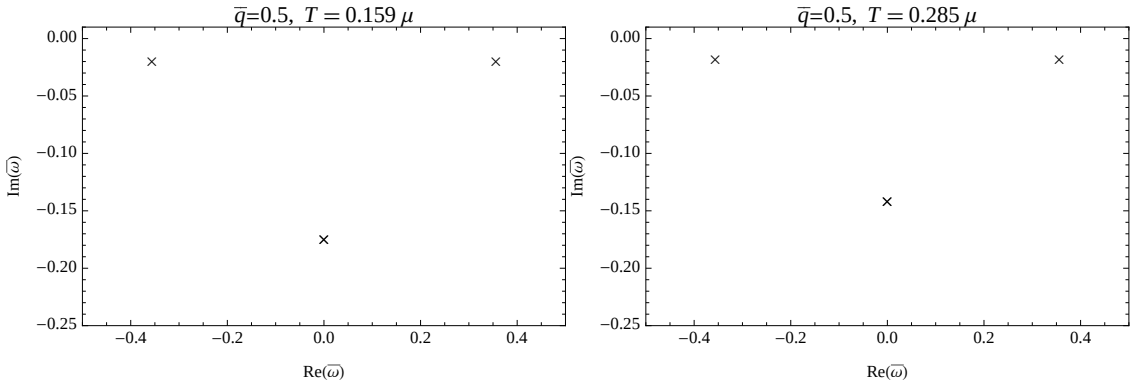

(c) (d)

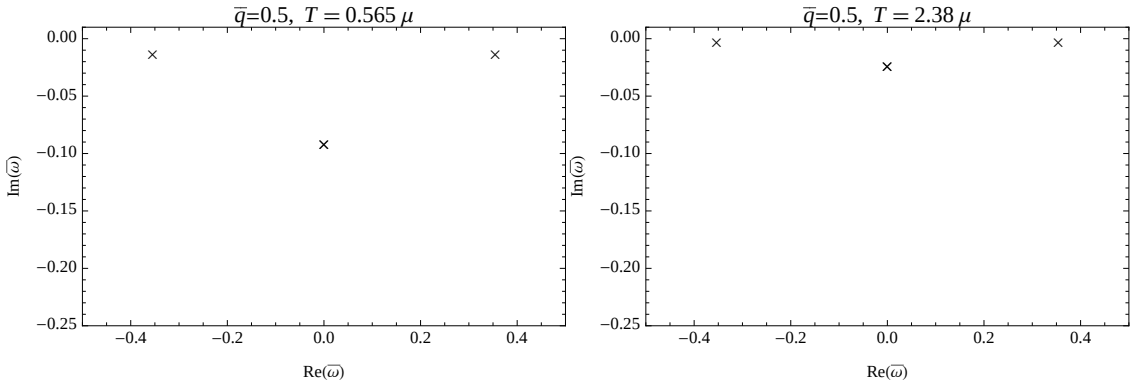

(e) (f)

Figure 4.7: Movement of the sound and diffusion poles in the complex frequency plane as the temperature is increased at fixed $\bar{q} = 0.5$.

as the temperature is increased. They do not have a significant effect on the low energy properties of the theory when $\bar{q} < 1$ and hence their temperature dependence is not shown.

Variation of the spectral functions with temperature

Up to this point, attention has been exclusively focused on the positions of the poles of the retarded Green's functions in the complex frequency plane. While these are interesting, they do not tell the full story of how charge and energy are transported in the theory. To investigate this, one needs to turn one's attention to the spectral functions of the energy density and charge density. These determine the average work done on the system when an external source of some frequency is applied to either the energy density or the charge density respectively. Despite the fact that the retarded Green's functions of both of these operators have the same set of poles, their spectral functions are quite different as shown in figures 4.8 and 4.9.

At very low temperatures, both spectral functions are dominated by the peak corresponding to sound propagation. As the temperature is increased, the spectral function of the energy density undergoes a fairly unremarkable change - the sound peak becomes narrower and taller (corresponding to a longer-lived excitation) but completely dominates at all temperatures. In contrast to this, the sound peak of the charge density spectral function becomes smaller (and narrower) as the temperature increases. At a sufficiently high temperature it becomes so small that the peak around $\bar{\omega} = 0$, corresponding to the high temperature diffusion mode, dominates the spectral function. At what temperature does this crossover occur? In figure 4.10, it is shown how the crossover value of μ/T (i.e. the value where the sound and diffusion peaks are of the same height) varies with q/μ. There is a clear linear relationship, signifying that the crossover occurs when

$$T_{\text{cross.}} \sim \mu^2/q, \tag{4.28}$$

and that diffusion dominates when $T \gg \mu^2/q$. Note that since we are studying the range $\bar{q} < 1$, this condition automatically implies that $T \gg \mu$. This crossover is reminiscent of the $\mu \to 0$ limit. In that limit, the fluctuations of $T^{\mu\nu}$ and J^μ decouple resulting in a hydrodynamic sound pole in the $T^{\mu\nu}$ correlators and a hydrodynamic diffusion pole in the J^μ correlators. The charge density spectral function in this limit is shown in [116]. However, it is not possible to interpret the crossover shown above to be due to approaching this limit, since it corresponds to the limit $\mu \ll q, T$ of the results, whereas the regime studied here is $q \ll \mu \ll T$.

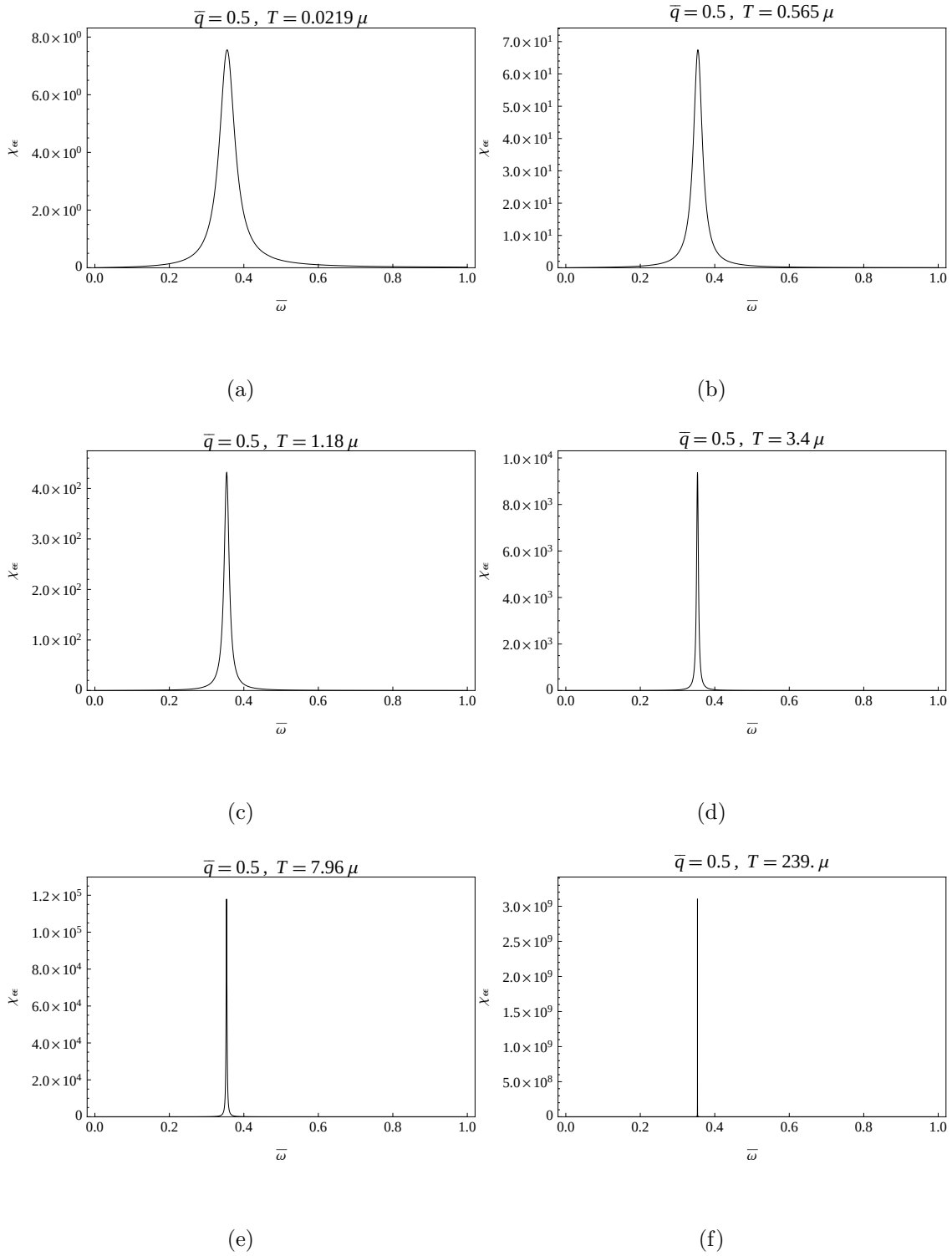

(a) (b)

(c) (d)

(e) (f)

Figure 4.8: The energy density spectral function for $\bar{q} = 0.5$ as the temperature is increased, in units of $2\mu^2 r_0/\kappa_4^2$. The peak due to sound propagation dominates at all temperatures.

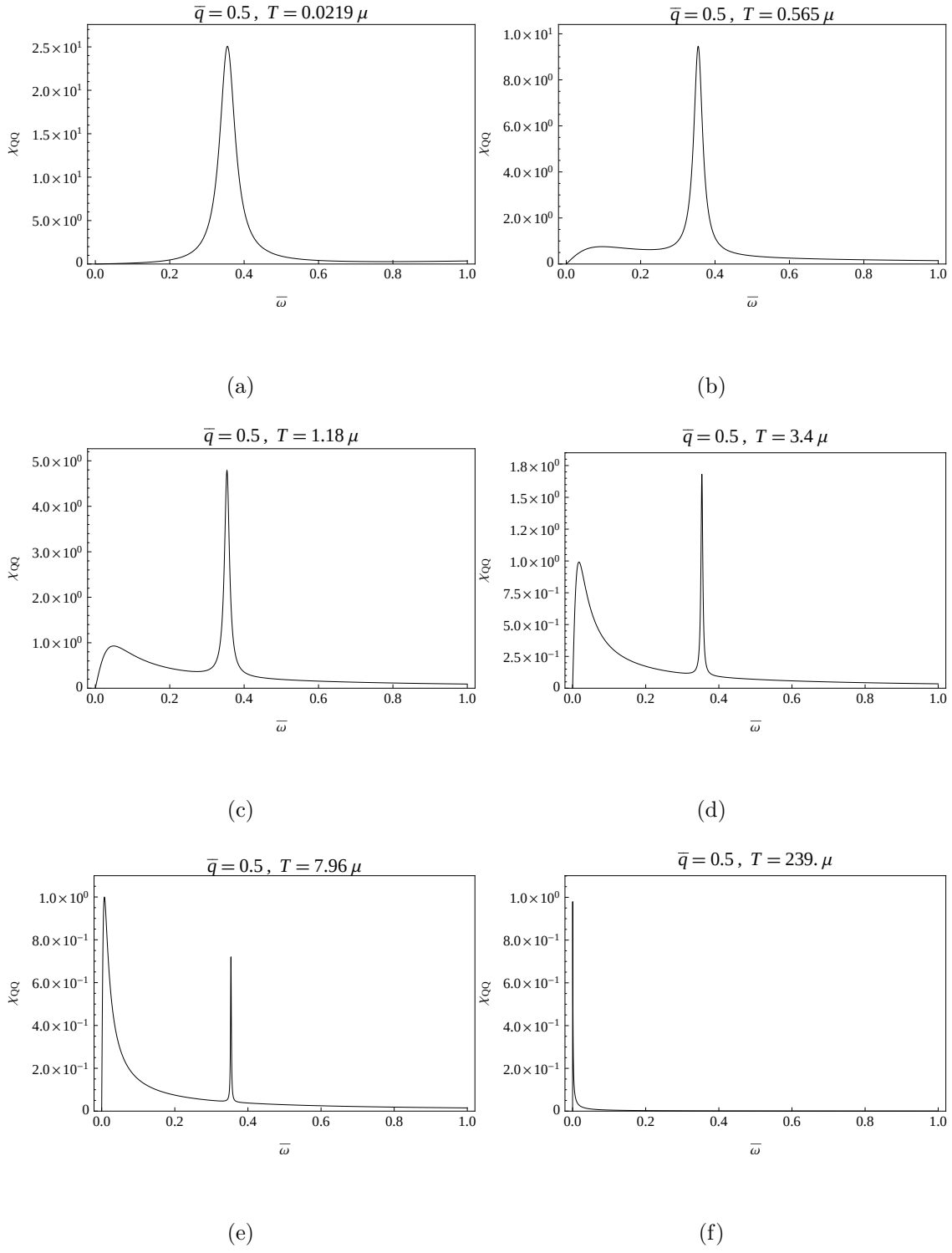

(a) (b)

(c) (d)

(e) (f)

Figure 4.9: The charge density spectral function for $\bar{q} = 0.5$ as the temperature is increased, in units of $2r_0/\kappa_4^2$. There is a crossover between sound domination and diffusion domination at high temperature.

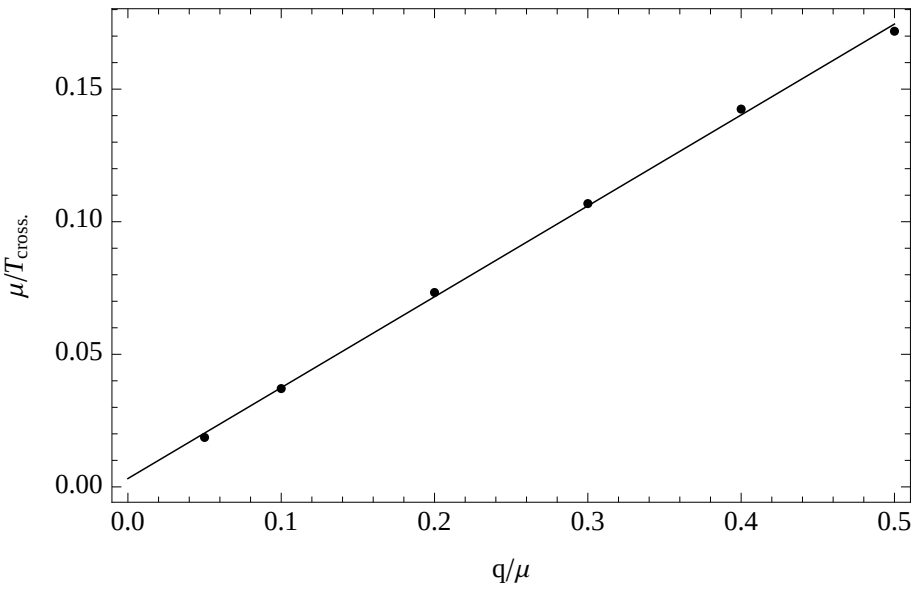

Figure 4.10: The dependence of the crossover value of μ/T upon q/μ. The best fit straight-line to these results has intercept ≈ 0.003 and gradient ≈ 0.34.

In the D3/D7 theory, the corresponding crossover occurred for $T_{\text{cross.}} \sim \sqrt{q\mu}$ and was reminiscent of the collisionless/hydrodynamic crossover in an LFL [2], but no such explanation is available here. In particular, the crossover observed here in the RN-AdS_4 theory occurs outside of the 'quantum liquid' regime $T \ll \mu$.

4.5 Dispersion relations at fixed temperature $T < \mu$

In the previous sections, it has been established how an increase in temperature affects the sound and diffusion modes that exist at some fixed, low momentum $q \ll \mu$. The next interesting object to study is the dispersion relations of these modes at a fixed temperature T and chemical potential μ. This is done by fixing T/μ and varying $\bar{q}$.

The sound mode dispersion relation

In [3], the dispersion relation at $T = 0$ and $\bar{q} \ll 1$ was found numerically to be of the form (4.1) with $v_s = 1/\sqrt{2}$ and $\Gamma_0 = 0.083$, which is remarkably close to the dispersion relation expected from the 'zero temperature hydrodynamics' described in the introduction and in [3], which has $\Gamma_0 = 0.072$ rather than 0.083.

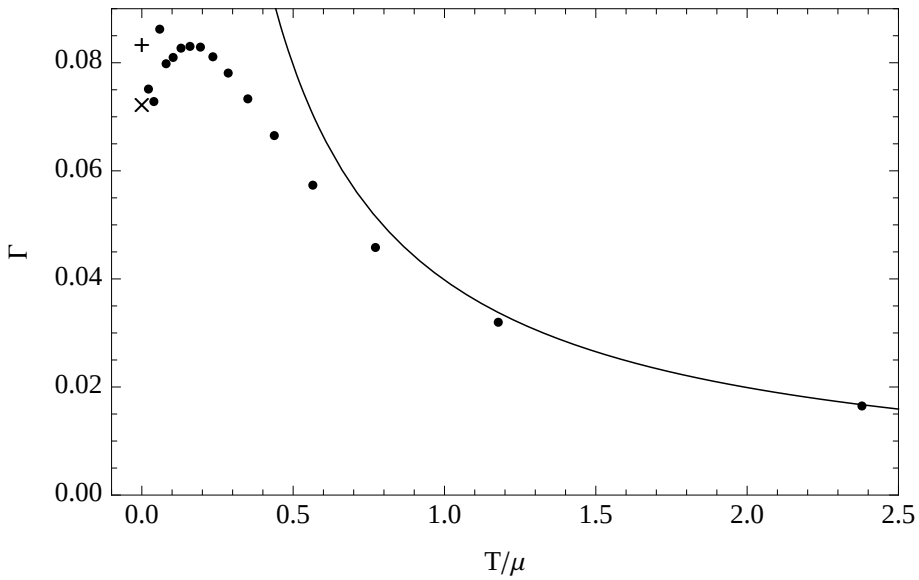

Figure 4.11: The temperature dependence of the quadratic term Γ in the imaginary part of the sound dispersion relation (4.4). Circles show our numerical results, the solid line shows the $\mu = 0$ analytic result (4.26), the '+' shows the $T = 0$ numerical result of [3] and the '$\times$' shows the prediction of '$T = 0$ hydrodynamics'.

Here a dispersion relation of the form (4.4) was found to be valid for non-zero temperatures also. The quadratic coefficient of the attenuation Γ as a function of temperature is shown in figure 4.11. These results were obtained by fitting over the range $0.01 \leq \bar{q} \leq 0.5$, and an example of the fit for $T = 0.0219\mu$ is shown in figure 4.12. At high temperatures $T \gg \mu$, it agrees with the $\mu = 0$ result (4.26), and at low temperatures $T \ll \mu$ it approaches a similar value to the $T = 0$ result of [3]. Although the results at very low T do not match smoothly onto the $T = 0$ numerical result of [3], they differ only by around 10% and it is believed that this is most likely caused by numerical inaccuracies, which grow as the temperature is lowered. The proximity of the numerical results to the prediction of '$T = 0$ hydrodynamics' is surprising - ultimately, an analytic calculation will be needed to determine whether these small discrepancies are due to inaccurate numerics, or whether this proximity is in fact a coincidence. The general trend of the results is clear however - as the temperature increases, the sound mode becomes more stable, as was observed in section 4.3.

When $\bar{q} \gtrsim 1$, this series form of the dispersion relation is useless. Figure 4.13 shows the dispersion relation of the sound mode when $q > \mu > T$, at two different temperatures: $T = 0$ and $T = 0.159\mu$. The dispersion relations have the same shape

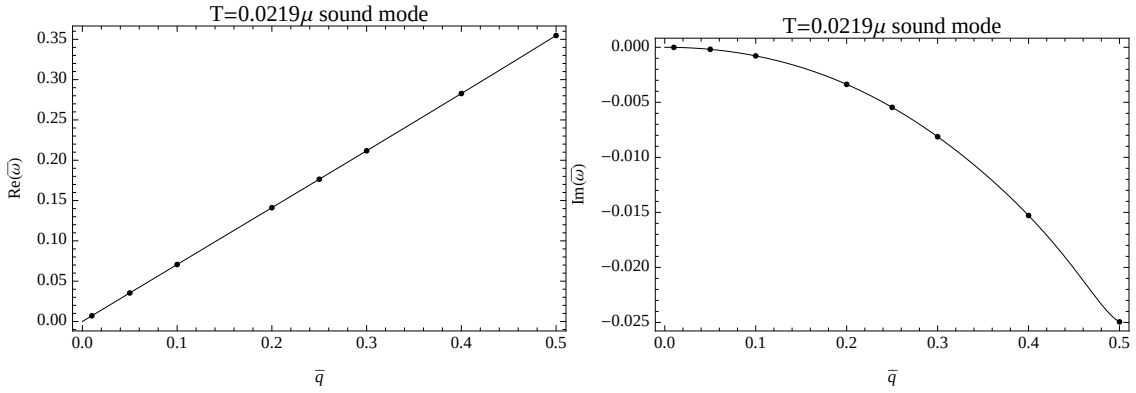

(a) (b)

Figure 4.12: The dispersion relation of the sound mode at $T = 0.0219\mu$ for $0.01 \leq \bar{q} \leq 0.5$. The circles show the numerical results and the solid line is the best fit $\bar{\omega} \approx \bar{q}/\sqrt{2} - i0.075\bar{q}^2 + O(\bar{q}^3)$.

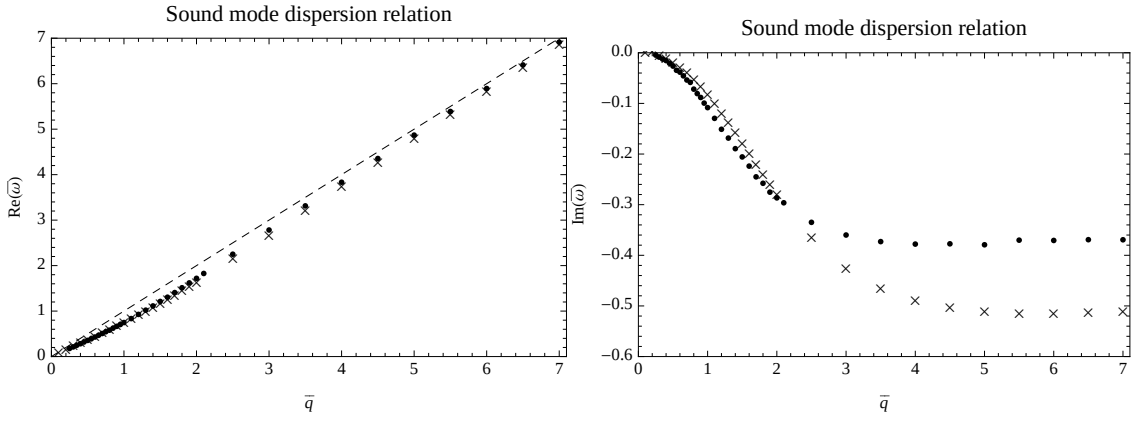

(a) (b)

Figure 4.13: The dispersion relation of the sound mode at two different temperatures: $T = 0$ (circles) and $T = 0.159\mu$ (crosses). The dashed line is the line $\mathrm{Re}\,(\bar{\omega}) = \bar{q}$.

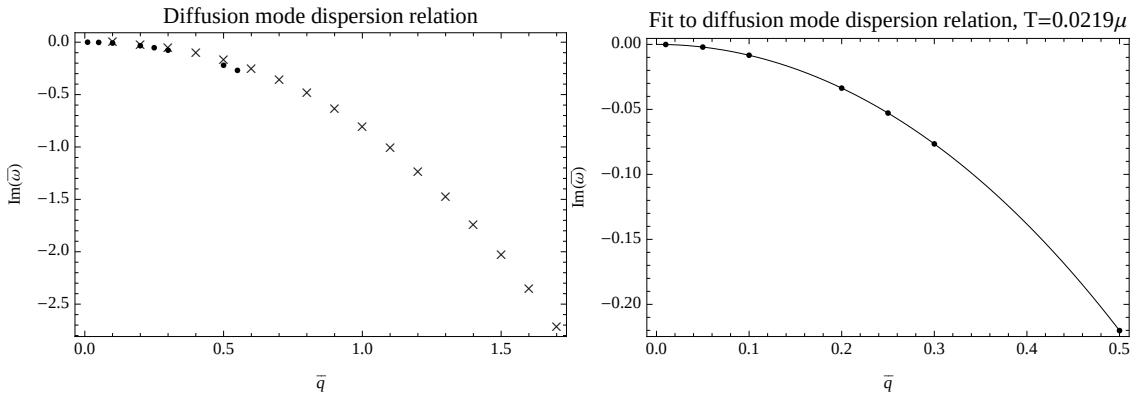

(a) Numerical results

(b) Best fit

Figure 4.14: The dispersion relation of the diffusion mode at two different temperatures: $T = 0.0219\mu$ (circles) and $T = 0.159\mu$ (crosses) with the polynomial best fit at $T = 0.0219\mu$ shown also (solid line). We cannot track the $T = 0.0219\mu$ mode for as high momenta as the $T = 0.159\mu$ mode.

at both temperatures - the real part asymptotes to $\bar{\omega} = \bar{q}$, and the imaginary part tends to a constant, in the region $q \gg \mu > T$.

The diffusion mode dispersion relation

Recall that at non-zero temperatures, the branch cut along the negative imaginary frequency axis becomes a series of poles and that the most stable of these becomes the $\mu = 0$ diffusion mode at high temperatures. Figure 4.14a shows the imaginary part of the dispersion relation of this pole at two fixed, low temperatures $T = 0.0219\mu$ and $T = 0.159\mu$ (its real part is always zero). At both temperatures, the pole recedes quickly into the complex plane as the momentum is increased. Performing a polynomial fit to the imaginary part in the range $0.01 \leq \bar{q} \leq 0.5$ at the very low temperature $T = 0.0219\mu$, a dispersion relation of the form (4.5) is found, with $D \approx 0.83$. The fit is shown in figure 4.14b. This therefore is an analogue, at low temperatures $T < q < \mu$, of the $\mu = 0$, $q \ll T$ hydrodynamic charge diffusion mode.

In fact, this quadratic form of the dispersion relation (4.5) is valid for all non-zero temperatures that could be accessed - the dependence of D upon T is shown in figure 4.15. D was extracted from a fit over the range $0.01 \leq \bar{q} \leq 0.5$. It decreases monotonically as the temperature is raised, in agreement with the results of section

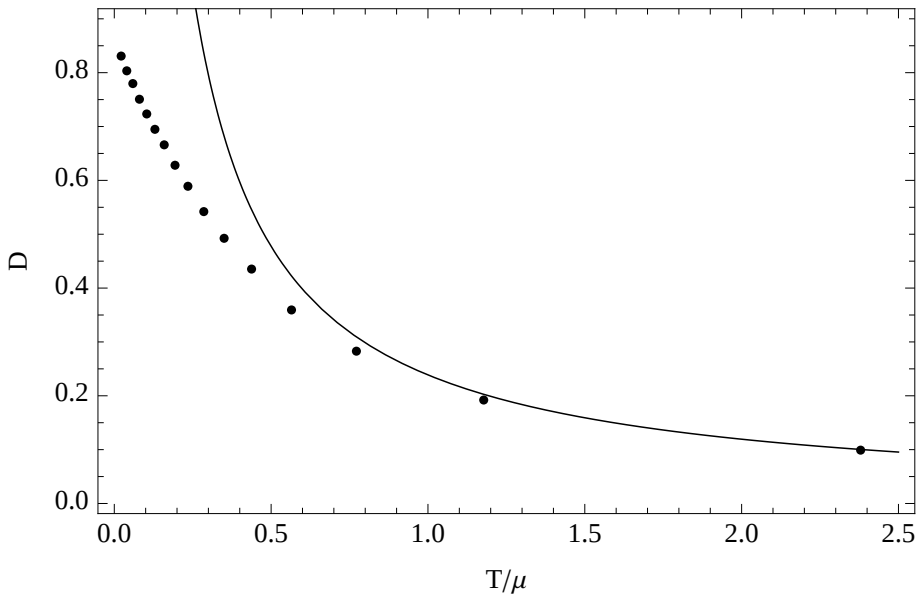

Figure 4.15: The temperature dependence of the quadratic coefficient D in the dispersion relation of the diffusion mode (4.5). The circles show the numerical results and the solid line is the analytic $\mu = 0$ result (4.27).

4.4, and approaches the $\mu = 0$ result (4.27) in the limit $T \gg \mu$. Again, it should be noted that this is despite the fact that the regime $\mu \gg q$ is studied.

It has not been possible to obtain the numerical accuracy required to access non-zero temperatures lower than $T = 0.0219\mu$ and hence it is impossible to say whether the mode exists with a quadratic dispersion relation for arbitrarily low non-zero temperatures. It is emphasized again that this mode does not exist at $T = 0$ itself (unlike the $T = 0$ 'R-spin diffusion' mode of [91]), as there is a branch cut in that case.

Dispersion relations of the secondary modes

Figures 4.16 and 4.17 show the dispersion relations of the second stablest ('secondary') propagating and purely imaginary modes at two different temperatures. These differ qualitatively from the sound and diffusion modes described above in that $\bar{\omega} \neq 0$ when $\bar{q} = 0$. At high momenta $q \gg \mu > T$, the propagating secondary modes have the same form as the sound modes - their real parts asymptote to $\mathrm{Re}\,(\bar{\omega}) = \bar{q}$ and their imaginary parts tend to a constant. The purely imaginary secondary mode recedes into the complex plane as the momentum is increased, and the rate at which this happens increases with the temperature.

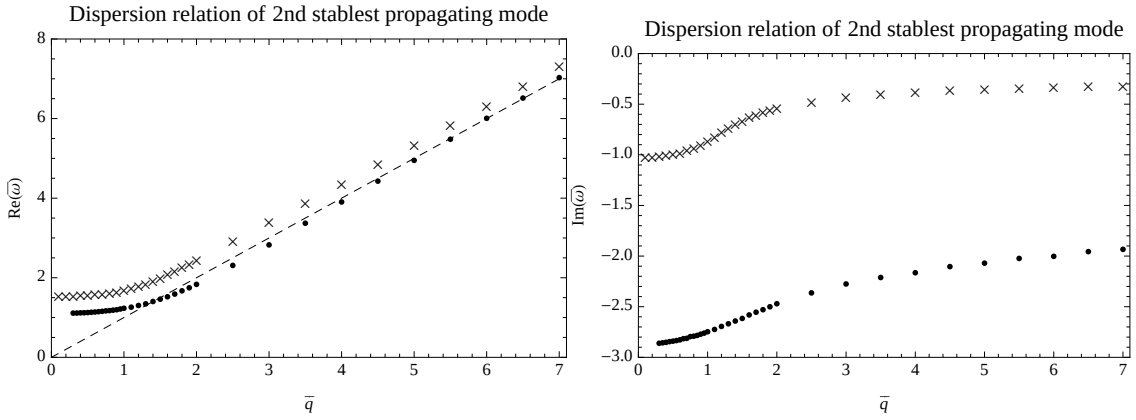

(a) (b)

Figure 4.16: The dispersion relation of the second stablest propagating mode at two different temperatures: $T = 0$ (circles) and $T = 0.159\mu$ (crosses). The dashed line is the line $\mathrm{Re}\,(\bar{\omega}) = \bar{q}$.

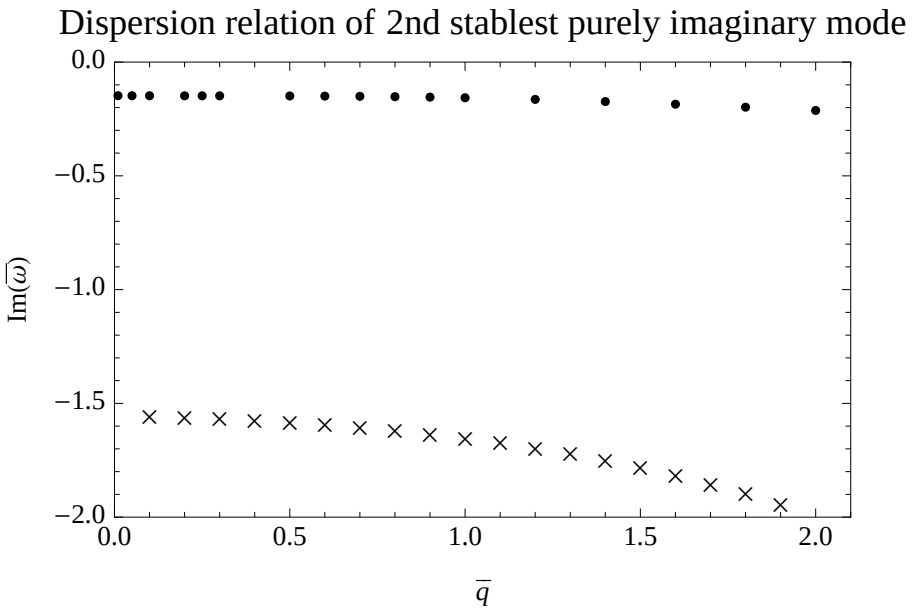

Figure 4.17: The dispersion relation of the second-stablest purely imaginary mode at two different temperatures: $T = 0.0219\mu$ (circles) and $T = 0.159\mu$ (crosses).

Movement of the poles in the complex frequency plane with momentum

It is instructive to view the simultaneous movements of these poles in the complex frequency plane as the momentum is increased. This is shown in figure 4.18 for $T = 0.159\mu$. It is apparent that as $\bar{q}$ is increased, the purely imaginary modes both become less stable as described previously. This figure shows that the diffusion mode destabilises much quicker than the secondary imaginary mode. The propagating modes show a different behaviour - their speeds both increase but their imaginary parts move in opposite directions and begin to approach each other in the complex plane as $\bar{q}$ increases. They eventually cross, before moving off horizontally together along the relativistic trajectory $\mathrm{Re}\,(\bar{\omega}) = \bar{q}$. At these high values of $\bar{q}$ it is clear that our original separation of modes into the stablest (sound and diffusion), second stablest etc. is of no value.

Variation of the spectral functions with momentum

Finally, attention is turned towards the spectral functions of the theory at low temperatures and as a function of the momentum $\bar{q}$. These are shown in figures 4.19 and 4.20 for $T = 0.159\mu$. At $\bar{q} = 0.5$, the lowest momentum shown, both spectral functions are completely dominated by the peak due to sound propagation. As the momentum is increased, this peak becomes smaller and wider and when $q \gtrsim \mu$, it no longer dominates the spectral function - a peak due to the secondary propagating mode also becomes visible. As the momentum is increased further, these two peaks merge into one peak which moves with speed $\mathrm{Re}\,(\bar{\omega}) = \bar{q}$ and constant width. This is a direct reflection of the two corresponding Green's function poles approaching each other in the complex plane. At high momenta, the value of the spectral function is very small at low frequencies $\bar{\omega} \lesssim \bar{q}$ and it only becomes significant when $\bar{\omega} \gtrsim \bar{q}$. Note that there is no significant difference between the charge density and energy density spectral functions in this regime.

4.6 An effective hydrodynamic scale

As discussed previously, when $\mu = 0$ there is a long-lived sound mode with momentum q provided that $q \ll T$, and when $T = 0$ there is a long-lived sound mode provided that $q \ll \mu$. In the first instance, this is the regime of applicability of hydro-

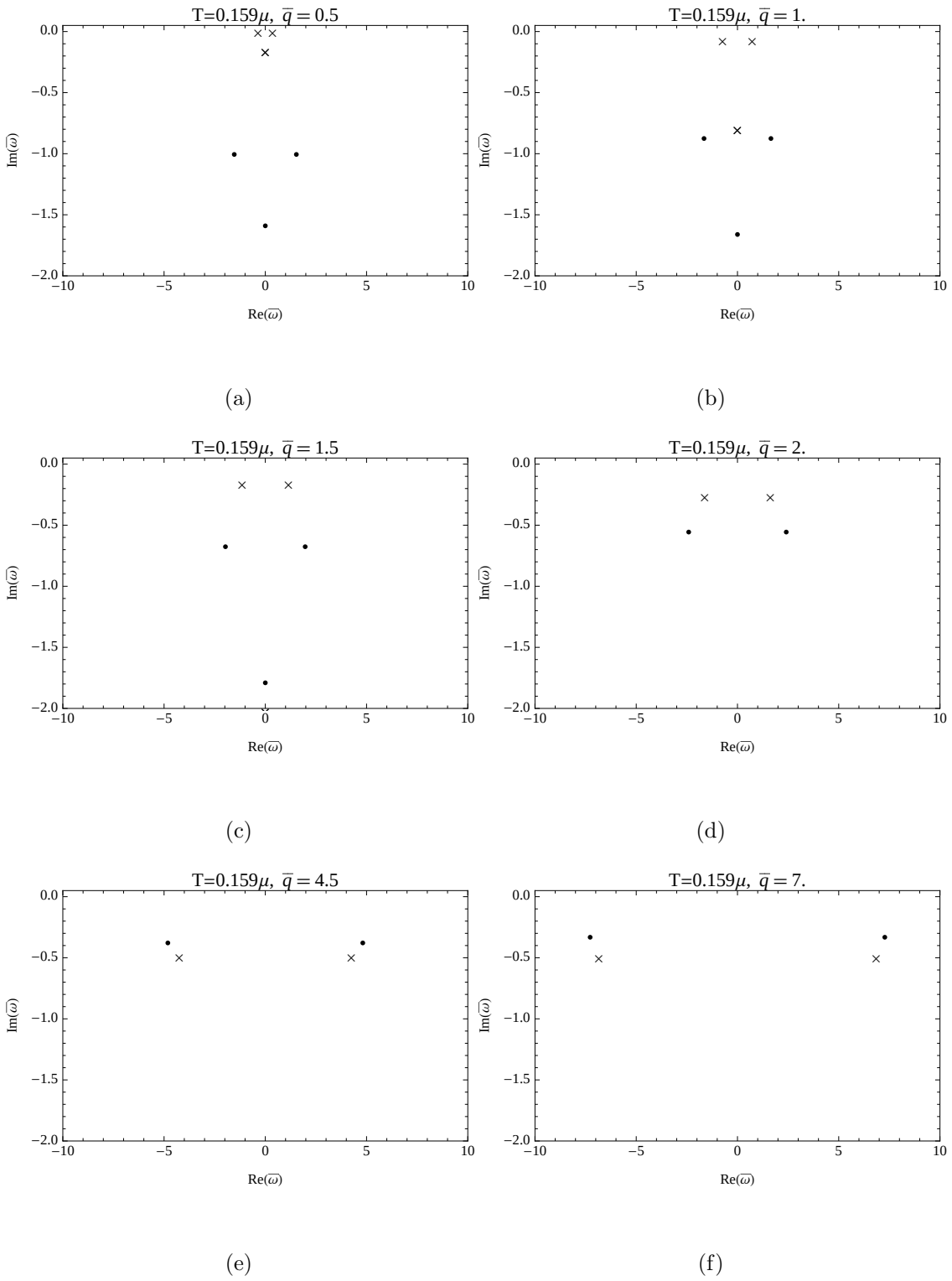

(a) (b)

(c) (d)

(e) (f)

Figure 4.18: Movement of the six longest-lived modes in the complex frequency plane as a function of momentum, for fixed $T = 0.159\mu$. The crosses denote the sound and diffusion modes, and the circles denote the secondary propagating and imaginary modes.

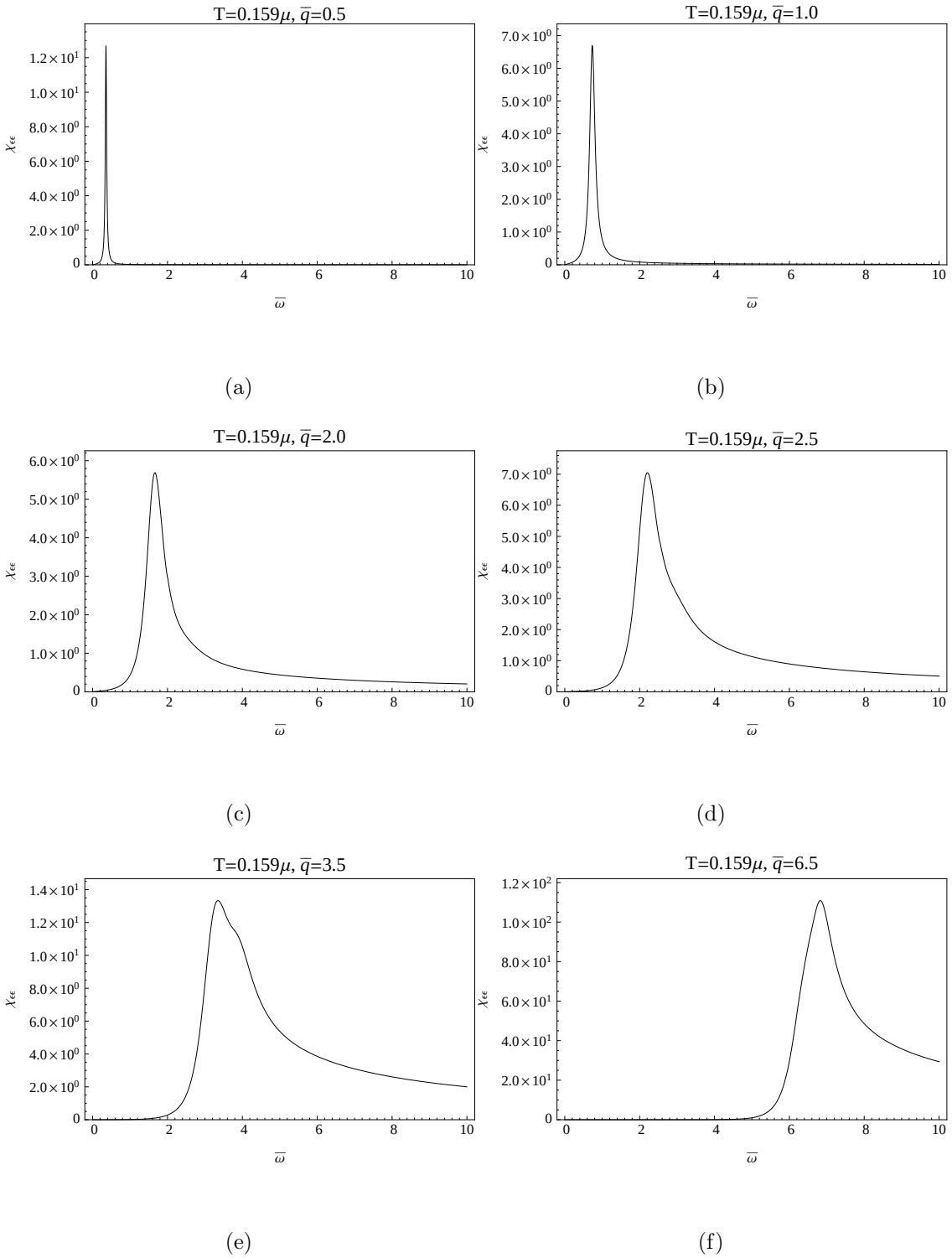

Figure 4.19: The energy density spectral function for $T = 0.159\mu$ as the momentum is increased, in units of $2\mu^2 r_0/\kappa_4^2$. As the momentum is increased, the peak due to sound propagation becomes less dominant.

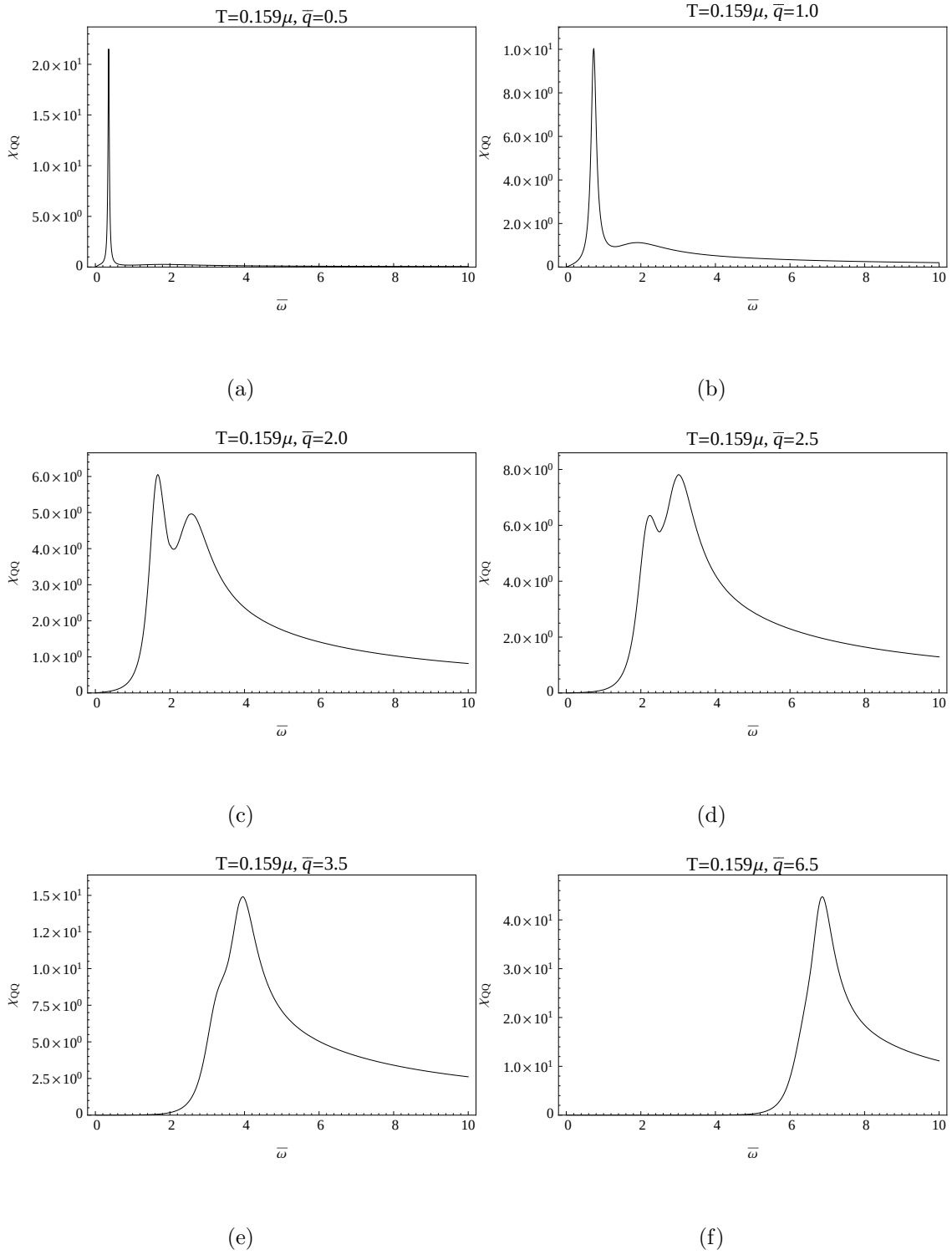

(a) (b) (c) (d) (e) (f)

Figure 4.20: The charge density spectral function for $T = 0.159\mu$ as the momentum is increased, in units of $2r_0/\kappa_4^2$. As the momentum is increased, the peak due to sound propagation becomes less dominant.

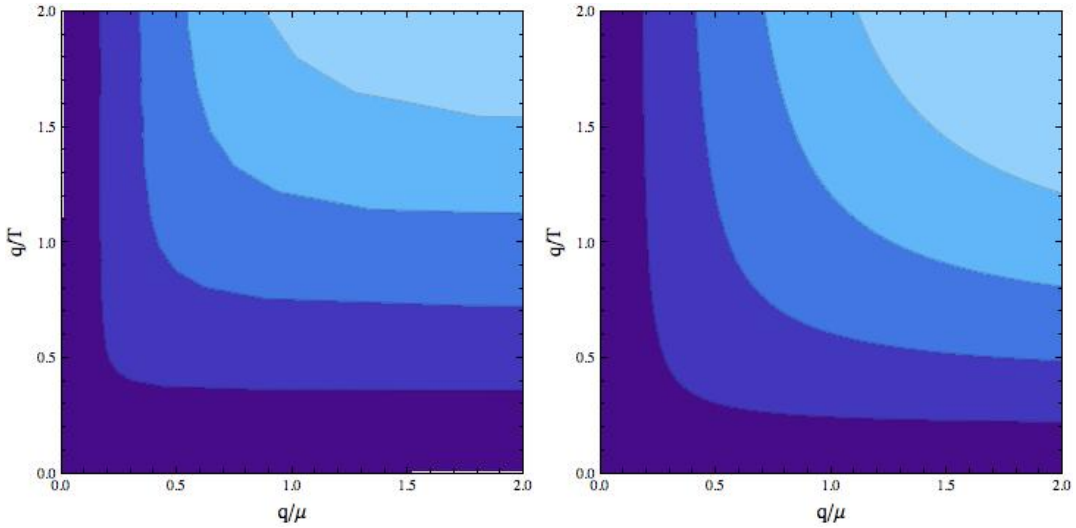

(a) Numerical results (b) Best fit

Figure 4.21: Contour plot showing $|\mathrm{Im}\,(\bar{\omega})\,|/\mathrm{Re}\,(\bar{\omega})$ for the sound mode as a function of q/μ and q/T and the best fit to these results: $a_0 = 10.1$ and $a_1 = 8.3$. Darker colours correspond to smaller values (i.e. more stable propagation) and the contours show the values 0.02, 0.04, 0.06, and 0.08.

dynamics and the condition on the momentum is such that the perturbations occur over much larger distance scales than the mean free path between thermal collisions.

The behaviour of the sound mode has been studied, when both T and μ are non-zero, to determine if there is some 'effective hydrodynamic scale' (or effective mean free path) which determines whether sound propagation is possible or not in this more general case. Figure 4.21a is a contour plot showing the value of $|\mathrm{Im}\,(\bar{\omega})\,|/\mathrm{Re}\,(\bar{\omega})$ - which is the ratio of the decay rate to the propagating frequency - for the sound mode as a function of q/μ and q/T. Darker colours correspond to smaller values (i.e. more stable propagation). There is a clear pattern in the plot - provided that *one* of q/T or q/μ is small enough, there is stable sound propagation. It suggests that there is an 'effective hydrodynamic scale' governing sound propagation which is qualitatively of the form $E_{\text{eff.}} = T\left(a_0 + \ldots + a_\alpha\left(\mu/T\right)^\alpha + \ldots + a_1\mu/T\right)$ where $\alpha \in (0,1)$. This reduces to the correct form in the $T = 0$ and $\mu = 0$ limits separately. A fit of the form $q/(a_0T + a_1\mu)$ could not quantitatively reproduce the plot above - suggesting that this ansatz is an oversimplification (for example, it neglects almost all terms of the form $(\mu/T)^\alpha$ in the denominator as well as higher order terms in q) - but does

give qualitatively the correct features for the sound propagation properties. Figure 4.21b shows the best fit to this form.

An effective hydrodynamic scale of this form is also consistent with the fact that the region $q \ll \mu \ll T$ reproduces the $\mu = 0$, $q \ll T$ results, as seen in section 4.3.

Chapter 5

Electron Star

Useful as it is, the Reissner-Nordström (RN) system exhibits a major complication, when using it in comparison with Condensed Matter systems. This comes from the peculiarity of Reissner-Nordström horizon. In particular it is well known (e.g. [113]) that at zero-temperature, i.e. at extremality, the area of the horizon does not vanish and given that the black hole's entropy is proportional to the horizon area, the system has non-zero entropy at zero temperature. This contradicts standard intuition from Condensed Matter. Many attempts have been made to construct systems that would have the necessary Holographic ingredients, the RN system provides, but circumventing the finite entropy limitation. One such system is the Electron Star. The system consists of an ideal fluid of bulk (in $3+1$ dimensions) fermions which is set-up in a similar way that the Neutron Star was constructed as a solution of Einstein's equations, resulting in the Tolman-Oppenheimer-Volkoff equations [117, 118]. In the infra-red regime and at zero temperature, the system asymptotes to a Lifshitz background geometry. The absence of a horizon resolves the finite entropy problem. Similarly at finite temperature, the system is a composite, consisting of an AdS-RN, that provides the temperature to the system, followed by the electron cloud and finally another AdS-RN up to the ultraviolet regime.

Another indication that extensions to the standard AdS-RN system need to be considered is that in many cases, RN black holes have been found to be thermodynamically unstable, transitioning to different systems. This transition involves the discharge of the black hole via various mechanisms, resulting in some bulk field carrying the charge that was "hiding" behind the horizon. Such mechanisms have been extensively explored and some indicative examples include, charged scalar field condensation [11], fermion Cooper pairing [119], D-branes emission [82, 120, 121], fermionic back-reaction [82], confinement [122–124] and lattice emergences [125]. Moreover

in [126] the more general issue of whether any finite-size-horizon black brane remains stable at zero temperature, has been addressed.

5.1 Background

As introduced in [127–129] the Electron Star emerges as a solution to the Einstein-Maxwell system with non-trivial stress-energy tensor. Namely, the Einstein equations are

$$R_{\mu\nu} - \frac{1}{2}g_{\mu\nu}R - \frac{3}{L^2}g_{\mu\nu} = \kappa^2\left[\frac{1}{e^2}\left(F_{\mu\sigma}F_{\nu}{}^{\sigma} - \frac{1}{4}g_{\mu\nu}F_{\rho\tau}F^{\rho\tau}\right) + T_{\mu\nu}\right] \tag{5.1}$$

while the Maxwell equations are

$$\nabla_{\alpha}F^{\beta\alpha} = e^2 J^{\beta} \tag{5.2}$$

Here the crucial difference to the AdS-RN system is the non-trivial energy-momentum tensor on the right-hand side of eq. (5.1), which given that one is dealing with a perfect fluid, is

$$T_{\mu\nu} = (p+\rho)u_{\mu}u_{\nu} + pg_{\mu\nu}\ ,\ J_{\mu} = \sigma u_{\mu} \tag{5.3}$$

Where p, ρ, σ are the pressure, energy and charge density respectively. Moreover u_{μ} is the velocity field which is normalized so that $u^2 = -1$, L is the characteristic length scale of the AdS, e is the electromagnetic coupling, κ Newton's constant (in $d = 3+1$). As is usual the case one makes the black-brane ansatz in search for solutions to this problem. Namely

$$ds^2 = L^2\left[-f(r)dt^2 + \frac{1}{r^2}(dx^2+dy^2) + g(r)dr^2\right] \tag{5.4}$$

for the metric, while for the gauge field

$$A = \frac{eL}{\kappa}h(r)dt \tag{5.5}$$

In order to unclutter the formalism, as well as in anticipation of numerical calculations, it makes sense to rescale the fields in order to absorb the various constants. To achieve this one rescales

$$p \to p = \frac{1}{L^2\kappa^2}\hat{p}\ ,\ \rho \to \rho = \frac{1}{L^2\kappa^2}\hat{\rho}\ ,\ \sigma \to \sigma = \frac{1}{eL^2\kappa}\hat{\sigma} \tag{5.6}$$

and works with the hatted variables. Introducing the ansatz (5.4, 5.5, 5.3) into the Einstein-Maxwell system, one gets the following system of equations for the fields to

be determined, i.e. f, g, h, p, ρ, σ

$$\hat{p}' + (\hat{p} + \hat{\rho})\frac{f'}{2f} - \frac{h'\hat{\sigma}}{\sqrt{f}} = 0 \tag{5.7}$$

$$\frac{1}{r}\left(\frac{f'}{f} + \frac{g'}{g} + \frac{4}{r}\right) + (\hat{p} + \hat{\rho})g = 0 \tag{5.8}$$

$$\frac{f'}{rf} - \frac{h'^2}{2f} + g(3 + \hat{p}) - \frac{1}{r^2} = 0 \tag{5.9}$$

$$h'' + \frac{rh'}{2}g(\hat{p} + \hat{\rho}) - g\sqrt{f}\hat{\sigma} = 0 \tag{5.10}$$

At first glance, it seems as if one has an under-determined system, since there are more fields than equations. However, if one takes into account the assumptions about the fluid, i.e. that it is an ideal fluid constituting of zero-temperature fermions[1] of unit charge and mass m. Filling up the fermionic states on has a density of states $\boldsymbol{g}(E) = \beta E\sqrt{E^2 - m^2}$[2]. Using that one can determine the pressure, energy and charge density through

$$\rho = \int_m^\mu dE E\boldsymbol{g}(E)\ ,\ \sigma = \int_m^\mu dE\boldsymbol{g}(E)\ ,\ p = \mu\sigma - \rho \tag{5.11}$$

where μ is the chemical potential. Now comes a quite drastic approximation - the locally flat space approximation. This means that the local chemical potential, which governs the fermions, is assumed to be the tangent frame value of the gauge field, i.e.

$$\mu_{local} = A_{\bar{t}} = \frac{1}{L\sqrt{f}}A_t = \frac{e}{\kappa}\frac{h}{\sqrt{f}} \tag{5.12}$$

Inserting this assumption into the definitions (5.11) and rescaling everything

$$\hat{\rho} = \hat{\beta}\int_{\hat{m}}^{\frac{h}{\sqrt{f}}} dE E^2\sqrt{E^2 - \hat{m}^2}\ ,\ \hat{\sigma} = \hat{\beta}\int_{\hat{m}}^{\frac{h}{\sqrt{f}}} dE E\sqrt{E^2 - \hat{m}^2}\ ,\ \hat{p} = \frac{h}{\sqrt{f}}\hat{\sigma} - \hat{\rho} \tag{5.13}$$

where $\hat{\beta} = \frac{e^4L^2}{\kappa^2}\beta$ and $\hat{m}^2 = \frac{\kappa^2}{e^2}m^2$. Intuitively the approximation used, precludes any gravitational and electromagnetic interactions, which however is acceptable. To see why assume that $\hat{\sigma} \sim 1$ and $e^2 \sim \kappa/L \ll 1$ which means that $\sigma L^3 \sim \frac{1}{e^3} \gg 1$. This is covered by the classical gravity limit, which is implicitly used and the fact that the Compton length of the fermions is much smaller that the curvature scale.

[1] The zero-temperature approximation is justified because any correction to that would be of the order $\frac{T}{\mu} \sim \mathcal{O}(\frac{\kappa}{eL}) \ll 1$. Here T, μ are the local quantities carrying metric components to account for their radial position.

[2] β is a free parameter of the system that will be later encountered.

Equations (5.13) eliminate three of the unknown fields, in the equations of motion, reducing them down to three, involving only f, g, h as dynamic fields

$$\frac{1}{r}\left(\frac{f'}{f}+\frac{g'}{g}+\frac{4}{r}\right)+\frac{gh\hat{\sigma}}{\sqrt{f}}=0 \tag{5.14}$$

$$\frac{f'}{rf}-\frac{h'^2}{2f}+g(3+\hat{p})-\frac{1}{r^2}=0 \tag{5.15}$$

$$h''+\frac{g\hat{\sigma}}{\sqrt{f}}\left(\frac{rhh'}{2}-f\right)=0 \tag{5.16}$$

For finite temperature, as discussed before, at the deep IR the space-time is that of AdS-RN. In particular using the forms (5.4,5.5), AdS-RN corresponds to

$$\begin{aligned} f &= \frac{1}{r^2}-\left(\frac{1}{r_+^2}+\frac{\hat{\mu}^2}{2}\right)\frac{r}{r_+}+\frac{\hat{\mu}^2}{2}\frac{r^2}{r_+^2} \\ g &= \frac{1}{r^4 f} \\ h &= \hat{\mu}\left(1-\frac{r}{r_+}\right) \end{aligned} \tag{5.17}$$

where r_+ is the location of the event horizon and $\hat{\mu}$ the chemical potential. It is clear from the above, and expressions (5.13) that the star cannot be supported for any temperature of the black hole. That is for a given mass $\hat{m}$ the star appears only when the AdS-RN parameters f, g, h, that are governed by the temperature as the only physical parameter of the black hole, become such that

$$\hat{m}=\frac{h}{\sqrt{f}}\ ,\ \frac{d}{dr}\frac{h}{\sqrt{f}}=0 \tag{5.18}$$

All the information is in place now, to compute the background solutions for $T>0$. This is done by taking the AdS-RN at lower and lower temperatures and solving the background equations (5.14,5.15,5.16) numerically in the exterior. In order to do so the coordinates have been switched ($r\to u$) so that the horizon is at $u=1$ and the AdS boundary at $u=0$. This allows for a better depiction of the full range of features. Moreover the controlling parameter used, is the dimensionless T/μ instead of just T. The results for $T/\mu=0.00003, 0.007, 0.027, 0.05, 0.07, 0.09, 0.12, 0.13$ are presented in fig. 5.1. What becomes immediately obvious is that there is a critical temperature, determined by eq. (5.18), over which the Electron Star background equations have no non-trivial solutions, or in other words a finite star cannot be sustained. Once the critical temperature is crossed the star emerges and as one continues to lower the temperature, it eventually dominates the full space-time. It

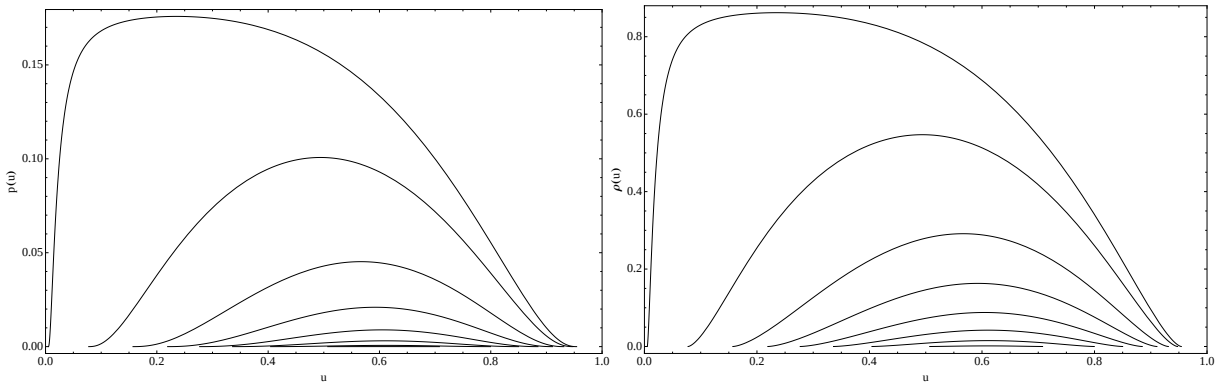

(a) Pressure

(b) Energy density

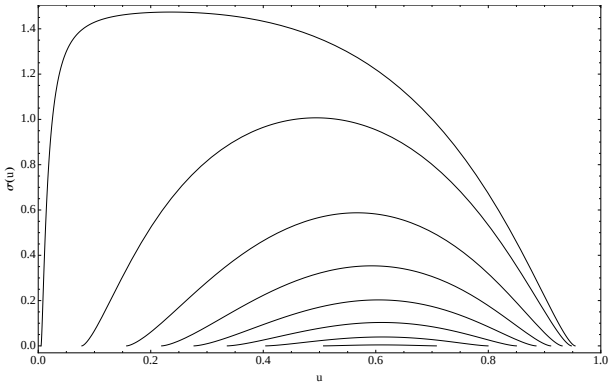

(c) Charge density

Figure 5.1: The Electron Star's development as a function of T/μ. The top curves correspond to $T/\mu = 0.00003$ and the bottom ones to $T/\mu = 0.13$. Here $\hat{m} = 0.36$, $\hat{\beta} = 19.951$.

should also be mentioned that the star eventually ends, at its surface (which is also a function of the temperature), determined by the position where all p, ρ, σ vanish. As mentioned before there are two free parameters in this system, i.e. $\hat{m}$ and $\hat{\beta}$, which affect the star dynamics. As it will be shown momentarily these two are tied in an interesting way at $T = 0$, but for now an indicative set of plots depicting the dependence of the star on them, is displayed in fig. 5.2.

The $T = 0$ case will now be examined more carefully. As seen above, as one lowers the temperature the Electron Star background tends to dominate the spacetime. Strictly at $T = 0$, another very interesting solution to (5.14,5.15,5.16) emerges.

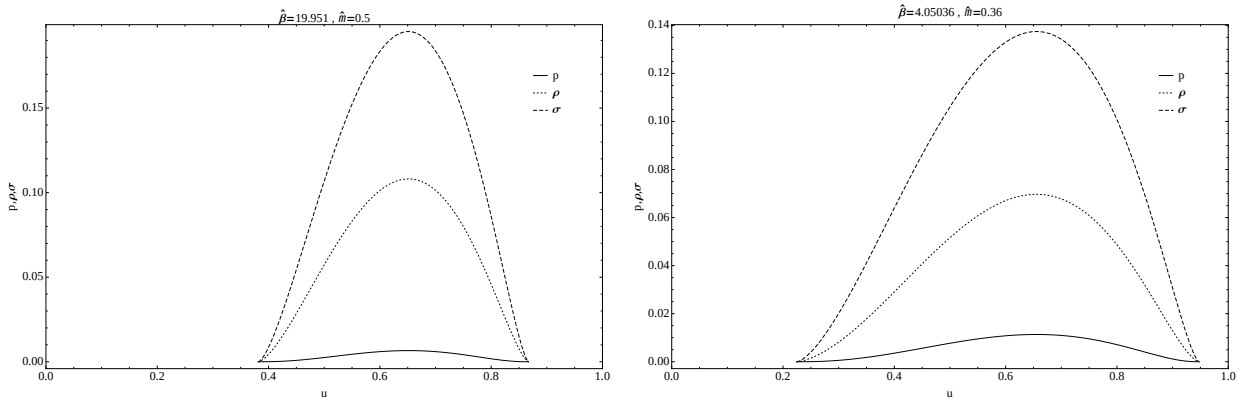

(a) $\hat{m} = 0.5, \hat{\beta} = 19.051$ (b) $\hat{m} = 0.36, \hat{\beta} = 4.05036$

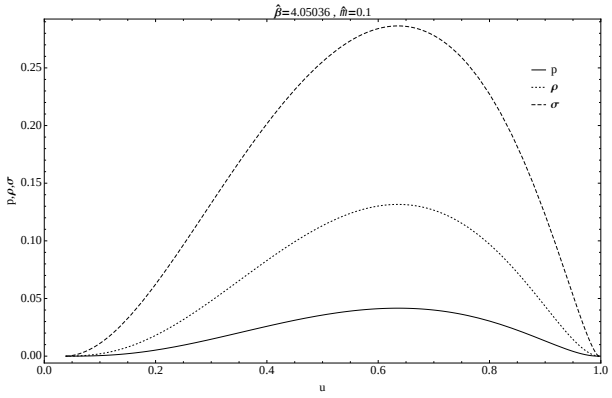

(c) $\hat{m} = 0.1, \hat{\beta} = 4.05036$

Figure 5.2: Dependence of the Electron Star background on the parameters $\hat{m}, \hat{\beta}$ for $T/\mu = 0.007$.

That is the Lifshitz solution, i.e.

$$f = \frac{1}{r^{2z}} \ , \ g = \frac{g_\infty}{r^2} \ , \ h = \frac{h_\infty}{r^z} \tag{5.19}$$

where z is dynamical critical exponent. By plugging the Lifshitz solution into the background equations, the parameters g_∞ and h_∞ are determined. In particular eliminating $\hat{\beta}$ from (eq. (5.14)) and (eq. (5.16)) yields

$$h_\infty^2 = \frac{z-1}{z} \tag{5.20}$$

and substituting this in (eq. (5.14)) results in

$$g_\infty^2 = \frac{36(z-1)z^4}{((1-\hat{m}^2)z-1)\hat{\beta}^2} \tag{5.21}$$

Using the last two equations in (eq. (5.15)), one gets a rather complicated relation between $z, \hat{\beta}, \hat{m}$, namely

$$\frac{1}{4}\left(\sqrt{-\frac{(z-1)z^4}{\beta^2\left((m^2-1)\,z+1\right)^3}}\left(\frac{\beta\sqrt{z-1}\sqrt{-m^2-\frac{1}{z}+1}\left(\left(2-5m^2\right)z-2\right)}{z^{3/2}}+72\right)\right.$$
$$\left.-3\beta m^4\sqrt{-\frac{(z-1)z^4}{\beta^2\left((m^2-1)\,z+1\right)^3}}\log\left(\frac{m}{\sqrt{-m^2-\frac{1}{z}+1}+\sqrt{\frac{z-1}{z}}}\right)-2(z+1)(z+2)\right)=0 \tag{5.22}$$

which albeit analytically intractable, can be numerically solved (fig. 5.3), meaning that out of $z, \hat{\beta}, \hat{m}$, only two are really independent. Taking sections of fig. 5.3 one

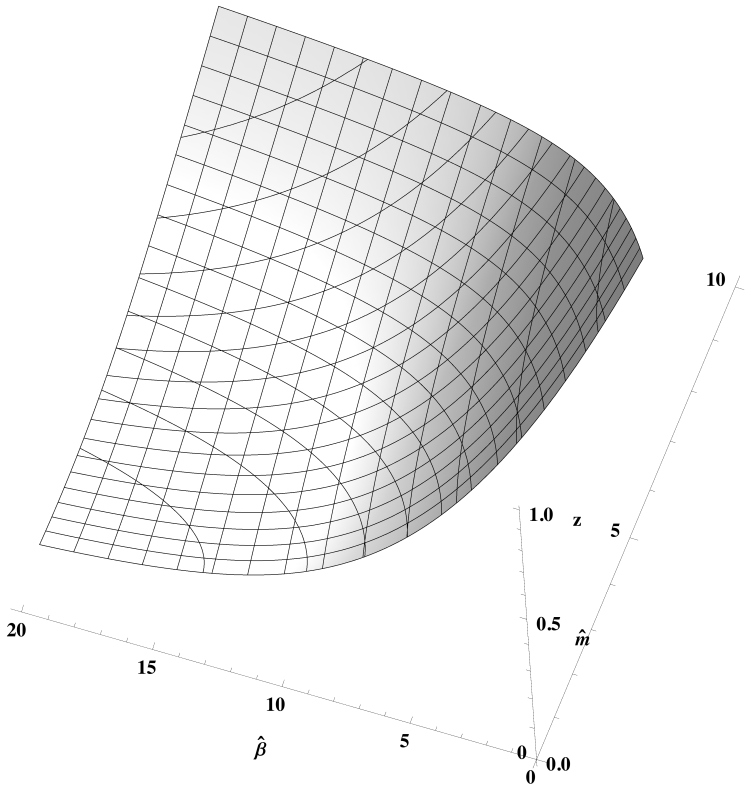

Figure 5.3: The surface defined by eq. (5.22).

gets $z = z(\hat{\beta})$ (fig. 5.4) and $z = z(\hat{m})$ (fig. 5.5).

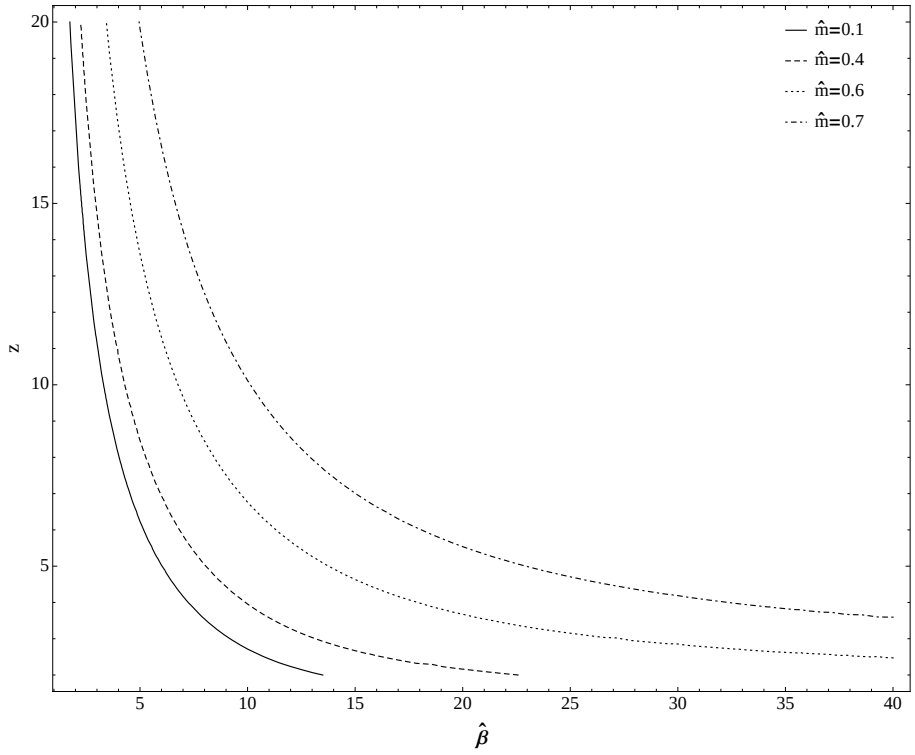

Figure 5.4: $(z, \hat{\beta})$ section of fig. 5.3, giving the critical exponent as a function of $\hat{\beta}$.

It is instructive to identify some significant limits of the parameter space of this model. At fixed $\hat{m}$ and $\hat{\beta} \to \infty$ the critical exponent is

$$z = \frac{1}{1-\hat{m}^2} + \frac{6^{4/3}\hat{m}^{2/3}}{(\hat{m}^2-1)^{4/3}(2\hat{m}^4-7\hat{m}^2+6)^{2/3}} \frac{1}{\hat{\beta}^{2/3}} + \dots \tag{5.23}$$

which at the massless limits ($\hat{m} \to 0$) becomes

$$z = 1 + \frac{6}{\hat{\beta}} + \dots \tag{5.24}$$

In the opposite limit $\hat{\beta} \to 0$

$$z = \frac{36}{(1-\hat{m}^2)^{3/2}} \frac{1}{\hat{\beta}} - 1 + \frac{3\hat{m}^4 \log(\frac{1+\sqrt{1-\hat{m}^2}}{\hat{m}})}{2(1-\hat{m}^2)^{3/2}} + \dots \tag{5.25}$$

An interesting connection with AdS-RN geometry can now be made. Setting $\hat{m}$ to 1 and taking $\hat{\beta} \to 0$ yields $z \to \infty$ which in turn recovers the near-horizon geometry of the AdS-RN black hole, i.e. and $AdS_2 \times \mathbb{R}^2$ space. In other words the back-reaction of the fermions becomes negligible.

Of course the (5.19) ansatz is asymptotically valid, i.e. when $r \to \infty$. Departures from that limit induce corrections which can be computed in a series form. In

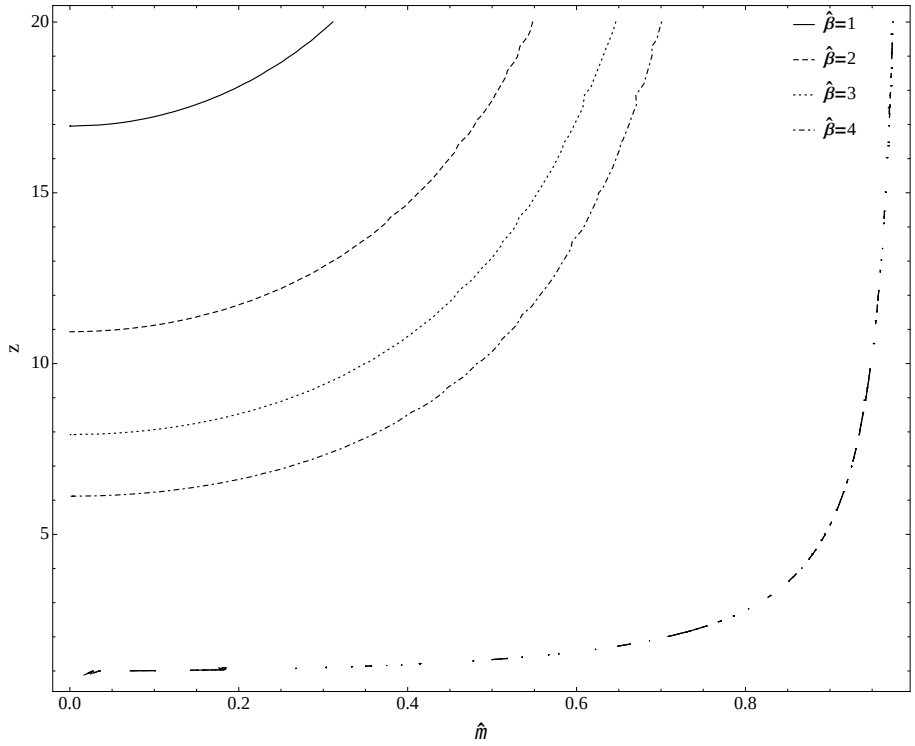

Figure 5.5: $(z, \hat{m})$ section of fig. 5.3, giving the critical exponent as a function of $\hat{m}$.

fact these corrections are necessary to define accurate boundary conditions for the perturbation fields, that will be encountered later on. Generically one writes

$$f = \frac{1}{r^{2z}} \left(1 + f_1 r^{\alpha_1} + f_2 r^{\alpha_2} + \ldots\right) \tag{5.26}$$

$$g = \frac{g_\infty}{r^2} \left(1 + g_1 r^{\alpha_1} + g_2 r^{\alpha_2} + \ldots\right) \tag{5.27}$$

$$h = \frac{h_\infty}{r^z} \left(1 + h_1 r^{\alpha_1} + h_2 r^{\alpha_2} + \ldots\right) \tag{5.28}$$

which can be inserted into the equations of motion and recursively determine the coefficients f_i, g_i, h_i, α_i. In fact solving for α_1 yields three solutions

$$\alpha_1^0 = 2 + z \tag{5.29}$$

$$\alpha_1^\pm = \frac{2+z}{2} \pm \frac{\sqrt{9z^3 - 21z^2 + 40z - 28 - \hat{m}^2 z(4-3z)^2}}{2\sqrt{(1-\hat{m}^2)z - 1}} \tag{5.30}$$

Out of the three solutions α_1^0 corresponds to a relevant deformation, which generates the finite temperature solution, α_1^- is negative and corresponds to the coupling of an irrelevant operator and α_1^+ is positive and corresponds to the expectation value of

that operator. The expressions for g_1 and h_1 are significantly more complicated

$$
\begin{aligned}
g_1 = & -36\alpha_1^3 + 18\alpha_1^2\left(\hat{\beta}g_\infty h_\infty^3\sqrt{(h_\infty-\hat{m})(h_\infty+\hat{m})}+2\right)\\
& +\hat{\beta}\alpha_1 g_\infty h_\infty\left(\left(4h_\infty^2-\hat{m}^2\right)\left(\hat{\beta}g_\infty h_\infty\left(h_\infty^2-\hat{m}^2\right)^2-6\sqrt{(h_\infty-\hat{m})(h_\infty+\hat{m})}\right)\right.\\
& \left.+36\sqrt{(h_\infty-\hat{m})(h_\infty+\hat{m})}\right)-6z^2\left(6\alpha_1+\hat{\beta}g_\infty h_\infty\sqrt{(h_\infty-\hat{m})(h_\infty+\hat{m})}\left(\hat{m}^2-4h_\infty^2\right)\right)\\
& +z\left(72\alpha_1^2-18\alpha_1\left(\hat{\beta}g_\infty h_\infty^3\sqrt{(h_\infty-\hat{m})(h_\infty+\hat{m})}+2\right)\right.\\
& \left.-\hat{\beta}g_\infty h_\infty\left(4h_\infty^2-\hat{m}^2\right)\left(\hat{\beta}g_\infty h_\infty\left(h_\infty^2-\hat{m}^2\right)^2-6\sqrt{(h_\infty-\hat{m})(h_\infty+\hat{m})}\right)\right)\\
& -2\hat{\beta}^2 g_\infty^2\left(h_\infty^2-\hat{m}^2\right)^2/\\
& 2\left(18\alpha_1^3+9\alpha_1^2\left(\hat{\beta}g_\infty h_\infty\left((h_\infty-\hat{m})(h_\infty+\hat{m})\right)^{3/2}-2\right)\right.\\
& +\hat{\beta}\alpha_1 g_\infty h_\infty\left((h_\infty-\hat{m})(h_\infty+\hat{m})\left(\hat{\beta}g_\infty h_\infty\left(h_\infty^2-\hat{m}^2\right)^2-6\sqrt{(h_\infty-\hat{m})(h_\infty+\hat{m})}\right)\right.\\
& \left.-18\sqrt{(h_\infty-\hat{m})(h_\infty+\hat{m})}\right)+6z^2\left(3\alpha_1+\hat{\beta}g_\infty h_\infty\left((h_\infty-\hat{m})(h_\infty+\hat{m})\right)^{3/2}\right)\\
& +z\left(-36\alpha_1^2+9\alpha_1\left(\hat{\beta}g_\infty h_\infty\sqrt{(h_\infty-\hat{m})(h_\infty+\hat{m})}\left(2\hat{m}^2-3h_\infty^2\right)+2\right)\right.\\
& \left.-\hat{\beta}^2 g_\infty^2 h_\infty^2\left(h_\infty^2-\hat{m}^2\right)^3+6\hat{\beta}g_\infty h_\infty\left((h_\infty-\hat{m})(h_\infty+\hat{m})\right)^{3/2}\right)+2\hat{\beta}^2 g_\infty^2\left(h_\infty^2-\hat{m}^2\right)^3\Big)
\end{aligned}
\tag{5.31}
$$

$$
\begin{aligned}
h_1 = & \hat{\beta}g_\infty\sqrt{(h_\infty-\hat{m})(h_\infty+\hat{m})}\left(3\alpha_1\left(h_\infty^2\left(3\hat{m}^2z-8\right)-6zh_\infty^4+2\hat{m}^2\right)\right.\\
& +4\hat{\beta}g_\infty h_\infty^5\sqrt{(h_\infty-\hat{m})(h_\infty+\hat{m})}-8\hat{\beta}\hat{m}^2 g_\infty h_\infty^3\sqrt{(h_\infty-\hat{m})(h_\infty+\hat{m})}\\
& \left.+4\hat{\beta}\hat{m}^4 g_\infty h_\infty\sqrt{(h_\infty-\hat{m})(h_\infty+\hat{m})}\right)/\\
& 2h_\infty\left(18\alpha_1^3+9\alpha_1^2\left(\hat{\beta}g_\infty h_\infty\left((h_\infty-\hat{m})(h_\infty+\hat{m})\right)^{3/2}-2\right)\right.\\
& +\hat{\beta}\alpha_1 g_\infty h_\infty\left((h_\infty-\hat{m})(h_\infty+\hat{m})\left(\hat{\beta}g_\infty h_\infty\left(h_\infty^2-\hat{m}^2\right)^2\right.\right.\\
& \left.\left.-6\sqrt{(h_\infty-\hat{m})(h_\infty+\hat{m})}\right)-18\sqrt{(h_\infty-\hat{m})(h_\infty+\hat{m})}\right)\\
& +6z^2\left(3\alpha_1+\hat{\beta}g_\infty h_\infty\left((h_\infty-\hat{m})(h_\infty+\hat{m})\right)^{3/2}\right)\\
& +z\left(-36\alpha_1^2+9\alpha_1\left(\hat{\beta}g_\infty h_\infty\sqrt{(h_\infty-\hat{m})(h_\infty+\hat{m})}\left(2\hat{m}^2-3h_\infty^2\right)+2\right)\right.\\
& \left.-\hat{\beta}^2 g_\infty^2 h_\infty^2\left(h_\infty^2-\hat{m}^2\right)^3+6\hat{\beta}g_\infty h_\infty\left((h_\infty-\hat{m})(h_\infty+\hat{m})\right)^{3/2}\right)+2\hat{\beta}^2 g_\infty^2\left(h_\infty^2-\hat{m}^2\right)^3\Big)
\end{aligned}
\tag{5.32}
$$

In general f_1 is unconstrained and has been set to unity in the previous expressions. Despite the complexity of the expressions, they can be iteratively solved to give as many terms as necessary.

It is interesting to notice that in the pure Lifshitz background the chemical potential $\mu = h/\sqrt{f}$ takes a constant value. This can be seen by the fact that the pressure,

energy and charge density of the Electron Star background are asymptotically constant (fig. 5.6).

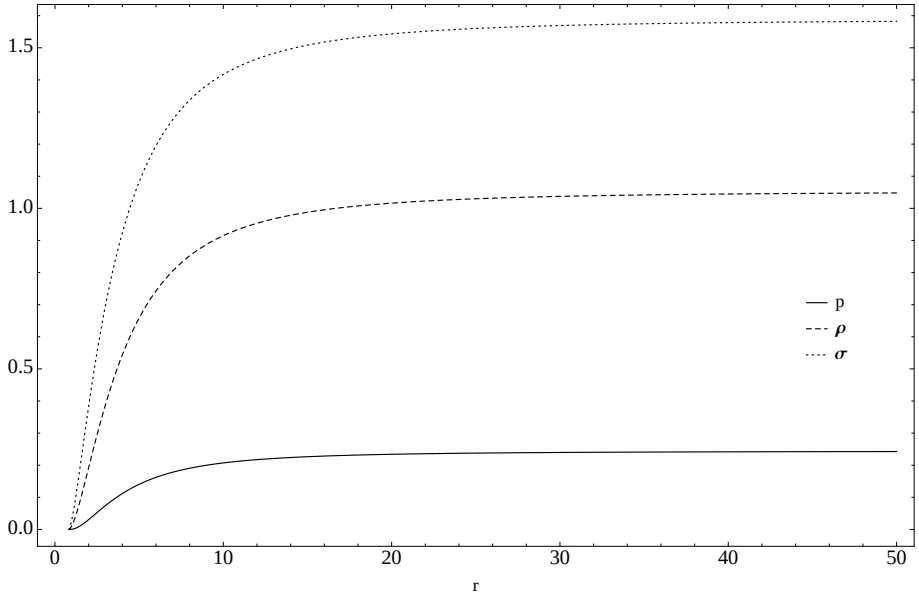

Figure 5.6: The pressure, energy and charge density for $z = 3, \hat{m} = 0.36$. In these coordinates $r \to \infty$ corresponds to the IR (Lifshitz).

Before carrying forward any further, another point about Lifshitz backgrounds needs to be stressed. It has been noticed (e.g. in [130]) that even though all the curvature scalars of this background, i.e. Ricci ($R = R_{\mu}{}^{\mu}$), Kretschmann ($K = R_{\mu\nu\rho\sigma}R^{\mu\nu\rho\sigma}$), are all finite at $r \to \infty$, at that limit the tidal forces on a test string diverge. This would indicate that there is a true, naked singularity at $r \to \infty$ which cannot be lifted by String Theory. This however is slightly misleading. Lishitz backgrounds are not solutions of vacuum Einstein's equations. In other words there needs to be matter contained in the space-time in order to support Lishitz backgrounds. This means that when one studies the nature of this space-time at $r \to \infty$, one has to take into account interactions with the relevant matter. Apparently, carefully incorporating these interactions resolves the singularity [131].

Concluding the discussion about the Electron Star background the space-time outside the Electron Star needs to be described. That exterior corresponds to an AdS-RN, but with modified parameters (compared to interior RN-AdS when $T > 0$). Those parameters are determined by matching the functions f, g, h across the star's surface when $T = 0$ or across the surface and across the interface between the star and the interior RN-AdS when $T > 0$. More explicitly one writes down the generic

RN-AdS functions as

$$f_{RN-AdS} = c^2\left(\frac{1}{r^2} - \hat{M}r + \frac{r^2}{2}\hat{Q}^2\right)\ ,\ g_{RN-AdS} = \frac{c^2}{r^4 f}\ ,\ h_{RN-AdS} = c\left(\hat{\mu} - r\hat{Q}\right) \tag{5.33}$$

where c is the speed of light which is now not necessarily equal to one. The rest of the parameters are the standard RN-AdS ones. Then by writing

$$f_{RN-AdS}|_{r=r_s} = f_{ES}|_{r=r_s} \tag{5.34}$$

$$g_{RN-AdS}|_{r=r_s} = g_{ES}|_{r=r_s} \tag{5.35}$$

$$g_{RN-AdS}|_{r=r_s} = g_{ES}|_{r=r_s} \tag{5.36}$$

one gets a system of equations that can be solved to compute $\hat{Q}, \hat{M}$ and c.

5.2 Thermo/Hydro-dynamics

Having reviewed the nature of the Electron-Star background, and before endeavouring to study the linear response of the this system, it is useful to examine its thermodynamic properties. This will provide a deeper understanding of the system and its usefulness. From the Holographic dictionary it is known that the on-shell Euclidean bulk action corresponds to the Free energy of the dual theory ($\hat{\Omega}$). In terms of the other thermodynamic parameters the free energy is

$$\hat{\Omega} = \hat{M} - \hat{\mu}\hat{Q} - \hat{s}T \tag{5.37}$$

where $\hat{s}$ is the Bekenstein-Hawking entropy, $\hat{M}$ the mass parameter of the AdS-RN black hole, $\hat{\mu}$ the chemical potential and $\hat{Q}$ the charge parameter of the AdS-RN black hole. From standard thermodynamics it is also known that

$$\hat{\Omega} = -\hat{p}\hat{V} \tag{5.38}$$

where $\hat{p}$ is the pressure and $\hat{V}$ the system's volume. The bulk action reads

$$S_E = \int d^4x\sqrt{g}\left[\frac{1}{2\kappa^2}\left(R + \frac{6}{L^2}\right) - \frac{1}{4e^2}F^2 + \hat{p}\right] + S_{GH} + S_{c.t.} \tag{5.39}$$

where S_{GH} is the Gibbons-Hawking term, necessary to make the variational problem well-defined and $S_{c.t.}$ is the counter-term prescribed by Holographic Renormalization, necessary to cancel the infinity that emerges at $r \to \partial AdS$ [73, 88]. In particular

$$S_{GH} = -\frac{1}{2\kappa^2}\int_{\partial AdS} d^3x\sqrt{\gamma}2K \tag{5.40}$$

and

$$S_{c.t.} = -\frac{1}{2\kappa^2}\int_{\partial AdS} d^3x \frac{4}{L}\sqrt{\gamma} + L\sqrt{\gamma}^{(3)}R \tag{5.41}$$

where γ is the determinant of the induced metric, K the extrinsic curvature and ${}^{(3)}R$ the three-dimensional Ricci scalar which in this case vanishes. Written out explicitly the action is

$$S_E = L^2\sqrt{f(r)g(r)}\left(r^2 g(r)f'(r)^2 + rf(r)\left(rf'(r)g'(r) + 2g(r)\left(-rf''(r) + 2f'(r)\right.\right.\right.$$
$$\left.\left.\left.+rh'(r)^2\right)\right) + 4f(r)^2\left(g(r)\left(r^2 g(r)\left(\hat{p}(r)+3\right) - 5\right) - rg'(r)\right)\right) / \left(4\kappa^2 r^4 f(r)^2 g(r)^2\right) \tag{5.42}$$

and after applying the background equations of motion one gets

$$S_E = \frac{L^2}{\kappa^2}\frac{d}{dr}\frac{f'(r) - 2h(r)h'(r)}{2r^2\sqrt{f(r)g(r)}} \tag{5.43}$$

Similarly

$$S_{GH} + S_{c.t.} = \frac{L^2\left(\varepsilon f'(\varepsilon) + 4f(\varepsilon)\left(\varepsilon\sqrt{g(\varepsilon)} - 1\right)\right)}{2\varepsilon^3\kappa^2\sqrt{f(\varepsilon)}\sqrt{g(\varepsilon)}} \tag{5.44}$$

where ε is an infinitesimal positive number, i.e. $\varepsilon \to 0$. Given that the background can be numerically computed, so can the action and consequently the free energy. The results are presented in fig. 5.7 and fig. 5.8. What one sees is that as the electron mass $\hat{m}$ decreases so does the free energy, at low temperatures[3]. Moreover as the temperature is increased, a transition to the pure AdS-RN appears (for each $\hat{m}$ there is a different transition temperature T_t) as the free energies of different Electron Star systems converge onto the AdS-RN free energy. Said differently for every electron mass there is a temperature over which the RN black hole becomes big enough that the Electron System ceases being supported and the black hole dominates the space-time. Furthermore by varying the critical exponent (z) one sees that the higher z is, the closer to the RN results one gets. This is in accordance with expectations, as at the limit where $z \to \infty$ one expects to recover the RN-AdS system. It should also be noted that the AdS-RN free energy is always larger that the Electron Star one, in the regime where the two systems can co-exist. This means that the Electron Star configuration is thermodynamically preferred to the pure AdS-RN.

Having numerically computed the background, more thermodynamical quantities can be computed. The entropy density[4] for example, which in the coordinate system

[3]Here temperature is measured with respect to the chemical potential through the dimensionless parameter $\frac{T}{\mu}$

[4]As in the case of temperature and Free Energy, entropy density is measure in units of chemical potential, which is the relevant scale. Seen in another way one computes the dimensionless entropy density.

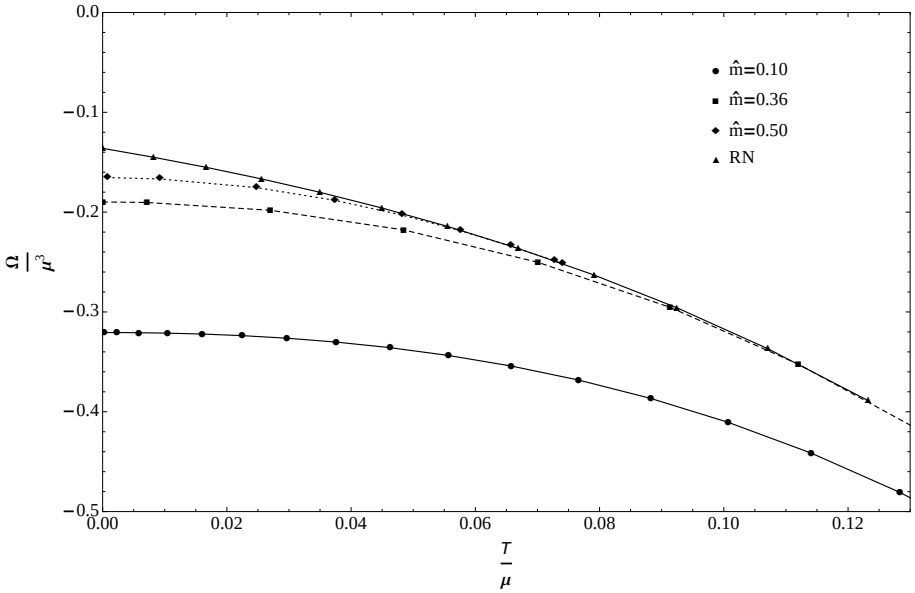

Figure 5.7: Free energy of the Electron Star system for three electron masses $\hat{m}$. The RN result is overlaid for comparison.

where the horizon is placed at $r = r_+ = 1$ is

$$\frac{s}{\mu^2} = \frac{2\pi}{r_+^2 \mu^2} = \frac{2\pi}{\mu^2} \tag{5.45}$$

Extracting the chemical potential from the outer (i.e. the one on the boundary side of space-time) RN one finds fig. 5.9, where the electron mass is varied and fig. 5.10 where the critical exponent dependence is examined. The striking characteristic compared to the RN case, is that the dimensionless entropy density vanishes as the temperature (also dimensionless) goes to zero. This seems to be circumventing one of the major issues encountered when studying the thermodynamics of theories dual to a pure RN-AdS system, since in those cases, as seen by the RN curve in fig. 5.9, the entropy density remains finite even at zero temperature, which is a bizarre result from the Condensed Matter point of view. With respect to the Electron Star parameters, one again sees that higher electron mass and higher critical exponent leads to faster convergence to RN.

Having the Free Energy and entropy of the system available, one can proceed to compute every thermodynamical quantity. What is more pertinent however is that one can compute at least one hydrodynamical quantity, namely the diffusion constant $\mathcal{D}$, for viscous fluids. It is known from standard liquid hydrodynamics (e.g. [28]) that the diffusion constant is related to the shear viscosity, the energy density and pressure,

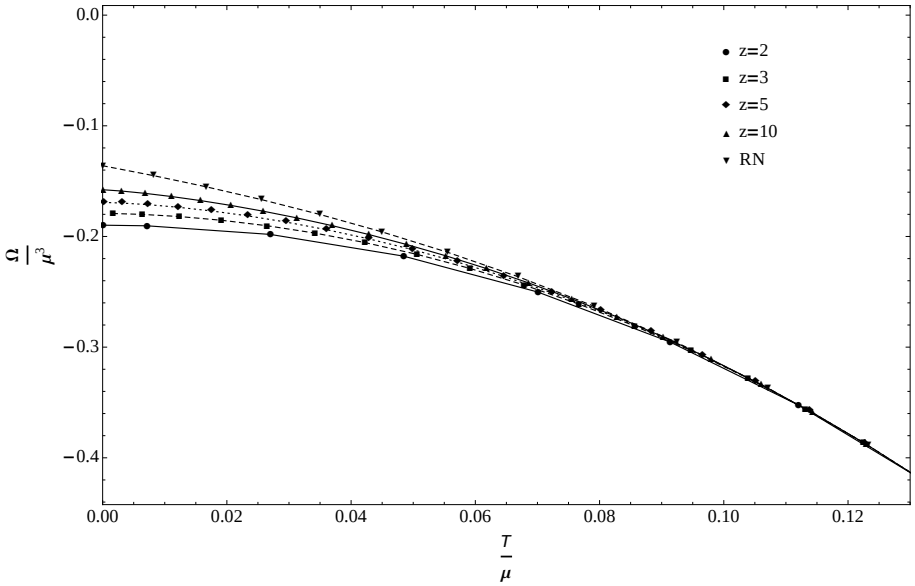

Figure 5.8: Free energy of the Electron Star system for four critical exponents z. The RN result is overlaid for comparison.

through

$$\mathcal{D} = \frac{\eta}{\epsilon + p} \tag{5.46}$$

The standard practice in Holography literature is to use the KSS[5] relation [132]

$$\frac{\eta}{s} = \frac{\hbar}{4\pi k_B} = \frac{1}{4\pi} \tag{5.47}$$

where in the last step natural units ($k_B = \hbar = 1$) have been used. Moreover, asymptotic symmetries indicate that the boundary theory should be conformal, imposing the relation

$$\epsilon - 2p = 0 \tag{5.48}$$

on energy density and pressure. Since the Electron Star system has not been examined in this way before and mainly out of caution concerning the potential numerical errors stemming from the fact that the background itself is only known numerically, both these statements will now be verified. The first to be examined is the conformality condition. The pressure can be extracted from the on-shell action through eq. (5.38) and the energy corresponds to the mass parameter of the outer RN part of the spacetime. It should be noted that since in the outer region $c \neq 1$ it has to be properly re-inserted in the calculation. From the numerical solution one indeed sees in fig. 5.11 that the condition holds.

[5]Kovtun-Son-Starinets

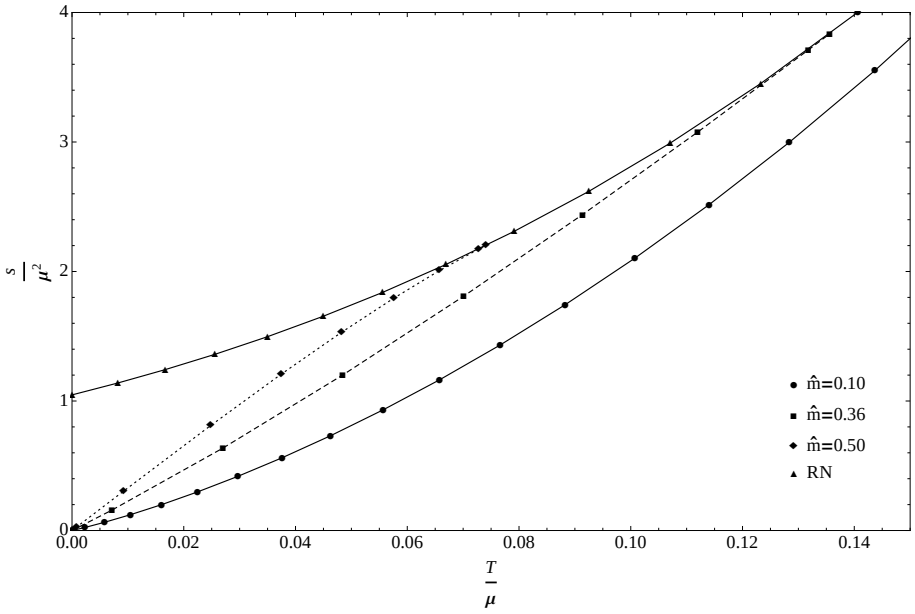

Figure 5.9: The entropy density of the Electron Star for three electron masses ($\hat{m}$). The RN result is overlaid for comparison.

The next one, i.e. the KSS relation is a bit more involved to verify. Since the entropy for this system is already known (5.45) one needs to calculate the shear viscosity in an independent way. To do that one makes use of the Kubo formula that relates the shear viscosity with the Green's function of the shear part (in this case xy) of the stress-energy tensor which, in turn, is computed, in standard Holographic practice, by calculating the solution of the perturbation to the gravity mode of the same symmetries [32, 109]. In particular

$$\eta = \lim_{\omega\to 0}\frac{1}{2\omega}\int dtd\boldsymbol{x}e^{\imath\omega t}\langle[T_{xy}(x),T_{xy}(0)]\rangle = -\lim_{\omega\to 0}\frac{1}{\omega}G(\omega,\mathbf{0}) \tag{5.49}$$

where in the last part $\mathbf{0}$ stands for zero momentum. To complete this calculation one needs the equation of motion for the xy component of the metric. The setup is similar to that described by eq. (4.6) and eq. (4.9) with the caveat that the background is a modified RN-AdS. The equations of motion are similarly

$$R_{\mu\nu}-\frac{1}{2}g_{\mu\nu}R-\frac{3}{L^2}g_{\mu\nu}=\kappa^2\left[\frac{1}{e^2}\left(F_{\mu\sigma}F_{\nu}{}^{\sigma}-\frac{1}{4}g_{\mu\nu}F_{\rho\tau}F^{\rho\tau}\right)\right] \tag{5.50}$$

perturbed at linear order. Fortunately at zero momentum, which is the case for this calculation, the Einstein's equation involving this mode, decouple giving

$$h_x{}^{y\prime\prime}(r)+\frac{f'_{out}(r)}{f_{out}(r)}h_x{}^{y\prime}(r)+\omega\frac{g_{out}(r)}{f_{out}(r)}h_x{}^{y}(r)=0 \tag{5.51}$$

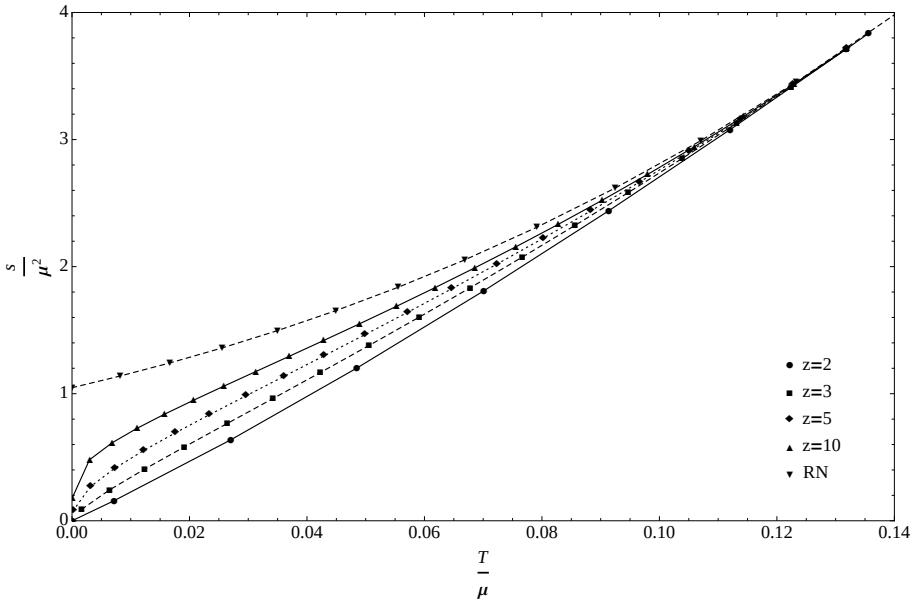

Figure 5.10: The entropy density for the Electron Star for four critical exponents (z). The RN result is overlaid for comparison.

where $f_{out}, g_{out}, h_{out}$ are the RN parameters for the outer RN part of the space-time determined by eq. (5.36). By expanding this equation near the boundary one sees that its solution admits a series expansion of the form

$$h_x{}^y = a_0 + a_1 r + a_2 r^2 + a_3 r^3 + a_4 r^4 + \dots \tag{5.52}$$

The indices of the equation (determined by setting $h_x{}^y = r^\nu f(r)$ and solving the resulting equation so that f is regular) for the regular singular point 0, are $\nu = 0, 3$[6], which indicates that the leading and sub-leading terms in the expansion are $\sim r^0$ and $\sim r^3$ and the rest of the coefficients are determined in terms of a_0, a_3. In fact

$$a_1 = 0 \ ; \ a_2 = a_0 \frac{\omega^2}{2c^2} \ ; \ a_4 = \frac{9 a_3 c^2 M - a_0 Q^2 \omega^2}{\omega^2} \tag{5.53}$$

where c, M, Q are the RN parameters for the outer region. These relations will be used as checks of our numerical solution. In order to proceed, eq. (5.51) will be solved numerically setting in-going boundary conditions on the horizon. Once the solution is found the checks mentioned above are performed to verify the numerical stability of the solution. Once the tests are passed the solution is fitted to the series expression, in order to determine the free parameters a_0 and a_3. Having determined these then

[6]This means that the solution can be written in the form $h_x{}^y \sim r^0(1 + \dots) + r^3(1 + \dots)$.

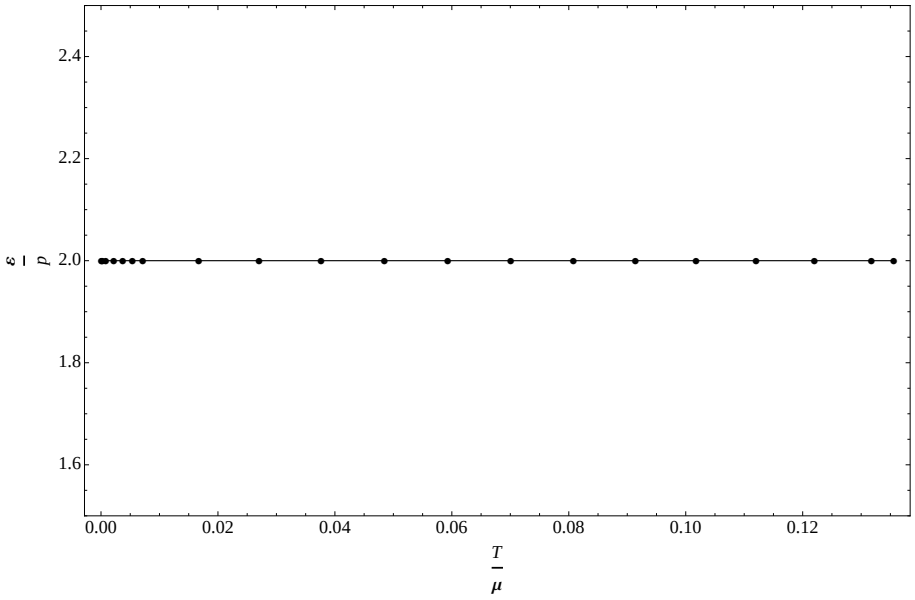

Figure 5.11: Verification of the conformality condition (5.48).

one can immediately determine the relative Green's function through the standard Holographic procedure (see e.g. [18])

$$G(\omega, \boldsymbol{k}) = (2\Delta - d)\frac{a_3(\omega, \boldsymbol{k})}{a_0(\omega, \boldsymbol{k})} \tag{5.54}$$

where d is the dimensionality of the boundary (here $d = 3$) and Δ the scaling dimension of the involved operator. The latter can either be computed by the indices of the governing equation of motion, at the boundary or through the standard formula

$$\Delta_{\pm} = \frac{d}{2} \pm \sqrt{\left(\frac{d}{2}\right)^2 + m^2} \tag{5.55}$$

which in this case ($m = 0$) yields $0, 3$. Hence the $\Delta = 3$. Combining eq. (5.49) and eq. (5.54) the results of fig. 5.12 are obtained, verifying that KSS does indeed hold. Now all the components are in place to compute the diffusion coefficient $\mathcal{D}$ through eq. (5.46). The results are presented in fig. 5.13 where the electron mass ($\hat{m}$) is varied and fig. 5.14 where the critical exponent (z) is varied.

It should be stressed here that this is the prediction of standard hydrodynamics, for this particular system. In the next section it will be compared and found to conditionally disagree with the full linear perturbation analysis of the system. For the time being, though one sees that at low temperature the diffusion coefficient vanishes as expected from standard Condensed Matter intuition. Moreover in accordance

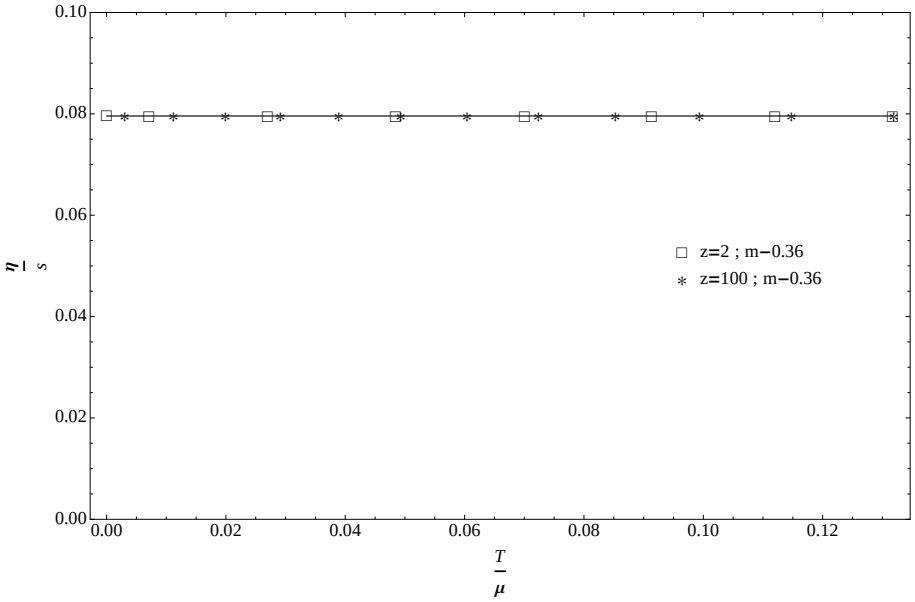

Figure 5.12: $\frac{\eta}{s}$ for two critical exponents. The solid line corresponds to the value $\frac{1}{4\pi}$.

with the already established fact that the Electron Star disappears at high enough temperatures, one sees that $\mathcal{D}$ converges to the RN values above a certain temperature (distinct for each electron mass). What can also be determined from these results is that the more massive the constituent electrons are the "quicker" (in terms of temperature) $\mathcal{D}$ converges to RN. Similarly the higher the critical exponent is the "quicker" the convergence to RN occurs. This is to be expected however, since it is known that at the infinite critical exponent limit ($z \to \infty$) one recovers the AdS_2 near horizon geometry corresponding to the RN black hole.

5.3 Shear channel

Now that all the necessary information is extracted from the background one can proceed to the full linear perturbation of the Electron Star system. What is going to be presented next, is a study of the low-lying poles of the correlators of the boundary theory, dual to the Electron Star system. The standard Holographic dictionary will be followed, according to which one needs to perturb the system and then examine the equation of motions of the fluctuations of all relevant bulk fields, as was done in the previous chapter for the Reissner-Nordstrom black hole. At first, attention will be focused on the shear channel (defined below).

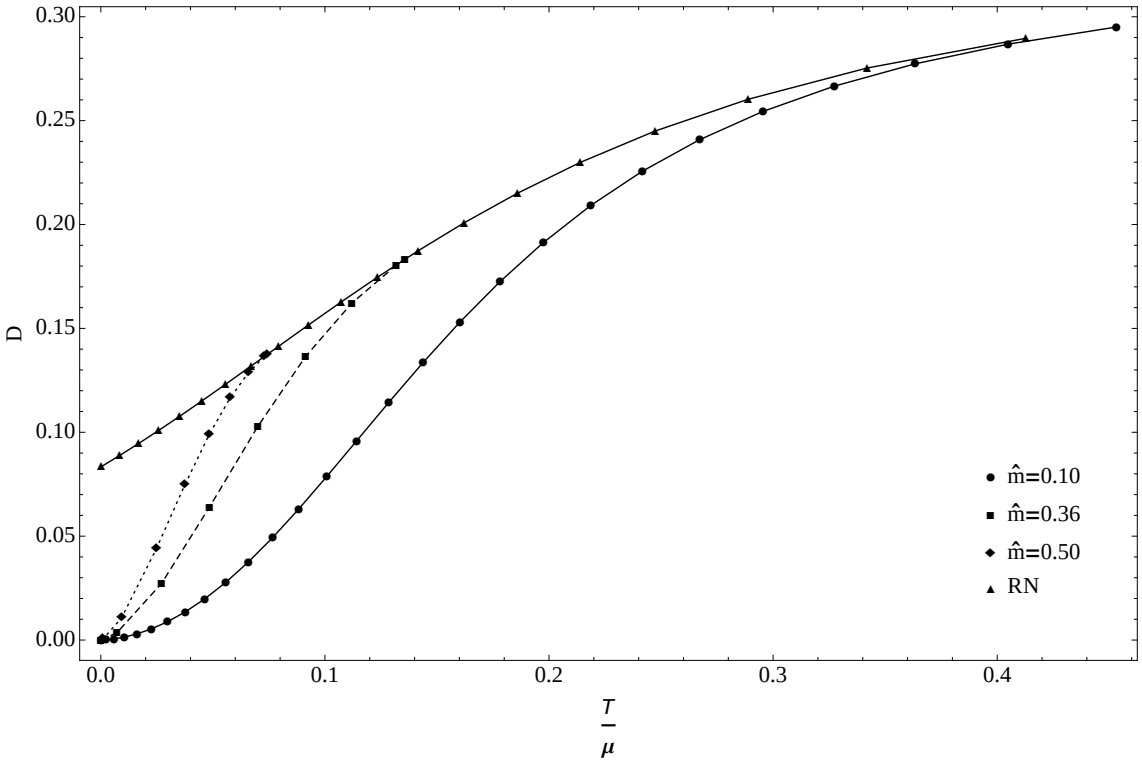

Figure 5.13: Diffusion coefficient for three electron masses as well as RN.

The starting point will be the action

$$S = \int d^x\sqrt{-g}\left[\frac{1}{2\kappa^2}\left(R+\frac{6}{L^2}\right) - \frac{1}{4e^2}F_{\mu\nu}F^{\mu\nu} - \rho(\sigma) + \sigma u^\mu(\partial_\mu\phi + A_\mu) + \lambda(u^\mu u_\mu + 1)\right] + S_{GH} + counterterms \tag{5.56}$$

The non-Einstein-Maxwell terms in this action comprise the so-called Schutz action at zero temperature [133]. This action should be varied with respect to the metric $g_{\mu\nu}$, the $U(1)$ gauge field A_μ, the four-velocity of the fluid u_μ, the charge density of the fluid σ, the Clebsch potential ϕ and the Lagrange multiplier λ, which imposes the requirement for a relativistic fluid that $u^2 = -1$. For simplicity, the fields will be rescaled so that the full action is proportional to $\frac{L^2}{\kappa^2}$

$$A_\mu \to \frac{eL}{\kappa}A_\mu\ ,\ \phi \to \frac{eL}{\kappa}\phi\ ,\ u_\mu \to Lu_\mu\ ,\ \sigma \to \frac{1}{eL^2\kappa}\sigma\ ,\ \lambda \to \frac{1}{L^2\kappa^2}\lambda \tag{5.57}$$

Note that when fluctuations of these fields will be considered shortly, they will inherit this rescaling also.

If one now makes the definitions

$$\mu(\sigma) \equiv \rho'(\sigma) = u^\mu(\partial_\mu\phi + A_\mu)\ ,\ p(\sigma) \equiv -\rho(\sigma) + \sigma\mu(\sigma) \tag{5.58}$$

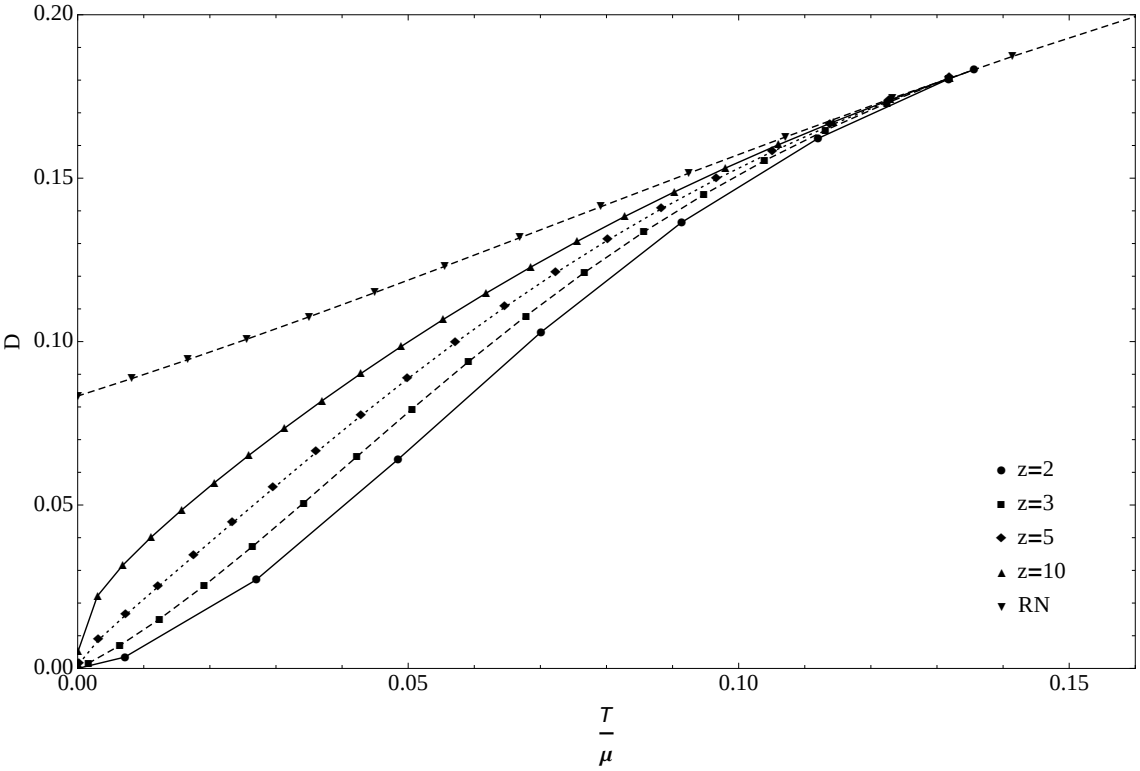

Figure 5.14: Diffusion coefficient for four critical exponents as well as RN.

then the energy-momentum tensor associated to the Schutz action is simply that of a perfect fluid

$$T^{\mu\nu}_{Schults} = (p+\rho)u^\mu u^\nu + pg^{\mu\nu} \tag{5.59}$$

with pressure p, energy density ρ, charge density σ and chemical potential μ.

In order to get the equations of motion for the perturbations, one has to excite all the involved fields as

$$\begin{aligned} g_{\mu\nu}(r) &\to g_{\mu\nu}(r) + h_{\mu\nu}(r,t,\boldsymbol{x}) \\ A_\mu(r) &\to A_\mu(r) + a_\mu(r,t,\boldsymbol{x}) \\ u_\mu(r) &\to u_\mu(r) + \delta u_\mu(r,t,\boldsymbol{x}) \\ \phi(r) &\to \phi(r) + \delta\phi(r,t,\boldsymbol{x}) \\ \sigma(r) &\to \sigma(r) + \delta\sigma(r,t,\boldsymbol{x}) \\ \lambda(r) &\to \lambda(r) + \delta\lambda(r,t,\boldsymbol{x}) \end{aligned} \tag{5.60}$$

The equations then come from varying the action. Furthermore, the non-radial spatial dependence for every field takes, without loss of generality, the trivial form

$$\phi(r,t,\boldsymbol{x}) = \exp[-\imath\omega t + \imath kx]\phi(r,\omega,k) \tag{5.61}$$

where ϕ stands for each field. This procedure results in twenty one equations. These split naturally into two decoupled sets of equations - the shear equations of motion, involving fields that are odd under $y \to -y$, and the longitudinal equations of motion, involving fields that are even under $y \to -y$. This decoupling is guaranteed at linear order in the fluctuations as the theory is invariant under $y \to -y$.

The shear degrees of freedom include $h_{xy}, h_{ty}, h_{ry}, a_y, \delta u_y$. By varying the action with respect to these one gets the equations

$$h_y{}^{x\prime\prime} - \imath k r^2 g h_y{}^{r\prime} + \left(\frac{f'}{2f} - \frac{g'}{2g} - \frac{2}{r}\right) h_y{}^{x\prime} - 2\imath k r^2 g \left(\frac{f'}{4f} + \frac{g'}{4g}\right) h_y{}^{r} + \omega^2 \frac{g}{f} h_y{}^{x} - \omega k r^2 g h_t{}^{t} = 0 \tag{5.62}$$

$$h_y{}^{t\prime\prime} - \imath\omega \frac{g}{f} h_y{}^{r\prime} + \left(\frac{3f'}{2f} - \frac{g'}{2g}\right) h_y{}^{t\prime} - \frac{2h'}{f} a_y' - 2\imath\omega \frac{g}{f}\left(\frac{g'}{4g} - \frac{f'}{4f} - \frac{1}{r}\right) h_y{}^{r} + \omega k \frac{g}{f} h_y{}^{x} - k^2 r^2 g h_y{}^{t} + 2\frac{g}{\sqrt{f}}(p+\rho)\delta u_y + 2\left(\frac{h'^2}{f} + g(p+\rho)\right) h_y{}^{t} = 0 \tag{5.63}$$

$$\left(\omega^2 - k^2 r^2 f\right) h_y{}^{r} + \imath\omega \frac{f}{g} h_y{}^{t\prime} - \imath k \frac{f}{g} h_y{}^{x\prime} + \frac{\imath\omega}{g}\left(\frac{2f}{r} + f'\right) h_y{}^{t} - 2\imath\omega \frac{h'}{g} a_y = 0 \tag{5.64}$$

$$a_y'' + \frac{1}{2}\left(\frac{f'}{f} - \frac{g'}{g}\right) a_y' + \frac{g}{f}(\omega^2 - k^2 r^2 f) a_y - h' h_y{}^{t\prime} + \imath\omega \frac{g}{f} h' h_y{}^{r} + g\sigma\delta u_y + \frac{h'}{2}\left(r g(p+\rho) - \frac{f'}{f} + \frac{g'}{g}\right) h_y{}^{t} = 0 \tag{5.65}$$

$$\delta a_y + \mu \delta u_y = 0 \tag{5.66}$$

where indices of the metric fluctuations $h_{\mu\nu}$ are raised and lowered using the background metric, a prime denotes a derivative with respect to r, and the dependence of the field fluctuations upon r, ω and k, and of the background fields upon r, have been suppressed for conciseness. Now the equations in this form are unmanageable. Thankfully, they may be considerably simplified. This is done by solving a subset of the equations of motion algebraically. In the shear sector one can solve equations (5.64) and (5.66) for $h_y{}^{r}$ and δu_y. Substituting the solutions for these fields into the remaining equations, one finds that there are only two linearly-independent equations of motion in the shear sector. These equations are naturally written in terms of the following gauge-invariant combinations of the fluctuations

$$Z_1(r,\omega,k) = \omega h_y{}^{x} - k r^2 f(r) h_y{}^{t}(r,\omega,k) \tag{5.67}$$

$$Z_2(r,\omega,k) = a_y(r,\omega,k) \tag{5.68}$$

These are invariant under both the bulk $U(1)$ gauge symmetry, which acts as

$$a_\mu(r,\omega,k) \to a_\mu(r,\omega,k) - \partial_\mu \Lambda(r,\omega,k) \tag{5.69}$$

and the bulk diffeomorphism symmetry which acts as

$$\begin{aligned} h_{\mu\nu}(r,x,t) &\to h_{\mu\nu}(r,x,t) - \nabla_\mu \xi_\nu(r,x,t) - \nabla_\nu \xi_\mu(r,x,t) \\ a_\mu(r,x,t) &\to a_\mu(r,x,t) - \xi^\alpha(r,x,t)\nabla_\alpha A_\mu(r) - A_\alpha \nabla_\mu \xi^\alpha(r,x,t) \\ \delta\sigma(r,x,t) &\to \delta\sigma(r,x,t) - \xi^\alpha(r,x,t)\nabla_\alpha \sigma(r) \end{aligned} \tag{5.70}$$

to linear order in the fluctuations, where ∇_μ is the covariant derivative with respect to the background metric. These particular combinations are natural in the language of the dual field theory operators as they guarantee that the relevant field theory Ward identities are satisfied (as seen above).

In terms of these fluctuations the the two linearly-independent equations of motion are

$$\begin{aligned} &Z_1'' + 2kr^2 h' Z_2' + \left(\frac{rg\sigma\mu}{2} + \frac{\omega^2 f' + 2k^2 r f^2}{f(\omega^2 - k^2 r^2 f)} \right) Z_1' + \frac{g}{f}(\omega^2 - k^2 r^2 f) Z_1 \\ &\quad + 2kr^2 \sqrt{f}\mu \left(\frac{2\omega^2 h'^2}{f(\omega^2 - k^2 r^2 f)} + \frac{g\sigma}{\mu} \right) Z_2 = 0 \end{aligned} \tag{5.71}$$

$$\begin{aligned} &Z_2'' + \frac{1}{2}\left(\frac{f'}{f} - \frac{g'}{g} \right) Z_2' - \frac{kh'}{\omega^2 - k^2 r^2 f} Z_1' + \frac{g}{f}(\omega^2 - k^2 r^2 f) Z_2 \\ &\quad - \left(\frac{2\omega^2 h'^2}{f(\omega^2 - k^2 r^2 f)} + \frac{g\sigma}{\mu} \right) Z_2 = 0 \end{aligned} \tag{5.72}$$

These are the equations that need to be solved numerically. In order however to compute physical quantities, like spectral functions, one needs the on-shell action, which from standard Holographic dictionary, correspond to the generating functional for the boundary theory. By perturbing the action to quadratic order in fluctuations ($\mathcal{O}(h^2)$), and imposing the equations of motion one gets, in terms of the original

degrees of freedom

$$
\begin{aligned}
S^{(2)}_{on-shell} = \int_{r\to 0} \frac{d\omega dk}{(2\pi)^2}\frac{L^2}{\kappa^2}\Big[& \frac{1}{4r^4\sqrt{fg}} h_t{}^x h_t{}^{x\prime} + \frac{\imath\omega\sqrt{g}}{4r^2\sqrt{f}}(h_t{}^x h_x{}^r - h_x{}^x h_t{}^r - h_y{}^y h_t{}^r) \\
& + \frac{\sqrt{f}}{8r^2\sqrt{g}}(h_t{}^t h_x{}^{x\prime} + h_x{}^x h_t{}^{t\prime} + h_y{}^y h_t{}^{t\prime} + h_t{}^t h_y{}^{y\prime} + h_x{}^x h_y{}^{y\prime} + h_y{}^y h_x{}^{x\prime}) \\
& - \frac{\imath k\sqrt{fg}}{4}(h_t{}^t h_x{}^r + h_y{}^y h_x{}^r) - \frac{\imath k\sqrt{g}}{4r^2\sqrt{f}} h_t{}^x h_t{}^r - \frac{1}{r^5\sqrt{fg}} h_t{}^{x2} \\
& + \frac{(rf' - 2f)}{16r^3\sqrt{fg}}(h_t{}^t h_x{}^x + h_t{}^t h_y{}^y + h_x{}^x h_y{}^y + h_y{}^y h_x{}^x - h_r{}^r h_x{}^x - h_r{}^r h_y{}^y - h_x{}^{22} - h_y{}^{y2}) \\
& \frac{\sqrt{f}}{4r^3\sqrt{g}}(h_t{}^{t2} + h_t{}^t h_r{}^r - h_t{}^t h_x{}^x - h_t{}^t h_y{}^y) + \frac{1}{2r^2\sqrt{fg}} a_t(a_t' + \imath\omega a_r) \\
& - \frac{\sqrt{f}}{2\sqrt{g}} a_x(a_x' - \imath k a_r) - \frac{h'}{4r^2\sqrt{fg}} a_t(h_r{}^r + h_t{}^t - h_x{}^x - h_y{}^y) - \frac{h'}{2r^2\sqrt{fg}} a_x h_T{}^x \\
& - \frac{\sqrt{g}\sigma}{2r^2} h_t{}^r \delta\phi + \frac{\sqrt{f}\sigma}{2r^2\sqrt{g}} \delta u_r \phi \\
& - \frac{\sqrt{f}}{4r^2\sqrt{g}} h_y{}^x h_y{}^{x\prime} + \frac{f^{3/2}}{4\sqrt{g}} h_y{}^t h_y{}^{t\prime} - \frac{\imath\omega\sqrt{fg}}{4} h_y{}^t h_y{}^r + \frac{\imath k\sqrt{fg}}{4} h_y{}^x h_y{}^r - \frac{\sqrt{f}}{2\sqrt{g}} a_y a_y' \\
& + \frac{\sqrt{f}(rf' - 2f)}{4r\sqrt{g}} h_y{}^{t2} - \frac{(rf' - 2f)}{4r^3\sqrt{fg}} h_x{}^{x2} + \frac{\sqrt{f}h'}{2\sqrt{g}} h_y{}^t a_y \Big] \\
& + counterterms
\end{aligned}
\tag{5.73}
$$

where the first fluctuation written in each term has argument $(r, -\omega, -k)$, the second has argument (r, ω, k), and a prime denotes a derivative with respect to r.

As we will work with the equations of motion for the gauge-invariant variables (5.68), we require the action to be written in terms of these variables also. It is not possible to write the full on-shell action in terms of these variables. This does not mean that any of the bulk gauge symmetries are broken but simply reflects the fact that the variables (5.68) are valid to linear order in fluctuations, whereas the action is quadratic in fluctuations. However, the derivative terms in the on-shell action can be written purely in terms of the gauge-invariant variables - this ensures that the relevant Ward identities of the field theory are satisfied. In terms of the gauge-invariant variables the on-shell action can be recast in the following form

$$
S^{(2)}_{on-shell} = \int_{r\to 0} \frac{d\omega dk}{(2\pi)^2}\frac{L^2}{\kappa^2}\left[Z_i(r,-\omega,-k)\mathcal{A}_{ij}Z_j'(r,\omega,k)\right] + non-derivative\ terms \tag{5.74}
$$

where the coefficients, though lengthy, are presented here for completeness:

$$\mathcal{A}_{11} = \frac{\sqrt{f}}{4r^2\sqrt{g}(\omega^2 - k^2r^2f)} \tag{5.75}$$

$$\mathcal{A}_{22} = -\frac{\sqrt{f}}{2\sqrt{g}} \tag{5.76}$$

$$\mathcal{A}_{12} = \mathcal{A}_{21} = 0 \tag{5.77}$$

$$\begin{aligned}\mathcal{A}_{33} =&[-4k^2r^2f^3\mu^4\sigma + r^2\omega^2(k^2r^2\mu + \sigma - 2\mu^2\sigma + \mu^4\sigma)f'^2 + 4f^2(k^2r^2\omega^2\mu - 2k^2r^2\omega^2\mu^3 \\ &+ \omega^2\sigma_\mu^4\sigma(\omega^2 + k^2r^3f')) + f(8\omega^4\mu^3 + 4k^2r^3\omega^2\mu f' + 4r\omega^2\sigma f' \\ &- r\mu^4\sigma f'(4\omega^2 + k^2r^3f'))]/[8r^2\omega^2\sqrt{f}(-\omega^2 + k^2r^2f)\sqrt{g}\mu^2(\mu(4\omega^2 - 2k^2r^2f + \\ &+ k^2r^3f')^2 + 2\mu^2\sigma(-4k^2r^2f^2 + 4f(\omega^2 + k^2r^3f') - rf'(4\omega^2 + k^2r^3f')) \\ &+ r\sigma(4k^2rf^2 - 4k^2r^2ff' + f'(8\omega^2 + k^2r^3f')))]\end{aligned} \tag{5.78}$$

$$\begin{aligned}\mathcal{A}_{44} =& [\sqrt{f}(\omega^2\mu(4\omega^2 - 2k^2r^2f + k^2r^3f')^2 + 2\omega^2\mu^2\sigma(-4k^2r^2f^2 + 4f(\omega^2 + k^2r^3f') \\ &+ -rf'(4\omega^2 + k^2r^3f')) + r\sigma(-4k^4r^3f^3 + 2\omega^2f'(4\omega^2 + k^2r^3f') \\ &- k^2r^2ff'(8\omega^2 + k^2r^3f') + 4f^2(2k^2r\omega^2 + k^4r^4f')))]/ \\ &[2\omega^2(\omega^2 - k^2r^2f)\sqrt{g}(\mu(4\omega^2 - 2k^2r^2f + k^2r^3f')^2 + 2\mu^2\sigma(-4k^2r^2f^2 \\ &+ 4f(\omega^2 + k^2r^3f') - rf'(4\omega^2 + k^2r^3f')) + r\sigma(4k^2rf^2 - 4k^2r^2ff' \\ &+ f'(8\omega^2 + k^2r^3f')))]\end{aligned} \tag{5.79}$$

$$\begin{aligned}\mathcal{A}_{55} =& -[f^{3/2}\sigma(4\omega^2 - 2k^2r^2f + k^2r^3f')^2\mu'^2]/[2r^2\omega^2\sqrt{g}(\mu(4\omega^2 - 2k^2r^2f + k^2r^3f')^2 \\ &+ 2\mu^2\sigma(-4k^2r^2f^2 + 4f(\omega^2 + k^2r^3f') - rf'(4\omega^2 + k^2r^4f')) + r\sigma(4k^2rf^2 \\ &- 4k^2r^2ff' + f'(8\omega^2 + k^2r^3f')))\sigma'^2]\end{aligned} \tag{5.80}$$

$$\begin{aligned}\mathcal{A}_{34} =& -[k(-4k^2r^2f^3\mu^2\sigma + 4f^2(-k^2r^2\omega^2\mu + \omega^2\sigma + \mu^2\sigma(\omega^2 + k^2r^3f')) + r\omega^2f'(r\sigma f' \\ &- r\mu^2\sigma f' + \mu(4\omega^2 + k^2r^3f')) + f(8\omega^4\mu + 4r\omega^2\sigma f' - r\mu^2\sigma f'(4\omega^2 + k^2r^3f')))]/ \\ &[4\omega^2(\omega^2 - k^2r^2f)\sqrt{g}\mu(\mu(4\omega^2 - 2k^2r^2f + k^2r^3f')^2 + 2\mu^2\sigma(-4k^2r^2f^2 \\ &+ 4f(\omega^2 + k^2r^3f') - rf'(4\omega^2 + k^2r^3f')) + r\sigma(4k^2rf^2 - 4k^2r^2ff') \\ &+ f'(8\omega^2 + k^2r^3f')))]\end{aligned} \tag{5.81}$$

$$\mathcal{A}_{35} = [\sqrt{f}\sigma(4k^2r^2f^2\mu^2 - 4f(2\omega^2 + k^2r^3\mu^2 f') + rf'(-4\omega^2 + \mu^2(4\omega^2 + k^2r^3f')))\mu']/$$
$$[4r^2\omega^2\sqrt{g}\mu(\mu(4\omega^2 - 2k^2r^2f + k^2r^3f')^2 + 2\mu^2\sigma(-4k^2r^2f^2 + 4f(\omega^2 + k^2r^3f')$$
$$- rf'(4\omega^2 + k^2r^3f')) + r\sigma(4k^2rf^2 - 4k^2r^2ff' + f'(8\omega^2 + k^2r^3f')))\sigma'] \qquad (5.82)$$

$$\mathcal{A}_{45} = -[kf\sigma(2f - rf')(-4\omega^2 + 2k^2r^2f - k^2r^3f')\mu']/[2\omega^2\sqrt{g}(\mu(4\omega^2 - 2k^2r^2f$$
$$+ k^2r^3f')^2 + 2\mu^2\sigma(-4k^2r^2f^2 + 4f(\omega^2 + k^2r^3f') - rf'(4\omega^2 + k^2r^3f'))$$
$$+ r\sigma(4k^2rf^2 - 4k^2r^2ff' + f'(8\omega^2 + k^2r^3f')))\sigma'] \qquad (5.83)$$

$$\mathcal{A}_{43} = -\mathcal{A}_{34} \qquad (5.84)$$
$$\mathcal{A}_{53} = \mathcal{A}_{34} \qquad (5.85)$$
$$\mathcal{A}_{54} = -\mathcal{A}_{45} \qquad (5.86)$$
$$(5.87)$$

where a prime denotes a derivative with respect to r.

It is also of interest to determine the off-shell action to quadratic order in the fluctuations in the gauge-invariant variables. This action has a Noether current corresponding to a global symmetry of the form

$$\phi(r,\omega,k) \to \exp[\imath\alpha]\phi(r,\omega,k)$$
$$\phi(r,-\omega,-k) \to \exp[-\imath\alpha]\phi(r,-\omega,-k) \qquad (5.88)$$

where ϕ represents the fluctuation of a generic field. This results in the existence of a quantity which is invariant under translations in the radial direction and this invariance can be used as a check on the numerical results obtained. As explained previously, the full quadratic action cannot be written in the variables (5.68). In fact, only the first-derivative squared terms in the action may be written in these variables. The conserved quantity depends on these terms, and also the single-derivative terms. This problem can be circumvented by adding purely real boundary counter-terms (different from the counter-terms the action) such that the single-derivative terms may be written in terms of the variables (5.68). These do not affect the equations of motion of the theory (and hence the Green's function poles), nor the spectral

functions (as they are purely real) but only the contact terms in the real part of the Green's function. Having done this, the off-shell action takes the form

$$S^{(2)}_{off-shel} = \int dr \frac{d\omega dl}{(2\pi)^2} \frac{L^2}{\kappa^2} \left[Z_i'(r,-\omega,-k) A_{ij} Z_j'(r,\omega,k) + Z_i(r,-\omega,-k) B_{ij} Z_j'(r,\omega,k) \right.$$
$$\left. + non-derivative terms \right] \tag{5.89}$$

where a prime denotes a derivative with respect to r. The coefficients are

$$A_{11} = \frac{\sqrt{f}}{4r^2\sqrt{g}(\omega^2 - k^2 r^2 f)} \tag{5.90}$$
$$A_{12} = A_{21} = 0 \tag{5.91}$$
$$A_{22} = -\frac{\sqrt{f}}{2\sqrt{g}} \tag{5.92}$$
$$B_{11} = \frac{rf' - 2f}{2\omega^2 r^3 \sqrt{fg}} \tag{5.93}$$
$$B_{12} = 0 \tag{5.94}$$
$$B_{21} = -\frac{k(rf' + 2f)}{2r\mu\sqrt{g}(\omega^2 - k^2 r^2 d)} \tag{5.95}$$
$$B_{22} = 0 \tag{5.96}$$
$$\tag{5.97}$$

Note that $A_{ij} = A_{ij}$ in the shear sector.

In order to proceed one needs to determine the boundary conditions, in order to numerically solve the equations of motion, and set up the numerical framework. The framework followed here will be the one prescribed in [112]. In particular it needs to be noted that the system consists of a coupled system of differential equation and hence it is not well-defined to talk about one-to-one solution-operator correspondence anywhere but strictly on the boundary. In other words it is only strictly on the boundary that the solution of each equation of motion provides information about a single, specific operator of the boundary theory. Given though that numerically one is never strictly on the boundary, but rather on a radial slice close to it, which defines a cut-off scale (r_Λ), one must take into account operator mixing effects. In essence the recipe in [112] consists of (numerically) finding a set of linearly independent solutions to the equations of motion, out of which, one forms a solution matrix which at the boundary reduces to a diagonal one. Out of this matrix one can extract all the relevant information about the boundary system. This process will now be briefly reviewed. The starting point is a system consisting of N fields Φ^I, $I \in \{1, \cdots, N\}$

governed by the bilinear action

$$S = \int d^d x \int dr \, \left[\partial_m \Phi^I A_{IJ}(x,r) \partial_n \Phi^J g^{mn} + \Phi^I B^m_{IJ}(x,r) \partial_m \Phi^J + \Phi^I C_{IJ}(x,r) \Phi^J\right] \tag{5.98}$$

where m, n span the Minkowski and radial coordinates ($x \sim x^\mu, z$). For the specific case in which this machinery will be implemented here, $N = 2$ and the two fields are the two gauge-invariant variables defined above. As usual, the non-radial directions are separated through a Fourier decomposition

$$\Phi^I(x^\mu, r) = \int \frac{d^d k}{(2\pi)^d} \Phi^I_k(r) \exp[-\imath k x] \tag{5.99}$$

which transforms the action into

$$S = \int \frac{d^d k}{(2\pi)^d} \int dr \left[\Phi'^I_{-k} A_{IJ}(k,r) \Phi'^J_k + \Phi^I_{-k} B_{IJ}(k,r) \Phi'^J_k + \Phi^I_{-k} C_{IJ}(k,r) \Phi^J_k\right] \tag{5.100}$$

where $k \equiv k^\mu$, $A_{IJ}(-k,r) = A_{IJ}(k,r)^*$, and similarly for B and C. Now the small issue of double counting arises, but is easily fixed by splitting the momentum integration into ($k_> = (\omega > 0, \mathbf{k})$) and ($k_< = (\omega < 0, \mathbf{k})$) and re-writing the action as

$$S = \int d\tilde{k}_> \int dr \left[2A^H_{IJ} \Phi'^I_{-k} \Phi'^J_k + B_{IJ} \Phi^I_{-k} \Phi'^J_k + B^\dagger_{IJ} \Phi'^I_{-k} \Phi^J_k + 2C^H_{IJ} \Phi^I_{-k} \Phi^J_k\right] \tag{5.101}$$

where $\int d\tilde{k}_> \equiv \frac{1}{(2\pi)^d} \int_0^\infty d\omega \int_{\mathbb{R}}^{d-1} d^{d-1}k$. One can now disregard the positive-negative momenta issue and just use the momentum variable $k = k_>$. The equations of motion can be recovered by varying Φ^I_{-k}, holding Φ^I_k fixed,

$$-2(A^H_{IJ} \Phi'^J_k)' + 2B^A_{IJ} \Phi'^J_k + (2C^H - B^{\dagger\prime})_{IJ} \Phi^J_k = 0 \tag{5.102}$$

where $M^{H,A}$ now stands for the (anti-)hermitian part $M^{H,A} = \frac{1}{2}(M \pm M^\dagger)$, for some matrix M. This is precisely how eq. (5.71) and eq. (5.72) where derived. In solving the equations of motion, one finds that near the boundary, the components of the vector Φ asymptote to $\Phi^I(r \to 0) \sim r^{\Delta^I_-} \phi^I_0 + ... + r^{\Delta^I_+} \phi^I_1 + ...$ Δ^I_- is the smallest exponent at the boundary $r = 0$. In order to compute the Green's functions of the dual quantum operators one needs to consider conveniently normalized fields $\Phi_k(r) = r^{\Delta^I_-} \bar{\Phi}^I_k(z)$ that close to the boundary have an expansion $\bar{\Phi}^I(r \to 0) = \phi^I_0 + \mathcal{O}(r^{\Delta^I_+ - \Delta^I_-})$, meaning that ϕ^I_0 can be interpreted as the source of the dual operator. The new fields can be treated collectively in the same formalism by defining the rescaling matrix $D^I{}_J = \delta^I{}_J z^{\Delta^J_-} = D^{\dagger\, I}{}_J$. Replacing Φ by $D\bar{\Phi}$ inside (eq. (5.101)) yields

$$S = \int d\tilde{k}_> \int dz \left[2\bar{A}^H_{IJ} \bar{\Phi}'^I_{-k} \bar{\Phi}'^J_k + \bar{B}_{IJ} \bar{\Phi}^I_{-k} \bar{\Phi}'^J_k + \bar{B}^\dagger_{IJ} \bar{\Phi}'^I_{-k} \bar{\Phi}^J_k + 2\bar{C}^H_{IJ} \bar{\Phi}^I_{-k} \bar{\Phi}^J_k\right], \tag{5.103}$$

where

$$\bar{A}^H = D^\dagger A^H D\,, \tag{5.104}$$

$$\bar{B} = D^\dagger B D + 2D'^\dagger A^H D\,, \tag{5.105}$$

$$\bar{C}^H = D^\dagger C^H D + D'^\dagger A^H D' + \frac{1}{2} D^\dagger B D' + \frac{1}{2} D'^\dagger B^\dagger D \tag{5.106}$$

One can now assume that the fields are indeed normalized this way and avoid the clutter caused by the barred symbols. Now consider a solution Φ_k^I of the coupled system. The boundary value of it acts as the source for the boundary theory operator O^I. Conversely the source of a particular operator, will be given by a vector $(\Phi_k^1(r), \Phi_k^2(r), ...)$ that, approaching the UV cut-off r_Λ, asymptotes, by construction, to a single component vector, $(\Phi_k^1(r), \Phi_k^2(r), ...) \overset{r\to r_\Lambda}{\to} (\varphi_k^1, 0, 0, ...)$. Similarly for every boundary operator. Therefore the bulk solution dual to a source $O^{I_0}(k)$ is given by a set $\{\Phi_k^I(r)\}$ that solves the equations of motion in the bulk and asymptote to $\Phi^J(r_\Lambda) = \delta^J{}_{I_0}\phi_0^{I_0}(k),\ J = 1, ..., N$, where $\phi_0^{I_0}(k) \equiv \varphi_k^{I_0}$ is the source of the corresponding operator $O^{I_0}(k)$. Since the system of equations of motion is coupled, at any other scale $r > r_\Lambda$ this set, $\{\Phi_k^I(z)\}$, will generically source a linear combination of all the operators. Hence, this set can be expressed in terms of the arbitrary boundary values, φ_k^J, as

$$\Phi_k^I(r) = F^I{}_J(k, r)\varphi_k^J \tag{5.107}$$

$$\Phi_{-k}^I(r) = F^I{}_J(-k, r)\varphi_{-k}^J = \varphi_{-k}^J F^\dagger{}_J{}^I(k, r) \tag{5.108}$$

The interesting dynamics of the fields are in this formalism contained in the solution matrix $F(k, z)^I{}_J = F(-k, z)^{*I}{}_J$, which is constructed to be normalized at the UV cut-off r_Λ as

$$F(k, r_\Lambda)^I{}_J = \delta_J^I \tag{5.109}$$

i.e. it reduces to a diagonal matrix, with each element corresponding to a specific boundary operator. Immediately two question arise - how does one construct this solution matrix and how can one extract the Green's function out of it. The latter is easier to address and therefore it will be treated first. Assuming that in some way one has constructed the solution matrix, the on-shell action can be rewritten in the form

$$\begin{aligned} S &= \int dk \int dr \left[\Phi_{-k}^I \left[e.o.m.(\Phi_k^I)\right] + \frac{d}{dr}[2A_{IJ}\Phi_{-k}^I \Phi_k'^J + B_{IJ}^\dagger \Phi_{-k}^I \Phi_k^J]\right] \\ &= \int dk\ \ \varphi_{-k}^I\, \mathcal{F}_{IJ}(k, z)\, \varphi_k^J\big|_{r_b}^{r_h}\,, \end{aligned} \tag{5.110}$$

where

$$\mathcal{F}(k,r) = 2F^\dagger A^H F' + F^\dagger B^\dagger F\,. \tag{5.111}$$

r_h is the position of the horizon and r_b the position of the boundary. In the present case those values are 1 and 0 respectively. It is now straightforward to generalize the standard Holographic approach [71] and write the Green's functions as

$$G^R_{IJ}(k) = -\lim_{r_\Lambda \to 0} \mathcal{F}_{IJ}(k, r_\Lambda) \tag{5.112}$$

One immediate property of these Green's functions can be derived by the conjugation properties of A, B, F defined above, i.e .

$$G^R_{IJ}(-k) = G^R_{IJ}(k)^* \tag{5.113}$$

It is important to notice at this point that the Green's function constructed in this fashion are not finite at the boundary. As prescribed by the Holographic Renormalization program [73], specific counter-terms need to be include in the action to compensate for the boundary infinities. These terms induce a change

$$\mathcal{F}_{IJ}(k, r_\Lambda) \to \mathcal{F}_{IJ}(k, r_\Lambda) - \mathcal{F}_{ct,IJ}(k, r_\Lambda) \tag{5.114}$$

These terms, presented in eq. (5.40) and eq. (5.41), have been appropriately introduced in the action used in this work.

Now the actual process of constructing the solution matrix will be considered, in particular in the context of numerical solutions. In order to construct these solutions a "shooting" method will be implemented. This means that a point close to the horizon will be picked, from which the integration will start, and on which boundary conditions (values and derivatives) will be set. The integration will be carried through the three parts of the space-time, i.e. first AdS-RN, Electron Star and finally the outer AdS-RN, all the way to a cut-off very close to the boundary, where the solutions will be checked using various numerical checks for stability and consistency. This checks include conservation of the current derived through the off-shell action, as well as the near-boundary solution of the equations of motion (what was defined before as a_0, a_2). In the presence of the horizon one imposes, as usual, in-going boundary conditions, which mirror the computation of the retarded Green's function. Hence, formally the solutions can be written as

$$\Phi^I_{(a)} = (r - r_h)^{-\frac{i\omega}{2T}} \left(e^I_{(a)} + O(r - r_H)\right) \tag{5.115}$$

realizing the IR boundary conditions. Here T is the Hawking temperature of the black hole in the inner region. The vectors $e_{(a)}$ should be used so as to provide

linearly independent solutions. In the present case, where two fields are involved, they are chosen to be

$$e^I_{(1)} = (1, 1) \tag{5.116}$$

$$e^I_{(2)} = (1, -1) \tag{5.117}$$

By performing the numerical integration for each boundary condition one obtains 2 independent solutions that extend in the range $r \in (r_\Lambda, r_h)$. These IR-normalized solutions can be arranged in a matrix, $H(k, r)$, in such a way that the J^{th} solution $(\Phi^1_{(J)}, \Phi^2_{(J)}, ..., \Phi^N_{(J)})$ appears as the J^{th} column, i.e.

$$H^I{}_J(k, r) = \Phi^I_{(J)}(k, r) \tag{5.118}$$

In the present case this is going to be a 2×2 matrix. Any in-going solution, can be written as a linear combination of the 2 independent solutions stemming from these boundary conditions. Consequently the matrix $F(k, r)$, consisting of the UV-normalized solutions must be related to $H(k, r)$. Given that by construction $F(k, r_\Lambda) = 1$ this relation must be

$$F(k, r) = H(k, r) \cdot H(k, r_\Lambda)^{-1} \tag{5.119}$$

Then the Green's functions is

$$G^R(k) = -\lim_{r_\Lambda \to 0} \mathcal{F}(k, r_\Lambda) = -\lim_{r_\Lambda \to 0} \left(2A^H(k, r_\Lambda)F'(k, r_\Lambda) + B^\dagger(k, r_\Lambda)\right) \tag{5.120}$$

where Holographic counter-terms have not been explicitly included. The near-boundary numerical check, i.e. the near-boundary behaviour of the fields, can be translated in this matrix language as

$$H^I{}_J(k, r \to 0) \sim \mathcal{A}(k)^I{}_J + z^{\Delta^I_+ - \Delta^I_-}\mathcal{B}(k)^I{}_J + ... \tag{5.121}$$

in the standard Holographic practice. Here $\mathcal{A}(k)$ and $\mathcal{B}(k)$ are equivalent to the connection coefficient found for example in [134], modified into matrices in order to fit this case. Inserting this expression into the Green's function one gets

$$G^R(k)^I{}_J = -\lim_{r_\Lambda \to 0} \left[2(\Delta^I_+ - \Delta^I_-)r_\Lambda^{\Delta^I_+ - \Delta^I_- - 1}\left(A^H(k, r_\Lambda)\mathcal{B}(k)\mathcal{A}(k)^{-1}\right) + B^\dagger(k, r_\Lambda)\right]^I{}_J \tag{5.122}$$

As is the case in many Holographic studies, of particular importance are the Quasi-Normal modes (QNMs) related to these Green's functions. Those correspond to poles of said Green's functions and even though the contain less information than

the full function, since they do not include the residue of each pole, they are easier to compute, particularly in cases where only numerical approaches are available like the present one, and contain enough information to calculate many interesting properties of the dual theory. In this coupled systems one can define a very useful operational criterion to locate QNMs. In particular one notices from eq. (5.122) that $G^R(k)$ is ill-defined whenever $\det \mathcal{A}(k) = 0$, hence the Green's function has poles whenever the inverse matrix $H(k, r_\Lambda)^{-1}$ does not exist. This is equivalent to demanding that the determinant of H vanishes at the cut-off, i.e.

$$\det[H(k_n, r_\Lambda)] = 0 \tag{5.123}$$

This is going to be the quantity computed in what follows to determine the position of a QNM.

Before presenting the main results it is useful, for completeness, to present the actual near-horizon boundary conditions determined after imposing in-going condition on the two coupled equations eq. (5.71) and eq. (5.72). By expanding the equations of motion close to the horizon and demanding that the regular part of the solution is expressed as a series, one has

$$Z_1^{reg}(u) = a_0 + a_1(1-u) + \dots \tag{5.124}$$

$$Z_2^{reg}(u) = b_0 + b_1(1-u) + \dots \tag{5.125}$$

Here the first two coefficients will be presented due to space limitations. However in the actual calculation the series has been continued up to sixth order, which provide enhanced numerical accuracy. Plugging in this ansatz into the equations of motion and iteratively solving, one finds that every coefficient can be computed in terms of a_0 and b_0. Those two parameters will provide the two linearly independent solutions by setting $(a_0, b_0) = (1, 1)$ for one of them and $(a_0, b_0) = (1, -1)$ for the other. Indicatively the first order coefficients for each field are presented here

$$\begin{aligned} a_1 =& a_0 \left(\varepsilon - \frac{\imath(\varepsilon-1)k^2}{\omega} - \frac{(\varepsilon-1)\left(2k^2+Q^2-6\right)}{Q^2+4\imath\omega-6} - \frac{8\imath(\varepsilon-1)Q^2\omega}{\left(Q^2-6\right)^2} \right) \\ &+ \frac{2b_0(\varepsilon-1)kQ\left(Q^2+2\imath\omega-6\right)}{Q^2+4\imath\omega-6} \end{aligned} \tag{5.126}$$

$$b_1 = -\frac{2\imath a_0(\varepsilon-1)kQ}{\omega\left(Q^2+4\imath\omega-6\right)} + \frac{2b_0(\varepsilon-1)\left(k^2+2Q^2\right)}{Q^2+4\imath\omega-6} - \frac{8\imath b_0(\varepsilon-1)Q^2\omega}{\left(Q^2-6\right)^2} + b_0 \tag{5.127}$$

Here ε is taken to be a very small ($0 < \varepsilon \ll 1$) number determining how close to the horizon the integration starts. Its appearance in these expressions highlights the point that one cannot just set the boundary conditions to either 1 or -1 since departure from the exact position of the horizon, which is numerically unavoidable, induces extra corrections. Having this series expansion, and the capacity to iteratively compute all terms up to what is required for numerical reasons, allows one to fully set boundary conditions for the gauge-invariant variables and their derivatives on the horizon. Therefore one has a well-defined differential problem that can be systematically studied.

The free parameters of the studied system are the temperature (in its dimensionless form) $\frac{T}{\mu}$, the injected (dimensionless) momentum $\frac{k}{\mu}$, the critical exponent z and the electron mass $\hat{m}$. The main target is to isolate the QNM corresponding to diffusion, in other words the lowest lying pole on the imaginary axis in the complex frequency plane [7]. The interest will be focused on extracting the diffusion coefficient of the dual theory and studying its dependence on temperature, momentum (dispersion relation) and then z and $\hat{m}$.

Putting all the ingredients together the complex frequency plane looks like fig. 5.15. In this plot the first three (in the sense that they are the lowest ones, or said differently they have the smallest (absolute) imaginary part) poles are presented, for a series of temperatures. The blob near the origin represents the lowest lying poles, which because they have the smallest imaginary part they are the longest-living ones (i.e. they attenuate with the slowest rate). The scaling imposed by the simultaneous plotting of the poles with non-vanishing real part, obscures these poles, which are the ones corresponding to diffusion and are the most interesting. Zooming into the origin, the diffusion mode, for various temperatures, looks like fig. 5.16. Since the purely imaginary pole is of maximum interest, from now on plots will be presented in one-dimensional form, only depicting the imaginary axis.

The first numerical study will attempt to extract the diffusion coefficient. It is expected that the diffusion mode behaves like

$$\omega = -\imath \mathcal{D}(T) k^2 + \dots \tag{5.128}$$

or in the proper dimensionless form

$$\frac{\omega}{c\mu} = -\imath \bar{\mathcal{D}}(T) \left(\frac{k}{\mu}\right)^2 + \dots \tag{5.129}$$

[7] By definition the frequencies of QNMs are complex [114].

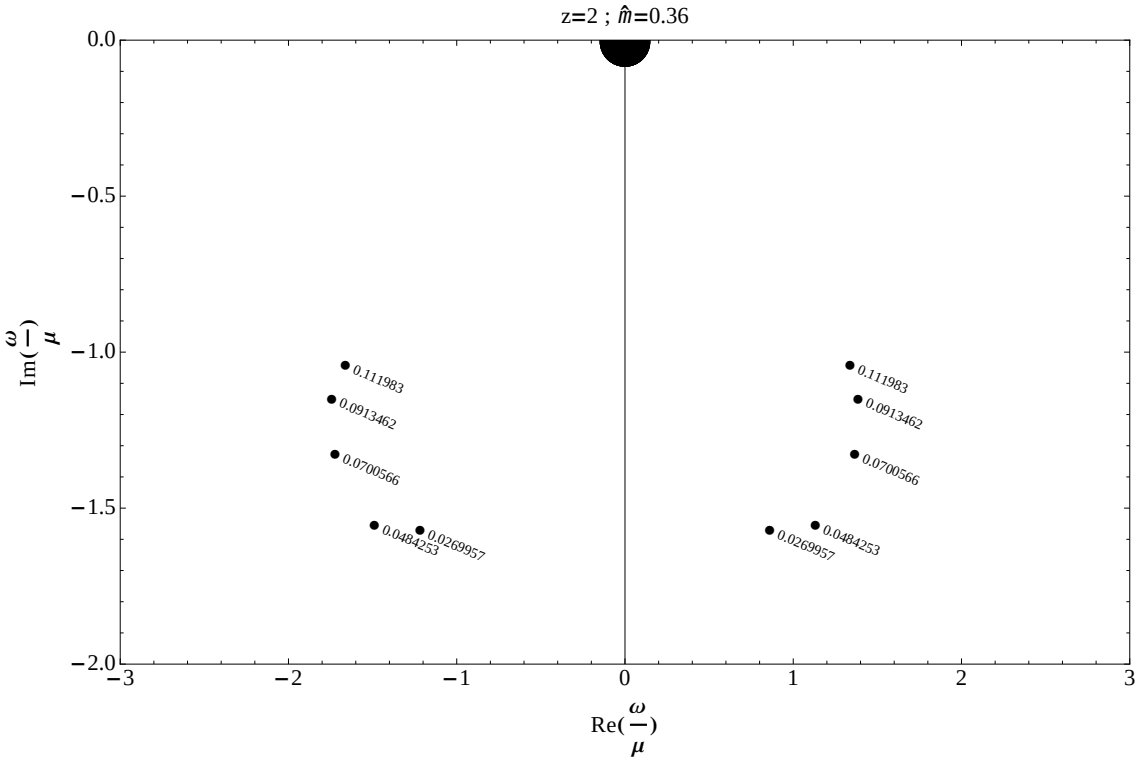

Figure 5.15: QNMs in the complex frequency (ω) plane for $\frac{k}{\mu} = 0.1$ and $\frac{T}{\mu} \simeq 0.11, 0.09, 0.07, 0.05, 0.03$.

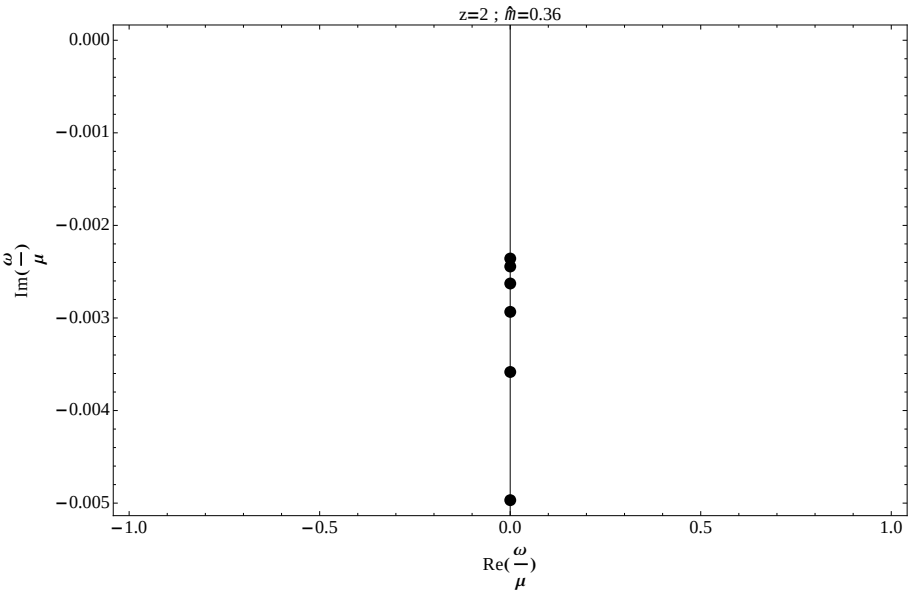

Figure 5.16: QNMs on the imaginary axis for $\frac{k}{\mu} = 0.1$ and $\frac{T}{\mu} \simeq 0.11, 0.09, 0.07, 0.05, 0.03$.

In order to extract $\mathcal{D}$ therefore, one can track the diffusion pole for a very small $\frac{k}{\mu}$, against temperature and then $\mathcal{D}(T) = -\Im\frac{\omega/\mu c}{(k/\mu)^2}$. The momentum value chosen is $k/\mu = 0.001$. The remaining free parameters are then z and $\hat{m}$, that is each pair defines a $\mathcal{D}(T)$ curve. Firstly the critical exponent z will be kept constant at $z = 2$ and variations of the electron mass $\hat{m}$ will be presented. These results are

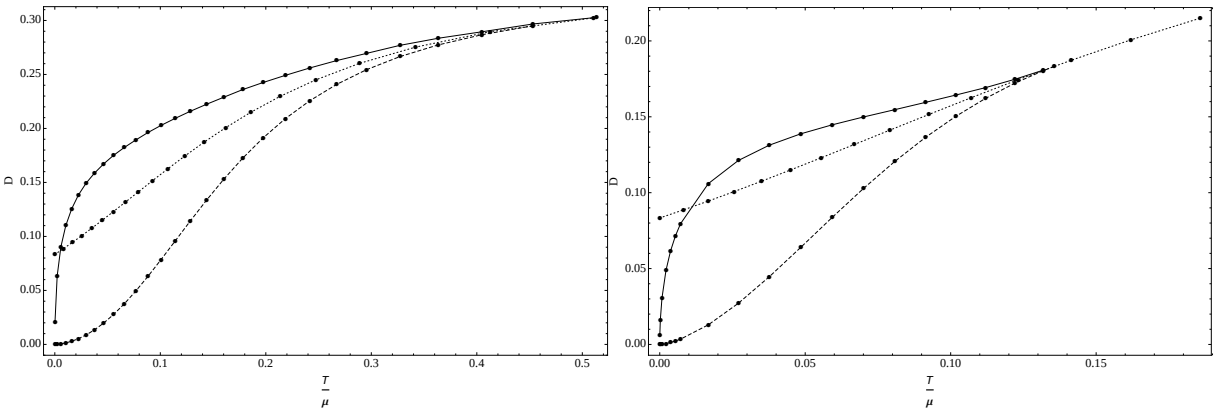

(a) $z = 2$; $\hat{m} = 0.10$

(b) $z = 2$; $\hat{m} = 0.36$

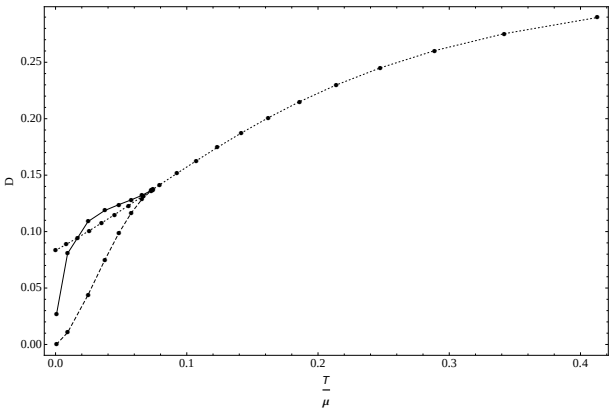

(c) $z = 2$; $\hat{m} = 0.50$

Figure 5.17: $\mathcal{D}(T)$ for $z = 2$ and $\hat{m} \in \{0.1, 0.36, 0.5\}$.

presented in fig. 5.17, where the solid lines correspond to the actual results, derived from the diffusion pole, while the RN result (dotted line) along with hydrodynamics expectation (dashed line) have been overlaid for comparison. Similarly in fig. 5.18 the diffusion constant (again from the pole, from hydrodynamics and for AdS-RN) is presented for four different critical exponents ($z \in \{3, 5, 10, 100\}$), keeping the

electron mass constant at $\hat{m} = 0.36$.

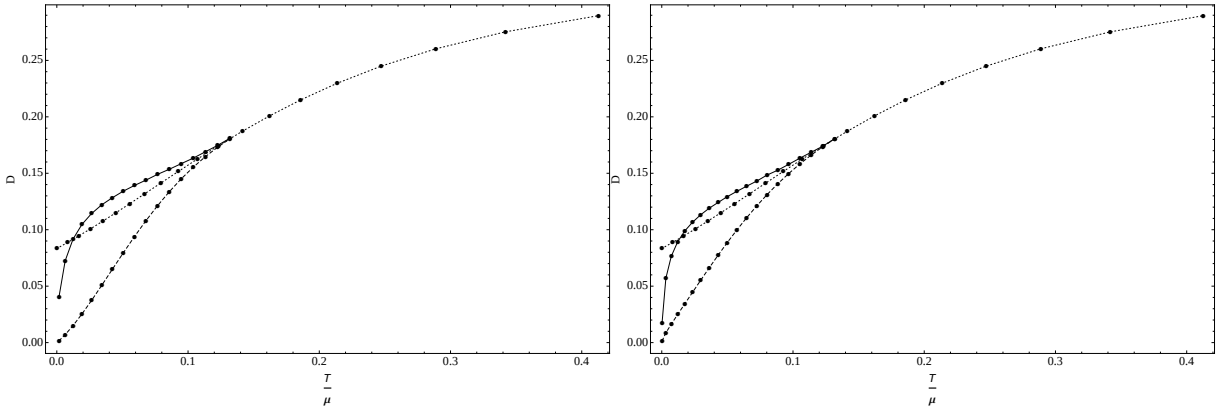

(a) $z = 3$; $\hat{m} = 0.36$

(b) $z = 5$; $\hat{m} = 0.36$

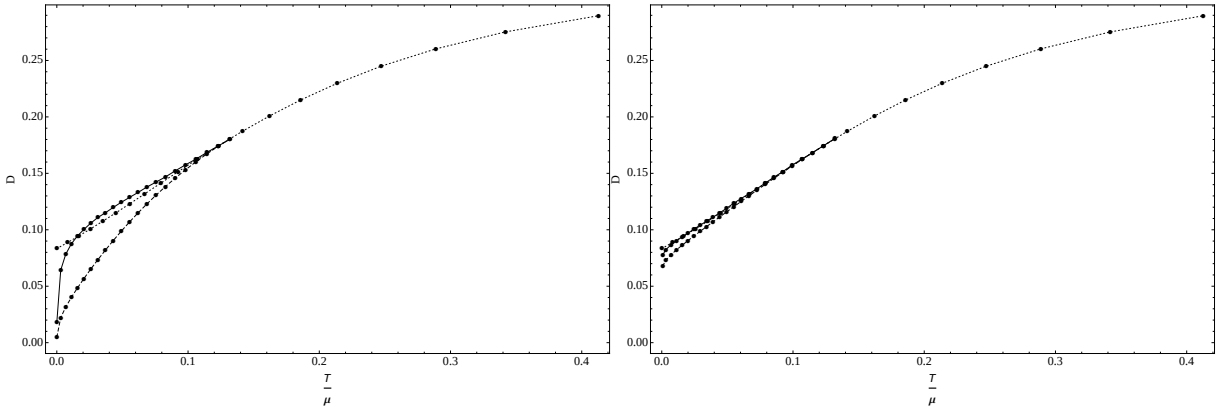

(c) $z = 10$; $\hat{m} = 0.36$

(d) $z = 100$; $\hat{m} = 0.36$

Figure 5.18: $D(T)$ for $\hat{m} = 0.36$ and $z \in \{3, 5, 10, 100\}$.

Let's summarize these results. The first, and easiest to describe, feature of the plots presented in this sections, is that for every pair of the parameters $z, \hat{m}$ there is a transition temperature above which the diffusion coefficient converges to the prediction for the pure AdS-RN system, i.e. when the Electron Star is absent. This is trivially expected since, as it has been noticed when studying the background, there is a finite range of temperatures within which the Electron Star is supported. Once the temperature exceeds the upper bound the black hole is hot/large enough to dominate the space-time, leaving no room for the star. The transition temperature appears to depend on the mass of the electron ($\hat{m}$). In particular the larger the mass the lower

the transition temperature. On the other hand the transition temperature seems to be very weakly correlated (if at all) with the critical exponent (z).

The more interesting and challenging part of these results is however related with the low-temperature behaviour of the diffusion constant. The striking characteristic is that it does not match the purely hydrodynamical prediction. The discrepancy seems not to be affected primarily by the electron mass, however the fact that an increase in $\hat{m}$ makes the transition towards the RN prediction quicker, suppresses the phenomenon. On the other hand this discrepancy seems to depend more strongly on the critical exponent. In particular the higher the critical exponent the closer the results are to both the hydrodynamics prediction and the RN. This should not be surprising since, as already noticed before, it is expected that at the limit $z \to \infty$ one should recover the AdS_2 near-horizon geometry. In other words the purely RN result.

What is striking and unexpected is that away from the limits when one recovers known systems, the system does not agree with hydrodynamical expectations. In order to understand this phenomenon one needs to consider the physical attributes of the system. What one has here is a system with two types of bulk charges - one that is behind the horizon (corresponding to the black hole) and one that is outside the horizon (corresponding to the electron star). Each of these charge sources, induces an electric flux through the boundary corresponding to boundary states. Depending on the source of the flux the phases are described as mesonic (Electron Star), fully fractionalised (RN) and partially fractionalised (ES and RN together) [135]. At low temperatures where ES and RN coexist the system is in the partially fractionlized phase, while above the transition temperature where there is only RN the system is in the fully fractionalised phase. Although this system has been studied at zero temperature in [135], here the system is heated up by taking the RN black hole away from extremality without however allowing the mesonic degrees of freedom to exchange heat with the fractionalised ones. This is because the Electron Star is assumed to remain at zero temperature (as explained above) no matter what the Hawking temperature of the black hole is. In other words on the boundary the systems consists of a set of two degrees of freedom that do not "communicate" thermodynamically and therefore the system is not in equilibrium. When the temperature is lowered enough, i.e the black hole is nearly extremal, eventually the phenomenon becomes irrelevant and diffusion ceases as expected by standard hydrodynamics, since the degrees of freedom "freeze" out, leading to $\mathcal{D}(T \to 0) = 0$.

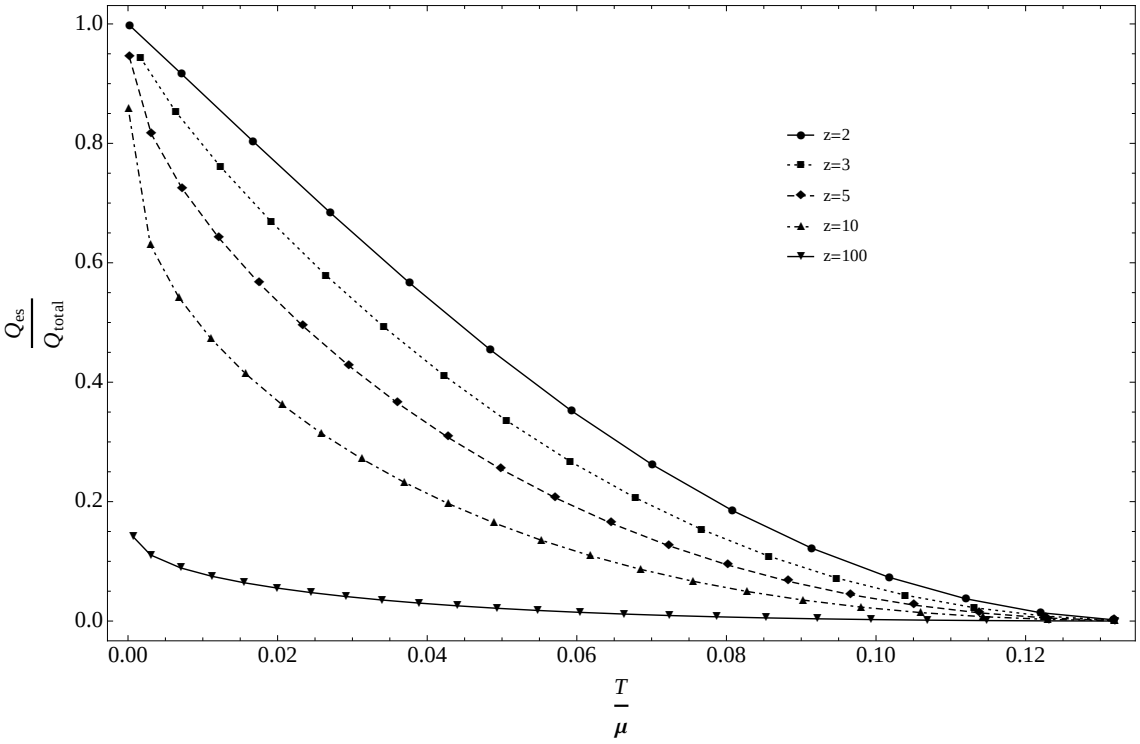

Figure 5.19: Fraction of Electron Star charge vs. z and $\frac{T}{\mu}$.

How can one quantify this phenomenon? A useful parameter is the ratio of the charge of the Electron Star over the total charge of the system [129]. This quantity measures how much of the boundary flux comes from the "frozen" mesonic degrees of freedom. Varying the critical exponent the ratio against temperature is presented in fig. 5.19, while the results varying the electron mass in fig. 5.20. What one sees from these is that the higher the critical exponent, the faster the transition from a partially to a fully fractionalised phase is. The more the system approaches the latter the more the diffusion constant agrees with both the hydrodynamical prediction and the pure RN, which corresponds to the fully fractionalised phase. Said differently for a fixed temperature (and electron mass) the charge ratio $\frac{Q_{es}}{Q_{total}} \to 0$ as $z \to \infty$, i.e the boundary flux is essentially sourced from behind the horizon, restoring the known hydrodynamical properties of the AdS-RN system. Similarly if one fixes the temperature and the critical exponent and varies the electron mass, it becomes apparent that as the mass grows the ratio goes to 0 again asymptoting to the AdS-RN system.

Trying to explain further this phenomenon the following was attempted. Assuming the form 5.46 for the diffusion coefficient what would happen if one had included more

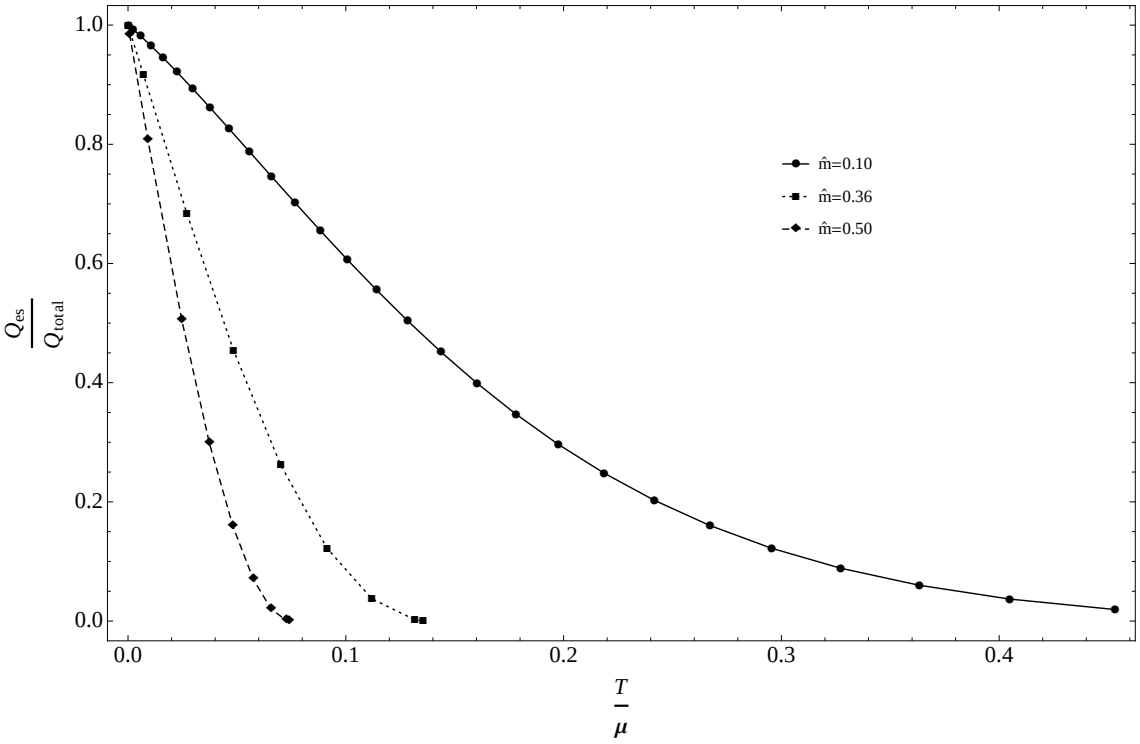

Figure 5.20: Fraction of Electron Star charge vs. $\hat{m}$ and $\frac{T}{\mu}$.

than the appropriate degrees of freedom in the diffusion process? To address that the denominator of 5.46 was split into two parts, on of which corresponds to the Electron Star, that is

$$\epsilon + p = \epsilon' + p' + \epsilon_{ES} + p_{ES} = \epsilon' + p' + \sigma\mu \tag{5.130}$$

where the equation of state for the Electron Star has been used. Assuming that degrees of freedom of the Electron Star do not diffuse and therefore removing them from the sum, one gets a hydrodynamical prediction that is much closer to the observed results. This observation has encouraged the interpretation of the two part boundary system, with one part being unaffected by the thermal fluctuations (that is the mesonic dof) whereas the other behaves as expected from hydrodynamics. The interplay between the two appears to be intricate and it is not easy to separate one from the other. In an attempt to make this interpretation more convincing the difference between observed $\epsilon_O + p_O$ and hydrodynamical $\epsilon_H + p_H$ has been computed, and it turns out that at low temperatures, where the mesonic dof dominate, it can be almost completely attributed to the Electron Star not interacting thermally. At the other end of the scale, i.e. at temperatures close to the transition, where more and more dof get fractionalised, the difference vanishes and the single RN black hole

	High $\frac{T}{\mu}$	Low $\frac{T}{\mu}$
z=2	$\sim (k/\mu)^{2.06}$	$\sim (k/\mu)^{2.003}$
z=3	$\sim (k/\mu)^{2.03}$	$\sim (k/\mu)^{2.08}$
z=10	$\sim (k/\mu)^{2.08}$	$\sim (k/\mu)^{2.08}$

Table 5.1: Dispersion relation for the lowest QNM, for various ES parameters and temperatures.

appears to account quite well for the observed diffusion coefficient.

In extracting the diffusion coefficient an important assumption has been made - that the imaginary part of the corresponding pole should behave quadratically (at least to first approximation) with momentum. This is an assumption that can and needs to be tested. In this last part of the current section the dispersion relation of the lowest lying pole will be examined. Of particular interest is its dependence (if any) on temperature and the two Electron Star parameters, i.e. the critical exponent and the electron mass. The way these results will be presented is the following - for each set of $(z, \hat{m})$ the position of the pole against the injected momentum $\frac{k}{\mu}$ will be plotted for the lowest and highest available temperatures [8]. The results are presented in fig. 5.21. The plots are made to be log-log so that a power law will be immediately identified as straight line. Inset in every plot is the estimate for the exponent of power-law relation fitting to the small-momentum data [9]. Since the presentation of the plots is quite compact, the actual results are summarized in table 5.1. What becomes apparent from fig. 5.21 and table 5.1 is that the imaginary part of the lowest lying QNM does in fact behave quadratically (to a very satisfactory numerical accuracy), independently of temperature, critical exponent and electron mass. It is also clear that there are corrections to the quadratic relation, as for higher momenta there is a deviation from the quadratic curve.

5.4 Sound channel

In this final section, preliminary work on the other channel, i.e sound, will be presented. What will be included is essentially the necessary analytic preparatory work,

[8] This form is chosen due to space limitation even though intermediate temperature have been examined and found to agree with what is presented here.

[9] In the inset the symbol k is used for the fitted relation. This is in fact $\frac{k}{\mu}$ but the symbol k was chosen for presentation reasons.

whereas the actual full numerical analysis will not be done here, due to space-time limitations. The sound channel consists of the following perturbation components: $h_{xy}, h_{xx}, h_{tt}, h_{yy}, h_{rt}, h_{rx}, h_{rr}, a_x, a_t, a_r, \delta\phi, \delta u_x, \delta u_t, \delta u_r, \delta\sigma, \delta\lambda$. By perturbing the action with respect to these components, one can extract the relevant equations of motion, which as mentioned before form a closed set and do not couple to the shear sector due to their symmetry properties (parity under $y \to -y$). The equations of motion are:

$$\begin{aligned} &h_t{}^{x\prime\prime} - \left(\frac{f'}{2f} + \frac{g'}{2g} + \frac{4}{r}\right) h_t{}^{x\prime} + \imath\omega r^2 g h_x{}^{r\prime} - \imath k r^2 g h_t{}^{r\prime} - \frac{\imath k}{2} r^2 g \left(\frac{f'}{f} + \frac{g'}{g}\right) h_t{}^{r} \\ &\quad + \frac{\imath\omega}{2} r^2 g \left(\frac{g'}{g} - \frac{f'}{f} - \frac{4}{r}\right) h_x{}^{r} + r^2 g\omega k \left(h_y{}^{y} + h_r{}^{r}\right) + 2r^2 h' \left(a_x' - \imath k a_r\right) \\ &\quad + 2r^2\sqrt{f} g\sigma(a_x + \imath k\delta\phi) = 0 \end{aligned} \tag{5.131}$$

$$\begin{aligned} &h_t{}^{t\prime\prime} + h_y{}^{y\prime\prime} + \left(\frac{f'}{f} - \frac{g'}{2g} - \frac{1}{r}\right) h_t{}^{t\prime} + \left(\frac{f'}{2f} - \frac{g'}{2g} - \frac{2}{r}\right) h_y{}^{y\prime} - 2\imath\omega \frac{g}{f} h_t{}^{r\prime} \\ &\quad + \left(\frac{1}{r} - \frac{f'}{2f}\right) h_r{}^{r\prime} + \imath\omega \left(\frac{2g}{rf} - \frac{g'}{f}\right) h_t{}^{r} + \omega^2 \frac{g}{f}(h_y{}^{y} + h_r{}^{r}) - \frac{2h'}{f}(a_t' + \imath\omega a_r) \\ &\quad + \left(\frac{2f'}{rf} - \frac{h'^2}{f} - \frac{2}{r^2}\right) h_r{}^{r} + \left(\frac{h'^2}{f} + g(p+\rho)\right) h_t{}^{t} - 2\frac{g\sigma}{\sqrt{f}}(a_t - \imath\omega\delta\phi) = 0 \end{aligned} \tag{5.132}$$

$$\begin{aligned} &h_x{}^{x\prime\prime} + h_y{}^{y\prime\prime} - 2\imath k r^2 g h_x{}^{r\prime} + \frac{2}{r} h_r{}^{r\prime} - \left(\frac{g'}{2g} + \frac{3}{r}\right)(h_x{}^{x\prime} + h_y{}^{y\prime}) + \imath k(2rg - r^2 g') h_x{}^{r} \\ &\quad - k^2 r^2 g(h_r{}^{r} + h_y{}^{y}) + \left(\frac{2f'}{rf} - \frac{h'^2}{f} - \frac{2}{r^2} + 2g(p+\rho)\right) h_r{}^{r} - \left(\frac{h'^2}{f} + g(p+\rho)\right) h_t{}^{t} \\ &\quad + \frac{2h'}{f}(a_t' + \imath\omega a_r) + 2\frac{g\sigma}{\sqrt{f}}(a_t - \imath\omega\delta\phi) + 4g\mu\delta\sigma - 4g\delta\lambda = 0 \end{aligned} \tag{5.133}$$

$$\begin{aligned} &h_x{}^{x\prime\prime} + h_t{}^{t\prime\prime} - 2\imath k r^2 g h_x{}^{r\prime} - 2\imath\omega \frac{g}{f} h_t{}^{r\prime} + \left(\frac{f'}{f} - \frac{g'}{g} - \frac{1}{g}\right) h_t{}^{t\prime} + \left(\frac{1}{r} - \frac{f'}{2f}\right) h_r{}^{r\prime} \\ &\quad + \left(\frac{f'}{2f} - \frac{g'}{2g} - \frac{2}{r}\right) h_x{}^{x\prime} - \imath\omega \left(\frac{g'}{f} - \frac{2g}{rf}\right) h_t{}^{r} - \imath k \left(r^2 g' + \frac{r^2 g f'}{f}\right) h_x{}^{r} + 2\omega k \frac{g}{f} h_t{}^{x} \\ &\quad + \omega^2 \frac{g}{f} h_x{}^{x} - k^2 r^2 g h_t{}^{t} + \frac{g}{f}(\omega^2 - k^2 r^2 f) h_r{}^{r} + \left(\frac{h'^2}{f} + g(p+\rho)\right) h_t{}^{t} \\ &\quad + \left(\frac{2f'}{rf} - \frac{h'^2}{f} - \frac{2}{r^2}\right) h_r{}^{r} - \frac{2h'}{f}(a_t' + \imath\omega a_r) - 2\frac{g\sigma}{\sqrt{f}}(a_t - \imath\omega\delta\phi) = 0 \end{aligned} \tag{5.134}$$

$$\frac{\imath\omega}{2}(h_x{}^{x\prime}+h_y{}^{y\prime})+\frac{\imath k}{2}h_t{}^{x\prime}+\frac{1}{2}k^2r^2gh_t{}^r+\frac{1}{2}\omega kr^2gh_x{}^r+\frac{\imath\omega}{r}h_r{}^r-g(p+\rho)h_t{}^r$$
$$-\imath\omega\left(\frac{f'}{4f}+\frac{1}{2r}\right)(h_x{}^x+h_y{}^y)-\imath k\left(\frac{f'}{2f}+\frac{1}{r}\right)h_t{}^x-\sqrt{f}\sigma(a_r+\delta\phi')=0 \tag{5.135}$$

$$\frac{\imath k}{2}(h_t{}^{t\prime}+h_y{}^{y\prime})-\frac{\imath\omega}{2r^2f}h_t{}^{x\prime}+\frac{g}{2f}\omega kh_t{}^r+\frac{g}{2f}\omega^2h_x{}^r+\imath k\left(\frac{f'}{4f}+\frac{1}{2r}\right)h_t{}^t$$
$$-\imath k\left(\frac{f'}{4f}-\frac{1}{2r}\right)h_r{}^r-\imath\frac{h'}{f}(\omega a_x+ka_t)=0 \tag{5.136}$$

$$\left(\frac{f'}{4f}-\frac{1}{2r}\right)(h_x{}^{x\prime}+h_y{}^{y\prime})-\frac{1}{r}h_t{}^{t\prime}+2\imath\omega\frac{g}{rf}h_t{}^r-\frac{\imath krg}{2f}(rf'-2f)h_x{}^r$$
$$-\left(\frac{h'^2}{2f}-\frac{g}{2}(p+\rho)\right)h_t{}^t-\frac{1}{2r^2f}\left(r^2h'^2-2rf'+2f\right)h_r{}^r+\frac{g}{2f}\omega^2h_x{}^x-\frac{k^2r^2g}{2}h_t{}^t$$
$$+\frac{g}{2f}(\omega^2-k^2r^2f)h_y{}^y+\frac{g}{f}\omega kh_t{}^x+\frac{h'}{f}(a_t'+\imath\omega a_r)-\frac{g\sigma}{\sqrt{f}}(a_t-\imath\omega\delta\phi)=0 \tag{5.137}$$

$$a_x''-\imath ka_r'+\frac{1}{2}\left(\frac{f'}{f}-\frac{g'}{g}\right)(a_x'-\imath ka_r)+\frac{g}{f}\omega(\omega a_x+ka_t)+\frac{h'^2}{r^2f}h_t{}^{x\prime}$$
$$+\imath\omega\frac{gh'}{f}h_x{}^r+g\sigma\delta u_x=0 \tag{5.138}$$

$$a_t''+\imath\omega a_r'+\frac{rg}{2}(p+\rho)(a_t'+\imath\omega a_r)-kr^2g(ka_t+\omega a_x)-\imath kr^2gh'h_x{}^r$$
$$+\frac{h'}{2}(h_x{}^{x\prime}+h_y{}^{y\prime}-h_t{}^{t\prime}-h_r{}^{r\prime})-g\sqrt{f}\sigma h_r{}^r+g\sigma\delta u_t-g\sqrt{f}\delta\sigma=0 \tag{5.139}$$

$$\imath\omega a_t'+\imath kr^2fa_x'-a_r(\omega^2-k^2r^2f)+\frac{\imath\omega}{2}h'(h_x{}^x+h_y{}^y-h_t{}^t-h_r{}^r)+\imath kh'h_t{}^x$$
$$+\sqrt{f}g\sigma h_t{}^r-f\sigma\delta u_r=0 \tag{5.140}$$

$$h_t{}^{r\prime}-\frac{\sqrt{f}}{g}\delta u_r'+\left(\frac{g'}{2g}-\frac{\sigma'}{\sigma}-\frac{2}{r}\right)h_t{}^r+\frac{\imath\omega}{2}(h_r{}^r+h_x{}^x+h_y{}^y-h_t{}^t)+\imath kh_t{}^x$$
$$+\frac{\sqrt{f}}{g}\left(\frac{g'}{2g}-\frac{f'}{2f}-\frac{\sigma'}{\sigma}+\frac{2}{r}\right)\delta u_r-\frac{\imath\omega}{\sqrt{f}}\delta u_t+\frac{\imath\omega}{\sigma}\delta\sigma-\imath kr^2\sqrt{f}\delta u_x=0 \tag{5.141}$$

$$a_x + \imath k\delta\phi + \mu\delta u_x = 0 \tag{5.142}$$

$$2\delta\lambda - \mu\delta\sigma - \frac{\sigma}{\sqrt{f}}(a_t - \imath\omega\delta\phi + \mu\delta u_t) = 0 \tag{5.143}$$

$$a_r + \delta\phi' + \mu\delta u_r = 0 \tag{5.144}$$

$$\frac{\mu'}{\sigma'}\delta\sigma + \mu h_t{}^t - \frac{1}{\sqrt{f}}(a_t - \imath\omega\delta\phi - \mu\delta u_t) \tag{5.145}$$

$$h_t{}^t + \frac{2}{\sqrt{f}}\delta u_t = 0 \tag{5.146}$$

where again indices of the metric fluctuations $h_{\mu\nu}$ are raised and lowered using the background metric, a prime denotes a derivative with respect to r, and the dependence of the field fluctuations upon r, ω and k, and of the background fields upon r, have been suppressed. It should be noted that one may also choose to parametrise deviations from equilibrium in terms of the variables $h_{\mu\nu}$, a_μ, δu_μ, $\delta\sigma$, δp and $\delta\rho$. This is convenient if one works directly at the level of equations of motion without invoking an action (as in section 2 of [127]). The bulk fluctuations of pressure and energy density are related to fluctuations of the Schutz variables via

$$\delta p = \frac{\sigma\mu'}{\sigma'}\delta\sigma \ , \ \delta\rho = \mu\delta\sigma \tag{5.147}$$

This set of equations is even more unmanageable than the shear sector. Again though they organize themselves in a much more convenient way, if one introduces the gauge-invariant variables

$$\begin{aligned} Z_3(r,\omega,l) =& \omega^2 h_x{}^x(r,\omega,k) + 2\omega k h_t{}^x(r,\omega,k) - k^2 r^2 f h_t{}^t(r,\omega,k) \\ & - \left(\omega^2 + \frac{k^2 r^3 f'}{2}\right) h_y{}^y(r,\omega,k) \end{aligned} \tag{5.148}$$

$$\begin{aligned} Z_4(r,\omega,l) =& \omega a_x(r,\omega,k) + k a_t(r,\omega,k) + \frac{k}{2} r h' h_y{}^y(r,\omega,k) \\ Z_5(r,\omega,l) =& \delta\sigma(r,\omega,k) + \frac{r\sigma'}{2} h_y{}^y \end{aligned} \tag{5.149}$$

These are invariant under, as were their shear counterparts, both $U(1)$ (5.69), as well as diffeomorphism transformations (5.70). Again not all of these equations are dynamic. Some of them, corresponding to constraint equations, can be solved algebraically and used to simplify the rest. In particular one can solve (5.134-5.136)

and (5.139-5.144) for the constraint fields ${h_r}^r$, ${h_t}^r$, ${h_t}^r$, a_r, δu_t, δu_x, δu_r, $\delta\phi$ and $\delta\lambda$. Substituting the solutions for these fields into the remaining equations, one finds that there are only three linearly independent equations in the sound (longitudinal) sector. These linearly-independent equations of motion may be written in the form

$$Z_3''(r) + C_{31}Z_3'(r) + C_{32}Z_4'(r) + C_{33}Z_5'(r) + C_{34}Z_3(r) + C_{35}Z_4(r) + C_{36}Z_5(r) = 0 \tag{5.150}$$

$$Z_4''(r) + C_{41}Z_3'(r) + C_{42}Z_4'(r) + C_{43}Z_5'(r) + C_{44}Z_3(r) + C_{45}Z_4(r) + C_{46}Z_5(r) = 0 \tag{5.151}$$

$$Z_3''(r) + C_{51}Z_3'(r) + C_{52}Z_4'(r) + C_{53}Z_5'(r) + C_{54}Z_3(r) + C_{55}Z_4(r) + C_{56}Z_5(r) = 0 \tag{5.152}$$

The coefficients of these equations are too lengthy and complicated to be put into print, which would anyway be of limited value. In fact they are computed through computer algebra software (in particular `Mathematica`) and are planned to accompany the upcoming publication of this work, in electronic form. Similarly unprintable is the on-shell action, which has also been computed in this way. Now, as was the case for the shear sector, all the necessary ingredients are available in order to proceed in a systematic numerical analysis of this system. Of particular interest will be the quest for zero-sound. For this extensive study one is referred to upcoming work.

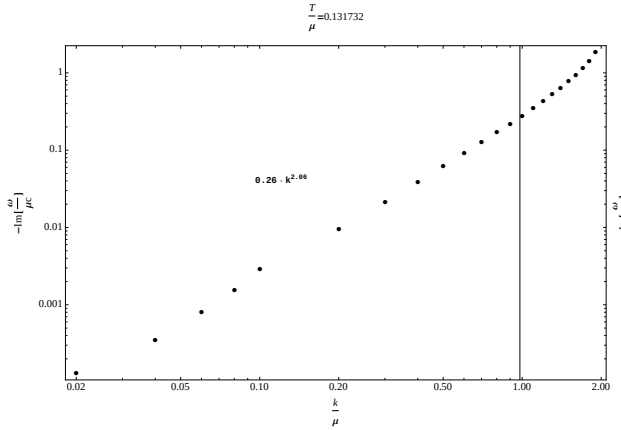

(a) $z = 2$, high

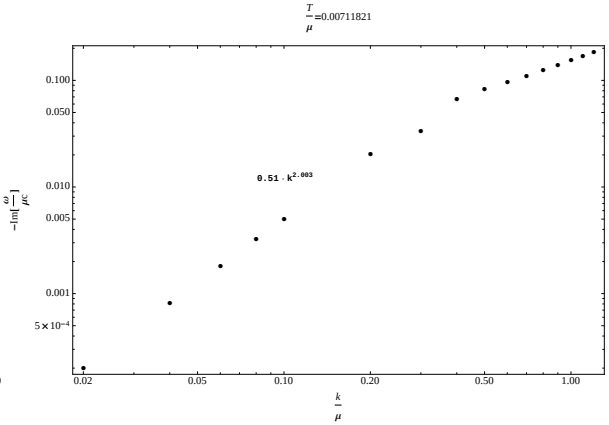

(b) $z = 2$, low

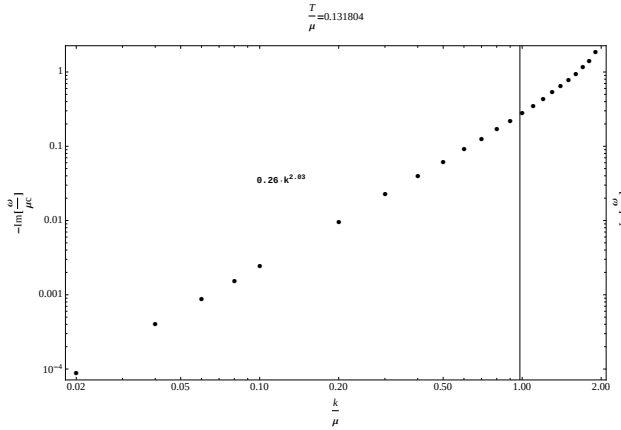

(c) $z = 3$, high

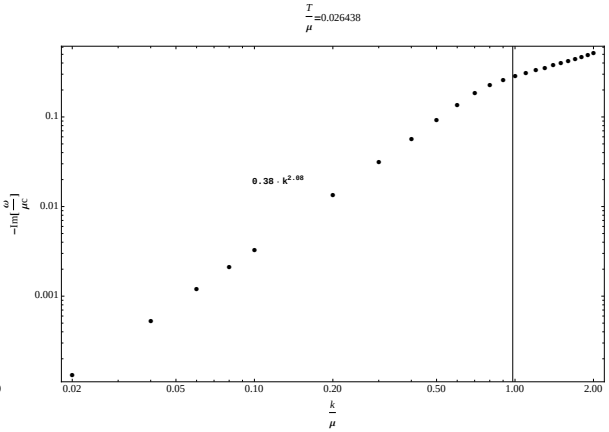

(d) $z = 3$, low

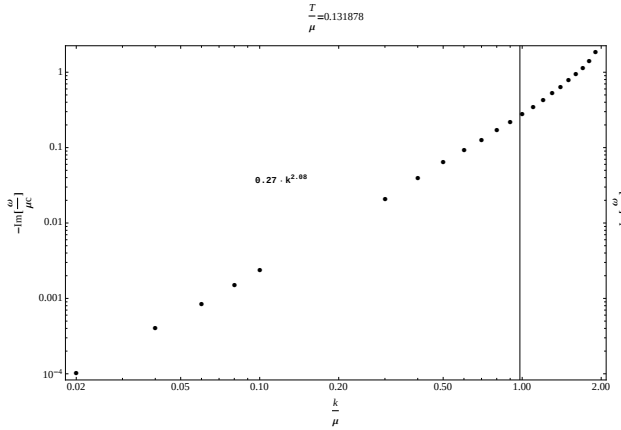

(e) $z = 10$, high

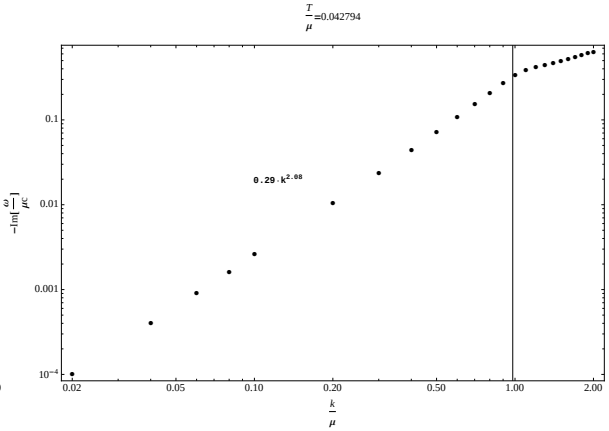

(f) $z = 10$, low

Figure 5.21: Dispersion relations.

Chapter 6

Conclusions and discussion

In the concluding chapter of this thesis the main results presented so far will be summarized. First the AdS_4 case will be reviewed, followed by the Electron Star.

6.1 AdS_4

In the studying the Anti-de Sitter Reissner–Nordström system the main results, in summary, are as follows:

i) When momentum $q \ll \mu$, the long-lived modes of the charge density and energy density Green's functions are the sound and diffusion-like modes with dispersion relations (4.4) and (4.5) respectively.

ii) When momentum $q \ll \mu$ and temperature $T \ll \mu$, the attenuation of the sound mode shows no significant temperature dependence, unlike in the strongly-coupled D3/D7 field theory and in Landau's theory of Fermi liquids. When $q \ll \mu$ and $T \gg \mu$, the sound and diffusion dispersion relations are well-approximated by the $\mu = 0$ results of [107, 109].

iii) When $q \ll \mu$, the energy density spectral function is dominated by the sound peak at all temperatures, whereas the charge density spectral function undergoes a crossover from sound domination at low temperatures to diffusion domination at high temperatures. This crossover is due to the changing residue at each pole, and occurs at a temperature $T_{\text{cross}} \sim \mu^2/q \gg \mu$.

iv) When $q \gg \mu$ and $T \ll \mu$, the sound and diffusion modes no longer dominate the energy density and charge density spectral functions, and the effects of other modes become important.

v) When both μ and T are non-zero, a long-lived sound mode will propagate provided that its momentum q is much less than either μ or T.

These results show that although many strongly-coupled field theories at large chemical potential (which have a gravitational dual) possess a $T = 0$ sound mode, these are not all LFL-like 'zero sound' modes (by which one means that they don't have the properties shown in figure 4.1) as was the case in the D3/D7 theory. However, there is still the possibility that there could be universal behaviour of the sound mode within subsets of strongly-coupled field theories with a gravitational dual. It is noted that the density-dependent physics in the D3/D7 and RN-AdS_4 theories arise through different holographic mechanisms (see [82, 136] for further discussion of this). In the D3/D7 theory, the background metric is fixed and it is the gauge field action - the DBI action - which alters the equation of motion of the gauge field from the $\mu = 0$ Maxwell equation (whose only long-lived mode is the high temperature charge diffusion mode). In contrast to this, the gauge field equation of motion in the RN-AdS_4 theory departs from the $\mu = 0$ Maxwell equation via couplings to the bulk metric fluctuations. The other major difference between these two field theories is the number of spatial dimensions, but it not expected that this will have a significant effect on the acoustic properties of the theory (provided that the number of field theory spatial dimensions is greater than one).

It would be very interesting to check whether the low temperature sound modes in other probe brane theories [92–96] share the LFL-like properties of the D3/D7 theory. This would help to establish whether it is the form of the DBI action, which implies that the non-zero density in the field theory is a density of fundamental matter (at least in the cases where the background geometry can be derived from string theory) rather than, for example, the R-charge density in the RN-AdS_4 theory, that generates these interesting properties or not. The effects of metric back-reaction (i.e. coupling between the field theory's charge density and energy density) are also yet to be computed for these probe brane theories. These may complete the LFL-like picture of acoustic propagation (by reproducing the full LFL sound attenuation curve - figure 4.1 - including the hydrodynamic regime), or they may result in deviations from it. No more insight can be gained into this from our back-reacted RN-AdS_4 results because of the difference in gauge field actions described previously. Although an expansion of the DBI action in powers of $F_{\mu\nu}$ yields the Maxwell action at lowest order, in field theory quantities this is an expansion in powers of μ/T which is the opposite limit from that in which any LFL-like properties of a theory would be exhibited.

In addition to those mentioned above, there are numerous other field theories with a gravitational dual which may possess interesting sound modes when $T \ll \mu$. Among the most interesting of these are dilatonic black holes [136–138] and geometries where

the bulk charge density is sourced by fermions [127, 129, 139–141]. It would also be worthwhile to determine the acoustic properties of more general truncations of super-gravity which admit more complicated solutions than RN-AdS_4 (for example, those of [111, 137, 142]), to determine whether the specific truncation chosen has a significant effect on these properties.

It has become clear that even this relatively simple holographic theory has many non-trivial features in its bosonic excitations. Among the most intriguing are the accuracy of the 'zero temperature hydrodynamics', and the crossover temperature $T_{\text{cross.}} \sim \mu^2/q$ between the charge density spectral function being dominated by the sound mode and the diffusion mode. It would be useful to have a clearer physical understanding of these properties, and also to determine if they are present in other field theories at non-zero chemical potential.

6.2 Electron Star

In studying the Electron Star system, in a non-zero temperature RN-AdS background, and in particular in the shear channel, the main results, in summary, are as follows:

i)The system possesses a QNM structure similar to many other gravitational systems, studied within Holography. In particular there is a long-lived or stable (i.e. very close to the origin of the complex frequency plane) pole on the imaginary axis (i.e. purely dissipative), which corresponds to diffusion in the system.

ii)The system is essentially composed of two kinds of degrees of freedom on the boundary - those related to the black-hole charge, i.e. the charge coming from behind the horizon and those related to the bulk fermionic charge of the Electron Star. The two sets of degrees of freedom are not in equilibrium, as one of them (the mesonic part) is constantly kept at zero temperature, while the other is heated up. This is reflected in the non-hydrodynamical low-temperature behaviour of the diffusion coefficient.

iii)The mixture of the two kinds of degrees of freedom is measure by the Electron Star to total charge ratio, which has been shown to depend on the system's temperature as well as the critical exponent and the electron mass. This ratio can be used as an order parameter to distinguish between the partially fractionalised and the fully fractionalised phases. Furthermore, as seen from the results presented here, it measures the departure from the hydrodynamical behaviour.

iv)A feature that has been observed in this analysis but was not elaborated on, since it is a negative result, is the absence of a real pole in the frequency plane. Such

a pole would correspond to a Fermi Surface in the boundary theory. This absence cannot be reliably accounted for and further study along with more robust numerical methods, appears to be required.

Moving forward in the exploration of the properties of this system, two directions should be pursued. Firstly and most importantly the bulk fermions must be allowed to thermally interact with the rest of the system so that it can relax and reach a proper equilibrium state. This entails the explicit treatment of the bulk fermions in the RN-AdS background, in place of the current approximation. This work is already under way.

Finally, the sound channel of the system has to be finalized. The existence of a zero-sound, as is the case in so many Holographic systems, should be examined. This work is almost completed and will be soon published.

Bibliography

[1] N. Beisert, C. Ahn, L. F. Alday, Z. Bajnok, J. M. Drummond, et al., *Review of AdS/CFT Integrability: An Overview*, *Lett.Math.Phys.* **99** (2012) 3–32, [arXiv:1012.3982].

[2] R. A. Davison and A. O. Starinets, *Holographic zero sound at finite temperature*, *Phys.Rev.* **D85** (2012) 026004, [arXiv:1109.6343].

[3] M. Edalati, J. I. Jottar, and R. G. Leigh, *Holography and the sound of criticality*, *JHEP* **1010** (2010) 058, [arXiv:1005.4075].

[4] P. Atkins and J. de Paula, *Atkins' Physical Chemistry*. OUP Oxford, 2010.

[5] J. M. Maldacena, *The Large N limit of superconformal field theories and supergravity*, *Adv.Theor.Math.Phys.* **2** (1998) 231–252, [hep-th/9711200].

[6] S. Gubser, I. R. Klebanov, and A. M. Polyakov, *Gauge theory correlators from noncritical string theory*, *Phys.Lett.* **B428** (1998) 105–114, [hep-th/9802109].

[7] E. Witten, *Anti-de Sitter space and holography*, *Adv.Theor.Math.Phys.* **2** (1998) 253–291, [hep-th/9802150].

[8] O. Aharony, S. S. Gubser, J. M. Maldacena, H. Ooguri, and Y. Oz, *Large N field theories, string theory and gravity*, *Phys.Rept.* **323** (2000) 183–386, [hep-th/9905111].

[9] J. Casalderrey-Solana, H. Liu, D. Mateos, K. Rajagopal, and U. A. Wiedemann, *Gauge/String Duality, Hot QCD and Heavy Ion Collisions*, arXiv:1101.0618.

[10] S. A. Hartnoll, *Lectures on holographic methods for condensed matter physics*, *Class.Quant.Grav.* **26** (2009) 224002, [arXiv:0903.3246].

[11] S. S. Gubser, *Breaking an Abelian gauge symmetry near a black hole horizon*, *Phys.Rev.* **D78** (2008) 065034, [arXiv:0801.2977].

[12] S. A. Hartnoll, C. P. Herzog, and G. T. Horowitz, *Building a Holographic Superconductor*, *Phys.Rev.Lett.* **101** (2008) 031601, [arXiv:0803.3295].

[13] S. A. Hartnoll, C. P. Herzog, and G. T. Horowitz, *Holographic Superconductors*, *JHEP* **0812** (2008) 015, [arXiv:0810.1563].

[14] H. Liu, J. McGreevy, and D. Vegh, *Non-Fermi liquids from holography*, *Phys.Rev.* **D83** (2011) 065029, [arXiv:0903.2477].

[15] M. Cubrovic, J. Zaanen, and K. Schalm, *String Theory, Quantum Phase Transitions and the Emergent Fermi-Liquid*, *Science* **325** (2009) 439–444, [arXiv:0904.1993].

[16] T. Faulkner, H. Liu, J. McGreevy, and D. Vegh, *Emergent quantum criticality, Fermi surfaces, and AdS(2)*, *Phys.Rev.* **D83** (2011) 125002, [arXiv:0907.2694].

[17] G. T. Horowitz, *Theory of Superconductivity*, *Lect.Notes Phys.* **828** (2011) 313–347, [arXiv:1002.1722].

[18] J. McGreevy, *Holographic duality with a view toward many-body physics*, *Adv.High Energy Phys.* **2010** (2010) 723105, [arXiv:0909.0518].

[19] M. Rangamani, *Gravity and Hydrodynamics: Lectures on the fluid-gravity correspondence*, *Class.Quant.Grav.* **26** (2009) 224003, [arXiv:0905.4352].

[20] G. Policastro, D. T. Son, and A. O. Starinets, *From AdS / CFT correspondence to hydrodynamics*, *JHEP* **0209** (2002) 043, [hep-th/0205052].

[21] G. Policastro, D. T. Son, and A. O. Starinets, *From AdS / CFT correspondence to hydrodynamics. 2. Sound waves*, *JHEP* **0212** (2002) 054, [hep-th/0210220].

[22] S. Bhattacharyya, V. E. Hubeny, S. Minwalla, and M. Rangamani, *Nonlinear Fluid Dynamics from Gravity*, *JHEP* **0802** (2008) 045, [arXiv:0712.2456].

[23] C. P. Herzog, *Lectures on Holographic Superfluidity and Superconductivity*, *J.Phys.* **A42** (2009) 343001, [arXiv:0904.1975].

[24] S. A. Hartnoll, *Horizons, holography and condensed matter*, arXiv:1106.4324.

[25] V. E. Hubeny, S. Minwalla, and M. Rangamani, *The fluid/gravity correspondence*, arXiv:1107.5780.

[26] V. E. Hubeny, *The Fluid/Gravity Correspondence: a new perspective on the Membrane Paradigm*, *Class.Quant.Grav.* **28** (2011) 114007, [arXiv:1011.4948].

[27] M. P. Heller, R. A. Janik, and P. Witaszczyk, *The characteristics of thermalization of boost-invariant plasma from holography*, *Phys.Rev.Lett.* **108** (2012) 201602, [arXiv:1103.3452].

[28] L. Landau and E. Lifshitz, *Fluid Mechnics*. Pergamon, 1966.

[29] R. Liboff, *Kinetic Theory: Classical, Quantum, and Relativistic Descriptions*. Graduate Texts in Contemporary Physics. Springer, 2003.

[30] P. Romatschke, *New Developments in Relativistic Viscous Hydrodynamics*, *Int.J.Mod.Phys.* **E19** (2010) 1–53, [arXiv:0902.3663].

[31] P. Kovtun, *Lectures on hydrodynamic fluctuations in relativistic theories*, *J.Phys.* **A45** (2012) 473001, [arXiv:1205.5040].

[32] D. T. Son and A. O. Starinets, *Hydrodynamics of r-charged black holes*, *JHEP* **0603** (2006) 052, [hep-th/0601157].

[33] S. Sachdev, *Quantum Phase Transitions*. Cambridge University Press, 2001.

[34] J. Negele and H. Orland, *Quantum Many-particle Systems*. Westview Press, 2008.

[35] M. Bellac, *Thermal Field Theory*. Cambridge Monographs on Mathematical Physics. Cambridge University Press, 2000.

[36] J. Kapusta and C. Gale, *Finite-Temperature Field Theory: Principles and Applications*. Cambridge Monographs on Mathematical Physics. Cambridge University Press, 2006.

[37] J. Polchinski, *Effective field theory and the Fermi surface*, hep-th/9210046.

[38] H. A. Kramers and G. H. Wannier, *Statistics of the two-dimensional ferromagnet. part i*, *Phys. Rev.* **60** (Aug, 1941) 252–262.

[39] H. A. Kramers and G. H. Wannier, *Statistics of the two-dimensional ferromagnet. part ii*, *Phys. Rev.* **60** (Aug, 1941) 263–276.

[40] L. Onsager, *Crystal statistics. i. a two-dimensional model with an order-disorder transition*, *Phys. Rev.* **65** (Feb, 1944) 117–149.

[41] A. Joyal and R. Street, *An introduction to tannaka duality and quantum groups*, in *Category theory*, pp. 413–492, Springer, 1991.

[42] R. Savit, *Duality in field theory and statistical systems*, *Rev. Mod. Phys.* **52** (Apr, 1980) 453–487.

[43] R. Rajaraman, *Solitons and Instantons: An Introduction to Solitons and Instantons in Quantum Field Theory*. North-Holland personal library. North-Holland Publishing Company, 1982.

[44] C. Vafa, *Geometric origin of Montonen-Olive duality*, *Adv.Theor.Math.Phys.* **1** (1998) 158–166, [hep-th/9707131].

[45] N. Seiberg and E. Witten, *Electric - magnetic duality, monopole condensation, and confinement in N=2 supersymmetric Yang-Mills theory*, *Nucl.Phys.* **B426** (1994) 19–52, [hep-th/9407087].

[46] J. de Boer, L. Maoz, and A. Naqvi, *Some aspects of the AdS / CFT correspondence*, hep-th/0407212.

[47] K.-H. Rehren, *QFT lectures on AdS-CFT*, hep-th/0411086.

[48] G. T. Horowitz and J. Polchinski, *Gauge/gravity duality*, gr-qc/0602037.

[49] H. Nastase, *Introduction to AdS-CFT*, arXiv:0712.0689.

[50] M. K. Benna and I. R. Klebanov, *Gauge-String Dualities and Some Applications*, arXiv:0803.1315.

[51] J. Soda, *AdS/CFT on the brane*, *Lect.Notes Phys.* **828** (2011) 235–270, [arXiv:1001.1011].

[52] J. Polchinski, *Introduction to Gauge/Gravity Duality*, arXiv:1010.6134.

[53] A. Strominger and C. Vafa, *Microscopic origin of the Bekenstein-Hawking entropy*, *Phys.Lett.* **B379** (1996) 99–104, [hep-th/9601029].

[54] S. Carlip, *Black Hole Thermodynamics and Statistical Mechanics*, *Lect.Notes Phys.* **769** (2009) 89–123, [arXiv:0807.4520].

[55] A. Sen, *Black Hole Entropy Function, Attractors and Precision Counting of Microstates*, *Gen.Rel.Grav.* **40** (2008) 2249–2431, [arXiv:0708.1270].

[56] M. Green, J. Schwarz, and E. Witten, *Superstring Theory: Volume 1, Introduction*. Cambridge Monographs on Mathematical Physics. Cambridge University Press, 1988.

[57] M. Green, J. Schwarz, and E. Witten, *Superstring Theory: Volume 2, Loop Amplitudes, Anomalies and Phenomenology*. Cambridge Monographs on Mathematical Physics. Cambridge University Press, 1987.

[58] E. Kiritsis, *String Theory in a Nutshell*. In a Nutshell. Princeton University Press, 2011.

[59] J. Polchinski, *String Theory*. Cambridge Monographs on Mathematical Physics. Cambridge University Press, 2005.

[60] J. Polchinski, *Tasi lectures on D-branes*, hep-th/9611050.

[61] C. Johnson, *D-Branes*. Cambridge Monographs on Mathematical Physics. Cambridge University Press, 2006.

[62] P. West, *Introduction to Strings and Branes*. Cambridge University Press, 2012.

[63] K. Becker, M. Becker, and J. Schwarz, *String Theory and M-Theory: A Modern Introduction*. Cambridge University Press, 2007.

[64] D. Freedman and A. Van Proeyen, *Supergravity*. Cambridge University Press, 2012.

[65] D. Tong, *String Theory*, arXiv:0908.0333.

[66] E. Witten, *Bound states of strings and p-branes*, *Nucl.Phys.* **B460** (1996) 335–350, [hep-th/9510135].

[67] Y. Makeenko, *Methods of Contemporary Gauge Theory*. Cambridge Monographs on Mathematical Physics. Cambridge University Press, 2002.

[68] S. S. Gubser, I. R. Klebanov, and A. A. Tseytlin, *Coupling constant dependence in the thermodynamics of N=4 supersymmetric Yang-Mills theory*, *Nucl.Phys.* **B534** (1998) 202–222, [hep-th/9805156].

[69] A. Fotopoulos and T. Taylor, *Comment on two loop free energy in N=4 supersymmetric Yang-Mills theory at finite temperature*, *Phys.Rev.* **D59** (1999) 061701, [hep-th/9811224].

[70] J.-P. Blaizot, E. Iancu, U. Kraemmer, and A. Rebhan, *Hard thermal loops and the entropy of supersymmetric Yang-Mills theories*, *JHEP* **0706** (2007) 035, [hep-ph/0611393].

[71] D. T. Son and A. O. Starinets, *Minkowski space correlators in AdS / CFT correspondence: Recipe and applications*, *JHEP* **0209** (2002) 042, [hep-th/0205051].

[72] C. Herzog and D. Son, *Schwinger-Keldysh propagators from AdS/CFT correspondence*, *JHEP* **0303** (2003) 046, [hep-th/0212072].

[73] K. Skenderis, *Lecture notes on holographic renormalization*, *Class.Quant.Grav.* **19** (2002) 5849–5876, [hep-th/0209067].

[74] M. Bianchi, D. Z. Freedman, and K. Skenderis, *Holographic renormalization*, *Nucl.Phys.* **B631** (2002) 159–194, [hep-th/0112119].

[75] P. Morse and H. Feshbach, *Methods of Theoretical Physics. Philip M. Morse,... Herman Feshbach,...* Mc Graw-Hill book Co, 1953.

[76] N. Birrell and P. Davies, *Quantum Fields in Curved Space*. Cambridge Monographs on Mathematical Physics. Cambridge University Press, 1984.

[77] P. Breitenlohner and D. Z. Freedman, *Stability in Gauged Extended Supergravity*, *Annals Phys.* **144** (1982) 249.

[78] G. Policastro, D. Son, and A. Starinets, *The Shear viscosity of strongly coupled N=4 supersymmetric Yang-Mills plasma*, *Phys.Rev.Lett.* **87** (2001) 081601, [hep-th/0104066].

[79] A. Karch, D. Son, and A. Starinets, *Zero Sound from Holography*, arXiv:0806.3796.

[80] A. Nunez and A. O. Starinets, *AdS / CFT correspondence, quasinormal modes, and thermal correlators in N=4 SYM*, *Phys.Rev.* **D67** (2003) 124013, [hep-th/0302026].

[81] K. Sfetsos and K. Skenderis, *Microscopic derivation of the Bekenstein-Hawking entropy formula for nonextremal black holes*, *Nucl.Phys.* **B517** (1998) 179–204, [hep-th/9711138].

[82] S. A. Hartnoll, J. Polchinski, E. Silverstein, and D. Tong, *Towards strange metallic holography*, *JHEP* **1004** (2010) 120, [arXiv:0912.1061].

[83] T. Faulkner, N. Iqbal, H. Liu, J. McGreevy, and D. Vegh, *From Black Holes to Strange Metals*, arXiv:1003.1728.

[84] G. T. Horowitz, J. E. Santos, and B. Way, *A Holographic Josephson Junction*, *Phys.Rev.Lett.* **106** (2011) 221601, [arXiv:1101.3326].

[85] M. Edalati, R. G. Leigh, and P. W. Phillips, *Dynamically Generated Mott Gap from Holography*, *Phys.Rev.Lett.* **106** (2011) 091602, [arXiv:1010.3238].

[86] R. A. Davison and N. K. Kaplis, *Bosonic excitations of the AdS_4 Reissner-Nordstrom black hole*, *JHEP* **1112** (2011) 037, [arXiv:1111.0660].

[87] M. Edalati, J. I. Jottar, and R. G. Leigh, *Transport Coefficients at Zero Temperature from Extremal Black Holes*, *JHEP* **1001** (2010) 018, [arXiv:0910.0645].

[88] M. Edalati, J. I. Jottar, and R. G. Leigh, *Shear Modes, Criticality and Extremal Black Holes*, *JHEP* **1004** (2010) 075, [arXiv:1001.0779].

[89] D. Nickel and D. T. Son, *Deconstructing holographic liquids*, *New J.Phys.* **13** (2011) 075010, [arXiv:1009.3094].

[90] M. Kulaxizi and A. Parnachev, *Comments on Fermi Liquid from Holography*, *Phys.Rev.* **D78** (2008) 086004, [arXiv:0808.3953].

[91] M. Ammon, J. Erdmenger, S. Lin, S. Muller, A. O'Bannon, et al., *On Stability and Transport of Cold Holographic Matter*, *JHEP* **1109** (2011) 030, [arXiv:1108.1798].

[92] M. Kulaxizi and A. Parnachev, *Holographic Responses of Fermion Matter*, *Nucl.Phys.* **B815** (2009) 125–141, [arXiv:0811.2262].

[93] L.-Y. Hung and A. Sinha, *Holographic quantum liquids in 1+1 dimensions*, *JHEP* **1001** (2010) 114, [arXiv:0909.3526].

[94] C. Hoyos-Badajoz, A. O'Bannon, and J. M. Wu, *Zero Sound in Strange Metallic Holography*, *JHEP* **1009** (2010) 086, [arXiv:1007.0590].

[95] B.-H. Lee, D.-W. Pang, and C. Park, *Zero Sound in Effective Holographic Theories*, *JHEP* **1011** (2010) 120, [arXiv:1009.3966].

[96] O. Bergman, N. Jokela, G. Lifschytz, and M. Lippert, *Striped instability of a holographic Fermi-like liquid*, *JHEP* **1110** (2011) 034, [arXiv:1106.3883].

[97] L. Landau, E. Lifshitz, and L. Pitaevskii, *Statistical Physics*. No. pt. 2 in Course of Theoretical Physics. Butterworth-Heinemann, 1980.

[98] L. Pitaevskii and E. Lifshitz, *Physical Kinetics*. No. v. 10. Elsevier Science, 1981.

[99] A. Abrikosov, L. Gorkov, I. Dzâlošinskij, and I. Dzialoshinskii, *Methods of Quantum Field Theory in Statistical Physics*. Dover books on advanced mathematics. Dover Publications, Incorporated, 1975.

[100] P. Nozieres and D. Pines, *Theory Of Quantum Liquids*. Advanced Books Classics. Westview Press, 1999.

[101] A. Abrikosov and I. Khalatnikov, *The theory of a fermi liquid (the properties of liquid 3he at low temperatures)*, *Reports on Progress in Physics* **22** (1959), no. 1 329.

[102] R. Belliard, S. S. Gubser, and A. Yarom, *Absence of a Fermi surface in classical minimal four-dimensional gauged supergravity*, *JHEP* **1110** (2011) 055, [arXiv:1106.6030].

[103] J. P. Gauntlett, J. Sonner, and D. Waldram, *Universal fermionic spectral functions from string theory*, *Phys.Rev.Lett.* **107** (2011) 241601, [arXiv:1106.4694].

[104] J. P. Gauntlett, J. Sonner, and D. Waldram, *Spectral function of the supersymmetry current*, *JHEP* **1111** (2011) 153, [arXiv:1108.1205].

[105] D. K. Brattan and S. A. Gentle, *Shear channel correlators from hot charged black holes*, *JHEP* **1104** (2011) 082, [arXiv:1012.1280].

[106] X.-H. Ge, K. Jo, and S.-J. Sin, *Hydrodynamics of RN AdS_4 black hole and Holographic Optics*, *JHEP* **1103** (2011) 104, [arXiv:1012.2515].

[107] C. P. Herzog, *The Sound of M theory*, *Phys.Rev.* **D68** (2003) 024013, [hep-th/0302086].

[108] A. S. Miranda, J. Morgan, and V. T. Zanchin, *Quasinormal modes of plane-symmetric black holes according to the AdS/CFT correspondence*, *JHEP* **0811** (2008) 030, [arXiv:0809.0297].

[109] C. P. Herzog, *The Hydrodynamics of M theory*, *JHEP* **0212** (2002) 026, [hep-th/0210126].

[110] A. Chamblin, R. Emparan, C. V. Johnson, and R. C. Myers, *Charged AdS black holes and catastrophic holography*, *Phys.Rev.* **D60** (1999) 064018, [hep-th/9902170].

[111] M. Cvetic, M. Duff, P. Hoxha, J. T. Liu, H. Lu, et al., *Embedding AdS black holes in ten-dimensions and eleven-dimensions*, *Nucl.Phys.* **B558** (1999) 96–126, [hep-th/9903214].

[112] M. Kaminski, K. Landsteiner, J. Mas, J. P. Shock, and J. Tarrio, *Holographic Operator Mixing and Quasinormal Modes on the Brane*, *JHEP* **1002** (2010) 021, [arXiv:0911.3610].

[113] R. Wald, *General Relativity*. University of Chicago Press, 2010.

[114] P. K. Kovtun and A. O. Starinets, *Quasinormal modes and holography*, *Phys.Rev.* **D72** (2005) 086009, [hep-th/0506184].

[115] H. Kodama and A. Ishibashi, *Master equations for perturbations of generalized static black holes with charge in higher dimensions*, *Prog.Theor.Phys.* **111** (2004) 29–73, [hep-th/0308128].

[116] C. P. Herzog, P. Kovtun, S. Sachdev, and D. T. Son, *Quantum critical transport, duality, and M-theory*, *Phys.Rev.* **D75** (2007) 085020, [hep-th/0701036].

[117] J. Oppenheimer and G. Volkoff, *On Massive neutron cores*, *Phys.Rev.* **55** (1939) 374–381.

[118] R. C. Tolman, *Static solutions of Einstein's field equations for spheres of fluid*, *Phys.Rev.* **55** (1939) 364–373.

[119] T. Hartman and S. A. Hartnoll, *Cooper pairing near charged black holes*, *JHEP* **1006** (2010) 005, [arXiv:1003.1918].

[120] D. Yamada, *Fragmentation of Spinning Branes*, *Class.Quant.Grav.* **25** (2008) 145006, [arXiv:0802.3508].

[121] B. McInnes, *Bounding the Temperatures of Black Holes Dual to Strongly Coupled Field Theories on Flat Spacetime*, *JHEP* **0909** (2009) 048, [arXiv:0905.1180].

[122] E. Witten, *Anti-de Sitter space, thermal phase transition, and confinement in gauge theories*, *Adv.Theor.Math.Phys.* **2** (1998) 505–532, [hep-th/9803131].

[123] T. Nishioka, S. Ryu, and T. Takayanagi, *Holographic Superconductor/Insulator Transition at Zero Temperature*, *JHEP* **1003** (2010) 131, [arXiv:0911.0962].

[124] G. T. Horowitz and B. Way, *Complete Phase Diagrams for a Holographic Superconductor/Insulator System*, *JHEP* **1011** (2010) 011, [arXiv:1007.3714].

[125] S. Sachdev, *Holographic metals and the fractionalized Fermi liquid*, *Phys.Rev.Lett.* **105** (2010) 151602, [arXiv:1006.3794].

[126] F. Denef and S. A. Hartnoll, *Landscape of superconducting membranes*, *Phys.Rev.* **D79** (2009) 126008, [arXiv:0901.1160].

[127] S. A. Hartnoll and A. Tavanfar, *Electron stars for holographic metallic criticality*, *Phys.Rev.* **D83** (2011) 046003, [arXiv:1008.2828].

[128] S. A. Hartnoll, D. M. Hofman, and A. Tavanfar, *Holographically smeared Fermi surface: Quantum oscillations and Luttinger count in electron stars*, *Europhys.Lett.* **95** (2011) 31002, [arXiv:1011.2502].

[129] S. A. Hartnoll and P. Petrov, *Electron star birth: A continuous phase transition at nonzero density*, *Phys.Rev.Lett.* **106** (2011) 121601, [arXiv:1011.6469].

[130] G. T. Horowitz and B. Way, *Lifshitz Singularities*, *Phys.Rev.* **D85** (2012) 046008, [arXiv:1111.1243].

[131] N. Bao, X. Dong, S. Harrison, and E. Silverstein, *The Benefits of Stress: Resolution of the Lifshitz Singularity*, *Phys.Rev.* **D86** (2012) 106008, [arXiv:1207.0171].

[132] P. Kovtun, D. T. Son, and A. O. Starinets, *Holography and hydrodynamics: Diffusion on stretched horizons*, *JHEP* **0310** (2003) 064, [hep-th/0309213].

[133] B. F. Schutz, *Perfect Fluids in General Relativity: Velocity Potentials and a Variational Principle*, *Phys.Rev.* **D2** (1970) 2762–2773.

[134] P. Benincasa, A. Buchel, and A. O. Starinets, *Sound waves in strongly coupled non-conformal gauge theory plasma*, *Nucl.Phys.* **B733** (2006) 160–187, [hep-th/0507026].

[135] S. A. Hartnoll and L. Huijse, *Fractionalization of holographic Fermi surfaces*, *Class.Quant.Grav.* **29** (2012) 194001, [arXiv:1111.2606].

[136] C. Charmousis, B. Gouteraux, B. Kim, E. Kiritsis, and R. Meyer, *Effective Holographic Theories for low-temperature condensed matter systems*, *JHEP* **1011** (2010) 151, [arXiv:1005.4690].

[137] S. S. Gubser and F. D. Rocha, *Peculiar properties of a charged dilatonic black hole in AdS_5*, *Phys.Rev.* **D81** (2010) 046001, [arXiv:0911.2898].

[138] K. Goldstein, S. Kachru, S. Prakash, and S. P. Trivedi, *Holography of Charged Dilaton Black Holes*, *JHEP* **1008** (2010) 078, [arXiv:0911.3586].

[139] V. G. M. Puletti, S. Nowling, L. Thorlacius, and T. Zingg, *Holographic metals at finite temperature*, *JHEP* **1101** (2011) 117, [arXiv:1011.6261].

[140] N. Iqbal, H. Liu, and M. Mezei, *Semi-local quantum liquids*, *JHEP* **1204** (2012) 086, [arXiv:1105.4621].

[141] S. Sachdev, *A model of a Fermi liquid using gauge-gravity duality*, *Phys.Rev.* **D84** (2011) 066009, [arXiv:1107.5321].

[142] M. Duff and J. T. Liu, *Anti-de Sitter black holes in gauged $N = 8$ supergravity*, *Nucl.Phys.* **B554** (1999) 237–253, [hep-th/9901149].